NASA TECHNICAL MEMORANDUM

NASA TM X-3070

NASA TM X-3070

STABILITY AND CONTROL CHARACTERISTICS AT MACH NUMBERS FROM 0.20 TO 4.63 OF A CRUCIFORM AIR-TO-AIR MISSILE WITH TRIANGULAR CANARD CONTROLS AND A TRAPEZOIDAL WING

by Ernald B. Graves and Roger H. Fournier

Langley Research Center
Hampton, Va. 23665

NATIONAL AERONAUTICS AND SPACE ADMINISTRATION • WASHINGTON, D. C. • JULY 1974

1. Report No.	2. Government Accession No.	3. Recipient's Catalog No.
NASA TM X-3070		

4. Title and Subtitle	5. Report Date
STABILITY AND CONTROL CHARACTERISTICS AT MACH NUMBERS FROM 0.20 TO 4.63 OF A CRUCIFORM AIR-TO-AIR MISSILE WITH TRIANGULAR CANARD CONTROLS AND A TRAPEZOIDAL WING	July 1974
	6. Performing Organization Code
7. Author(s)	8. Performing Organization Report No.
Ernald B. Graves and Roger H. Fournier	L-9577
	10. Work Unit No.
9. Performing Organization Name and Address	760-67-01-03
NASA Langley Research Center Hampton, Va. 23665	11. Contract or Grant No.
	13. Type of Report and Period Covered
12. Sponsoring Agency Name and Address	Technical Memorandum
National Aeronautics and Space Administration Washington, D.C. 20546	14. Sponsoring Agency Code

15. Supplementary Notes

16. Abstract

Investigations have been conducted in the Langley 8-foot transonic pressure tunnel and the Langley Unitary Plan wind tunnel at Mach numbers from 0.20 to 4.63 to determine the stability and control characteristics of a cruciform air-to-air missile with triangular canard controls and a trapezoidal wing.

The results indicate that canards are effective in producing pitching moment throughout most of the test angle-of-attack and Mach number range and that the variations of pitching moment with lift for trim conditions are relatively linear. There is a decrease in canard effectiveness with an increase in angle of attack up to about Mach 2.50 as evidenced by the beginning of coalescence of the pitching-moment curves. At a Mach number above 2.50, there is an increase in effectiveness at moderate to high angles of attack. Simulated launch straps have little effect on the lift and pitch characteristics but do cause an increase in drag, and this increase in drag induces a rolling moment at a zero roll attitude where the straps cause an asymmetric geometric shape. The canards are not suitable devices for roll control and, at some Mach numbers and roll attitudes, are not effective in producing pure yawing moments.

17. Key Words (Suggested by Author(s))	18. Distribution Statement
Canard controls Stability and control Air-to-air missile	Unclassified – Unlimited STAR Category 01

19. Security Classif. (of this report)	20. Security Classif. (of this page)	21. No. of Pages	22. Price*
Unclassified	Unclassified	233	$6.00

*For sale by the National Technical Information Service, Springfield, Virginia 22151

STABILITY AND CONTROL CHARACTERISTICS AT MACH NUMBERS FROM 0.20 TO 4.63 OF A CRUCIFORM AIR-TO-AIR MISSILE WITH TRIANGULAR CANARD CONTROLS AND A TRAPEZOIDAL WING

By Ernald B. Graves and Roger H. Fournier
Langley Research Center

SUMMARY

Investigations have been conducted in the Langley 8-foot transonic pressure tunnel and the Langley Unitary Plan wind tunnel at Mach numbers from 0.20 to 4.63 to determine the stability and control characteristics of a cruciform air-to-air missile with triangular canard controls and a trapezoidal wing.

The results indicate that canards are effective in producing pitching moment throughout most of the test angle-of-attack and Mach number range and that the variations of pitching moment with lift for trim conditions are relatively linear. There is a decrease in canard effectiveness with an increase in angle of attack up to about Mach 2.50 as evidenced by the beginning of coalescence of the pitching-moment curves. At a Mach number above 2.50, there is an increase in effectiveness at moderate to high angles of attack. Simulated launch straps have little effect on the lift and pitch characteristics but do cause an increase in drag, and this increase in drag induces a rolling moment at a zero roll attitude where the straps cause an asymmetric geometric shape. The canards are not suitable devices for roll control and, at some Mach numbers and roll attitudes, are not effective in producing pure yawing moments.

INTRODUCTION

The National Aeronautics and Space Administration is providing continuous support in the field of missile research and development. As a part of this effort, wind-tunnel tests have been performed on a model of a cruciform air-to-air type missile with canard controls to determine the stability, control, and performance characteristics at subsonic, transonic, and supersonic Mach numbers. The model body had a fineness ratio of about 22 and used a hemispheric nose. Triangular canard surfaces were used for controls and fixed trapezoidal wings were located at the rear of the body. Three straps were placed on the body to simulate launch hangers for the vehicle.

The tests were conducted in the Langley 8-foot transonic pressure tunnel at Mach numbers from 0.20 to 1.20 and in the Langley Unitary Plan wind tunnel at Mach numbers from 1.75 to 4.63. The angle of attack was varied from approximately -4^{o} to 24^{o} at a constant Reynolds number of 6.56×10^{6} per meter. Various roll attitudes were investigated.

SYMBOLS

The aerodynamic coefficients are referenced to both the body and stability axis systems. The moment reference is at the 55-percent body length location, 51.85 cm aft of the model nose.

A	reference area (based on d), 0.001408 m^2
A_c	canard reference area, 0.001936 m^2
a_n	normal acceleration, g units
b	reference span, canard surface, 4.345 cm
C_A	axial-force coefficient, Axial force/qA
$C_{A,b}$	base axial-force coefficient, Base axial force/qA
C_{BM}	coefficient of canard bending moment about root chord, Bending moment/qA_cb
C_D	drag coefficient, Drag/qA
$C_{D,b}$	base drag coefficient, Base drag/qA
$C_{D,o}$	drag coefficient at zero lift
C_{HM}	coefficient of canard hinge moment about hinge line, Hinge moment/qA_cc
C_L	lift coefficient, Lift/qA
C_{L_α}	lift-curve slope taken through $\alpha = 0^{o}$, per deg
$C_{L,trim}$	trim lift coefficient

ERRATA

NASA Technical Memorandum X-3070

STABILITY AND CONTROL CHARACTERISTICS AT MACH NUMBERS FROM 0.20 TO 4.63 OF A CRUCIFORM AIR-TO-AIR MISSILE WITH TRIANGULAR CANARD CONTROLS AND A TRAPEZOIDAL WING

By Ernald B. Graves and Roger H. Fournier

July 1974

Page 3: The definition for the symbol C_m should read as follows:

pitching-moment coefficient, Pitching moment/$qA\ell$

Issued March 1976

C_l	rolling-moment coefficient, Rolling moment/qAd
C_m	pitching-moment coefficient, Pitching moment/qAℓ
C_{m_δ}	pitch control parameter, $\Delta C_m / \Delta \delta_{pitch}$, per deg
C_N	normal-force coefficient, Normal force/qA
C_{NF}	coefficient of canard normal force, Normal force/qA_c
C_n	yawing-moment coefficient, Yawing moment/qAd
C_Y	side-force coefficient, Side force/qA
c	reference chord, canard, 8.890 cm
d	maximum body diameter, 4.238 cm
ℓ	reference length, 94.27 cm
M	free-stream Mach number
q	free-stream dynamic pressure
r	radius, cm
W	weight, N
x_{ac}	aerodynamic center, percent ℓ
x_{cg}	center of gravity, percent ℓ
α	angle of attack, deg
δ_c	canard deflection angle (subscripts 1, 2, 3, and 4 indicate canard surface in a clockwise direction from rear, $\delta_{c,1}$ being the canard on top of the body for $\phi = 0^o$), deg
δ_{pitch}	canards deflected to provide pitching moment (positive leading edge up), deg; for $\phi = 0^o$, 2 controls and for $\phi = -45^o$, 4 controls

δ_{roll} canards (4) deflected to produce negative rolling moment, deg

δ_{yaw} canards deflected to provide yawing moment (positive leading edge right), deg; for $\phi = 0^{o}$, 2 controls and for $\phi = -45^{o}$, 4 controls

ϕ model roll angle (positive clockwise viewed from rear), deg; $\phi = -45^{o}$ when canards and wings are in × position with launch straps on top of body

ϕ_c canard roll angle, deg

APPARATUS AND TESTS

Tunnels

The investigation was conducted in the Langley 8-foot transonic pressure tunnel and in the Langley Unitary Plan wind tunnel. These tunnels are variable-pressure continuous-flow facilities. The 8-foot tunnel has a slotted test section which is about 2.44 meters square and has a Mach number range from about 0.20 to 1.30.

The Unitary Plan wind tunnel has two test sections, each about 1.22 meters square and about 2.13 meters long. The nozzle leading to each test section is of the asymmetric sliding block type which permits a continuous variation in Mach number from about 1.47 to 2.86 in the low Mach number test section and from about 2.3 to 4.7 in the high Mach number test section.

Model

A drawing of the model ($\phi = -90^{o}$) is presented as figure 1 and a photograph of the model ($\phi = 0^{o}$) in the test section is shown as figure 2. The model fuselage had a fineness ratio of about 22 and incorporated a hemispheric nose. The aft 17 percent of the fuselage was slightly enlarged in diameter in order to attach the wings. The all-movable cruciform canards had wedge-shaped airfoil sections and a modified triangular planform with rounded leading edges. The in-line wing had a trapezoidal planform and side fairings for attachment to the body. Two mounting hangers (launch straps) were located on the body between the canards and wings. A third hanger was located on the body slightly aft of the leading edge of the wings.

Tests

The investigation was performed under the following test conditions:

Tunnel	Mach number	Reynolds number per meter	Stagnation temperature, K	Transition grit size
8 foot	0.20 to 1.20	6.56×10^6	332	No. 90
Unitary Plan	1.75 to 2.86	6.56×10^6	339	No. 50
Unitary Plan	3.95 to 4.63	6.56×10^6	353	No. 45

The dewpoint temperature for these tests was maintained sufficiently low to insure negligible condensation effects in all the test facilities. Boundary-layer transition strips were placed 3.05 cm aft the model nose and 1.02 cm aft, streamwise, on all lifting surfaces. Sand, sparsely sprinkled, in 0.16-cm-wide strips was used except at Mach numbers of 3.95 and 4.63 where the sand particles were individually placed three diameters apart.

Measurements

Aerodynamic forces and moments were measured by means of a six-component electrical strain-gage balance located within the model and, in turn, rigidly fastened to a sting-support system. Pressures in the model balance chamber were measured by means of a single static orifice. The model base was feathered to the outer diameter so that no base area existed.

Angles of attack have been corrected for sting and balance deflection due to aerodynamic loads and for tunnel airflow misalinement. Axial-force and drag coefficients have been adjusted to free-stream static conditions acting over the model balance chamber. Typical values of base drag and base axial-force coefficients are presented in figure 3.

In addition, some tests were made with instrumented canard controls to measure the control surface normal force, hinge moment, and root bending moment.

PRESENTATION OF RESULTS

The results of wind-tunnel tests on the model are presented as follows:

DISCUSSION

Longitudinal Characteristics

Pitch control data are presented in figure 4 for the model at $\phi = 0^{o}$ (2 controls) and in figure 5 for $\phi = -45^{o}$ (4 controls). The pitching-moment and lift data, although they exhibited some irregular variations, are relatively linear throughout most of the operating lift coefficient range at all test Mach numbers. Deflection of the canards for pitch control leads to some nonlinear pitching-moment variations near $C_L = 0$ for Mach numbers up to about 2.0; however, the data indicate linear characteristics near all trim conditions. The low-lift nonlinearities are probably caused by canard wake on the wing since the effects tend to disappear at the higher lift coefficients.

There is a decrease in canard effectiveness with increase in angle of attack up to about Mach 2.50 as evidenced by the beginning of coalescence of the C_m curves and, in

some instances, an increase in canard deflection will lead to no increase or even a decrease in pitching moment. At Mach numbers above 2.50, there is an increase in effectiveness at moderate to high angles of attack.

The effects of the launch straps and hangers on the longitudinal characteristics of the model are shown in figures 6 and 7. These data indicate that other than an expected increase in C_A or C_D, there is little effect of the launch straps on the longitudinal characteristics.

For this test sequence, the model was rolled to a ϕ attitude of -14.04° (fig. 8) with $\delta_{c,1}$ and $\delta_{c,3}$ equal to 5° and $\delta_{c,2}$ and $\delta_{c,4}$ equal to 20° and then pitched in a vertical plane. This procedure simulates an out-of-plane pitch-yaw maneuver in the $\phi = -14.04^\circ$ plane. Figure 9 shows results for the model rolled to a ϕ attitude of -26.57° with $\delta_{c,1}$ and $\delta_{c,3}$ equal to 10° and $\delta_{c,2}$ and $\delta_{c,4}$ equal to 20°, and then pitched in a vertical plane to simulate the pitch-yaw maneuver at $\phi = -26.57^\circ$.

A summary of the longitudinal stability, control, and performance characteristics is presented in figure 10. The results (fig. 10(a)) indicate that the canards are effective in producing pitching moment throughout the Mach number range, the effectiveness being about 50 percent greater at $\phi = -45^\circ$ (4 controls) than at $\phi = 0^\circ$ (2 controls). The total variation in aerodynamic center location is a little less than 10 percent of the body length throughout the entire speed range of the test. Figure 10(b) shows the normal accelerations available at $\phi = 0^\circ$ and -45° for canard deflections of 20° at various supersonic Mach numbers and altitudes for several model center-of-gravity locations with a nominal weight loading W/A of 35 910 N/m^2 (750 lbf/ft^2). This figure can be used to determine the maneuvering capability for a number of conditions, and to establish the operational bounds of altitude, missile speed, and center of gravity for specified maneuvering capability. For example, at $M = 2$ and $\phi = -45^\circ$, the missile with a center-of-gravity location of 0.55ℓ is capable of about 40g at 3.05 km (10 000 ft), about 20g at 9.15 km (30 000 ft), and about 10g at 18.29 km (60 000 ft). Obviously, since the g capability is directly proportional to dynamic pressure, the g potential increases with increasing Mach number and decreasing altitude. The maneuverability is also directly related to the stability level and, all other factors being equal, the g potential increases as the center of gravity is moved aft. The lower g capability at $\phi = 0^\circ$ is due to the lower control power.

Lateral Characteristics

The effects of model roll orientation ϕ on the lateral coefficients are presented in figure 11. These data indicate induced side force, roll, and yaw occurring at angles of attack beyond about 6° for Mach numbers through the lower supersonic range. At Mach numbers above about 4, the induced effects are somewhat lessened. The large

induced effects at the higher angles of attack would be expected because of the asymmetry of the lifting surfaces at these roll conditions.

The effect of the launch straps on the lateral data is shown in figures 12 and 13. These data indicate that the induced effects at $\phi = 0^{\circ}$ (fig. 12) are caused in part by the launch straps since, for example, there are essentially no induced rolling moments with the launch straps off at $\phi = 0^{\circ}$. The launch straps cause little induced effects at $\phi = -45^{\circ}$. These results would be expected since the launch straps cause an asymmetrical model configuration for $\phi = 0^{\circ}$ whereas the configuration is symmetrical for $\phi = -45^{\circ}$.

The results presented in figures 14 and 15 generally show that the controls deflected for out-of-plane maneuvering at $\phi = -14.04^{\circ}$ and -26.57° increase the induced rolling and yawing moments of the vehicle at Mach numbers to 2.86. At the higher Mach numbers the effect is considerably reduced.

For research purposes, the roll control effectiveness of the canards at supersonic speeds is presented in figures 16 and 17. At angles of attack to about 6°, there is little or no roll control available with the canards throughout the Mach number range. In addition, the canard roll control at the higher angles of attack is extremely nonlinear. It appears that canards are not a satisfactory means of obtaining roll control, and some other means such as ailerons or wing tabs are necessary.

Data showing the pure yaw control effectiveness of the canards are presented in figures 18 and 19. For the model at $\phi = 0^{\circ}$, the canards are effective in producing yawing moment throughout the supersonic Mach number range, although there is a reduction in yaw effectiveness with an increase in Mach number. At subsonic Mach number and supersonic Mach numbers to 2.86, however, there is a large reduction in yaw control effectiveness with angle of attack so that in the α range between about 10° and 15°, the canards produce little or no yawing moment. This effect is probably caused by interference flow fields from the canards reacting on the wing surfaces in this range of Mach number and angle of attack. For the model at $\phi = -45^{\circ}$, the canards are effective in producing yawing moment throughout the range of angle of attack and Mach number, although there are some regions in which reductions in yaw control effectiveness occur.

Canard Loading

Figures 20 and 21 present normal-force, hinge-moment, and bending-moment coefficients for the canard at roll attitudes from 0° to 180° through the angle-of-attack range and at deflections of 0° and 20°. These results are limited to Mach numbers of only 1.75 and 2.50 but should be useful in providing some indication of the isolated canard surface loading characteristics.

CONCLUSIONS

Results of tests on a cruciform, canard-controlled missile configuration at Mach numbers from 0.20 to 4.63 lead to the following conclusions:

1. The canards were effective in producing pitching moment throughout most of the test angle-of-attack and Mach number range, and the variations of pitching moment with lift for trim conditions were relatively linear.

2. There is a decrease in canard effectiveness with increase in angle of attack up to about Mach 2.50 as evidenced by the beginning of coalescence of the pitching-moment curves. At Mach numbers above 2.50, there is an increase in effectiveness at moderate to high angles of attack.

3. Simulated launch straps had little effect on the lift and pitch characteristics but did cause an increase in drag, and this increase in drag induced a rolling moment at a zero roll attitude where the straps caused an asymmetric geometric shape.

4. The canards were not suitable devices for roll control and, at some Mach numbers and roll attitudes, were not effective in producing pure yawing moments.

Langley Research Center,
National Aeronautics and Space Administration,
Hampton, Va., May 13, 1974.

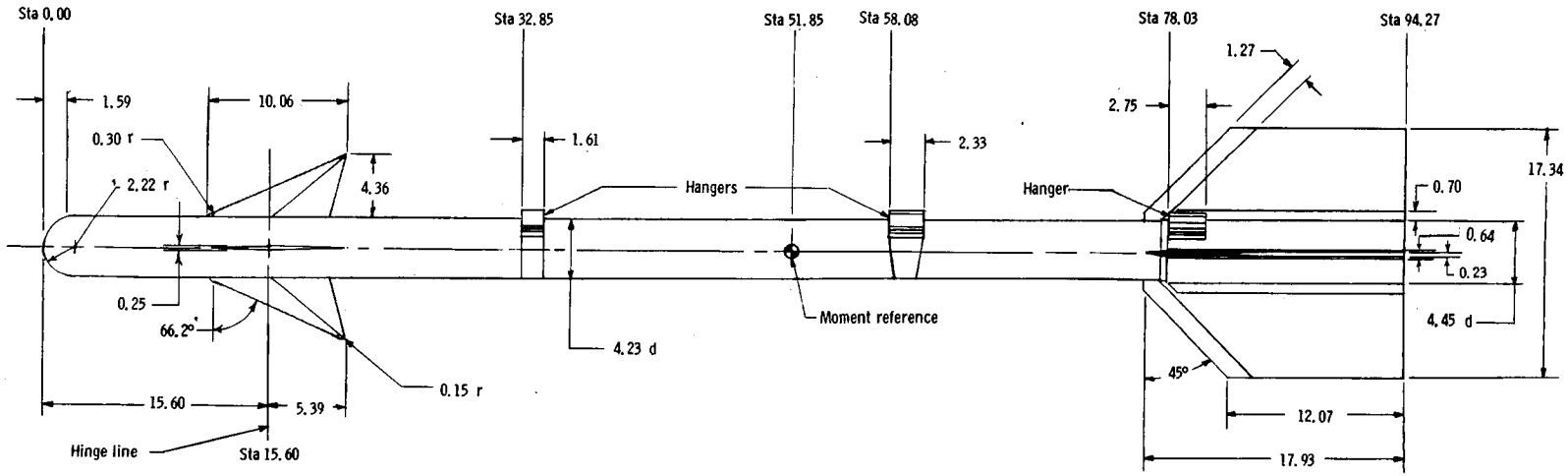

Figure 1.- Model drawing. $\phi = -90^{o}$. (All dimensions are in centimeters.)

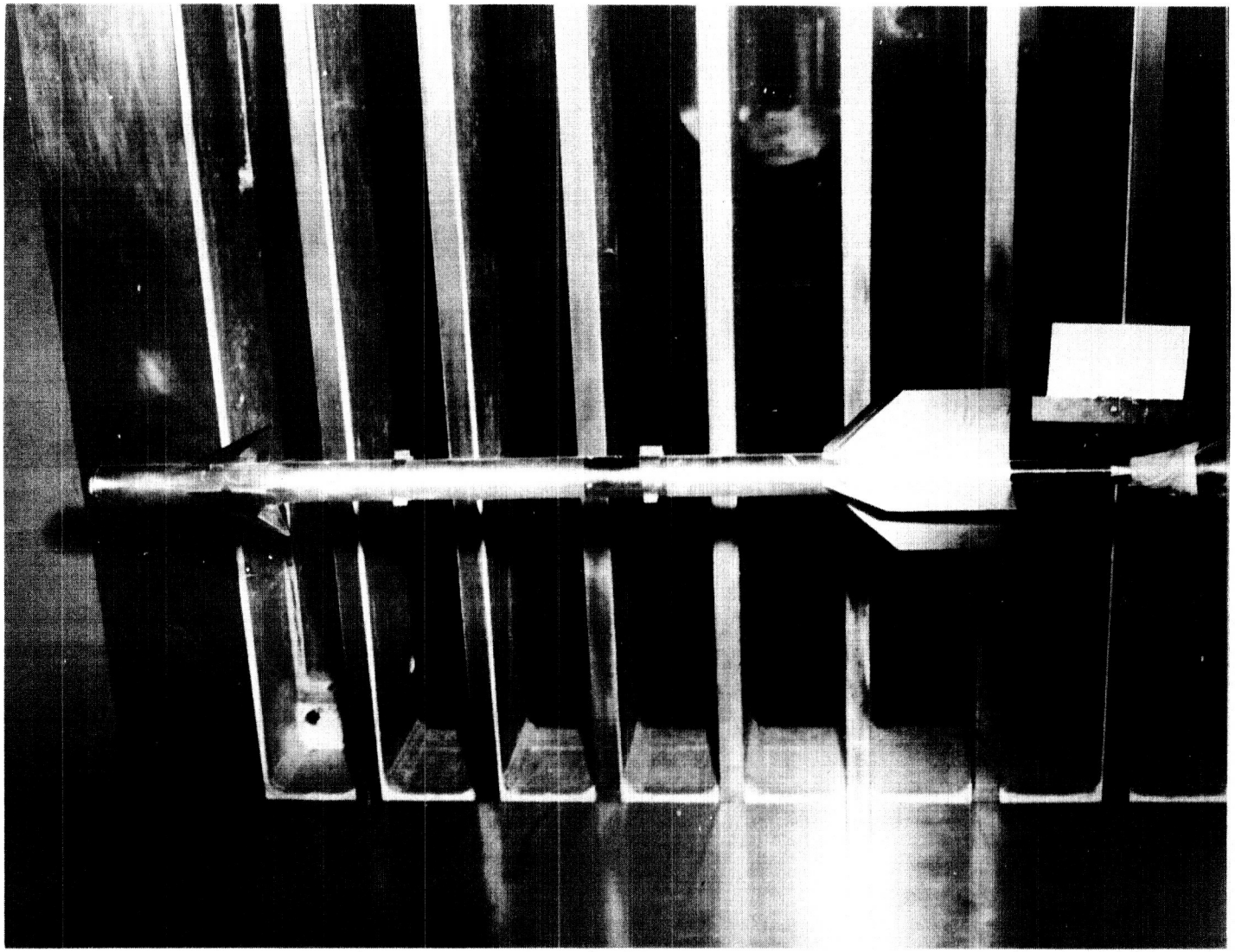

L-72-6196

Figure 2.- Typical model photograph. $\phi = 0^{o}$.

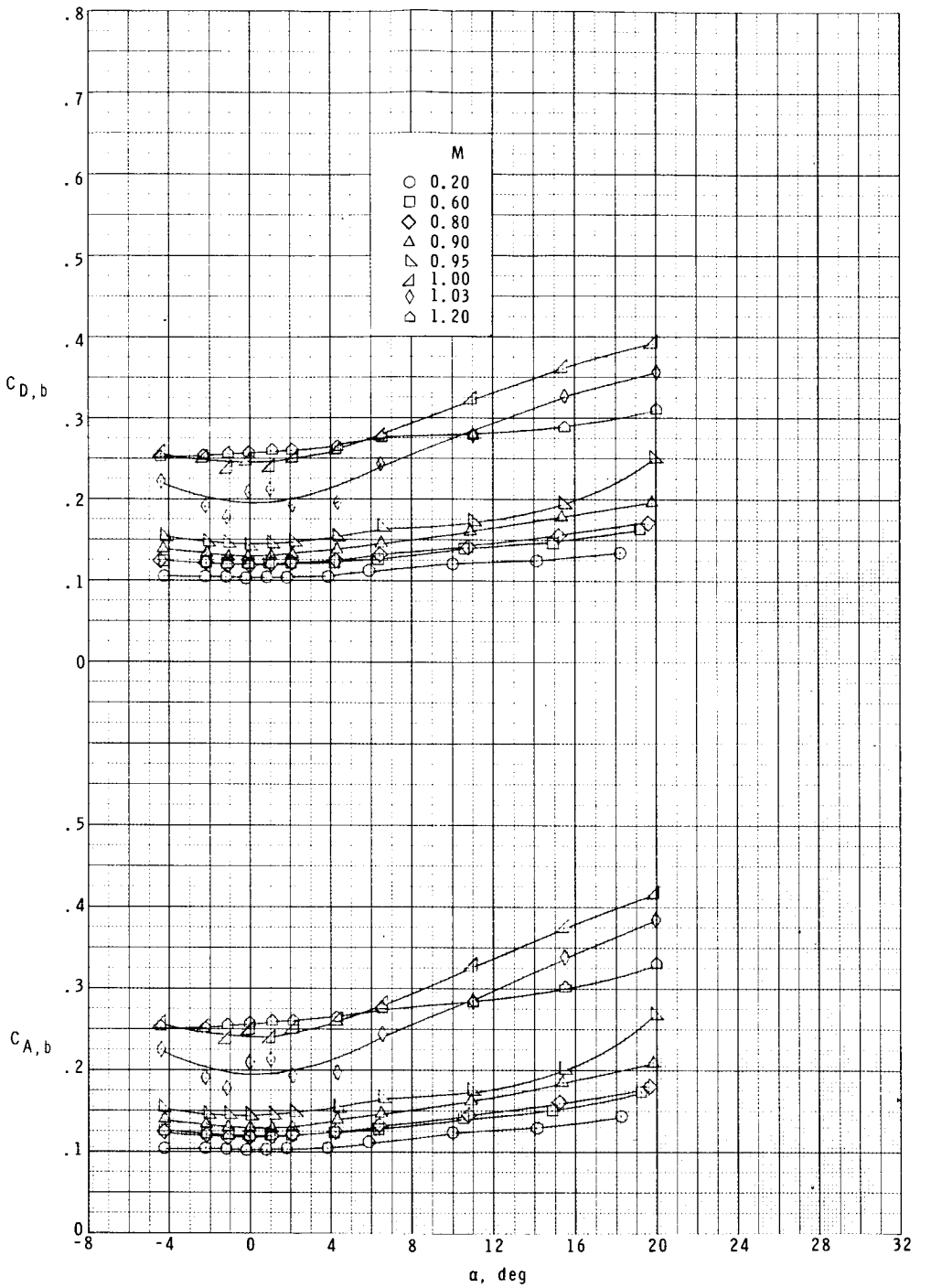

(a) M = 0.20 to M = 1.20.

Figure 3.- Typical values of base axial-force and drag coefficients.

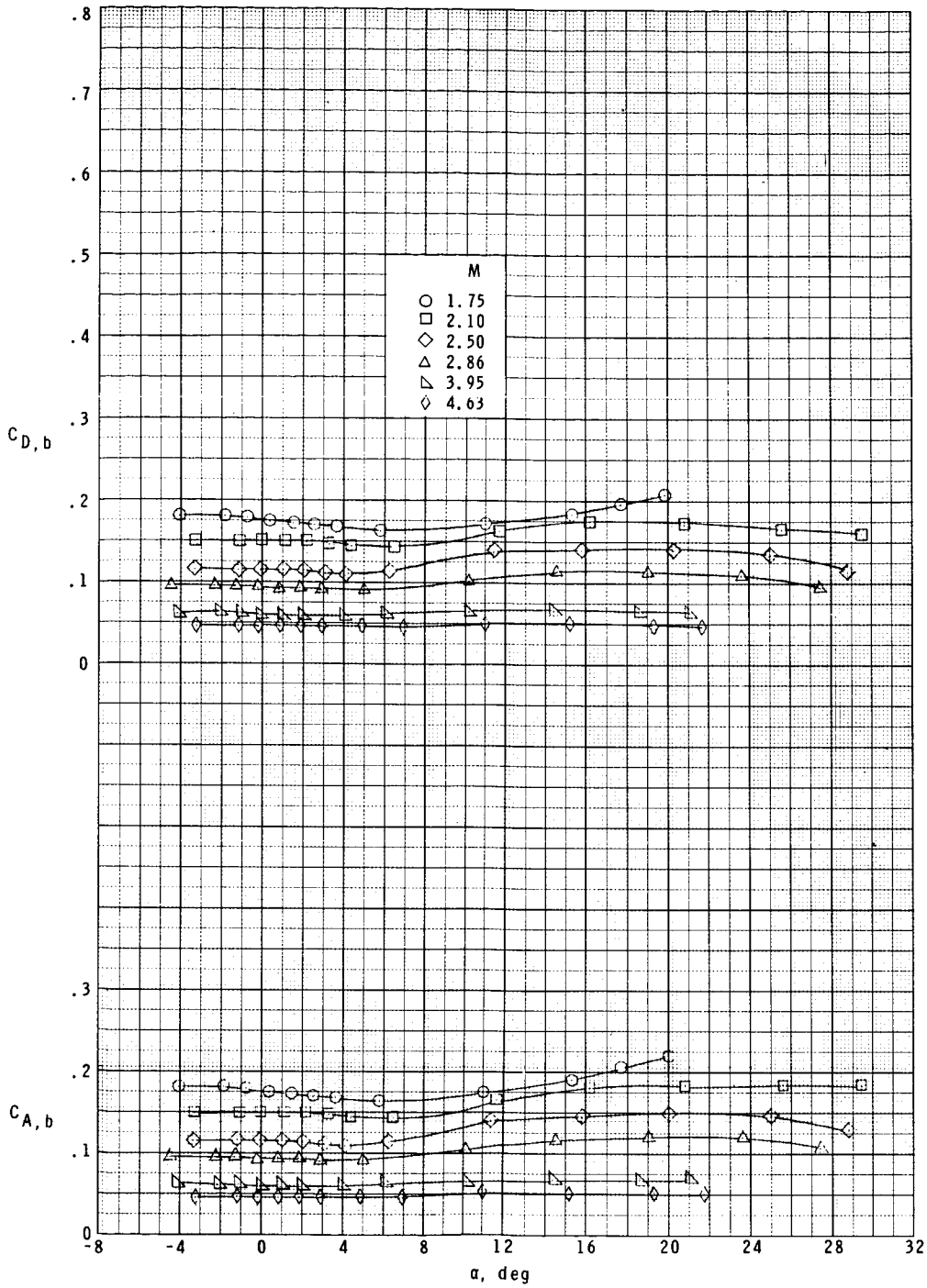

(b) M = 1.75 to M = 4.63.

Figure 3.- Concluded.

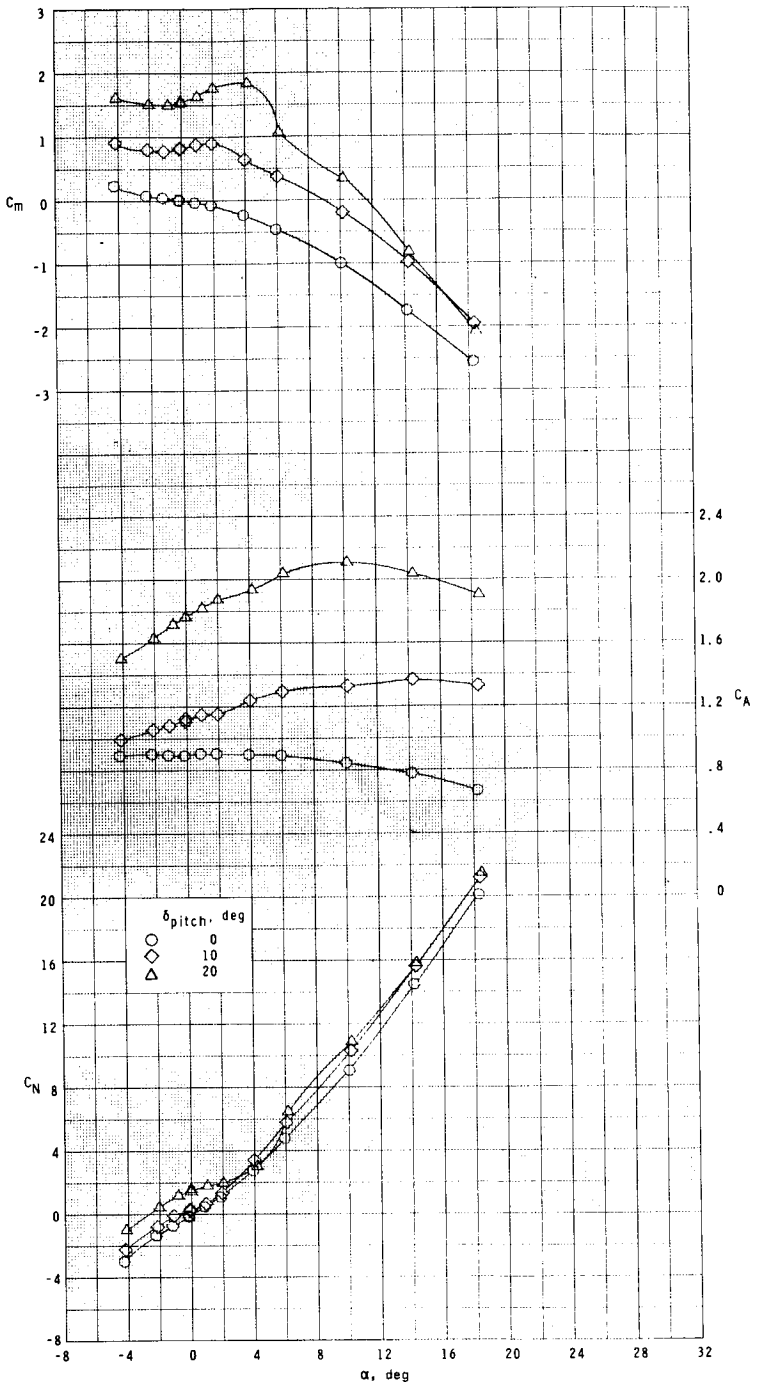

(a) M = 0.20.

Figure 4.- Pitch control effectiveness. $\phi = 0^o$.

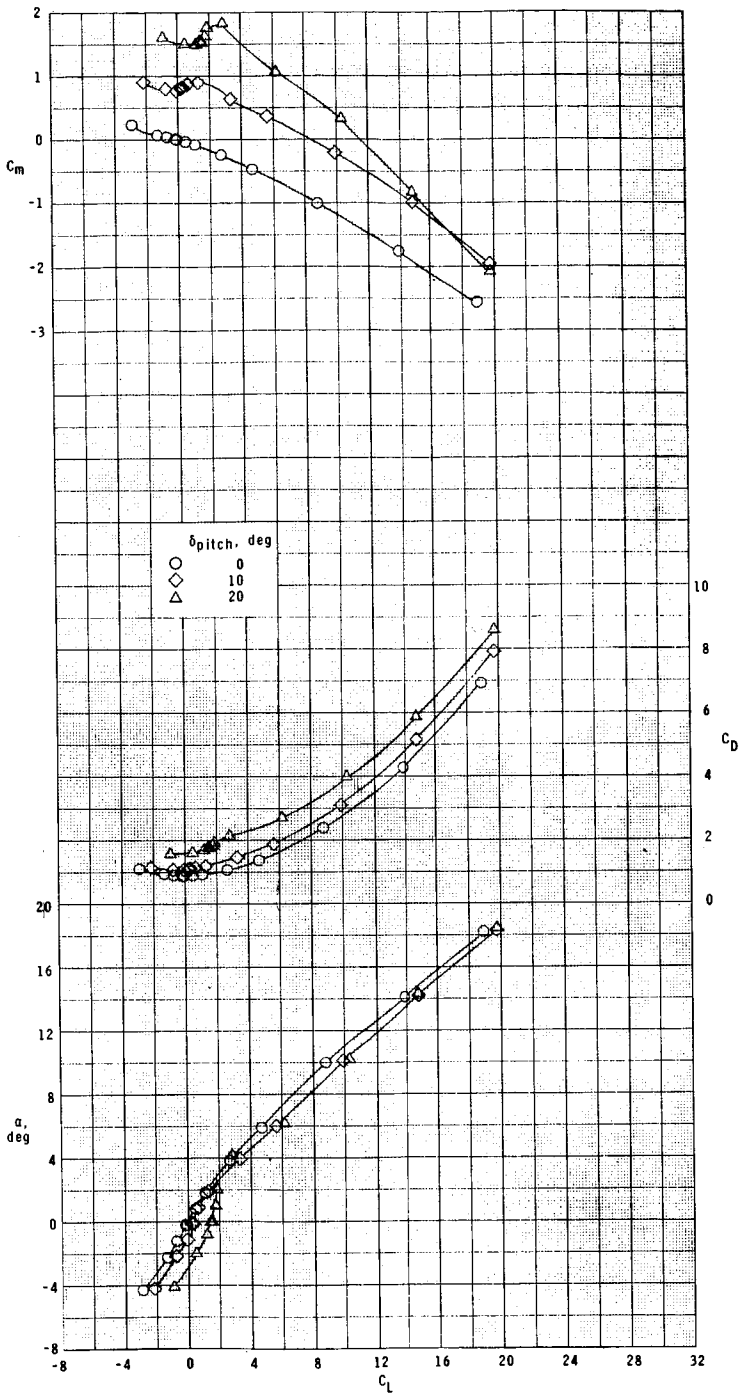

(a) Concluded.

Figure 4.- Continued.

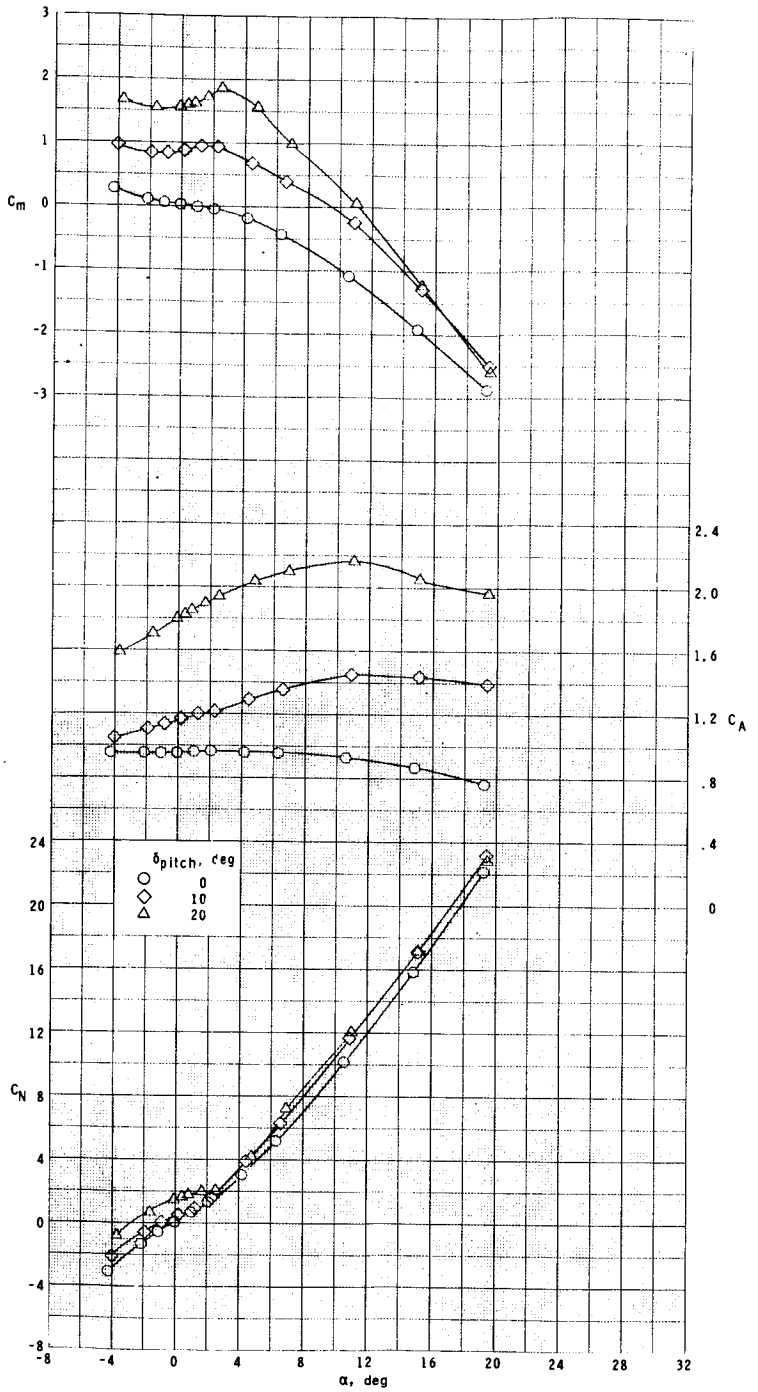

(b) M = 0.60.

Figure 4.- Continued.

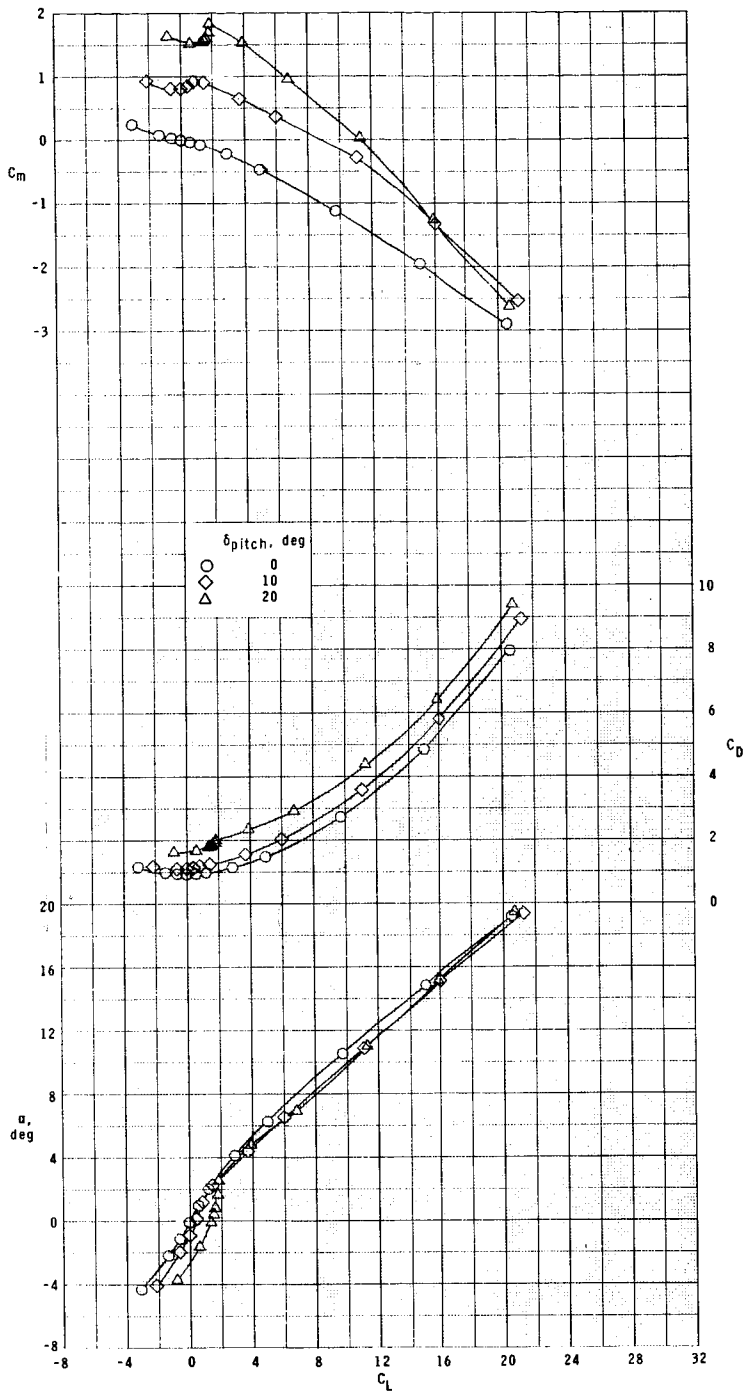

(b) Concluded.

Figure 4.- Continued.

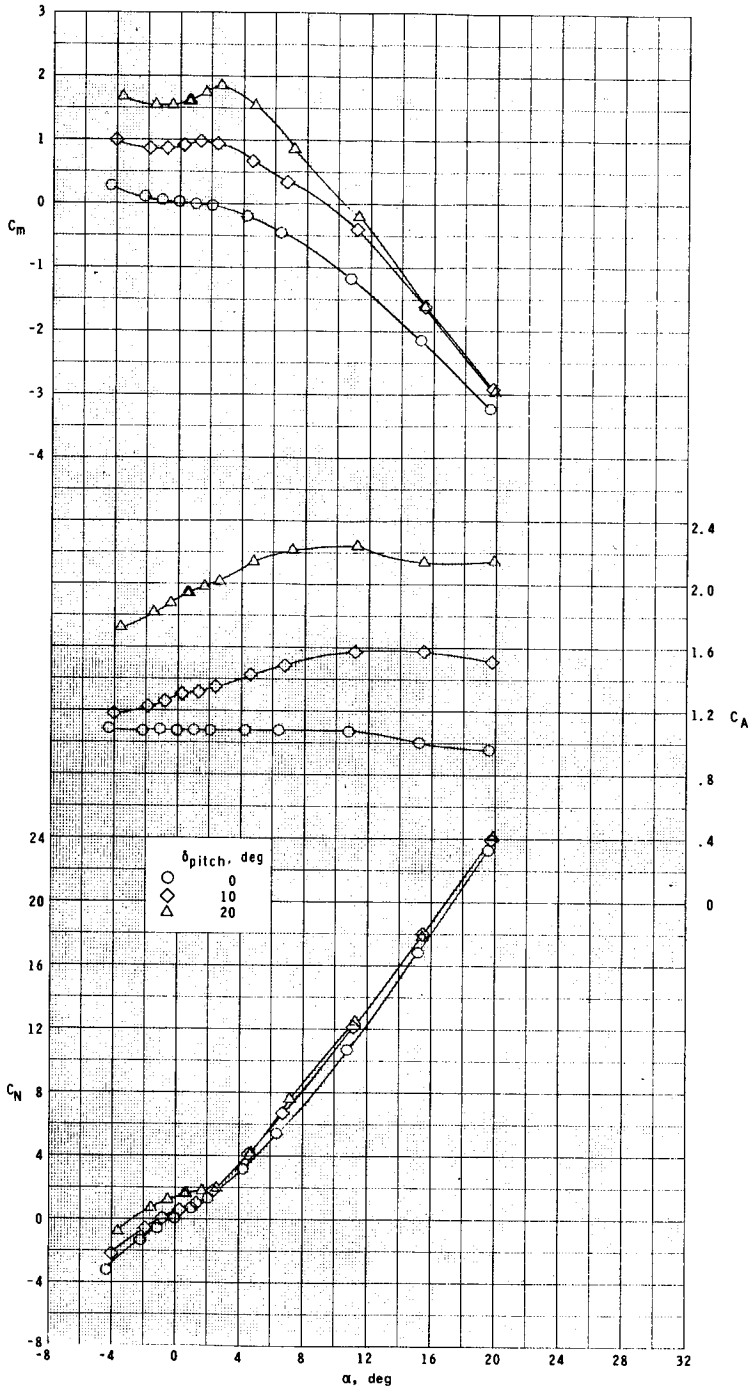

(c) M = 0.80.

Figure 4.- Continued.

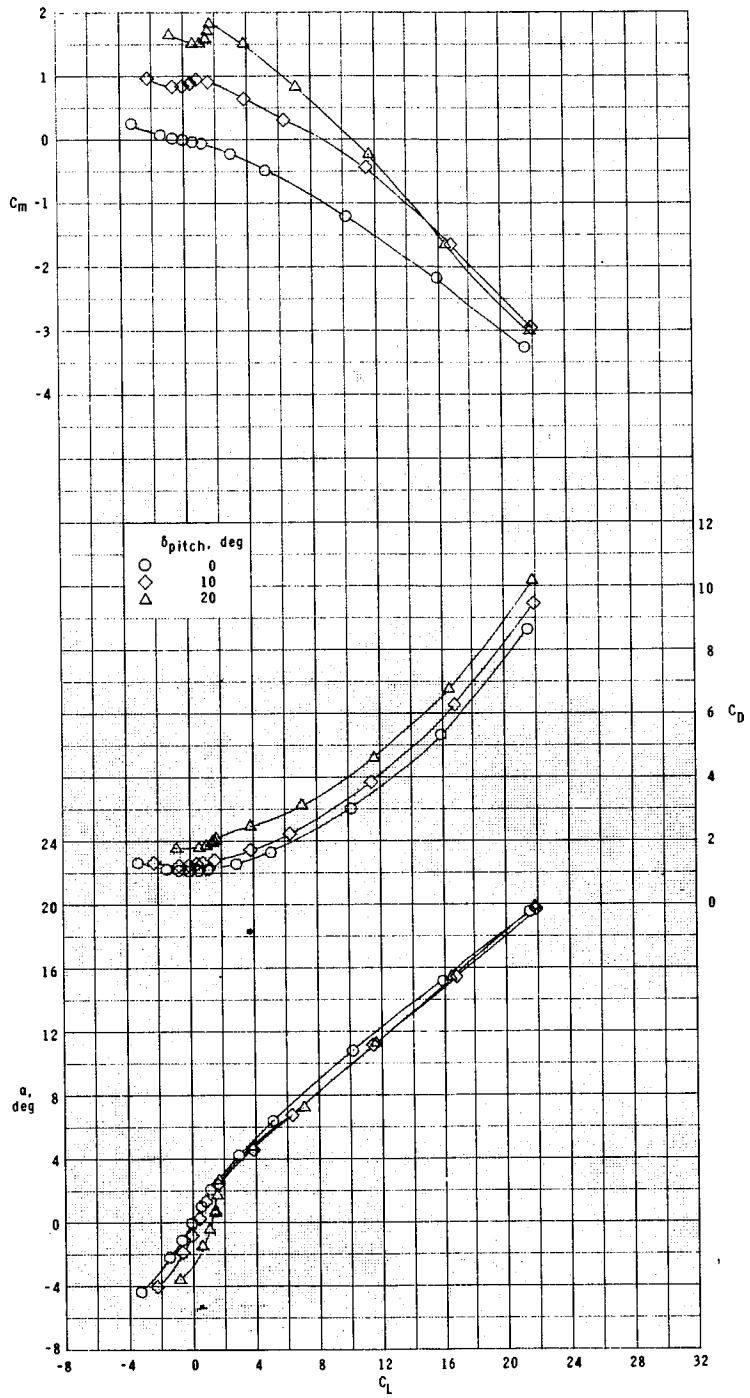

(c) Concluded.

Figure 4.- Continued.

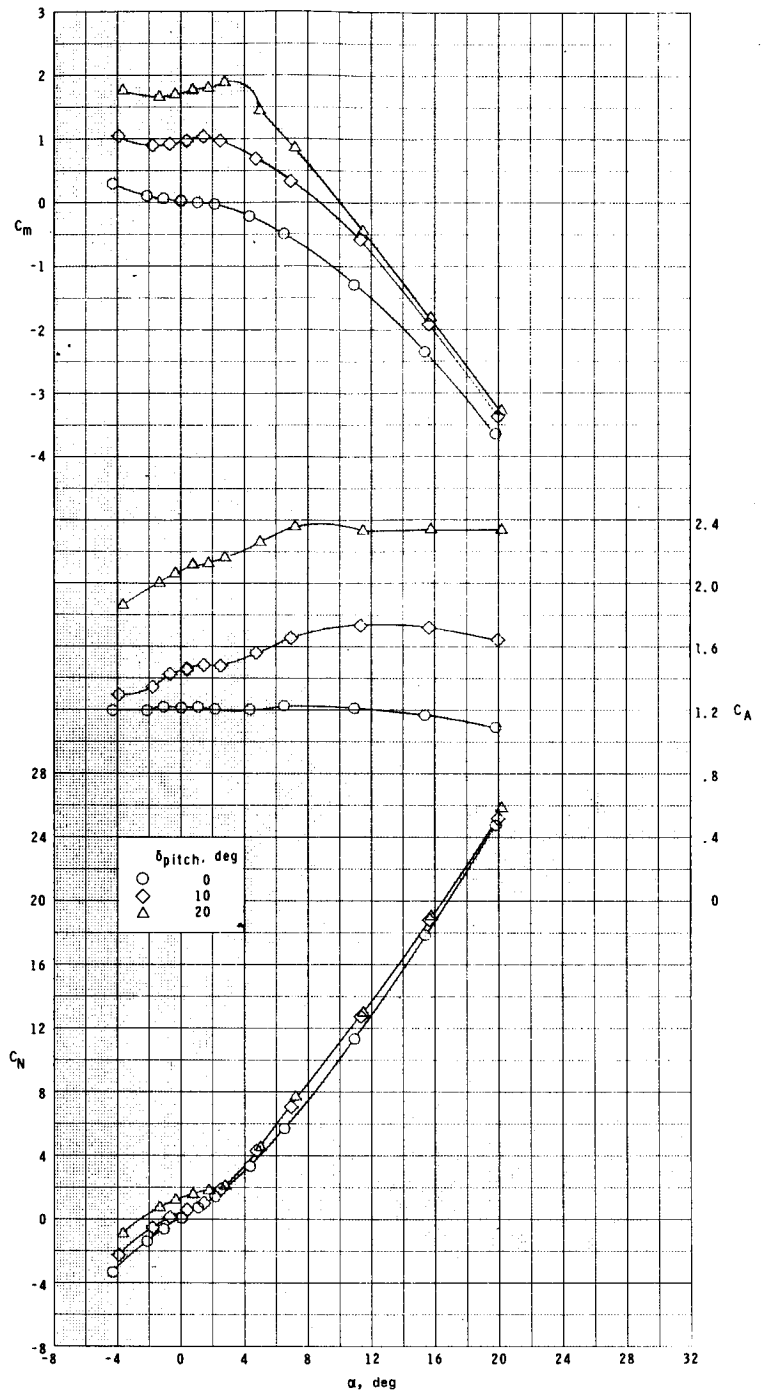

(d) M = 0.90.

Figure 4.- Continued.

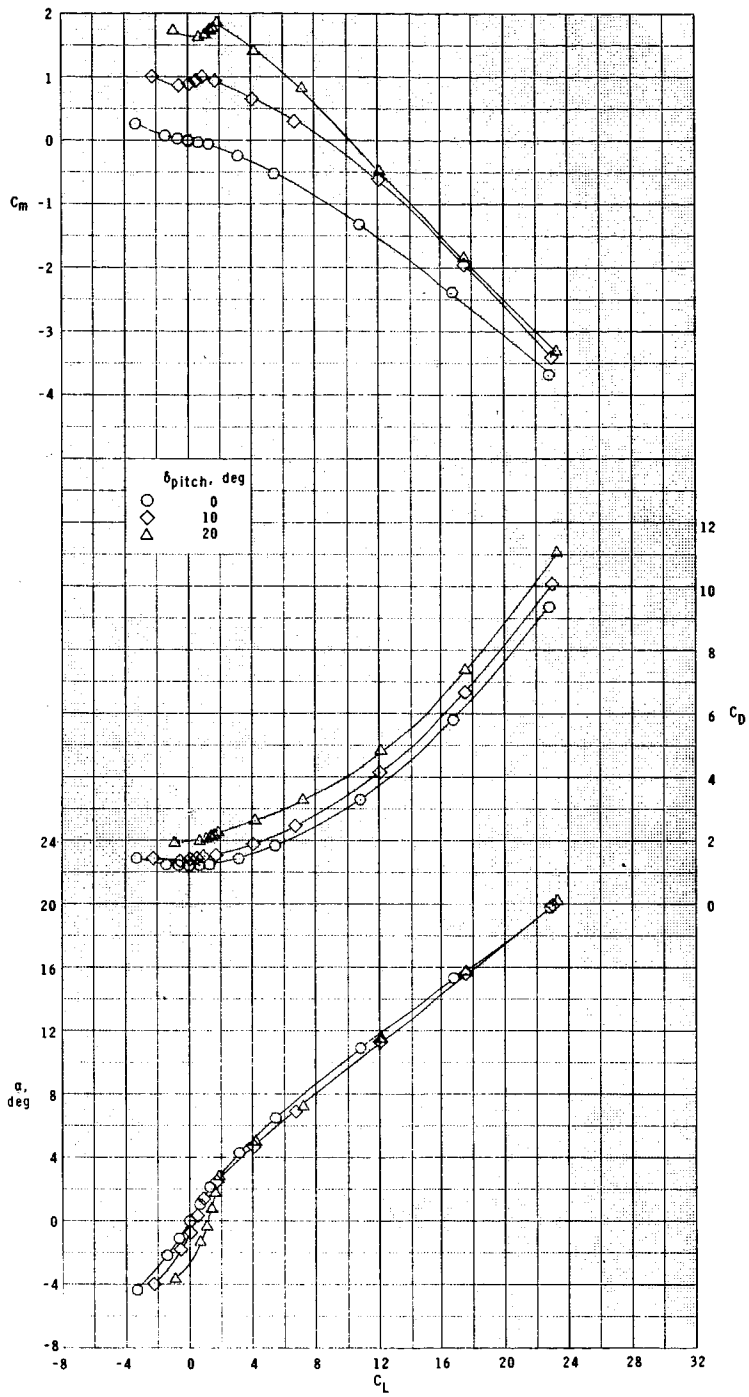

(d) Concluded.

Figure 4.- Continued.

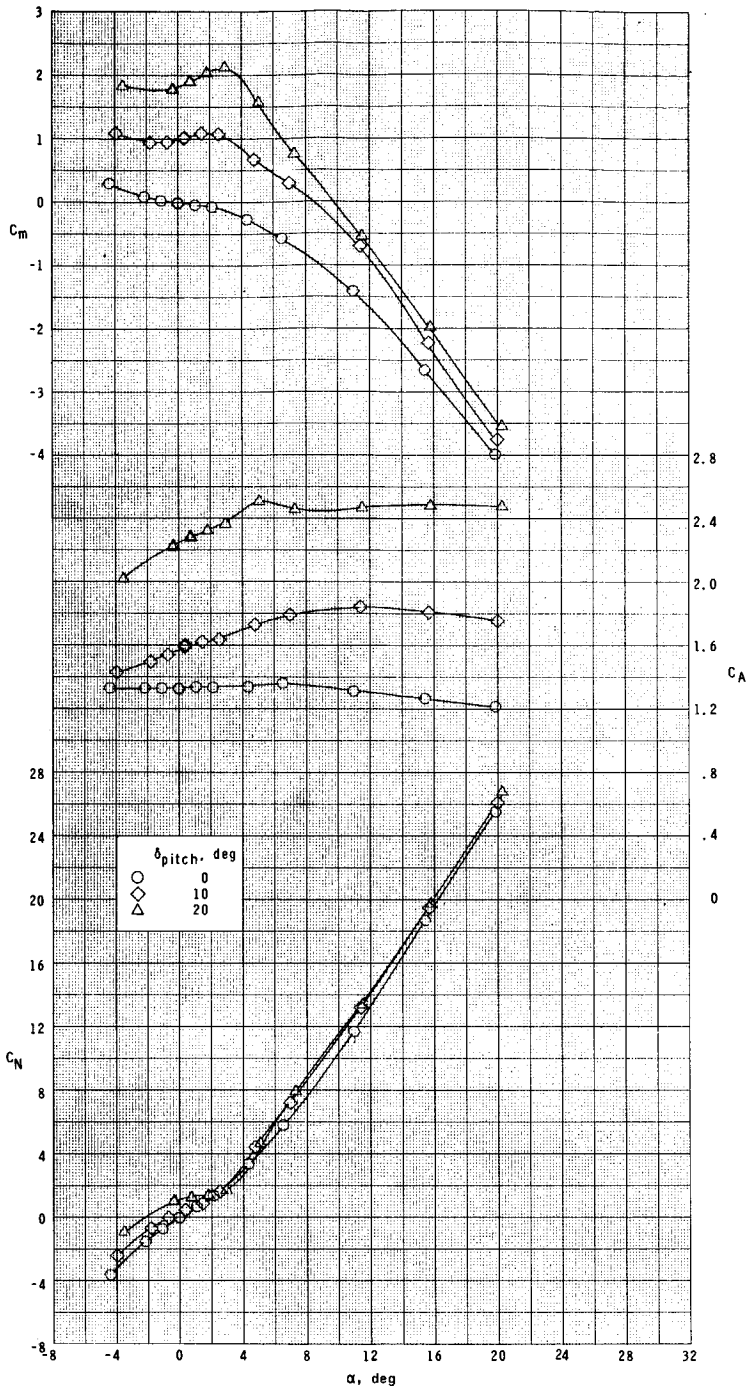

(e) M = 0.95.

Figure 4.- Continued.

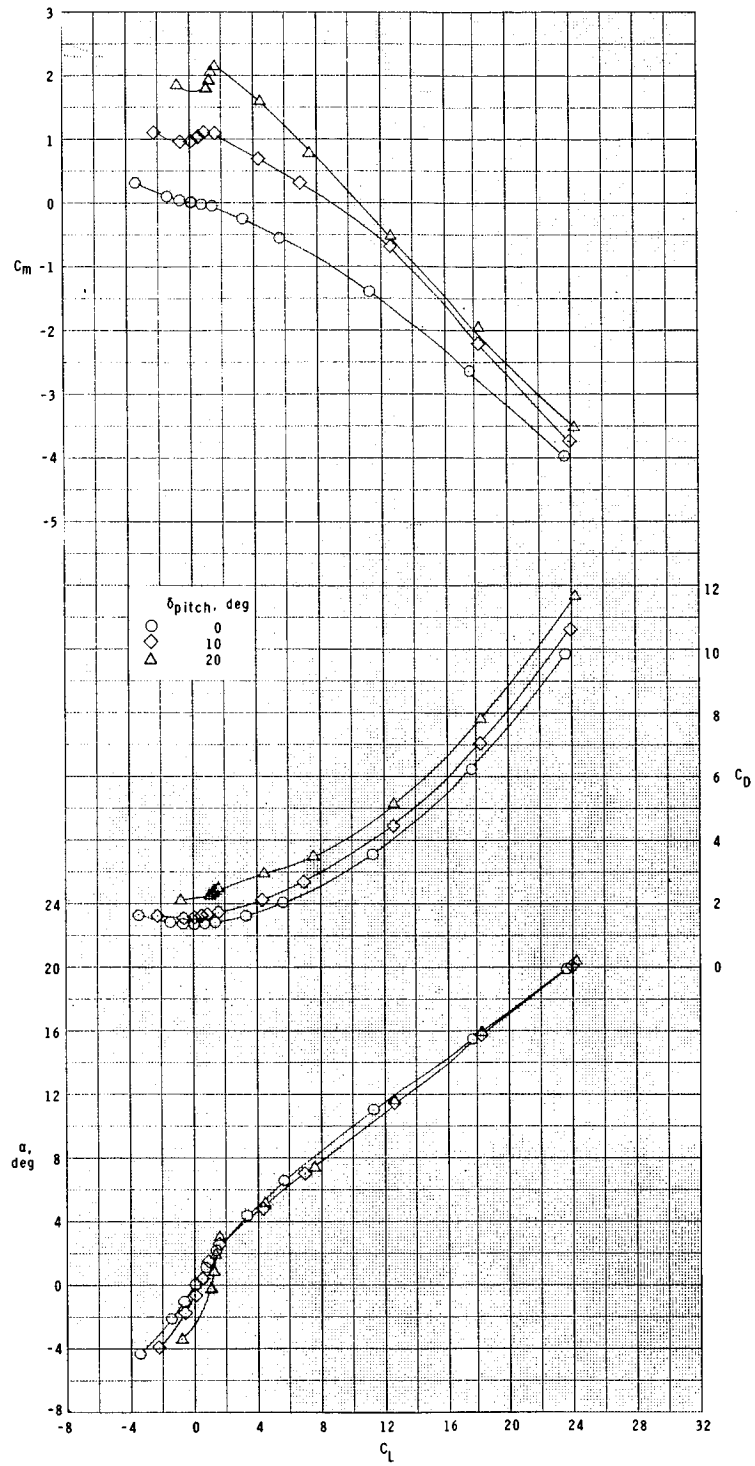

(e) Concluded.

Figure 4.- Continued.

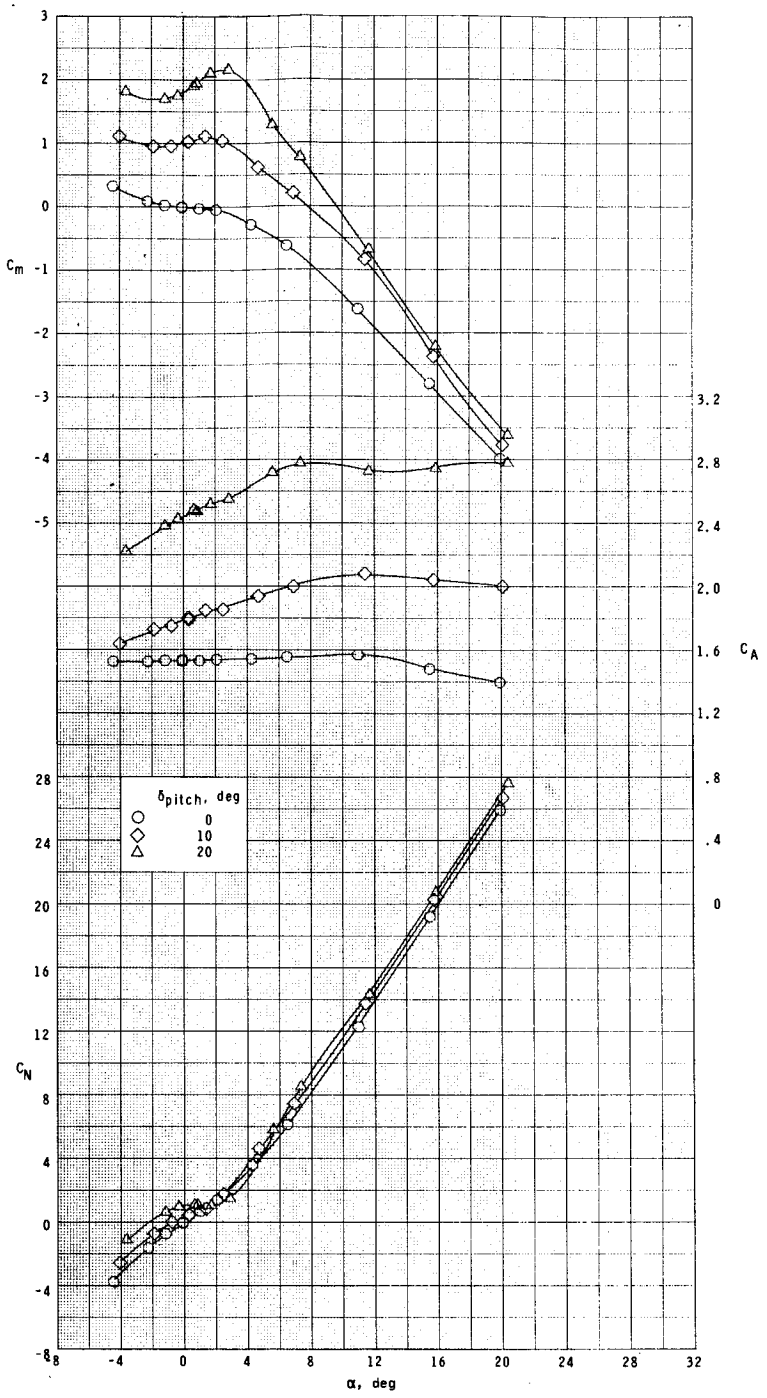

(f) M = 1.00.

Figure 4.- Continued.

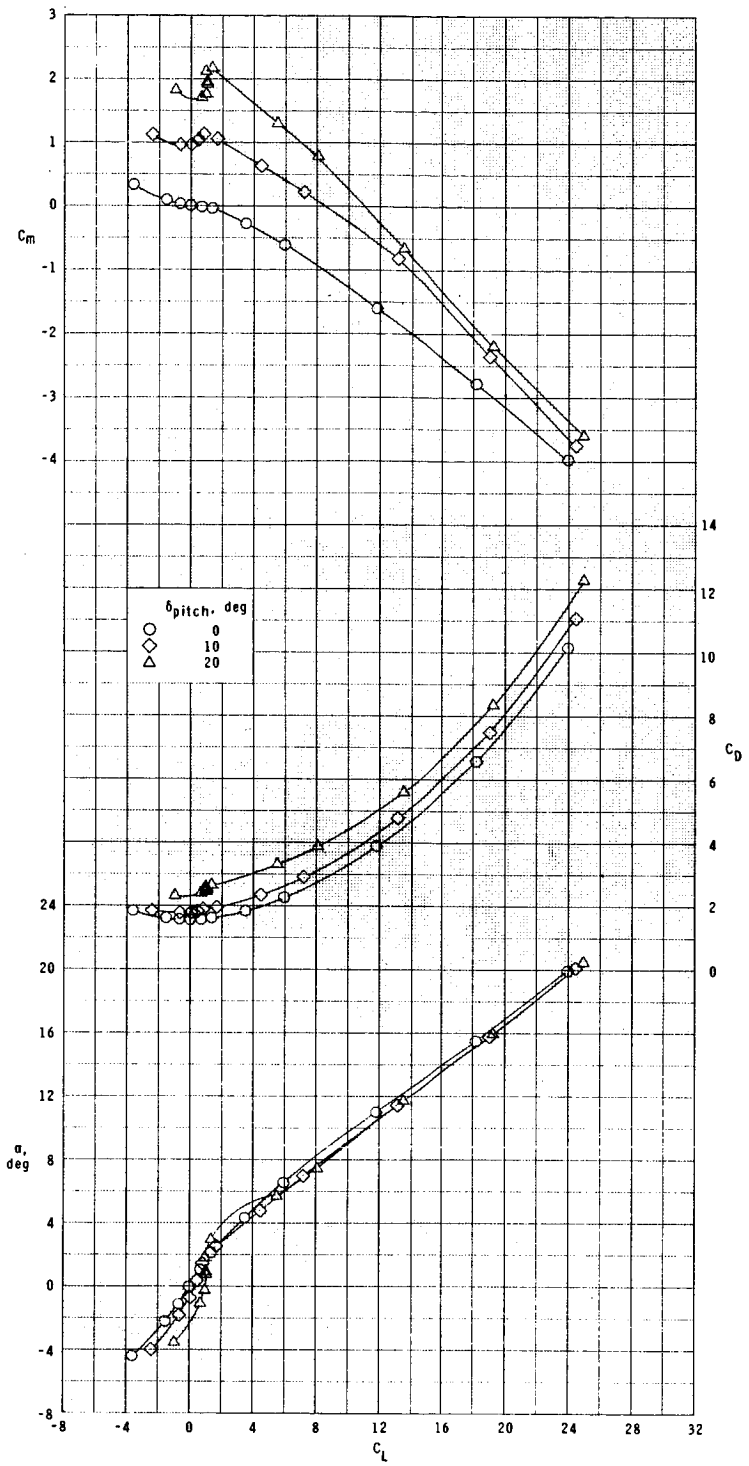

(f) Concluded.

Figure 4.- Continued.

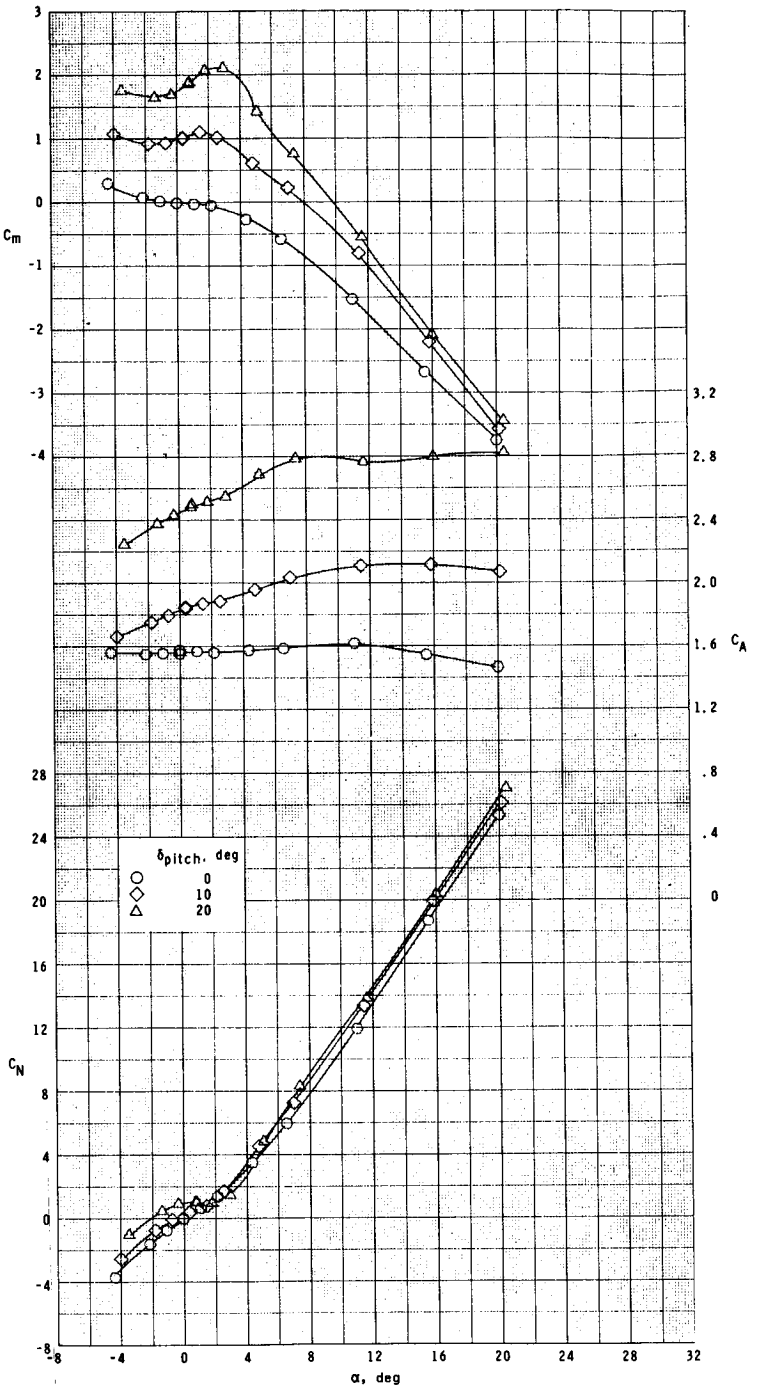

(g) M = 1.03.

Figure 4.- Continued.

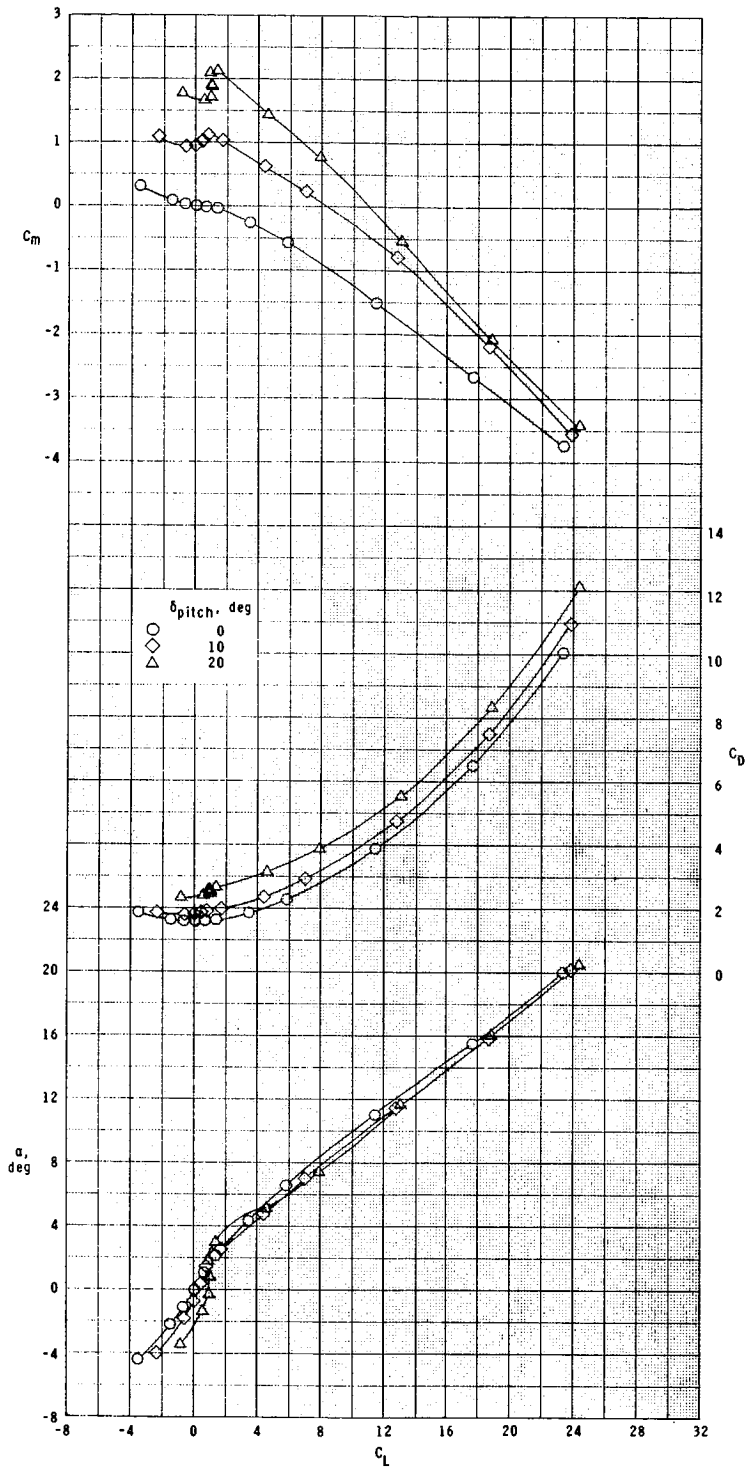

(g) Concluded.

Figure 4.- Continued.

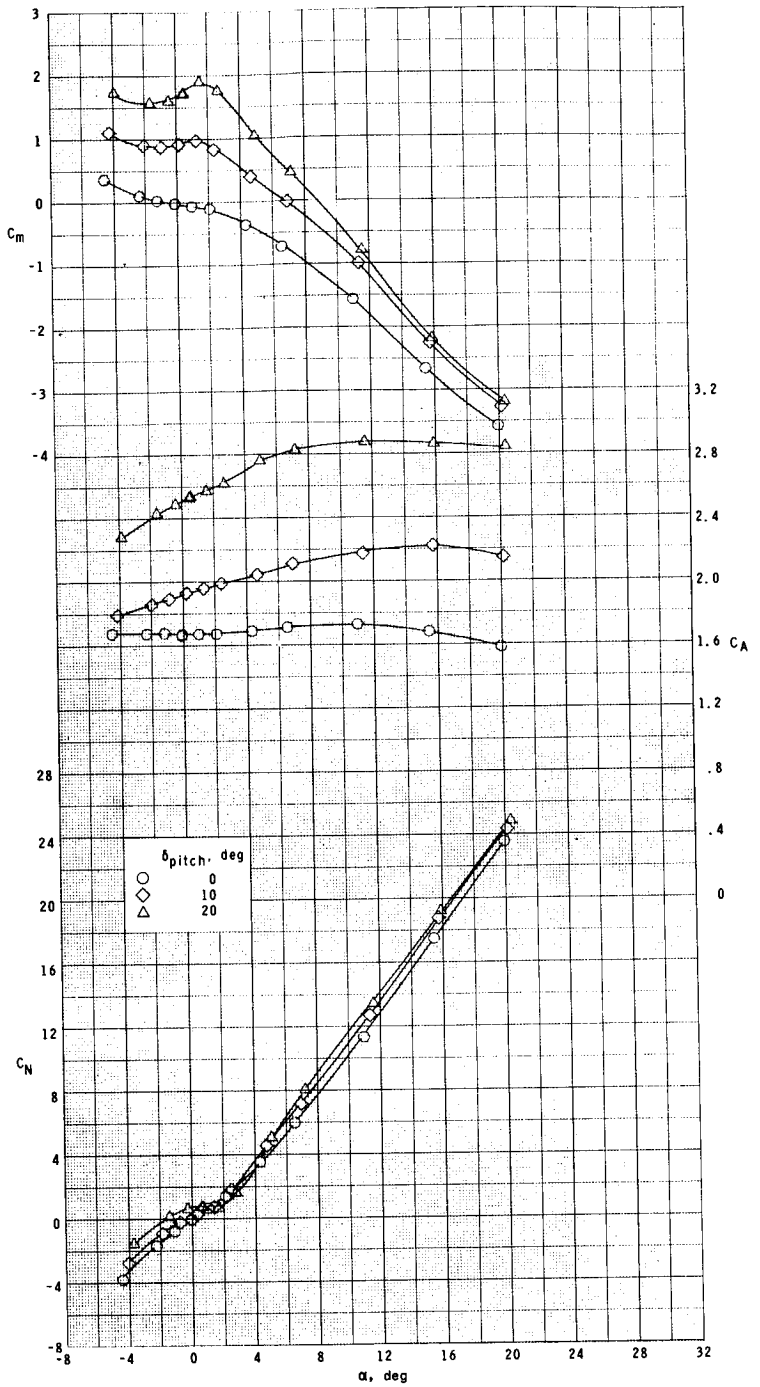

(h) M = 1.20.

Figure 4.- Continued.

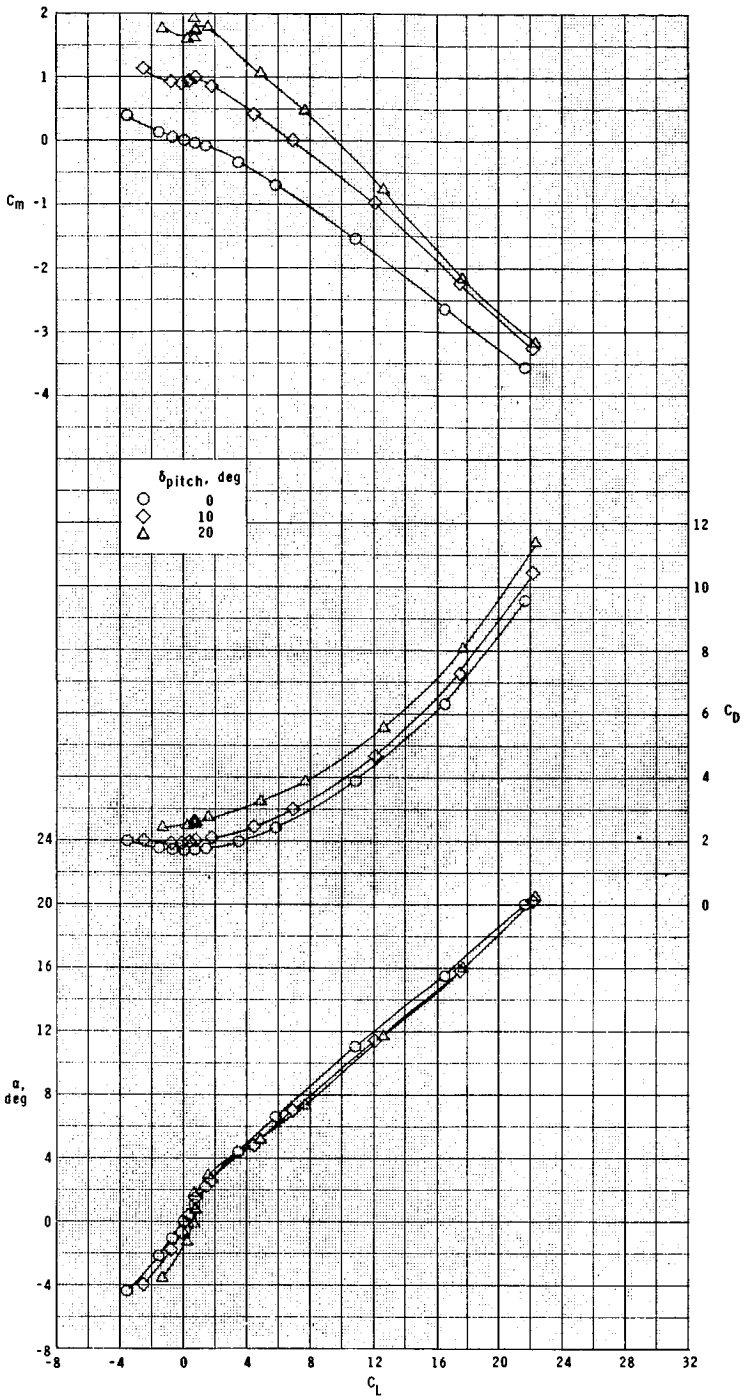

(h) Concluded.

Figure 4.- Continued.

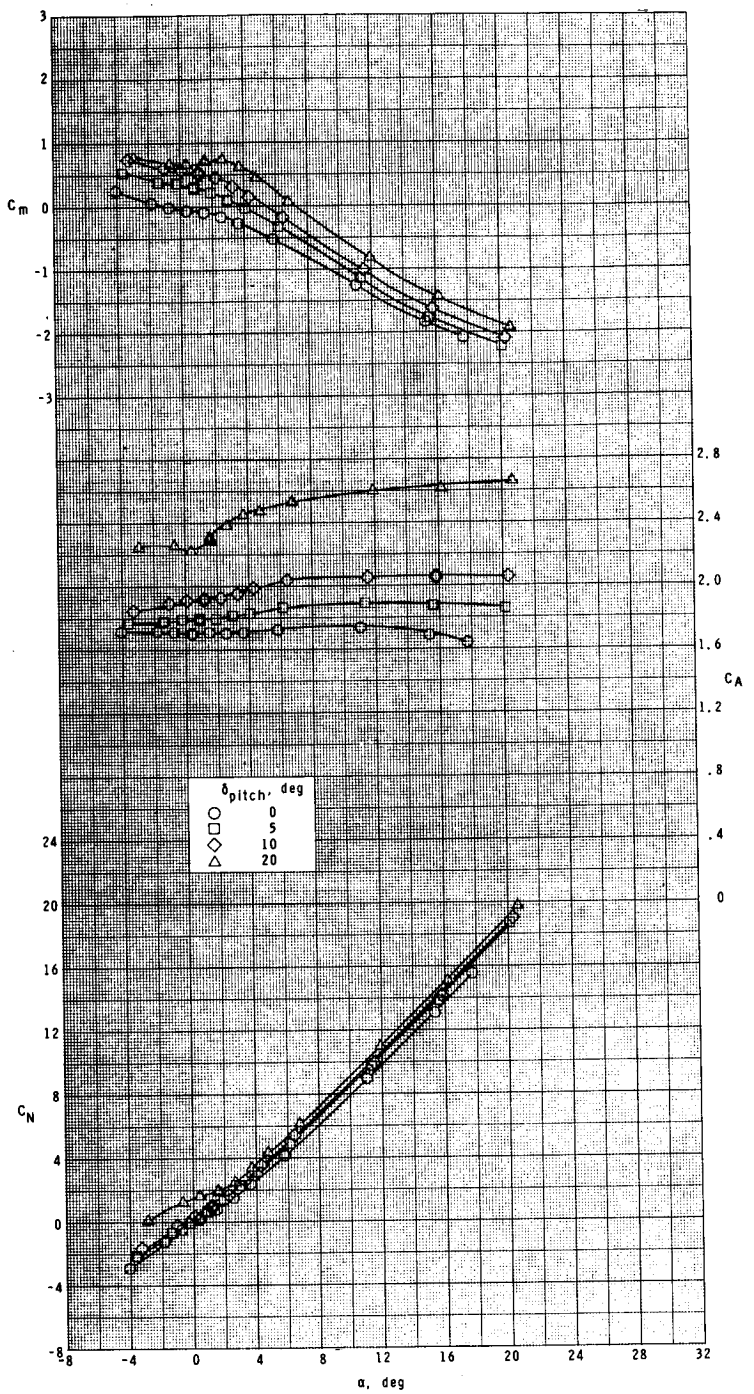

(i) M = 1.75.

Figure 4.- Continued.

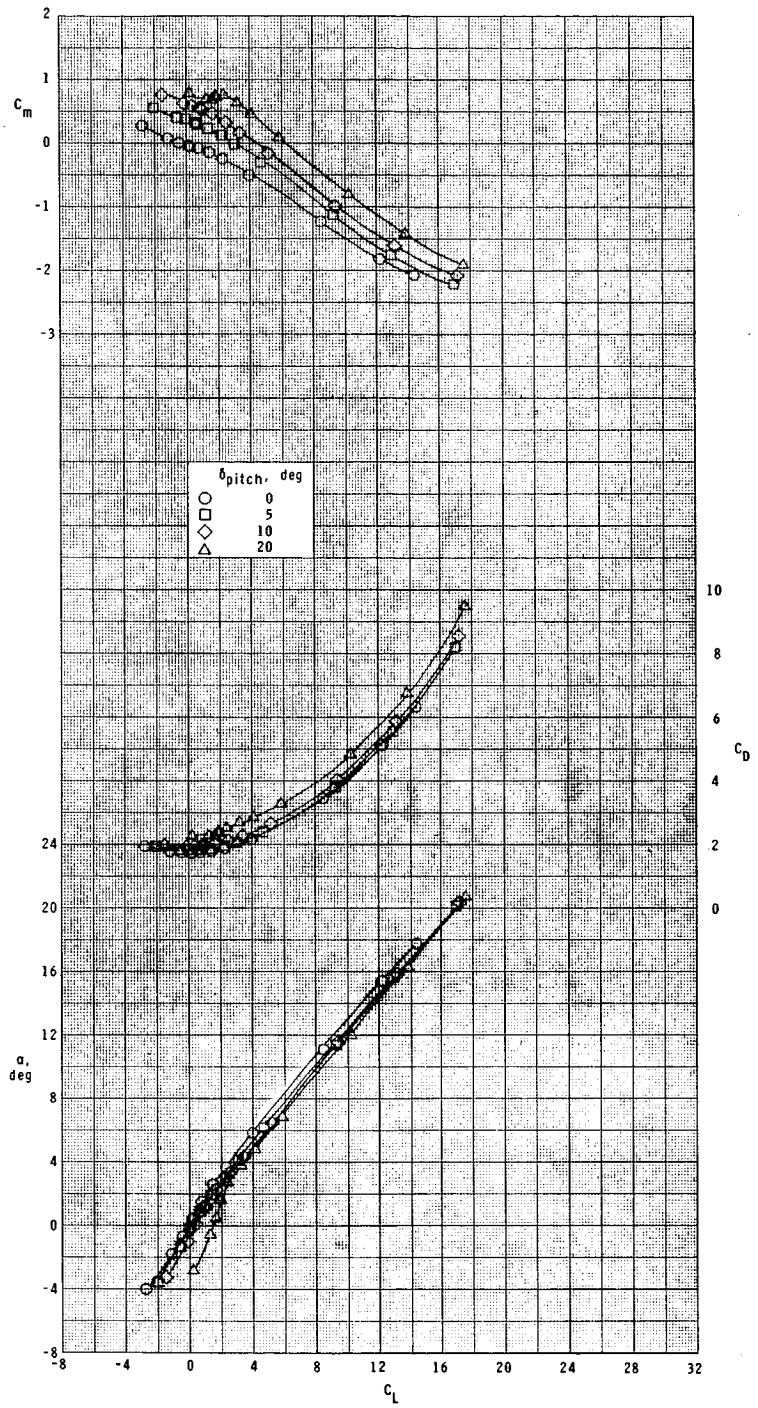

(i) Concluded.

Figure 4.- Continued.

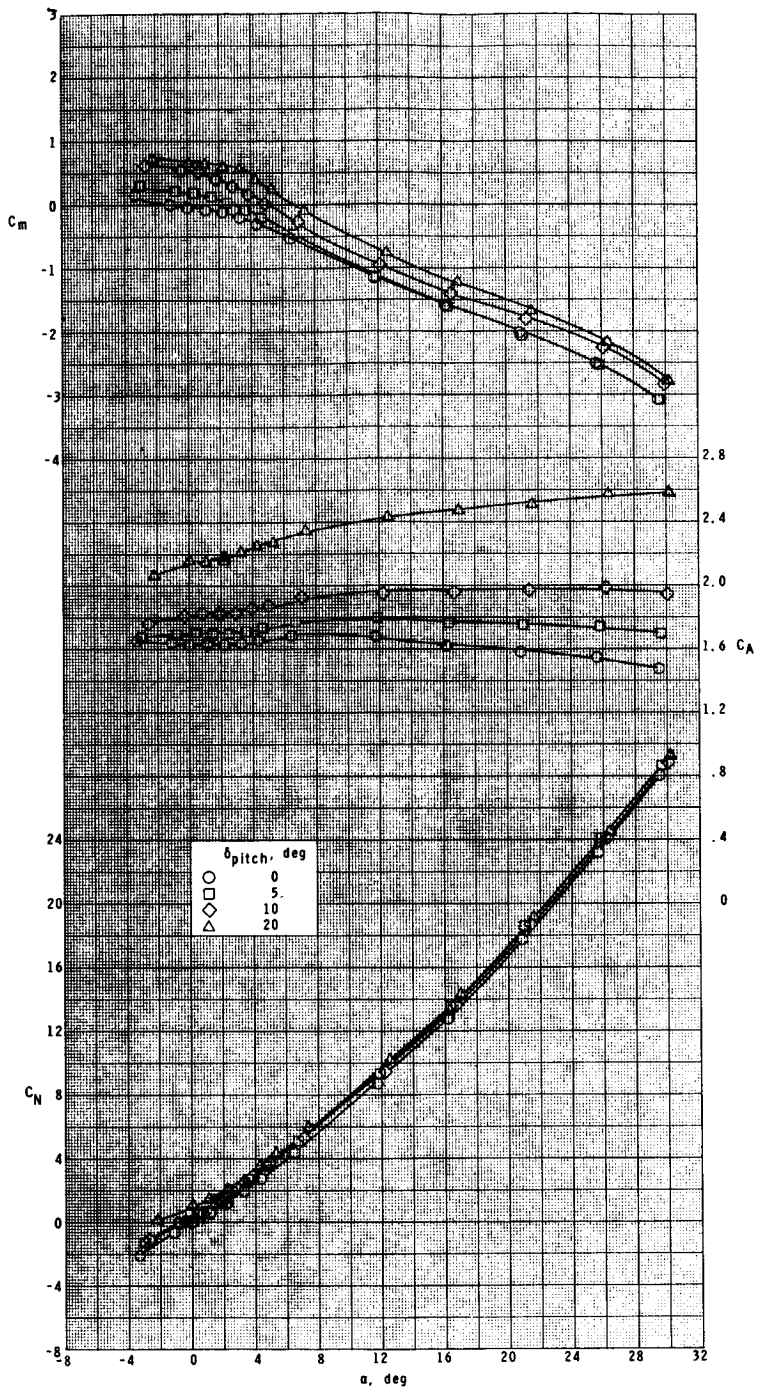

(j) M = 2.10.

Figure 4.- Continued.

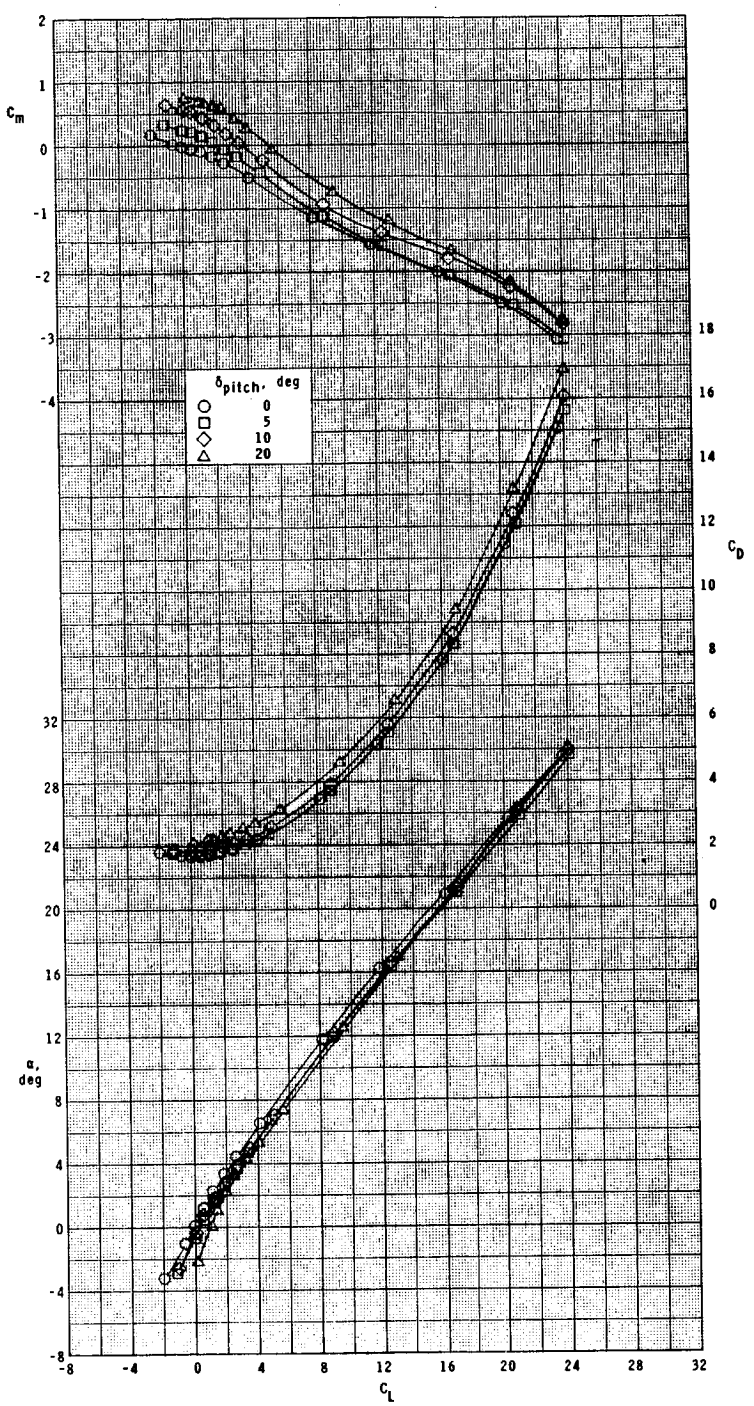

(j) Concluded.

Figure 4.- Continued.

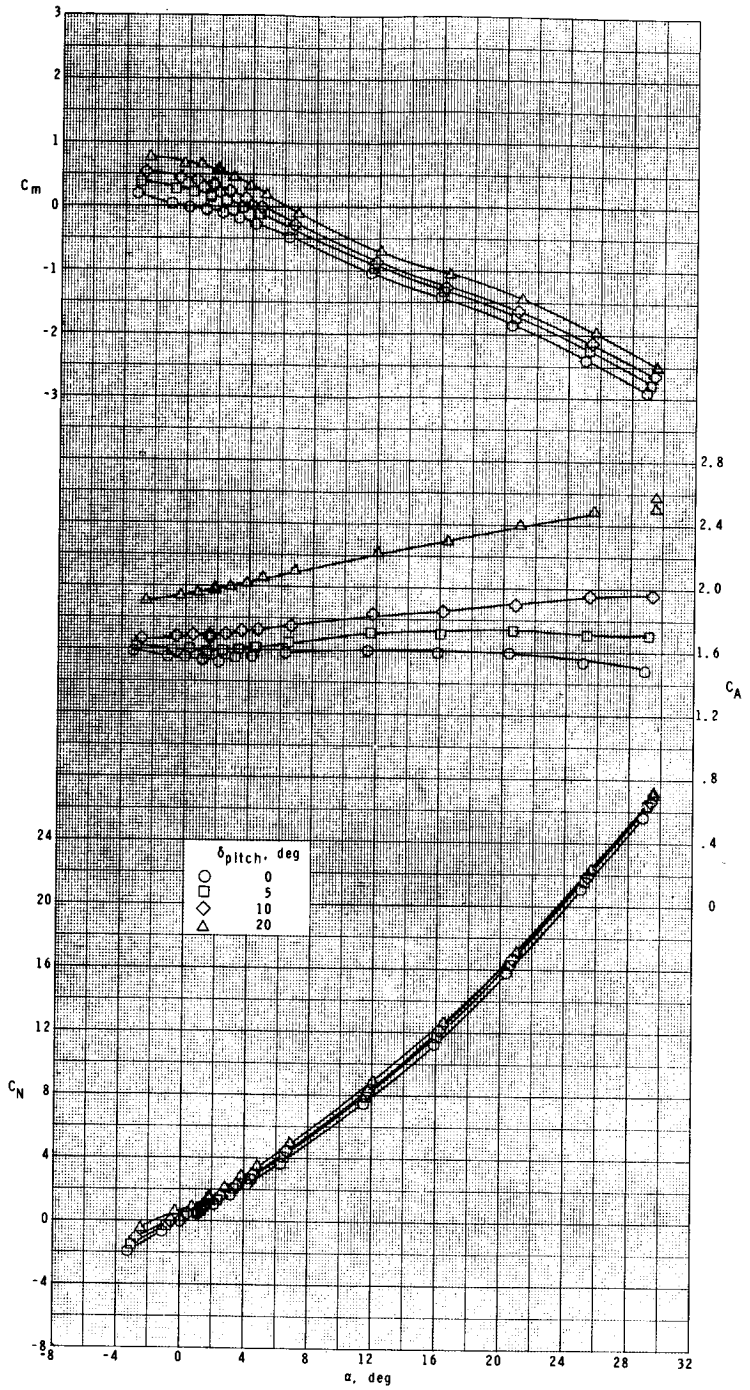

(k) M = 2.50.

Figure 4.- Continued.

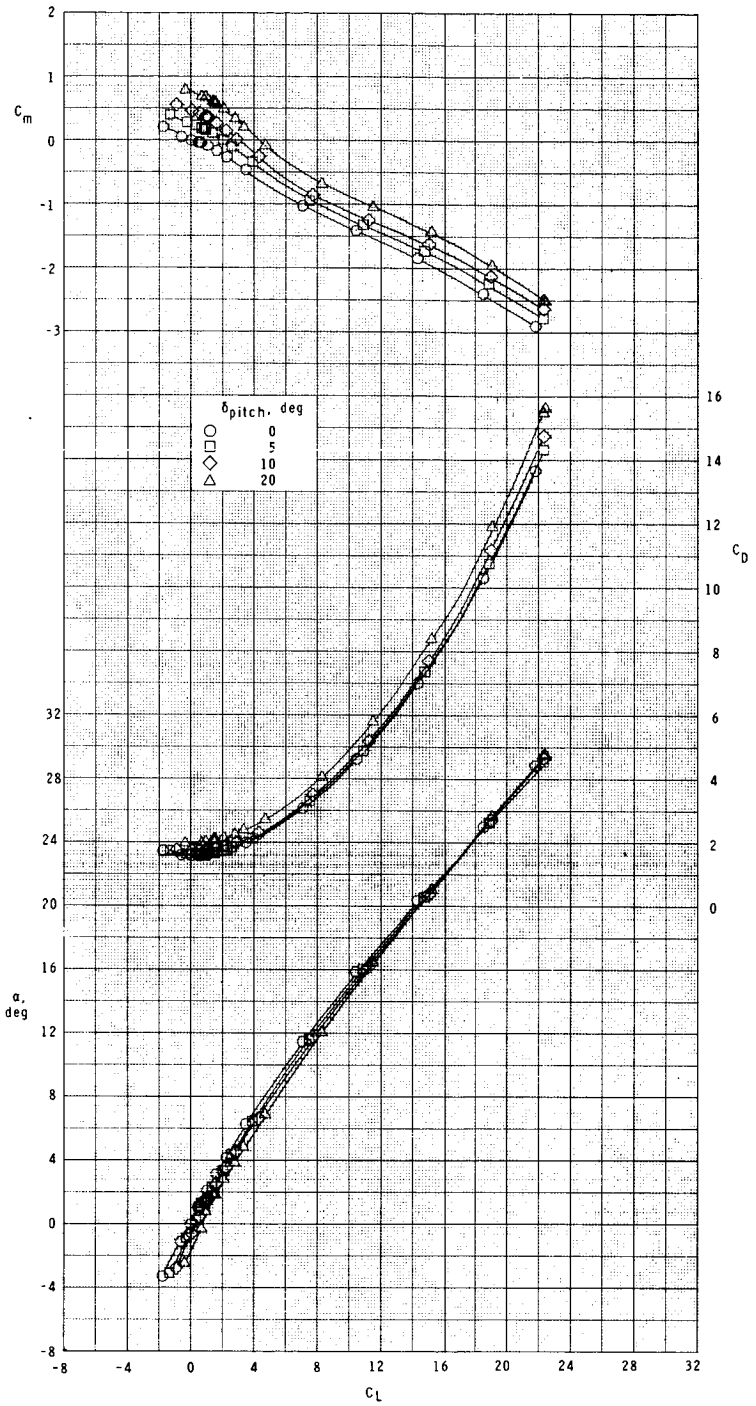

(k) Concluded.

Figure 4.- Continued.

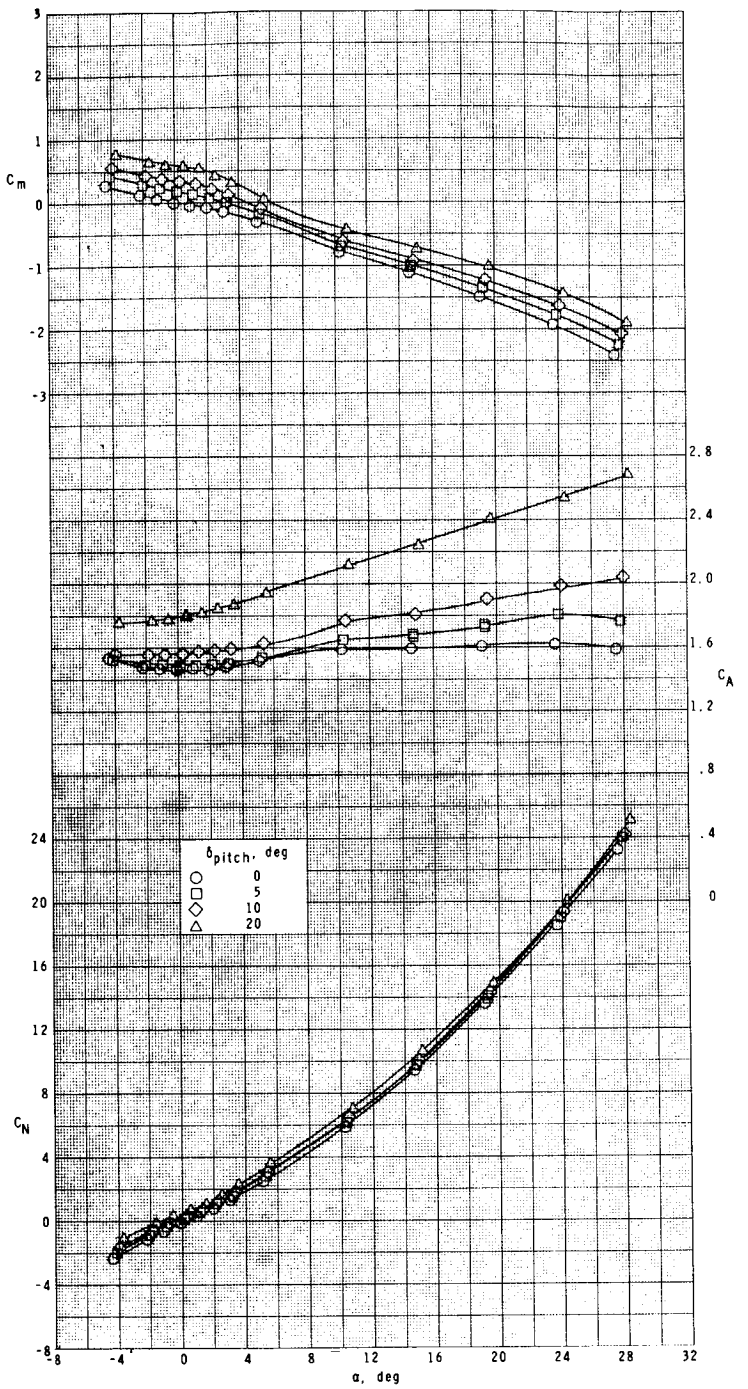

(l) M = 2.86.

Figure 4.- Continued.

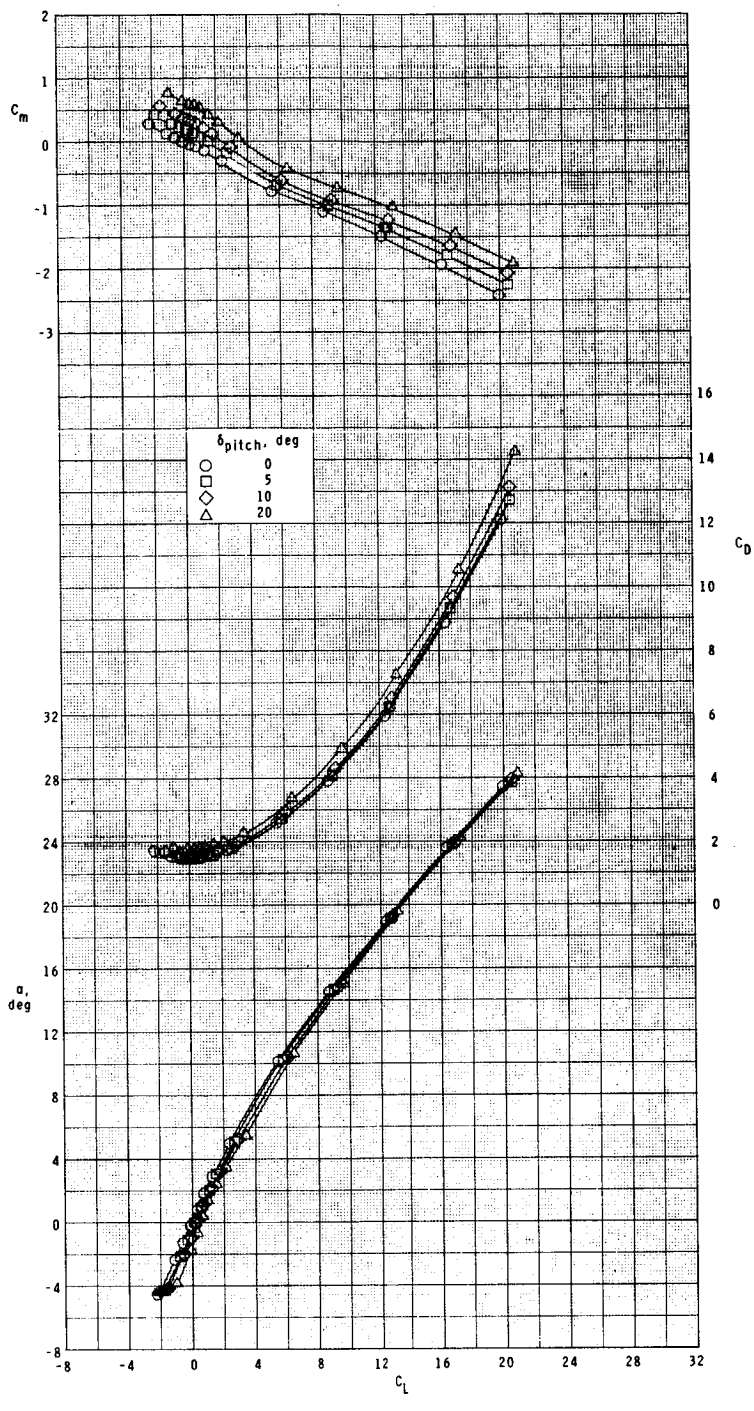

(l) Concluded.

Figure 4.- Continued.

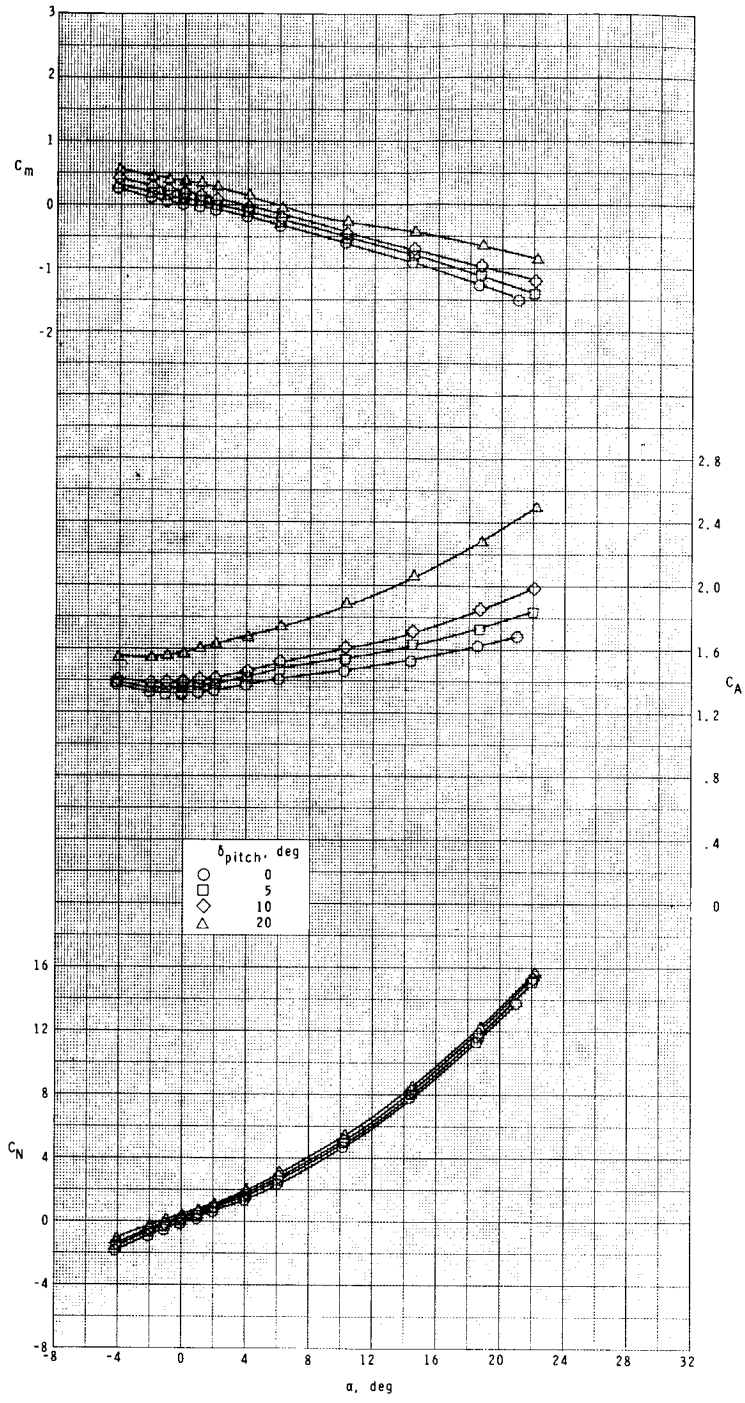

(m) M = 3.95.

Figure 4.- Continued.

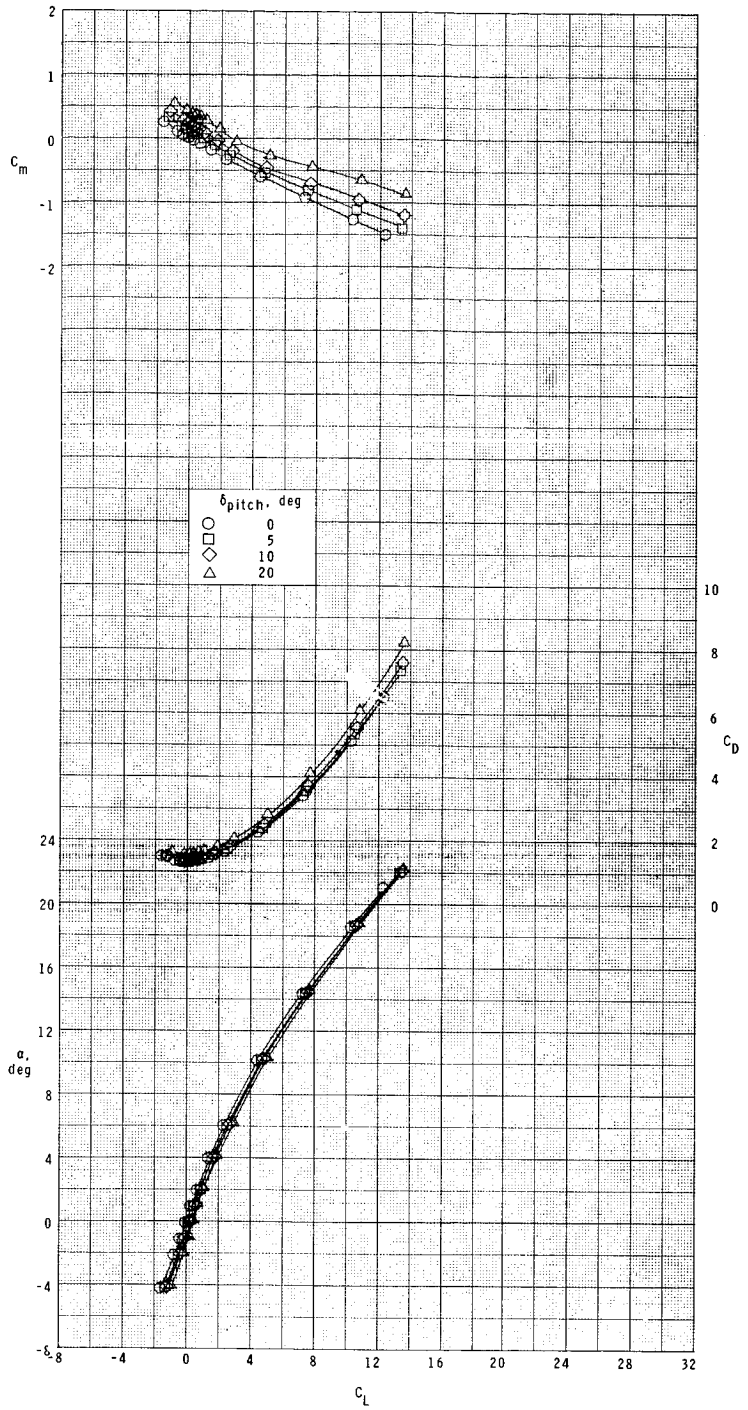

(m) Concluded.

Figure 4.- Continued.

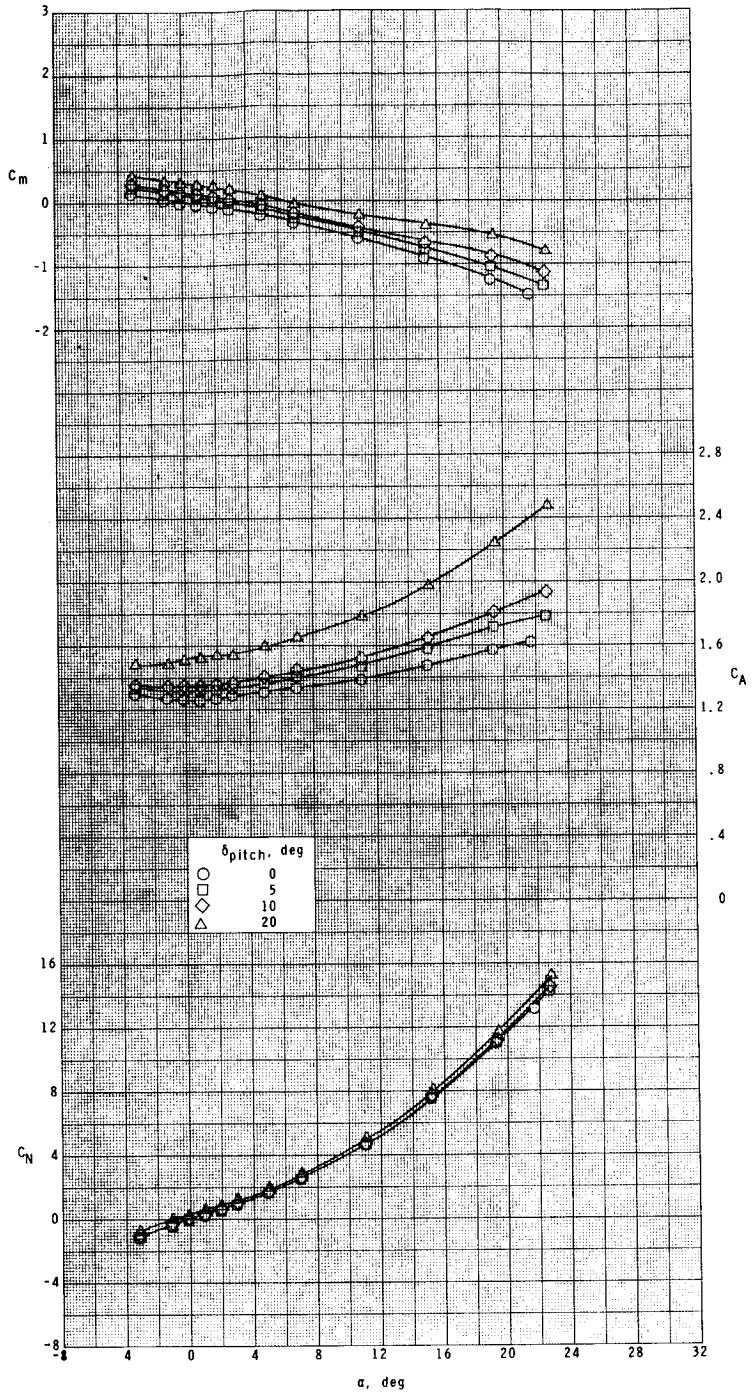

(n) M = 4.63.

Figure 4.- Continued.

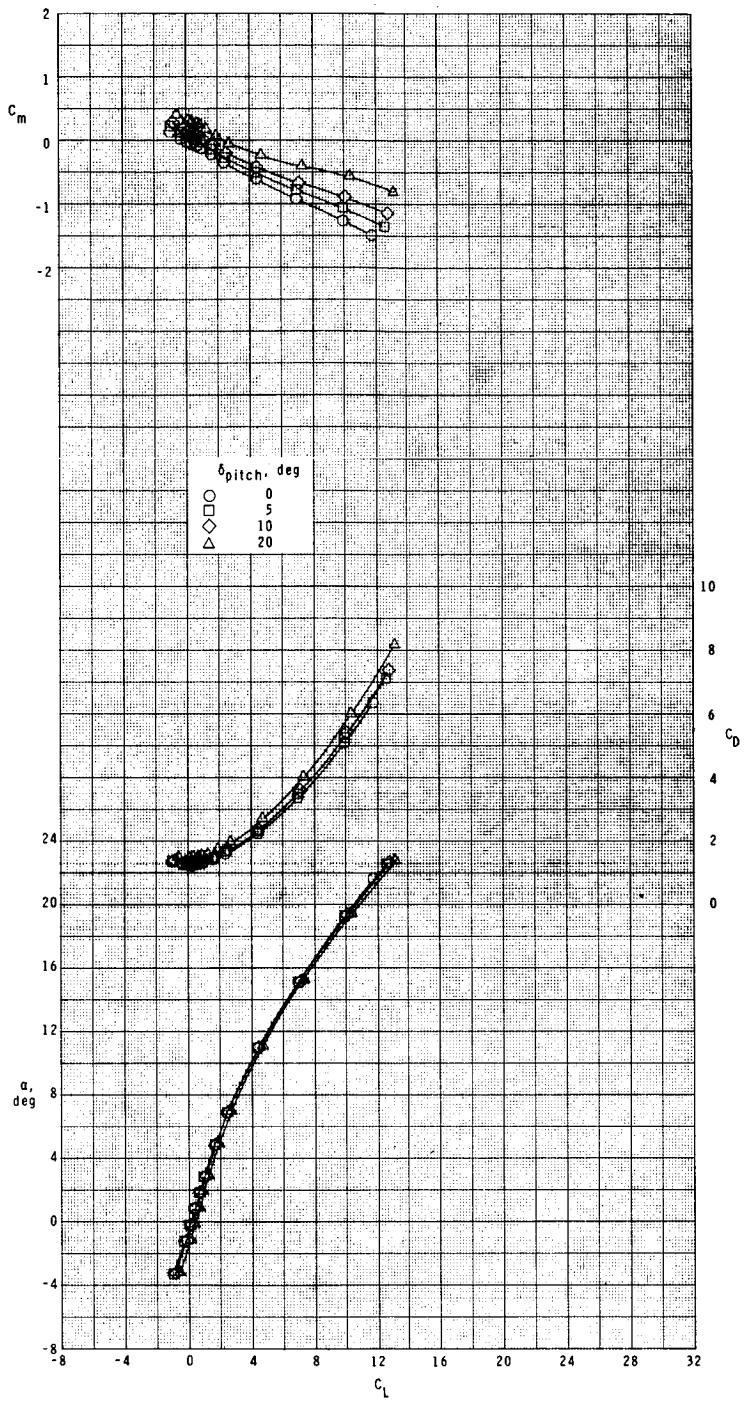

(n) Concluded.

Figure 4.- Concluded.

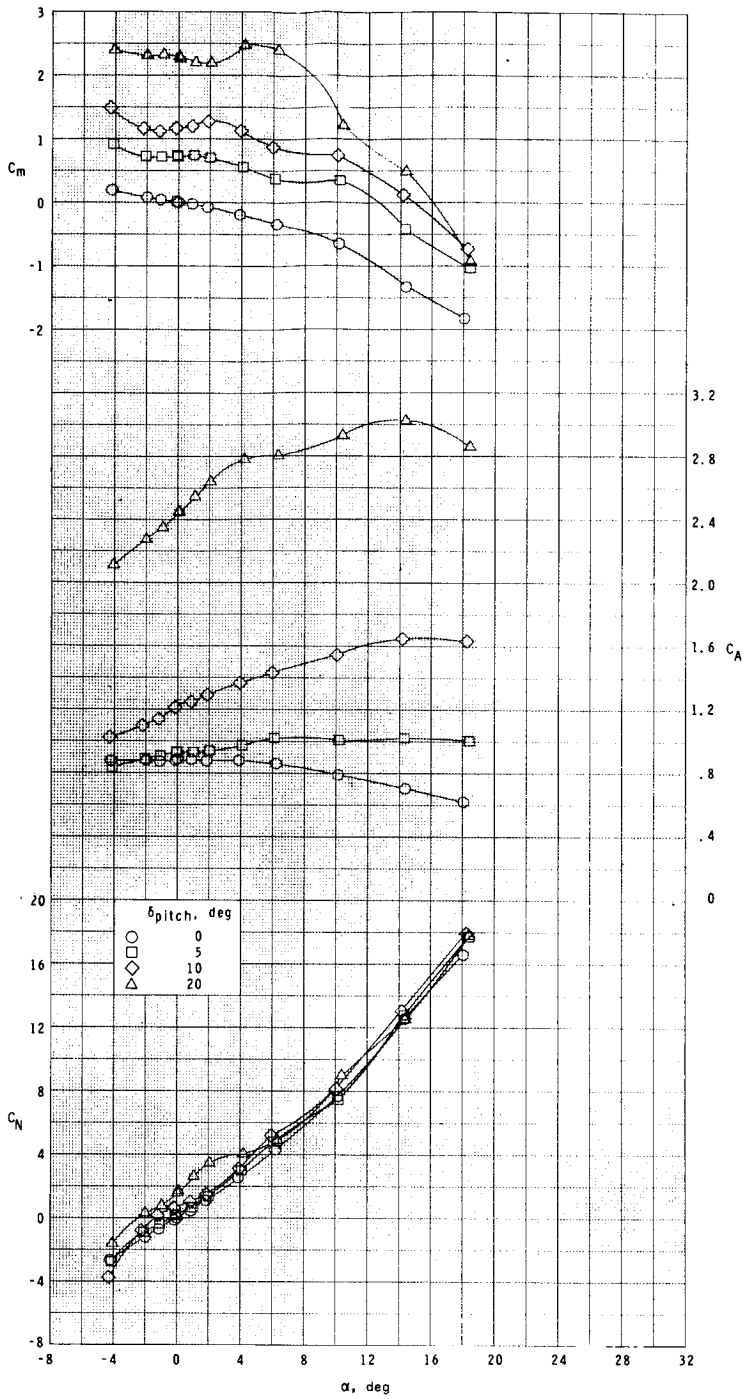

(a) M = 0.20.

Figure 5.- Pitch control effectiveness. $\phi = -45^{o}$.

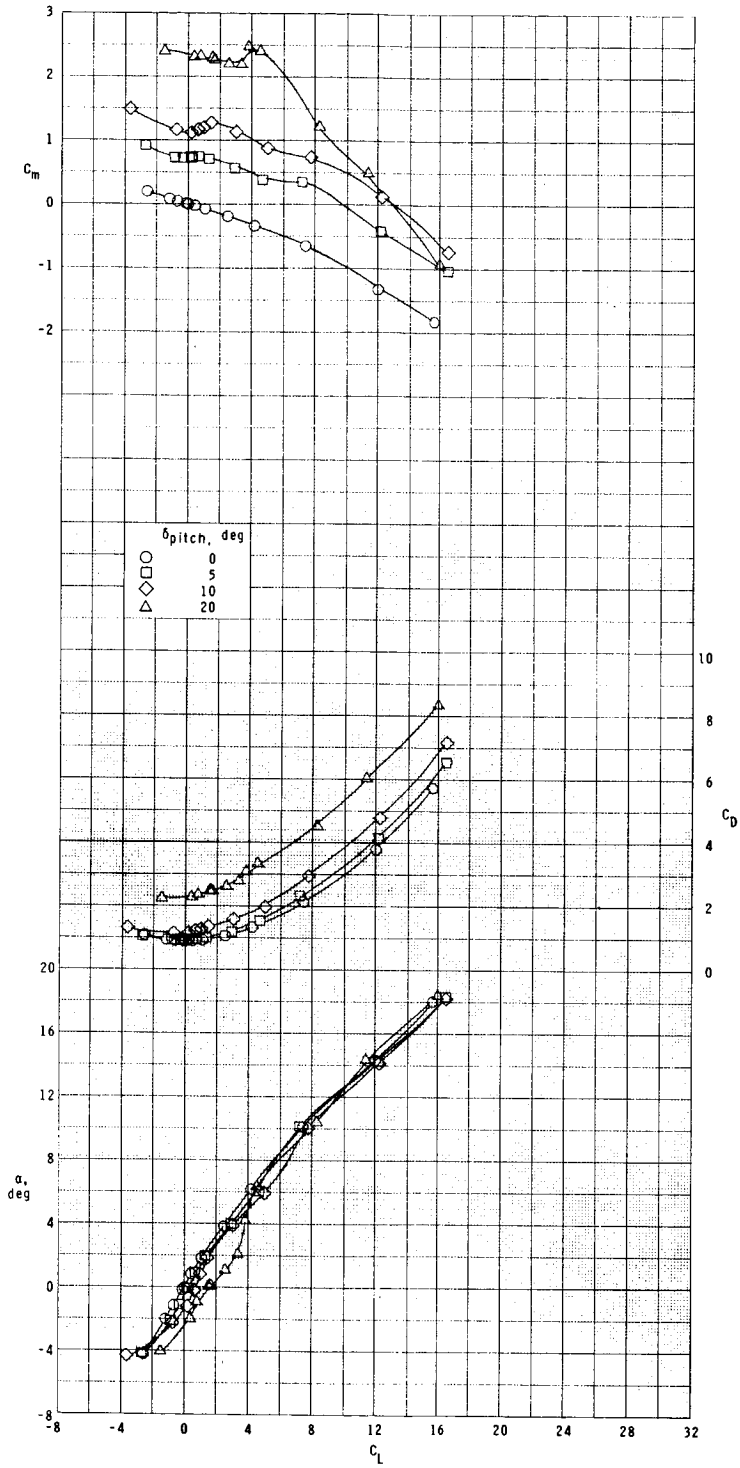

(a) Concluded.

Figure 5.- Continued.

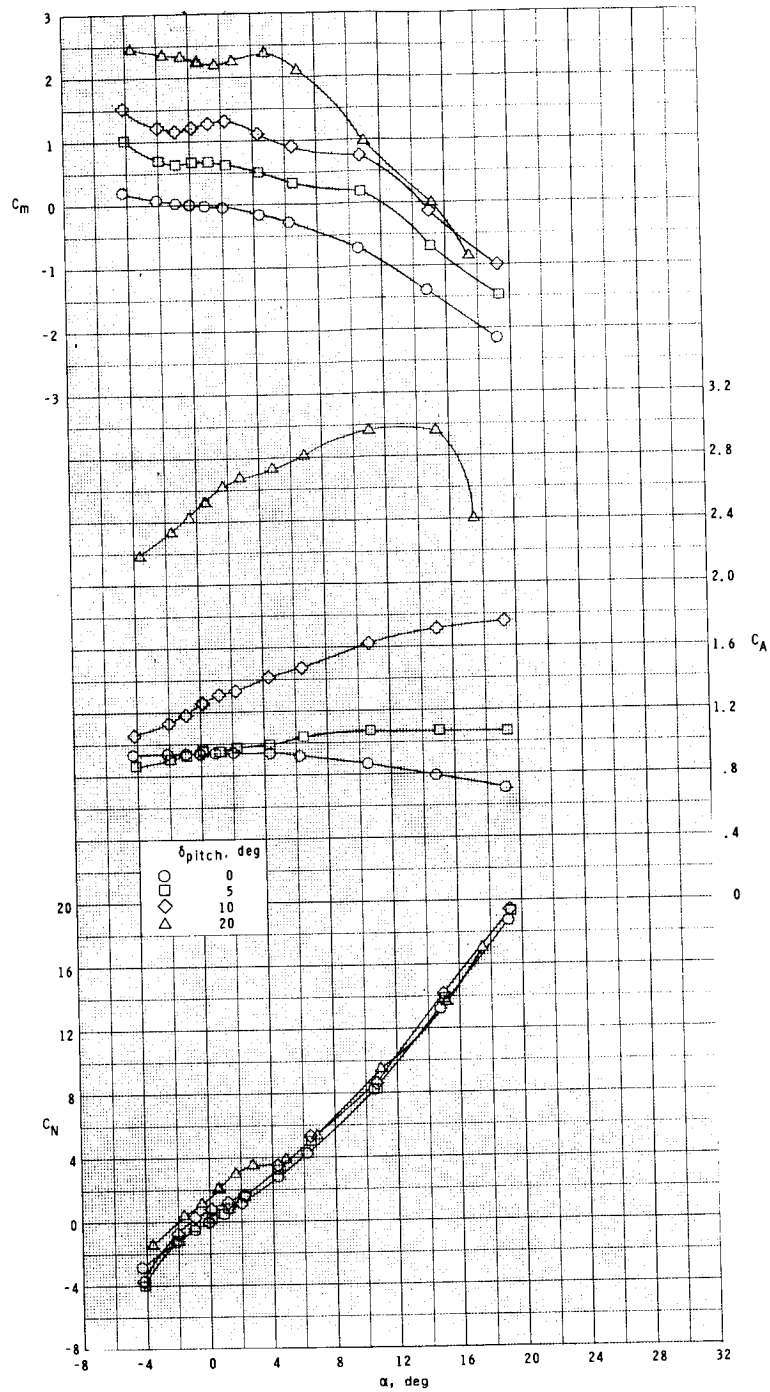

(b) M = 0.60.

Figure 5.- Continued.

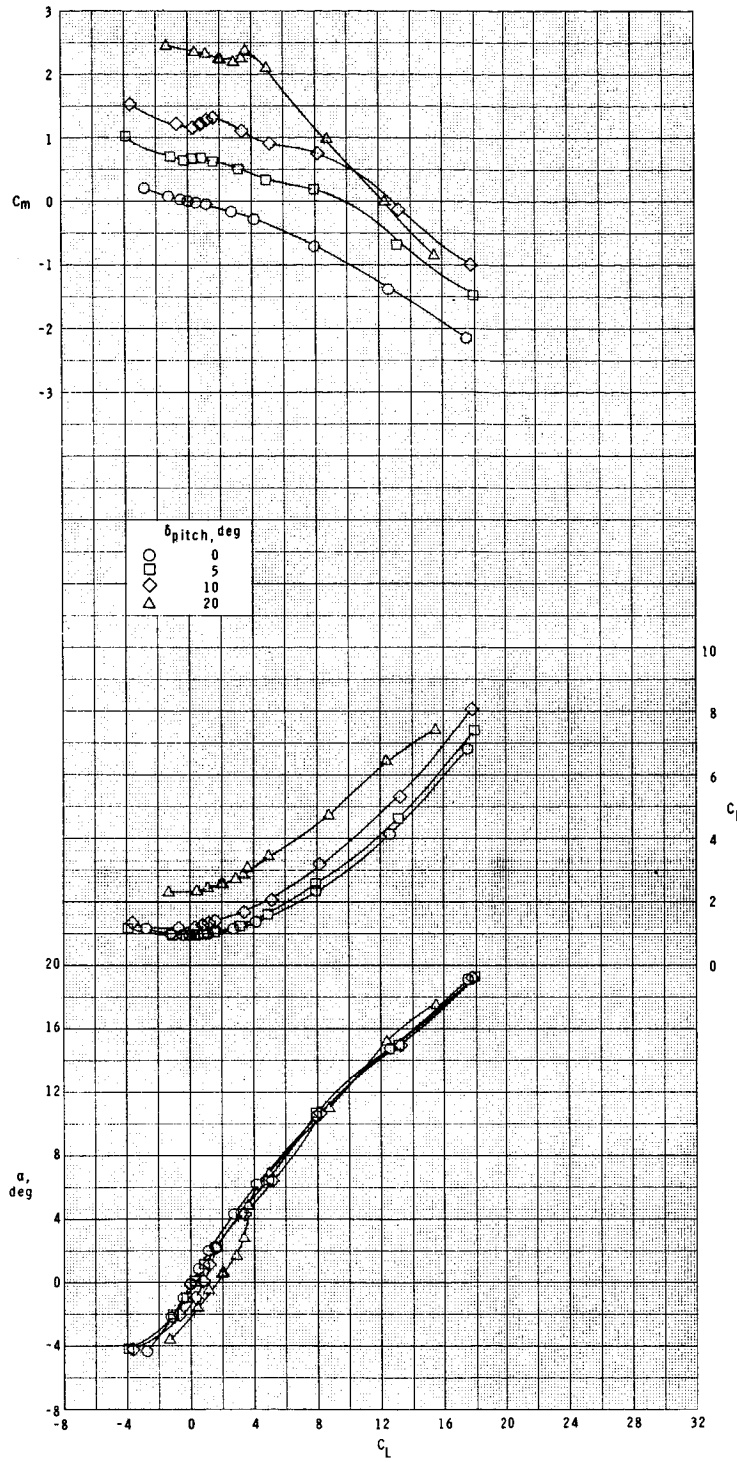

(b) Concluded.

Figure 5.- Continued.

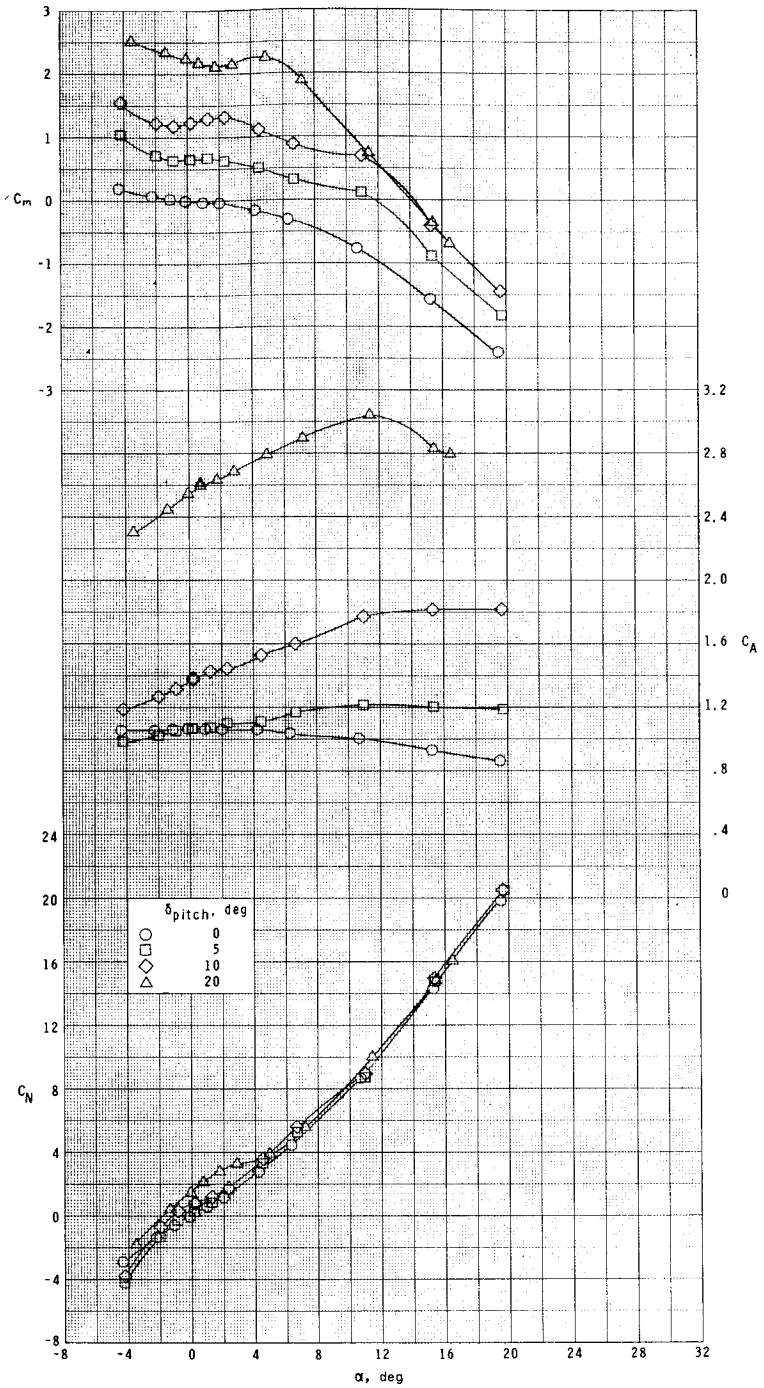

(c) M = 0.80.

Figure 5.- Continued.

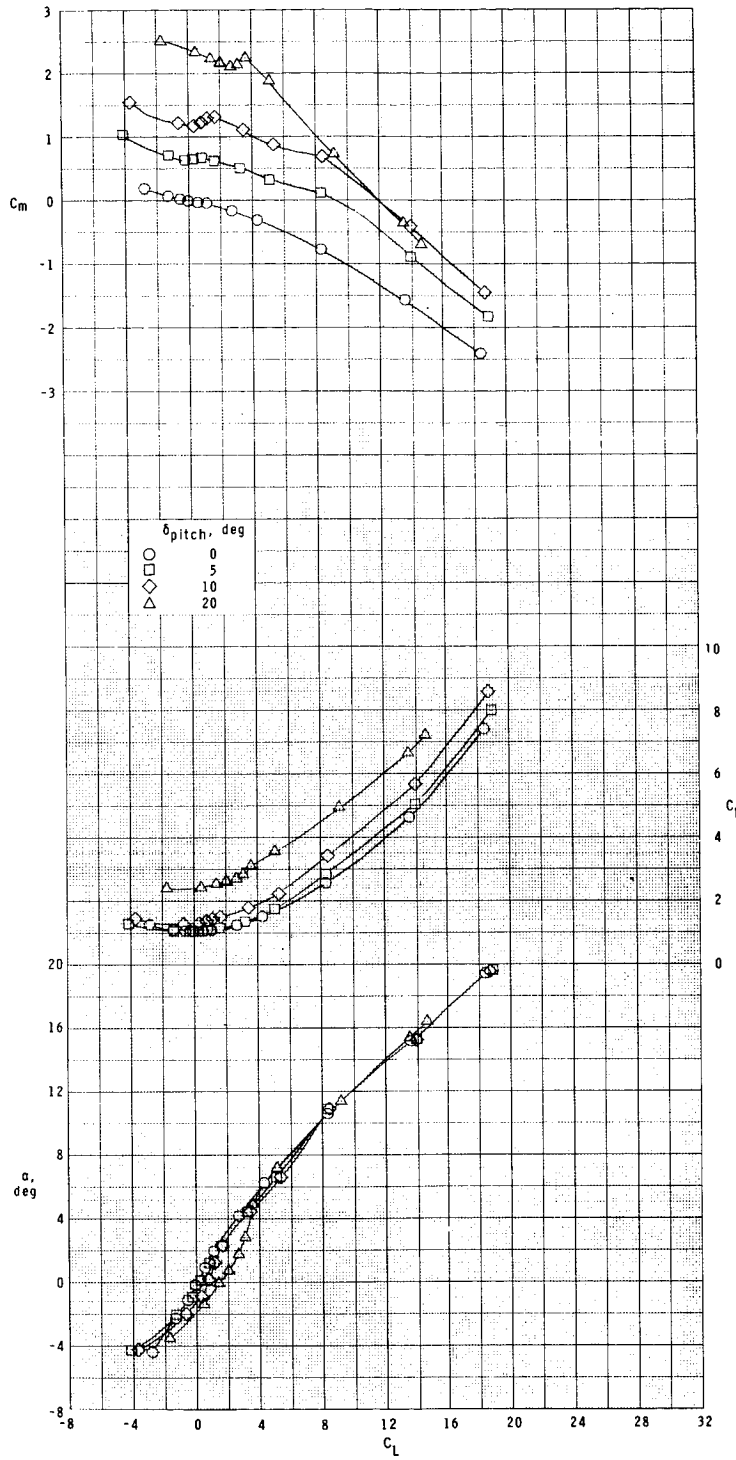

(c) Concluded.

Figure 5.- Continued.

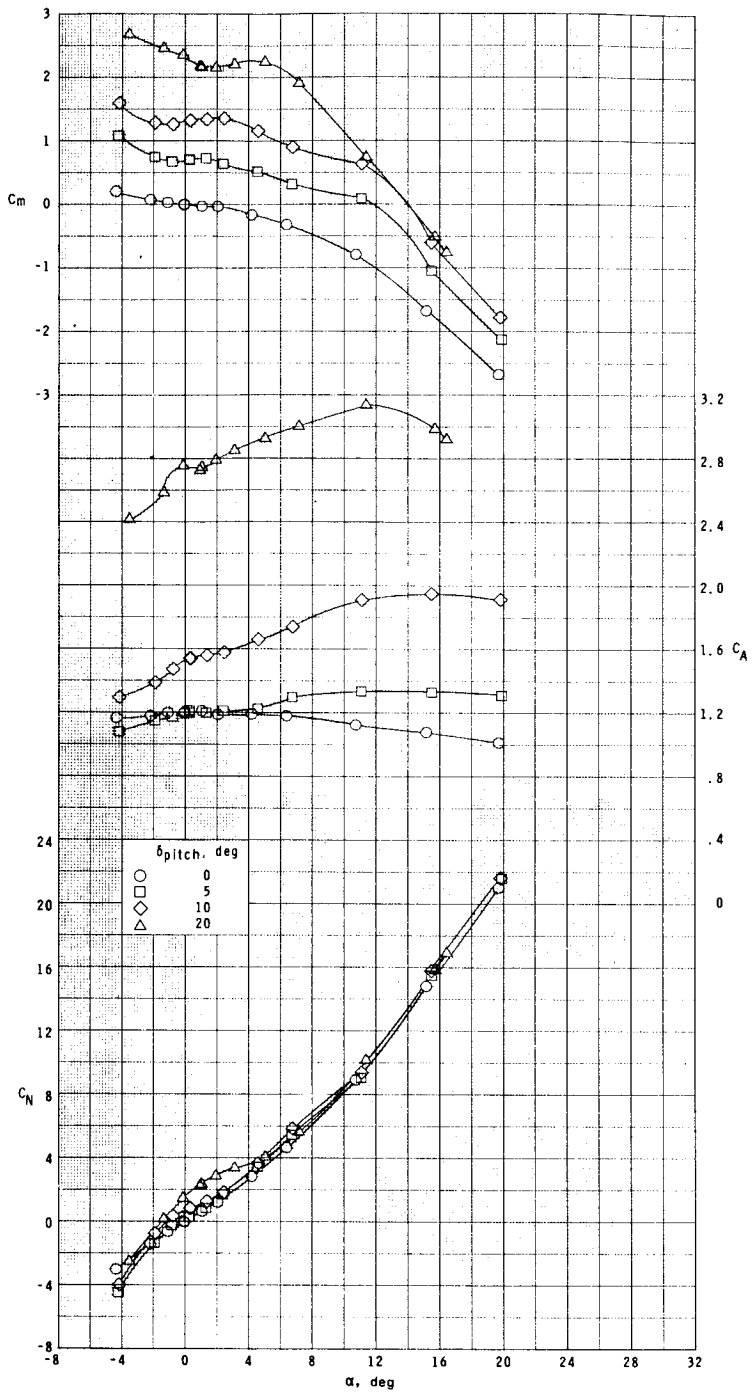

(d) M = 0.90.

Figure 5.- Continued.

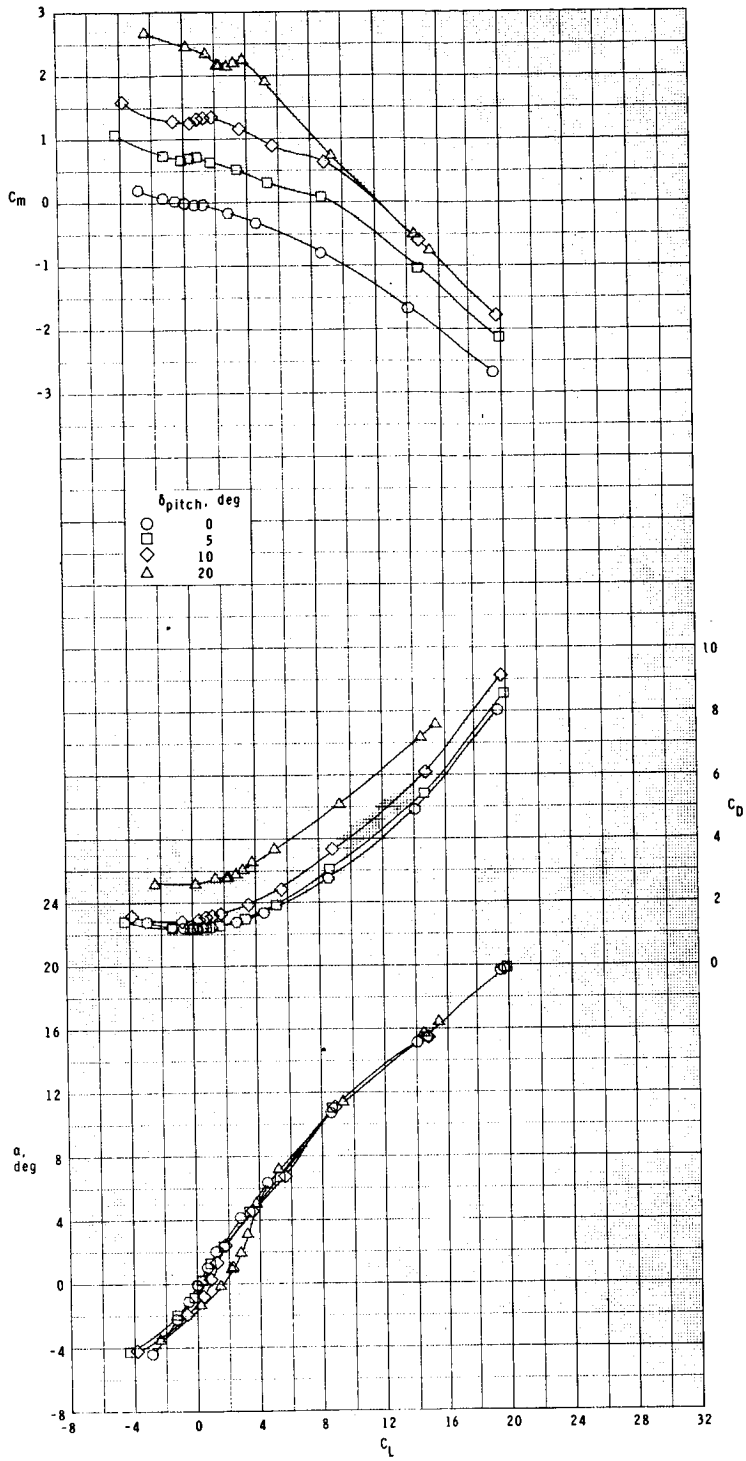

(d) Concluded.

Figure 5.- Continued.

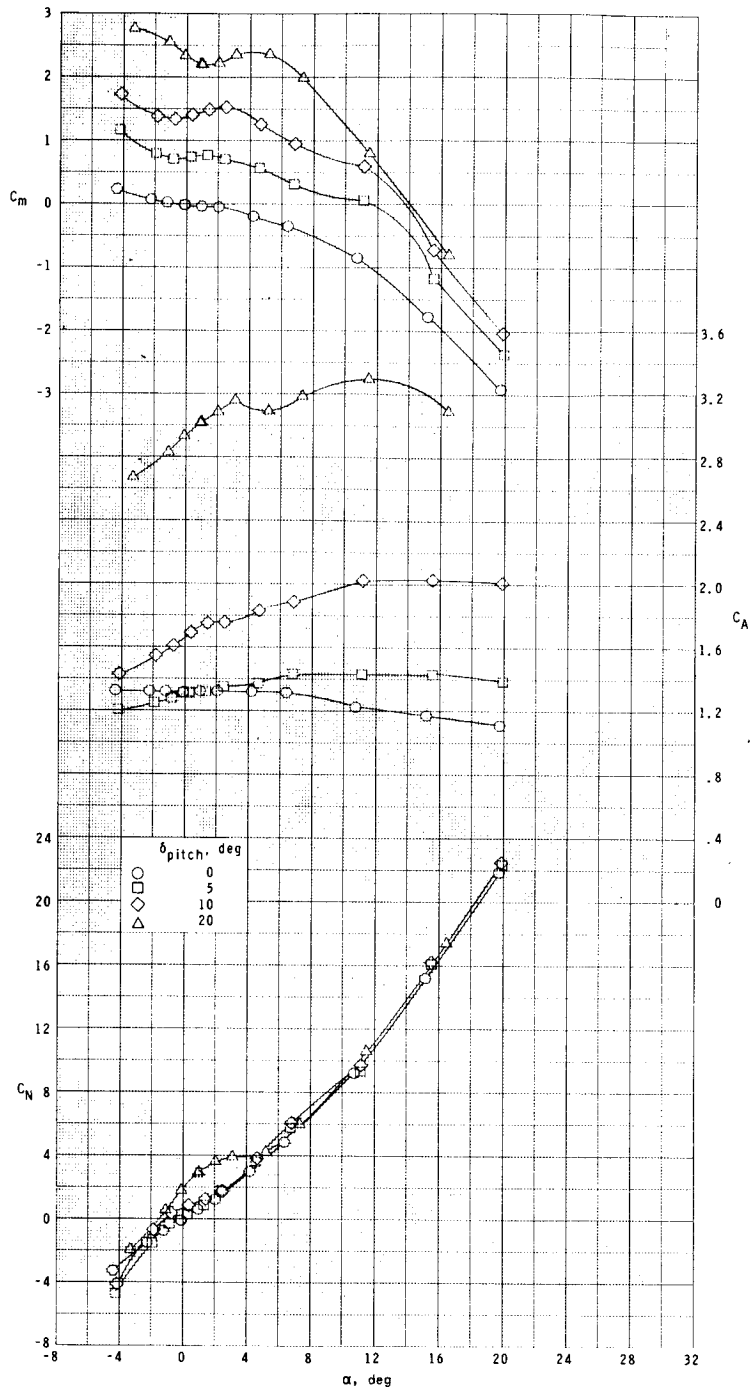

(e) M = 0.95.

Figure 5.- Continued.

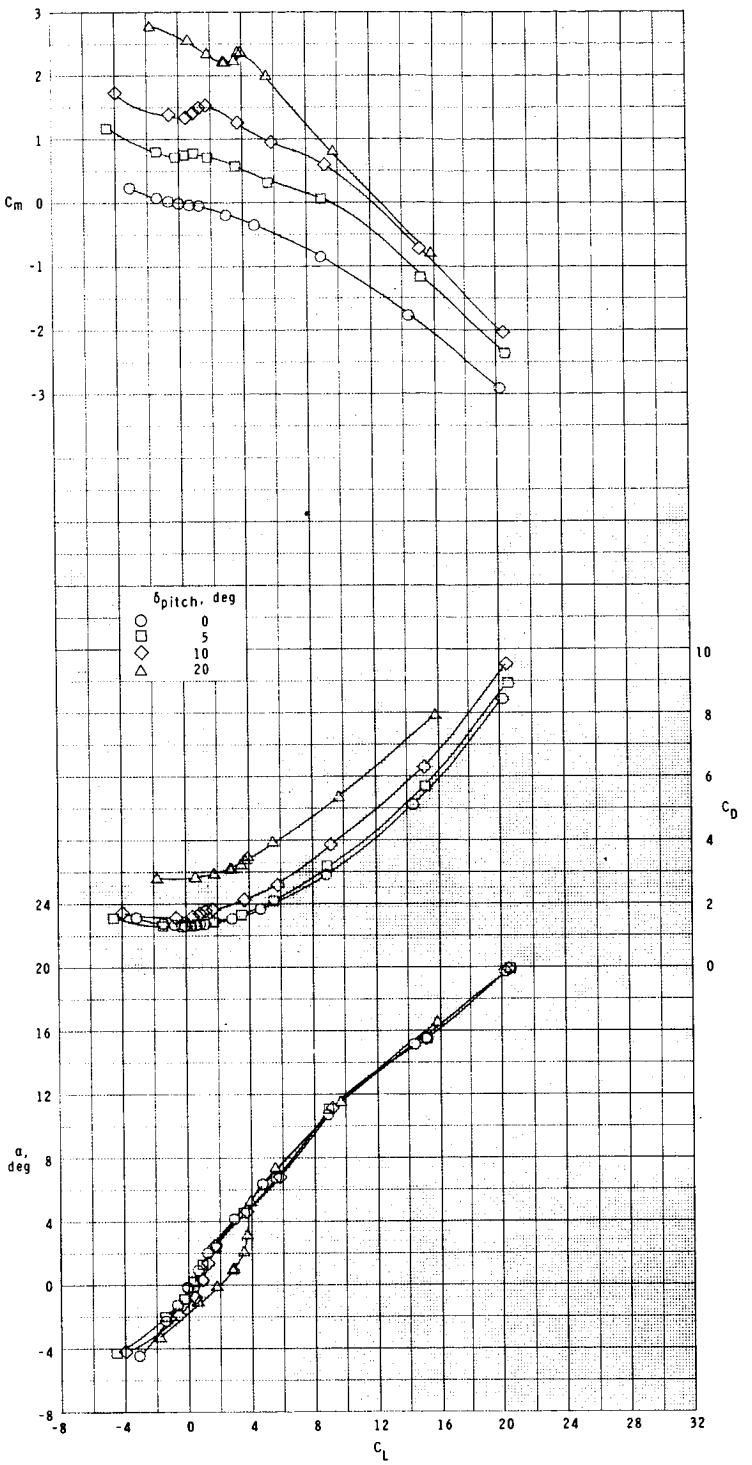

(e) Concluded.

Figure 5.- Continued.

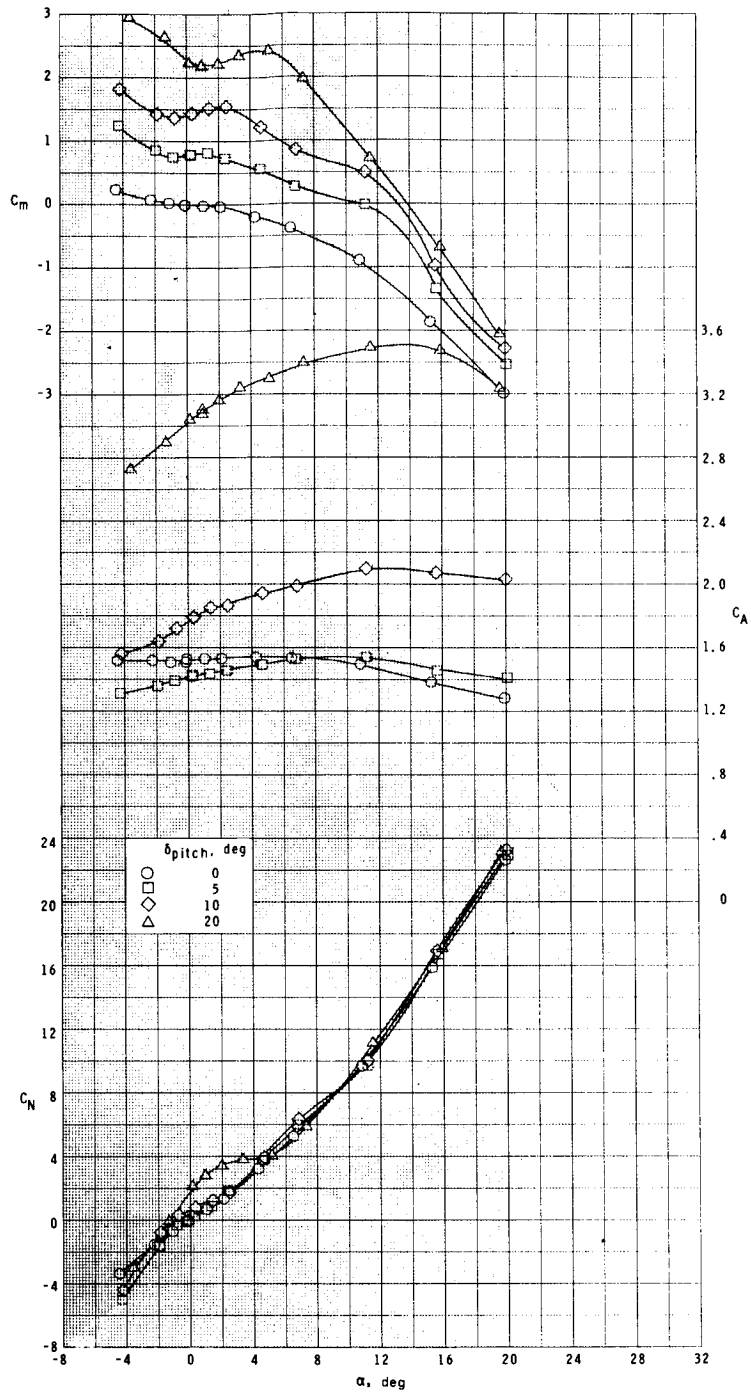

(f) M = 1.00.

Figure 5.- Continued.

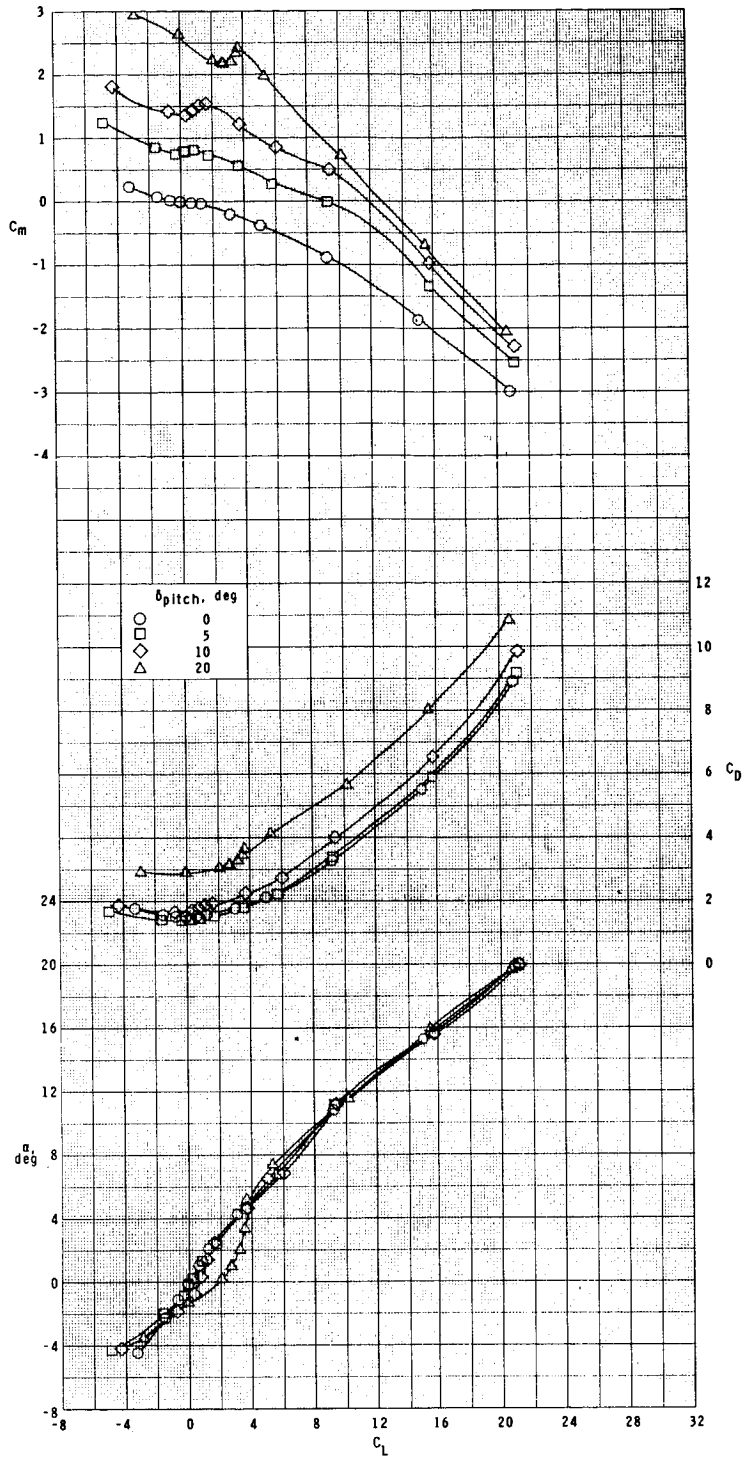

(f) Concluded.

Figure 5.- Continued.

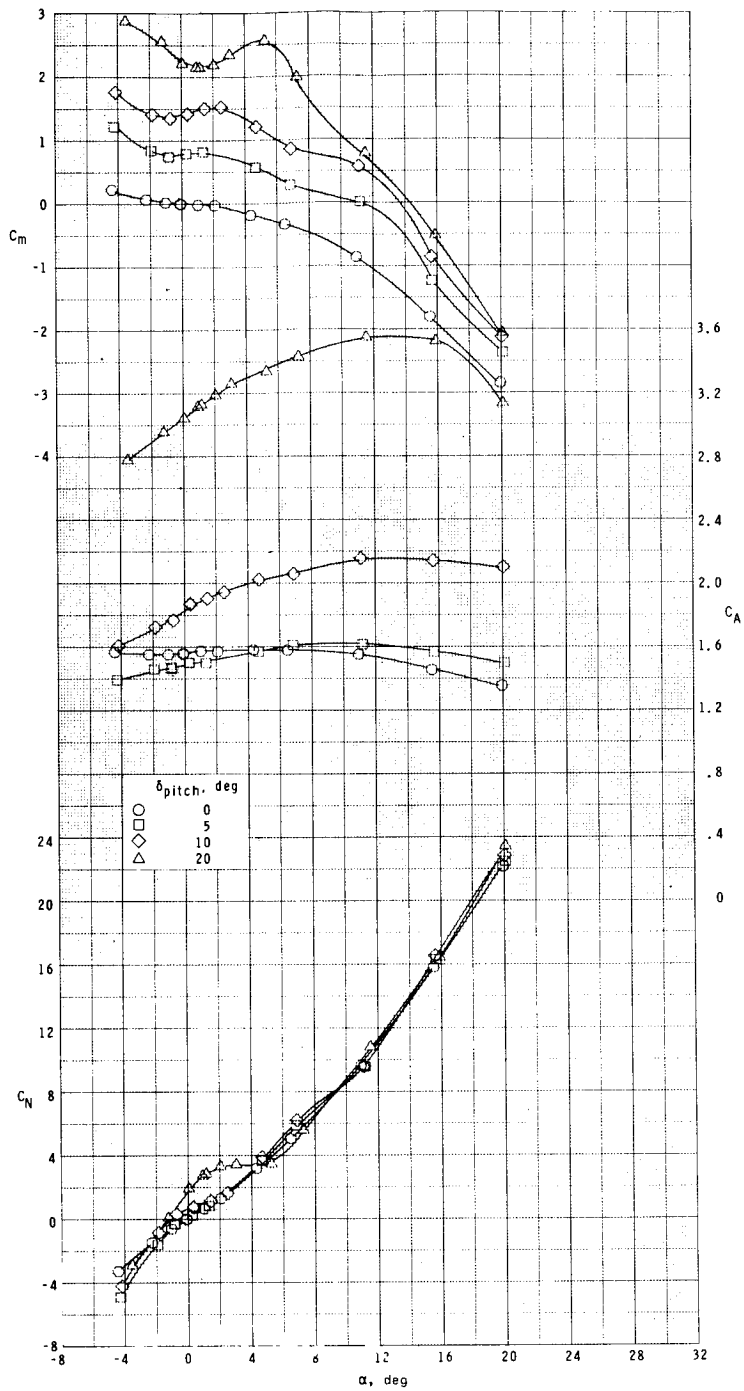

(g) M = 1.03.

Figure 5.- Continued.

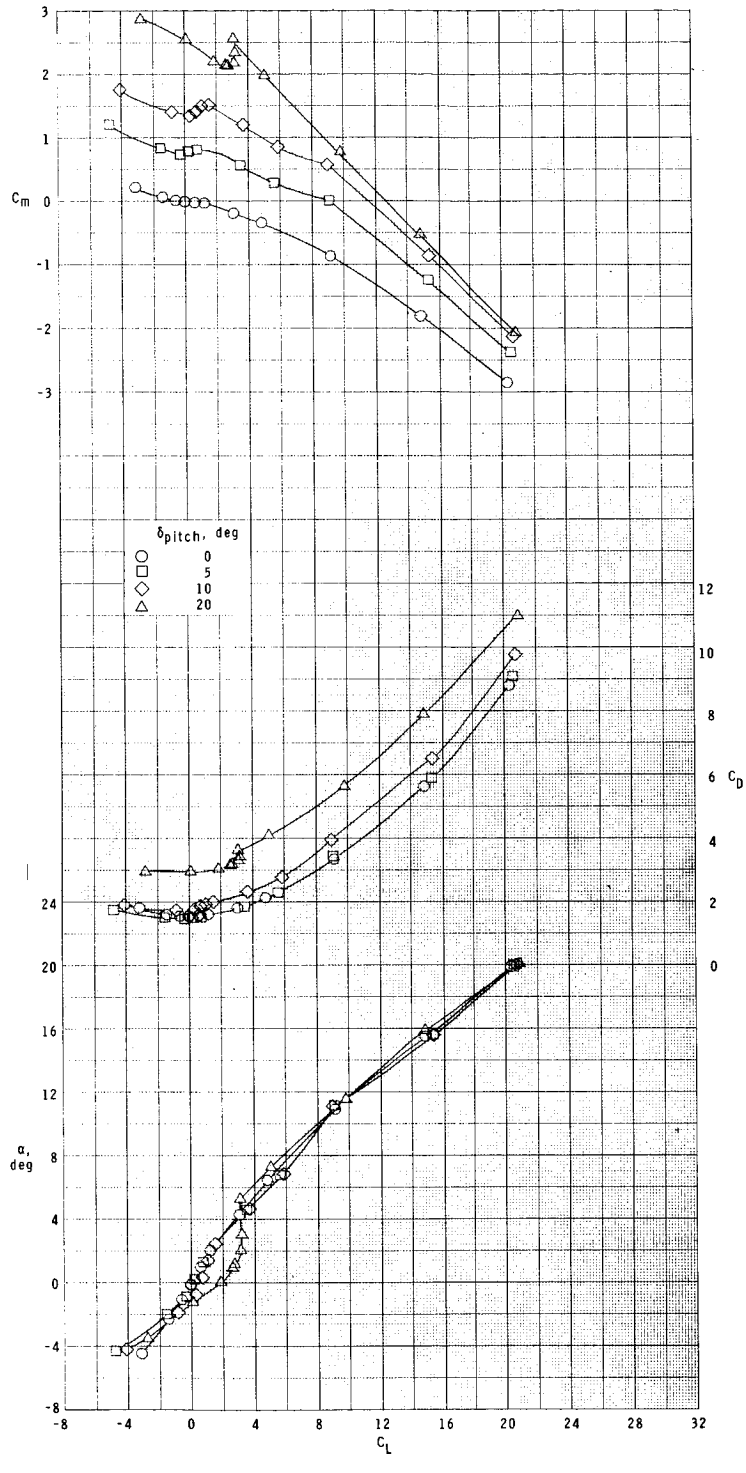

(g) Concluded.

Figure 5.- Continued.

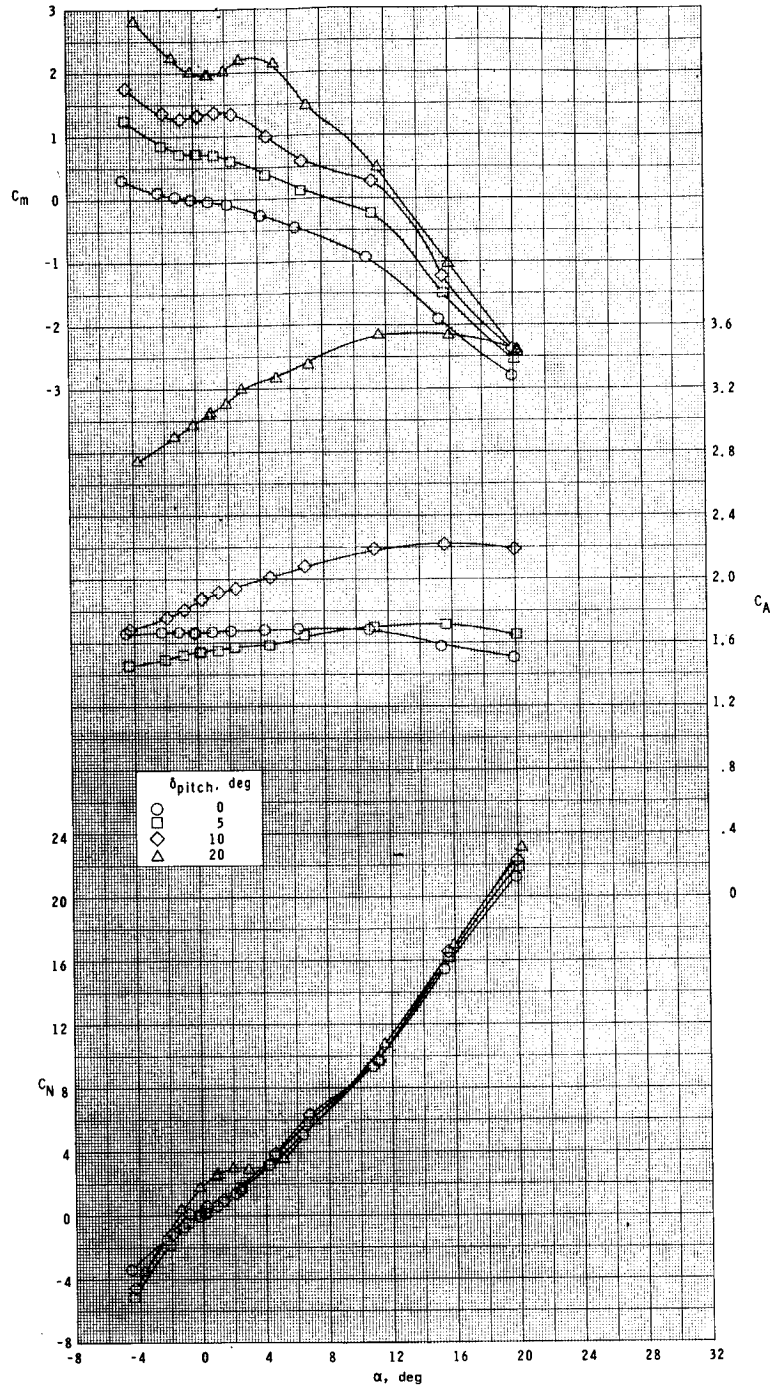

(h) M = 1.20.

Figure 5.- Continued.

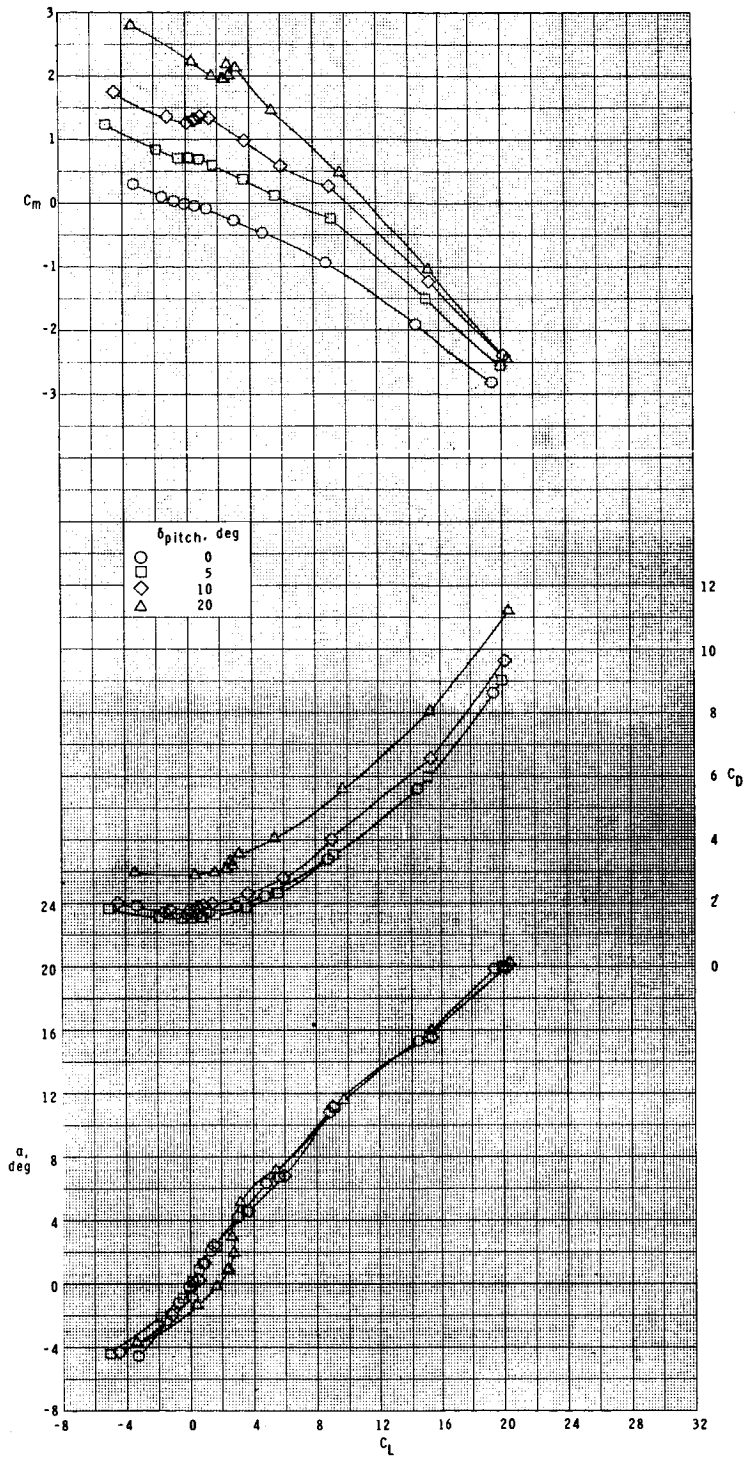

(h) Concluded.

Figure 5.- Continued.

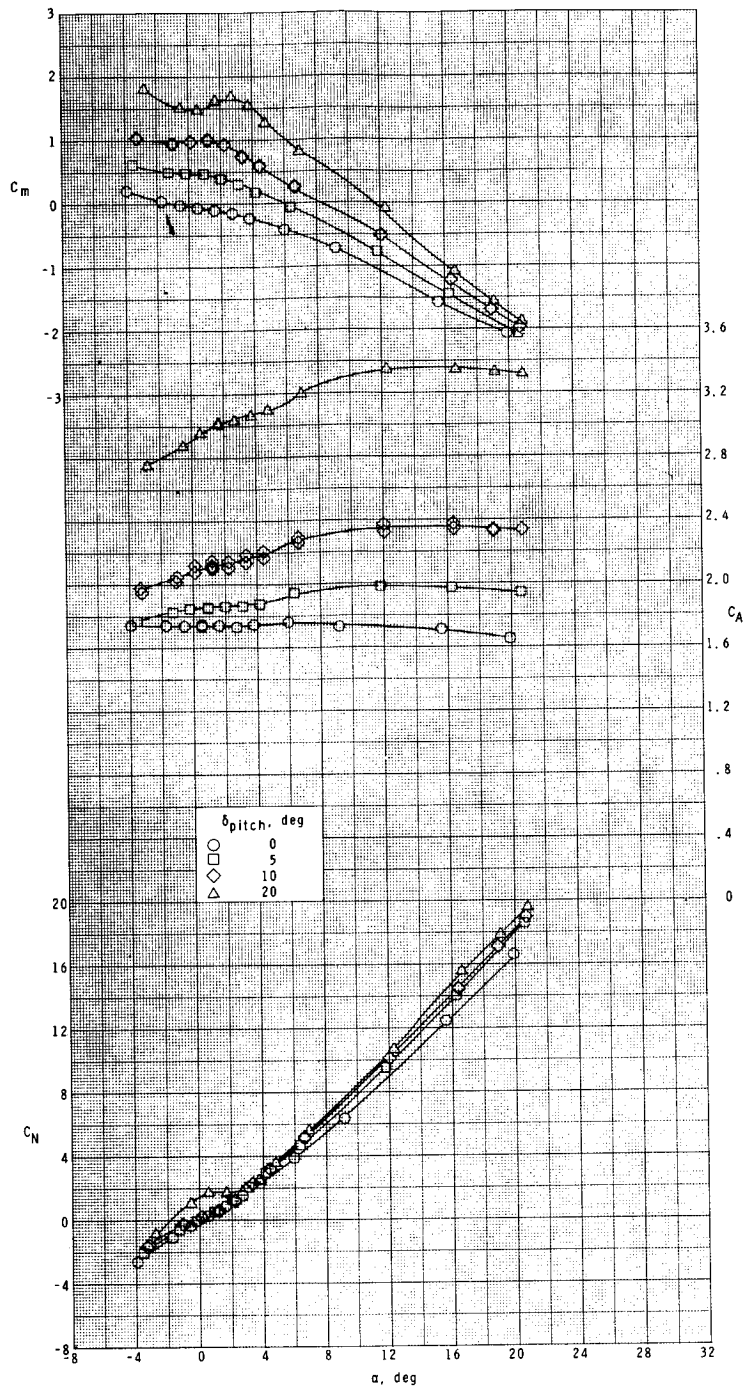

(i) M = 1.75.

Figure 5.- Continued.

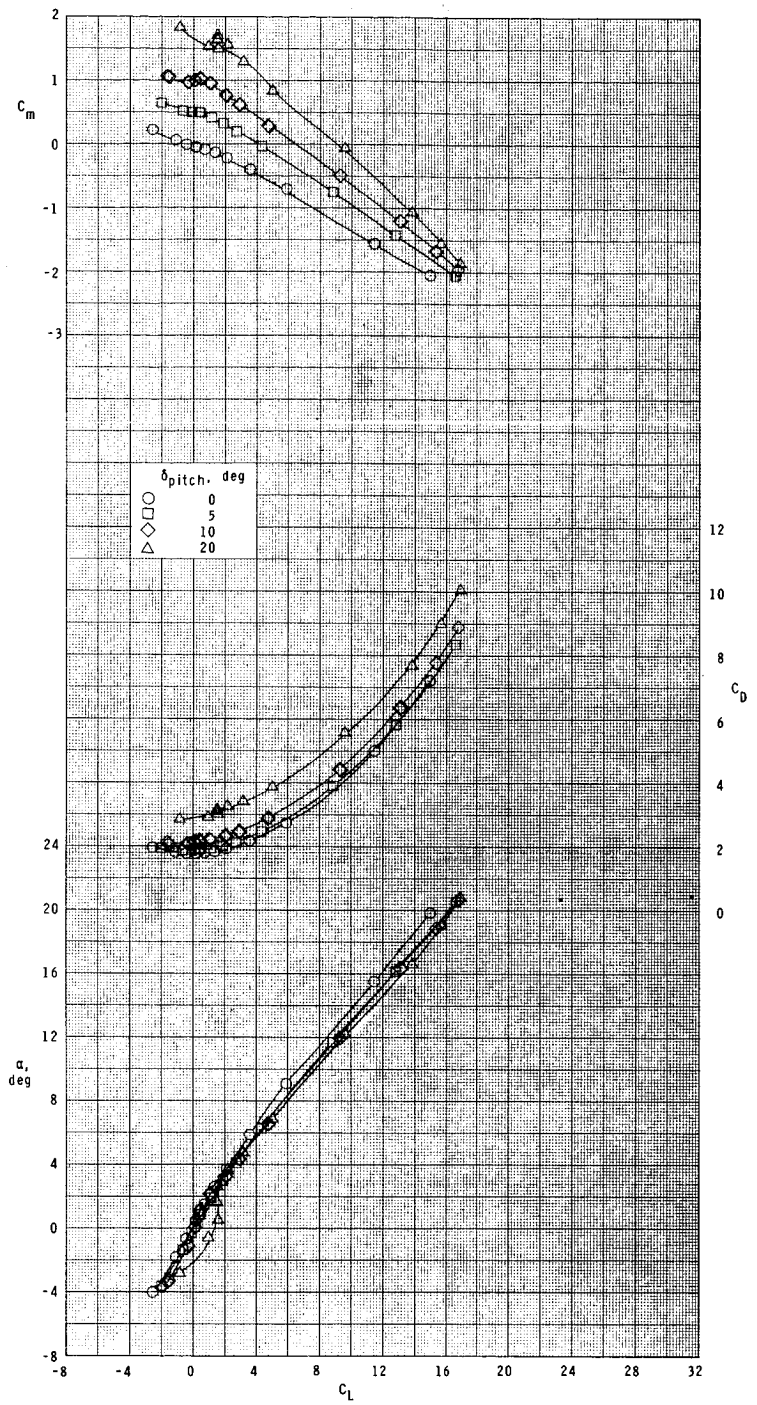

(i) Concluded.

Figure 5.- Continued.

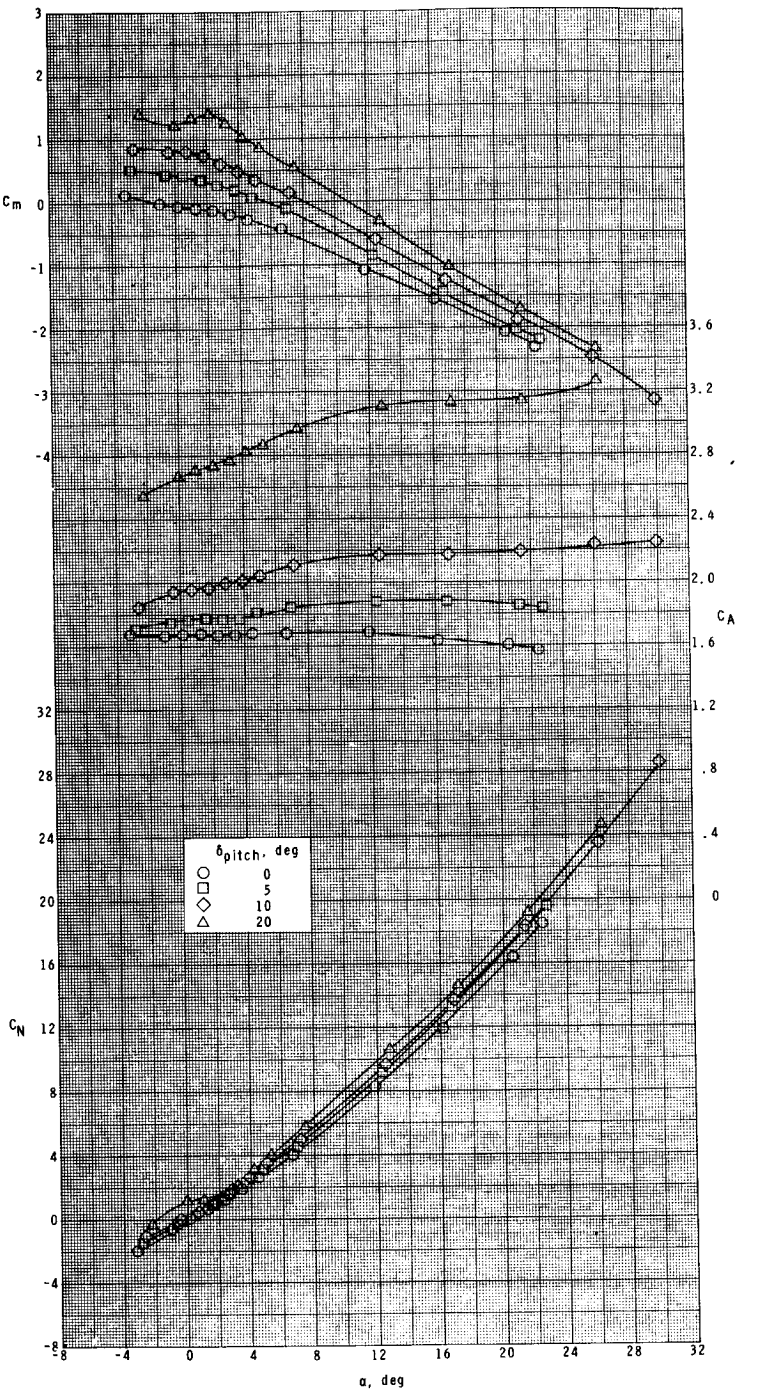

(j) M = 2.10.

Figure 5.- Continued.

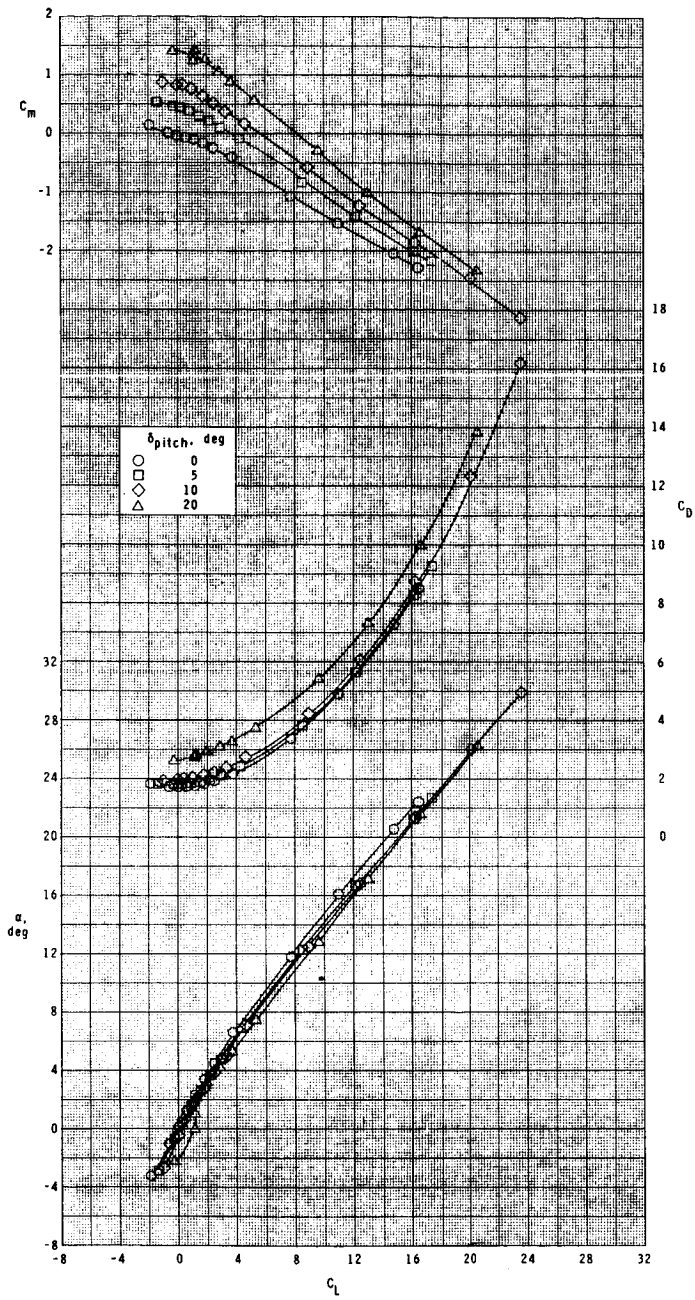

(j) Concluded.

Figure 5.- Continued.

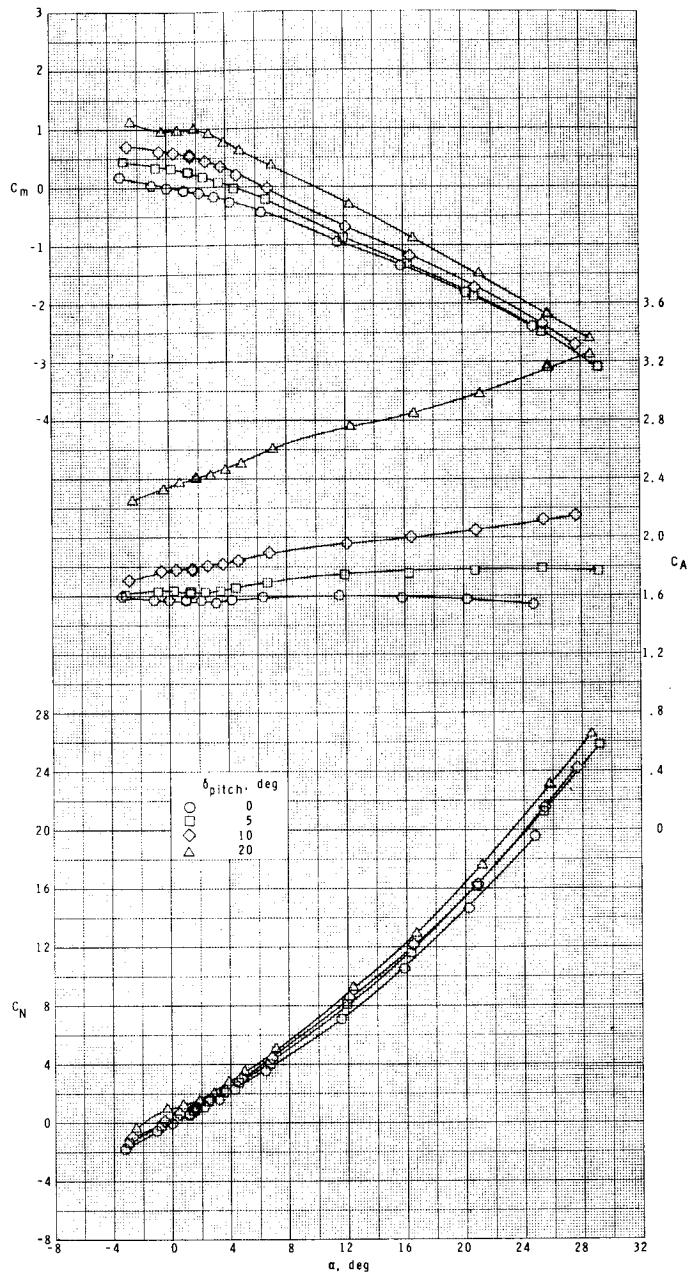

(k) M = 2.50.

Figure 5.- Continued.

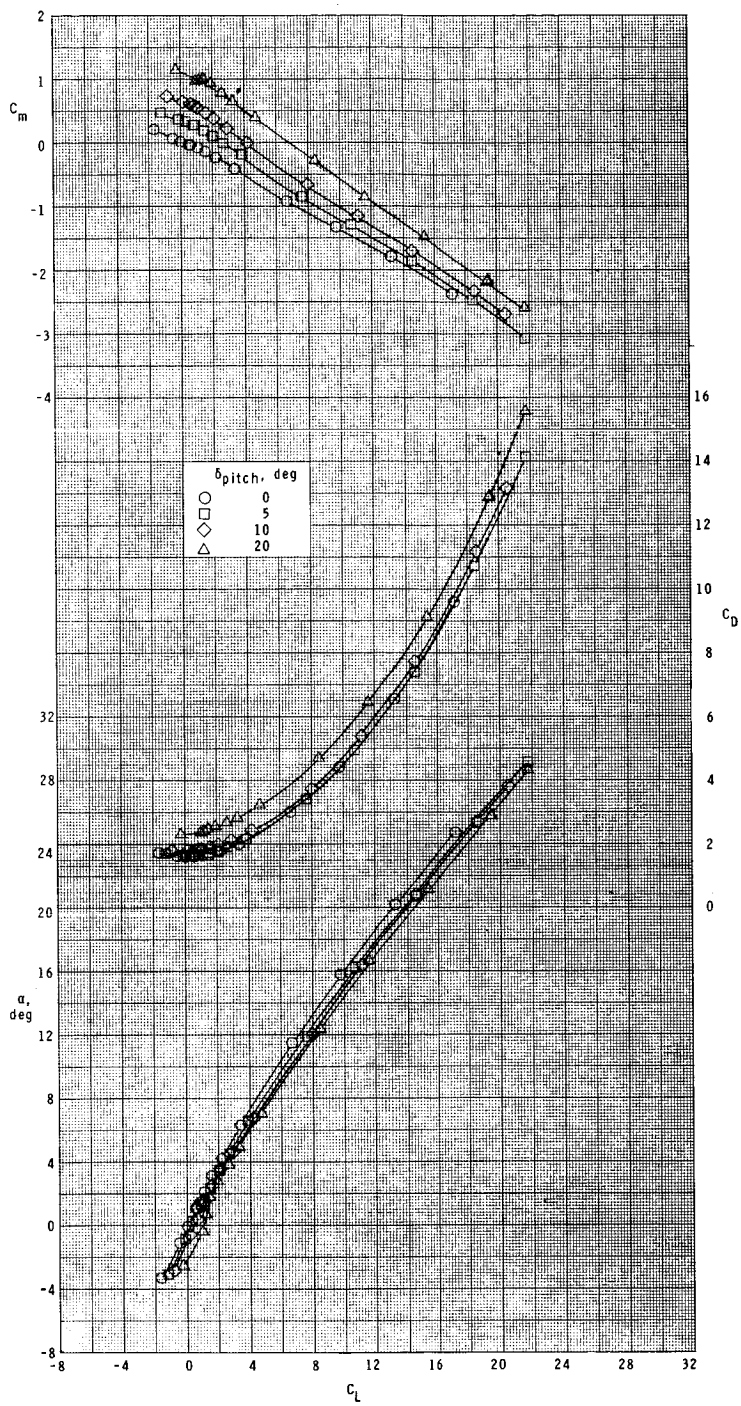

(k) Concluded.

Figure 5.- Continued.

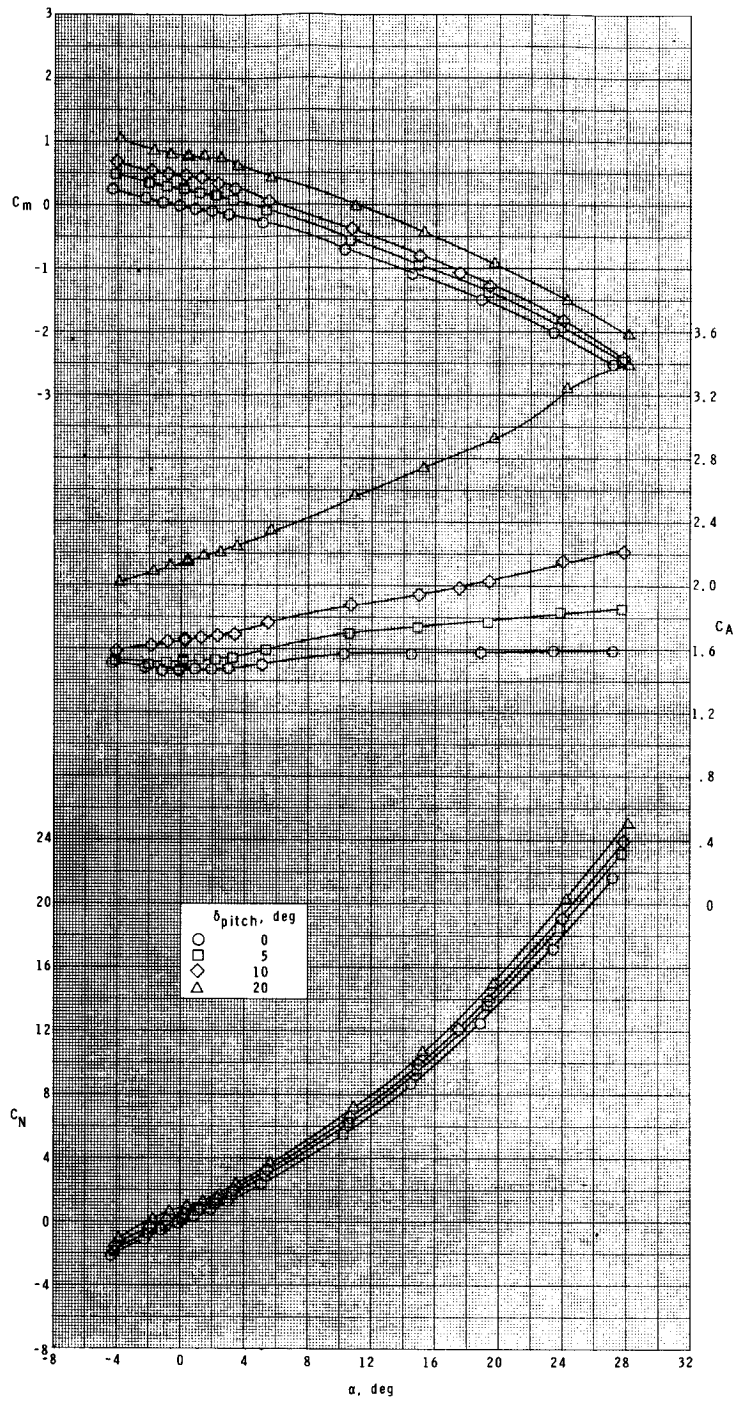

(l) M = 2.86.

Figure 5.- Continued.

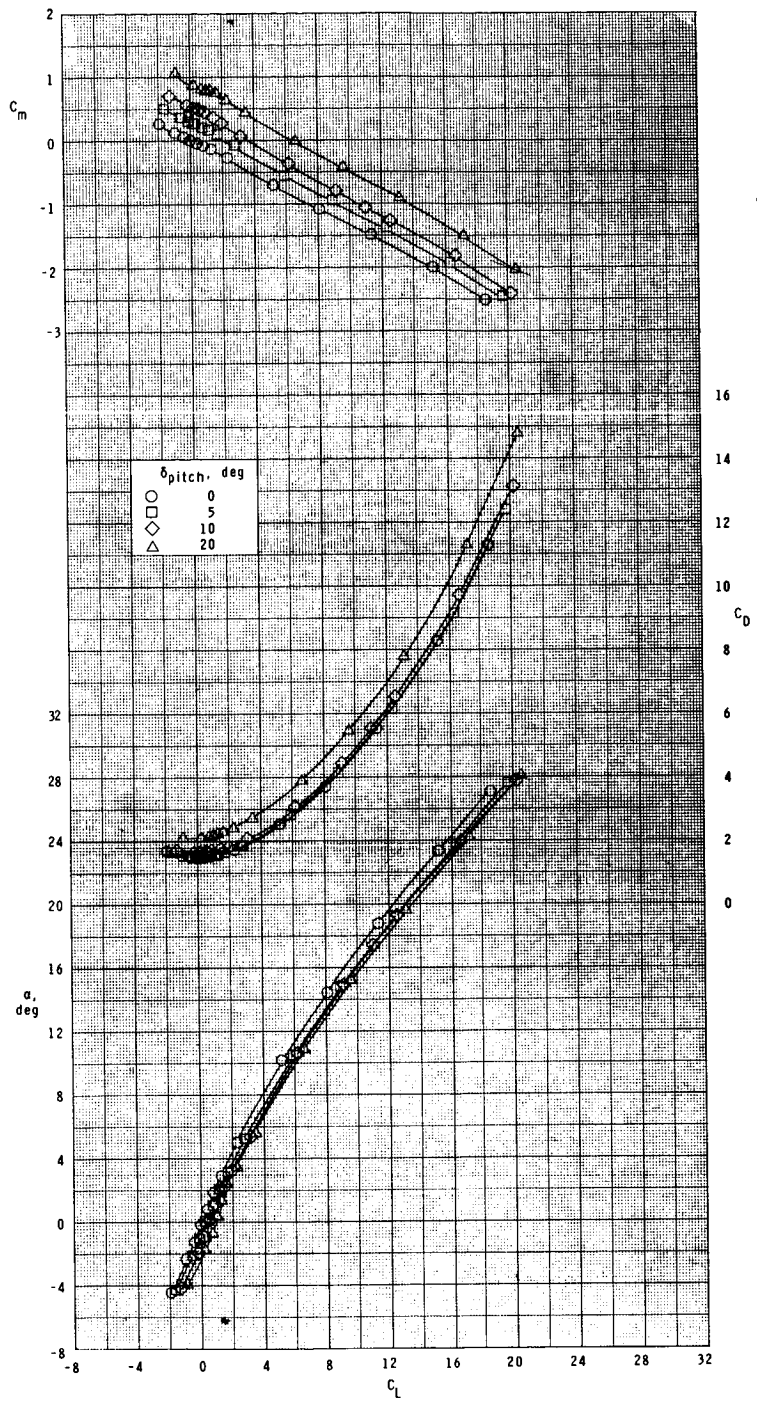

(l) Concluded.

Figure 5.- Continued.

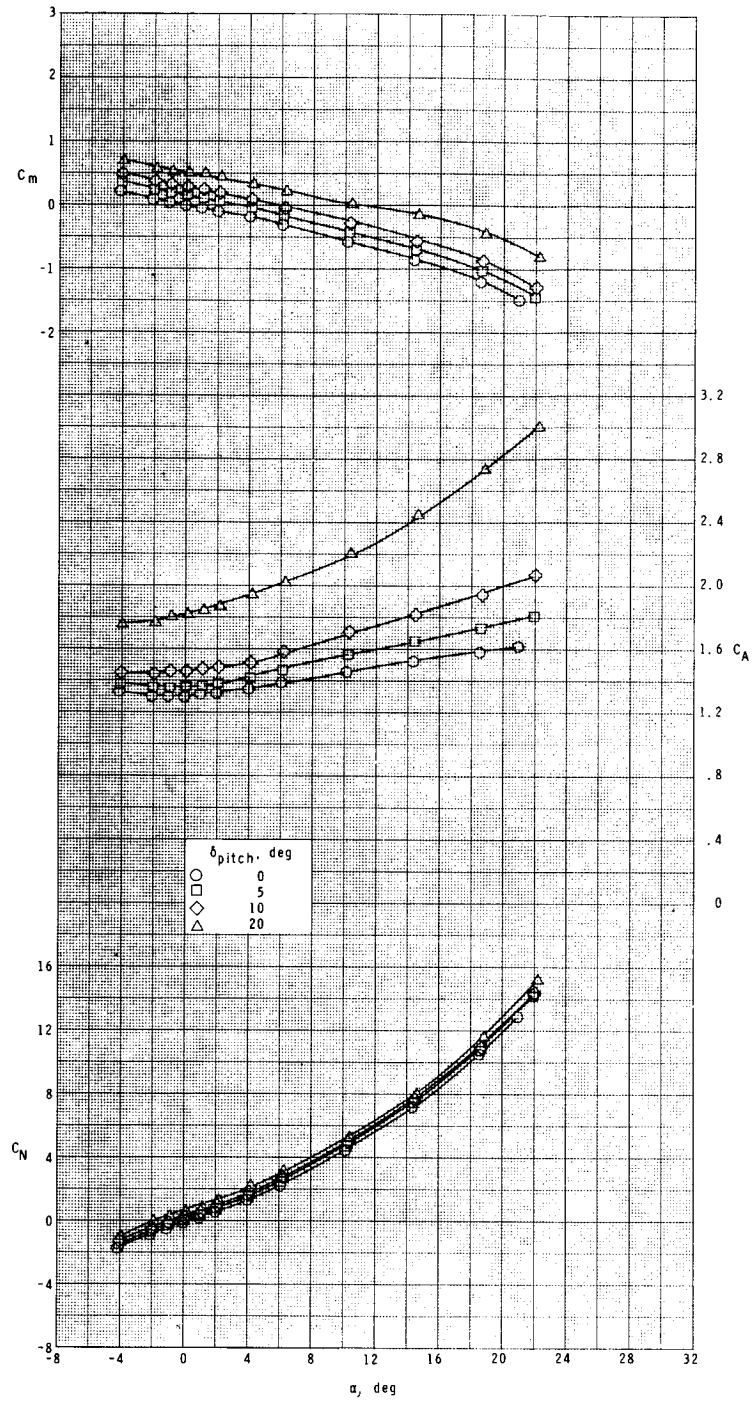

(m) M = 3.95.

Figure 5.- Continued.

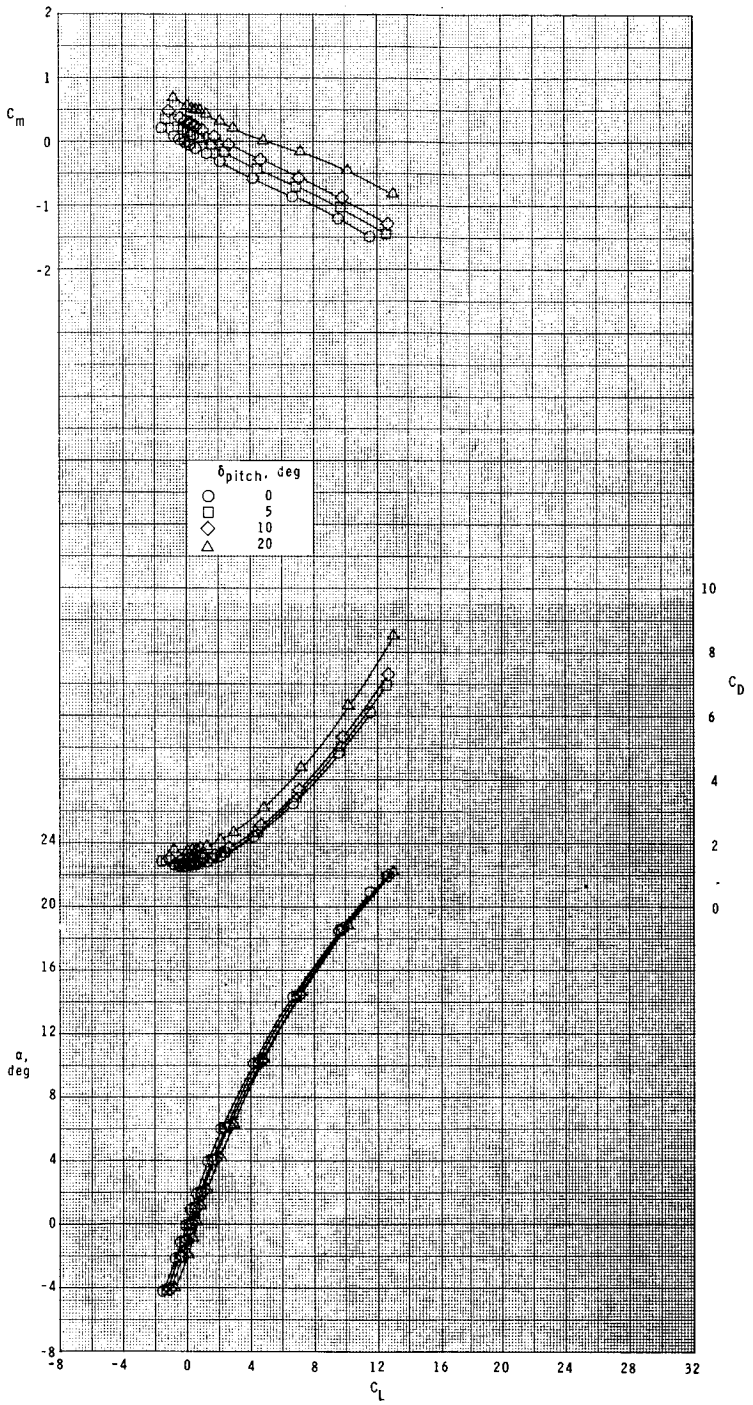

(m) Concluded.

Figure 5.- Continued.

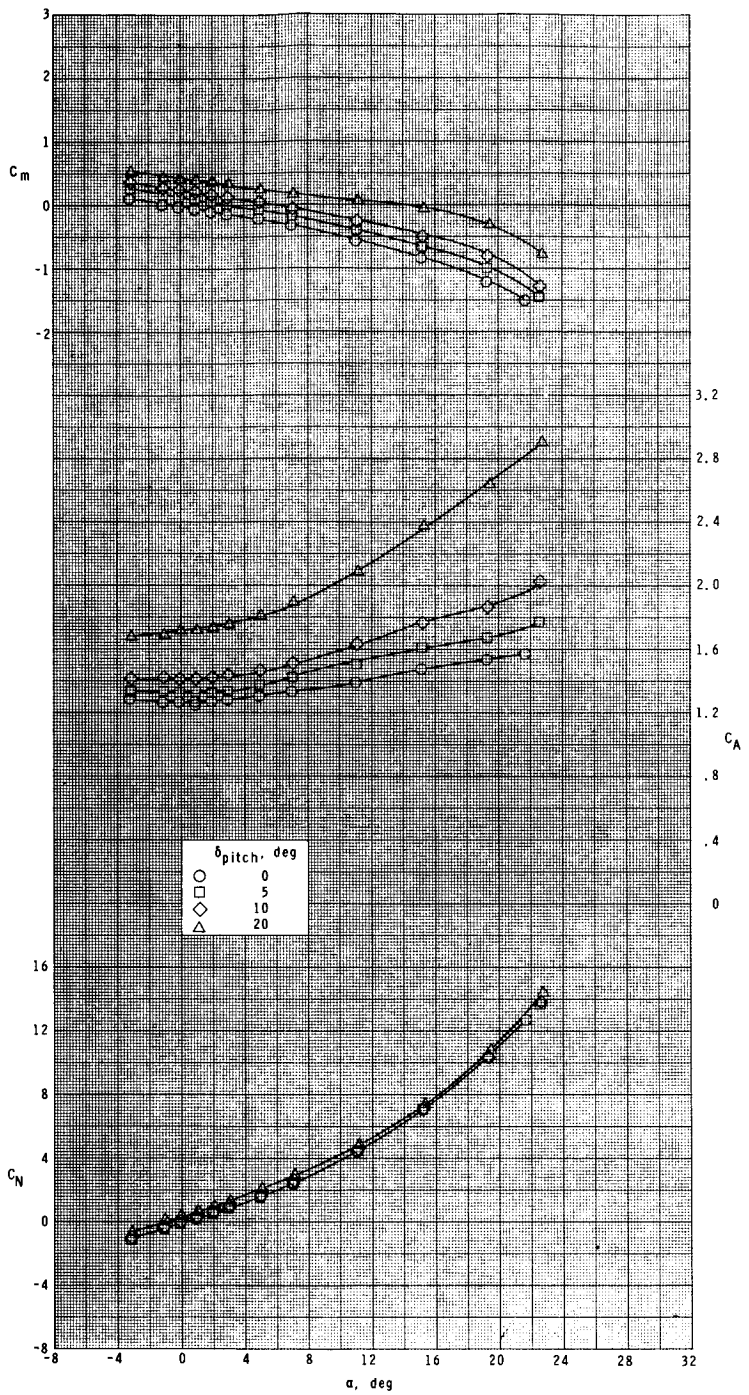

(n) M = 4.63.

Figure 5.- Continued.

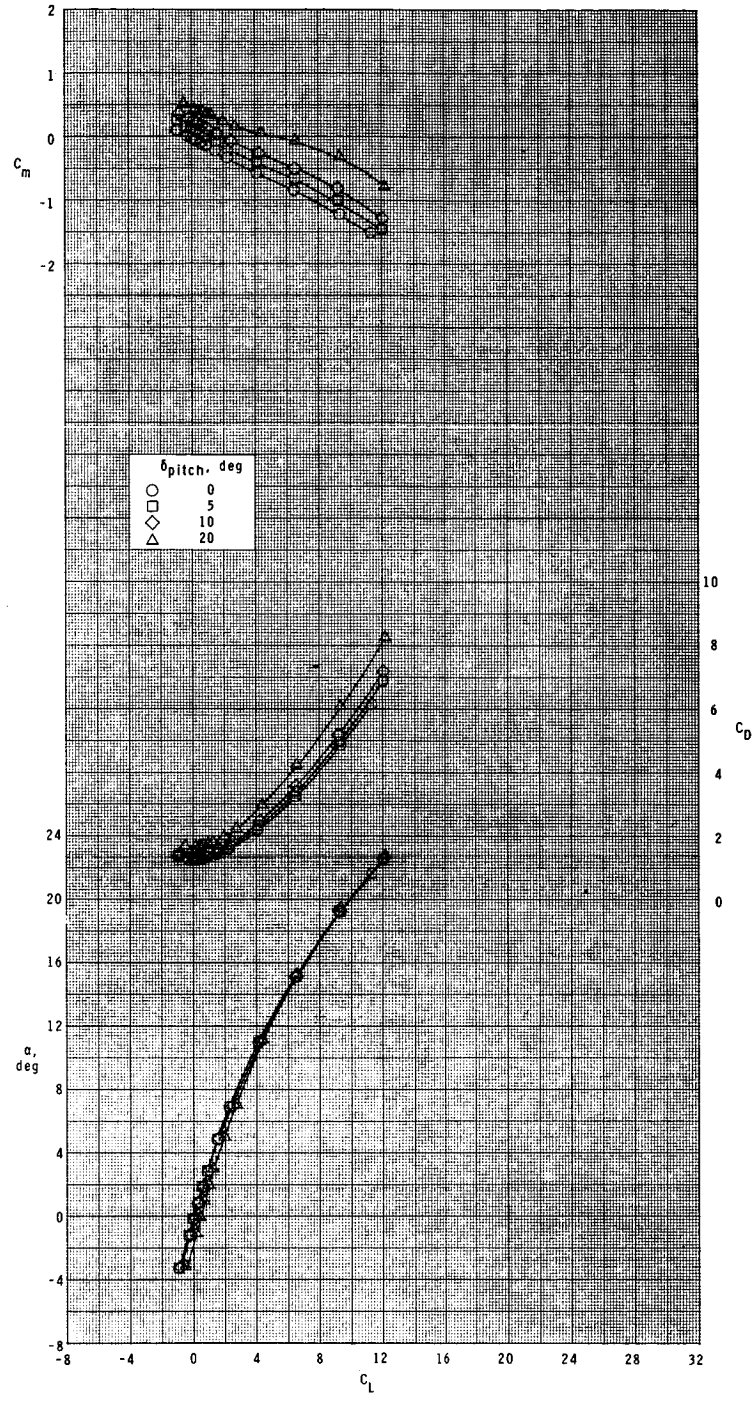

(n) Concluded.

Figure 5.- Concluded.

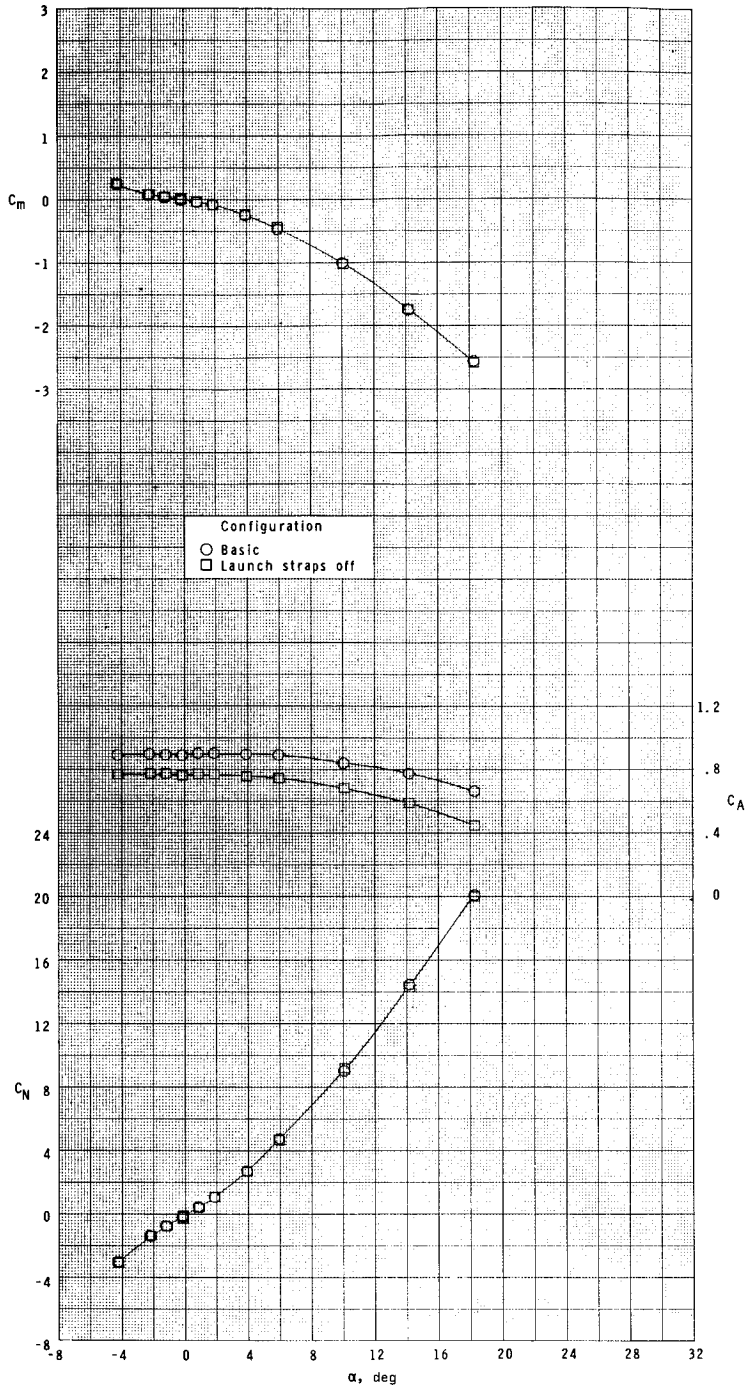

(a) M = 0.20.

Figure 6.- Effect of launch straps on the longitudinal characteristics. $\phi = 0^{o}$.

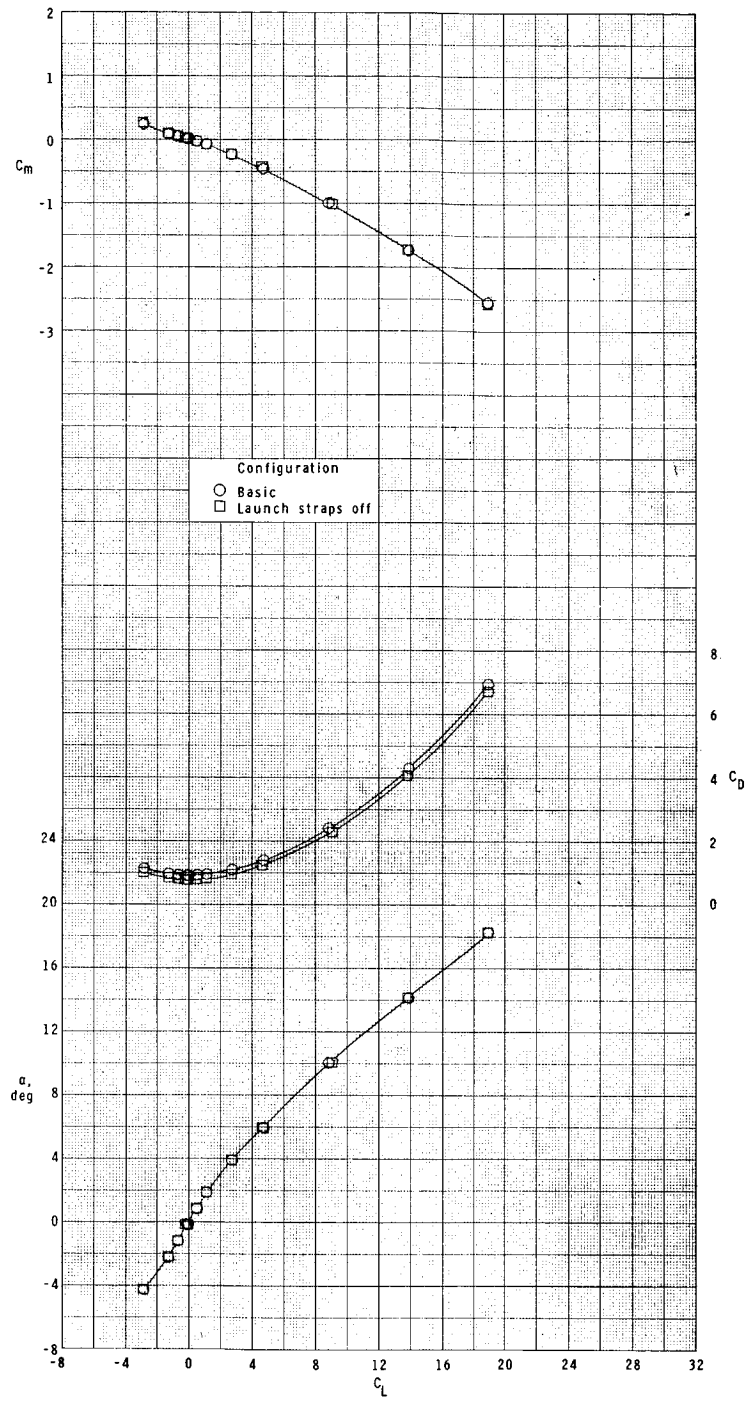

(a) Concluded.

Figure 6.- Continued.

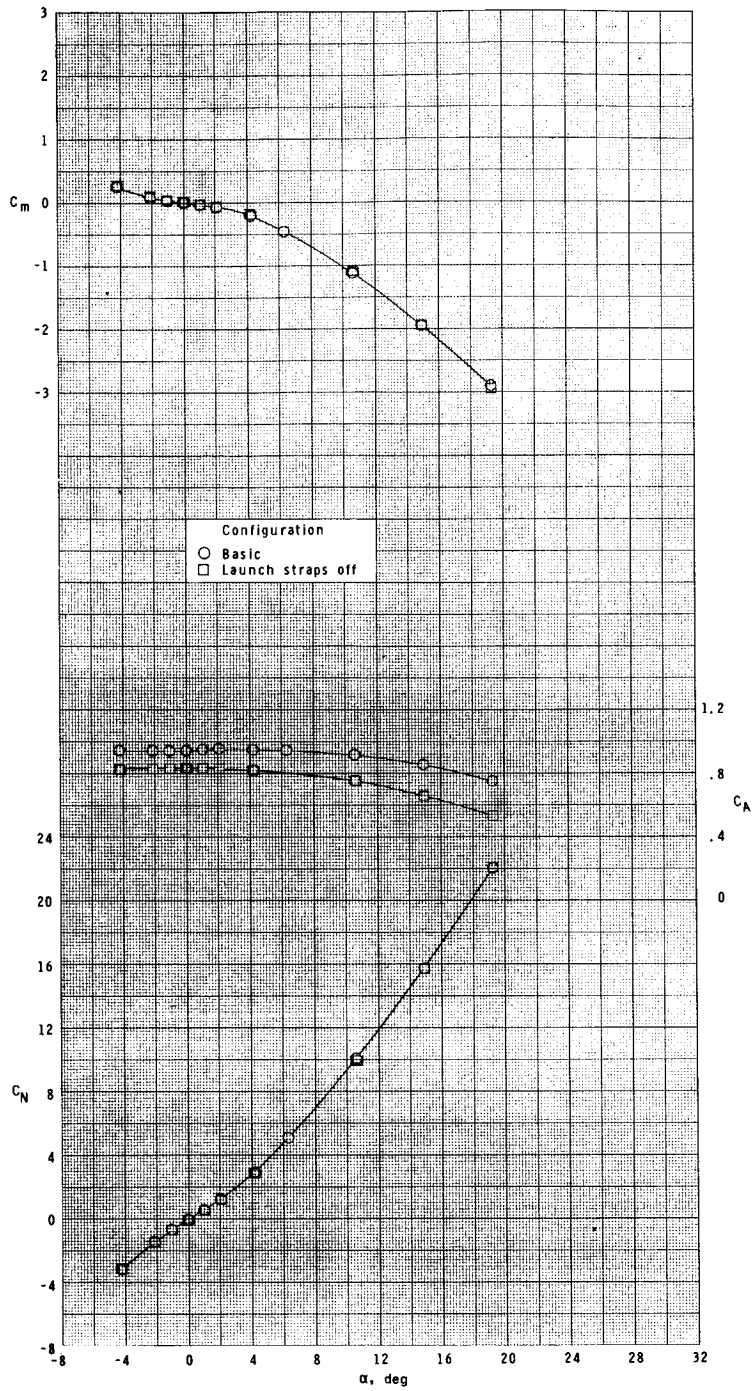

(b) M = 0.60.

Figure 6.- Continued.

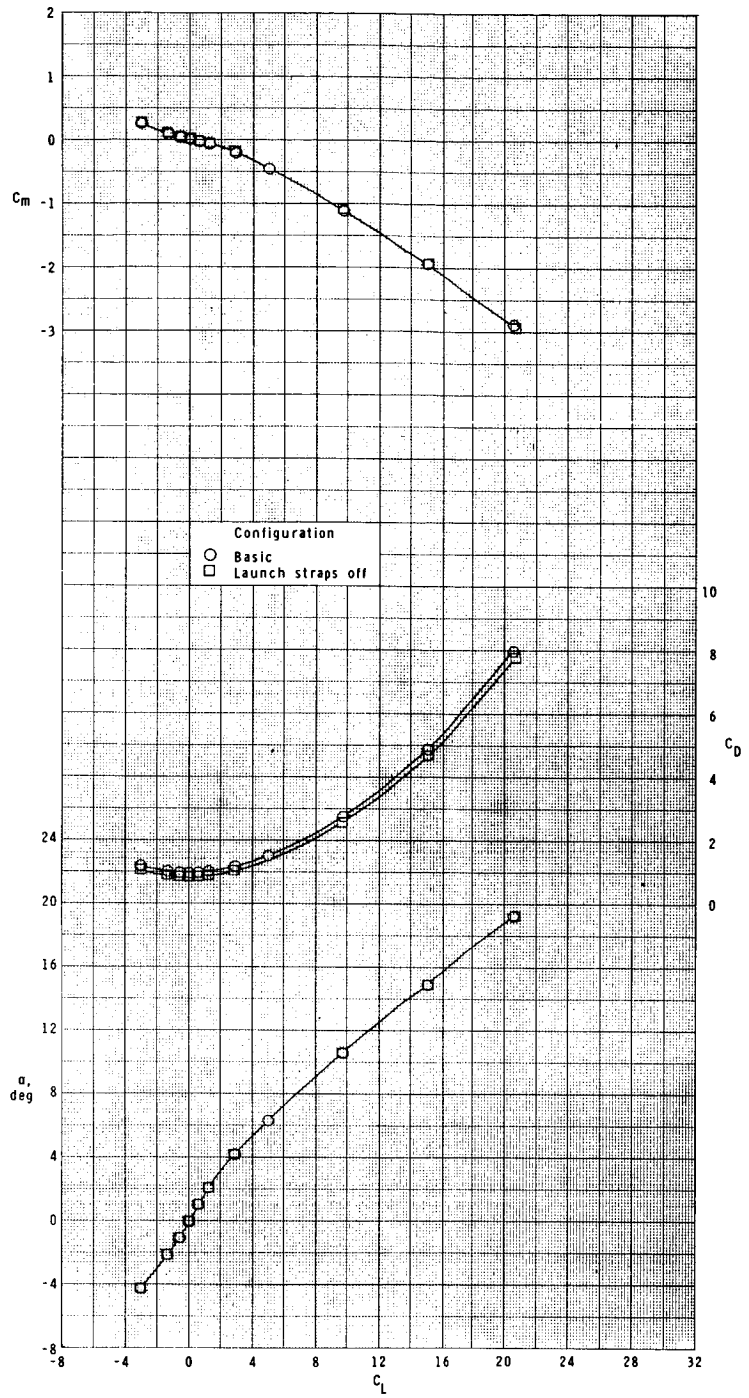

(b) Concluded.

Figure 6.- Continued.

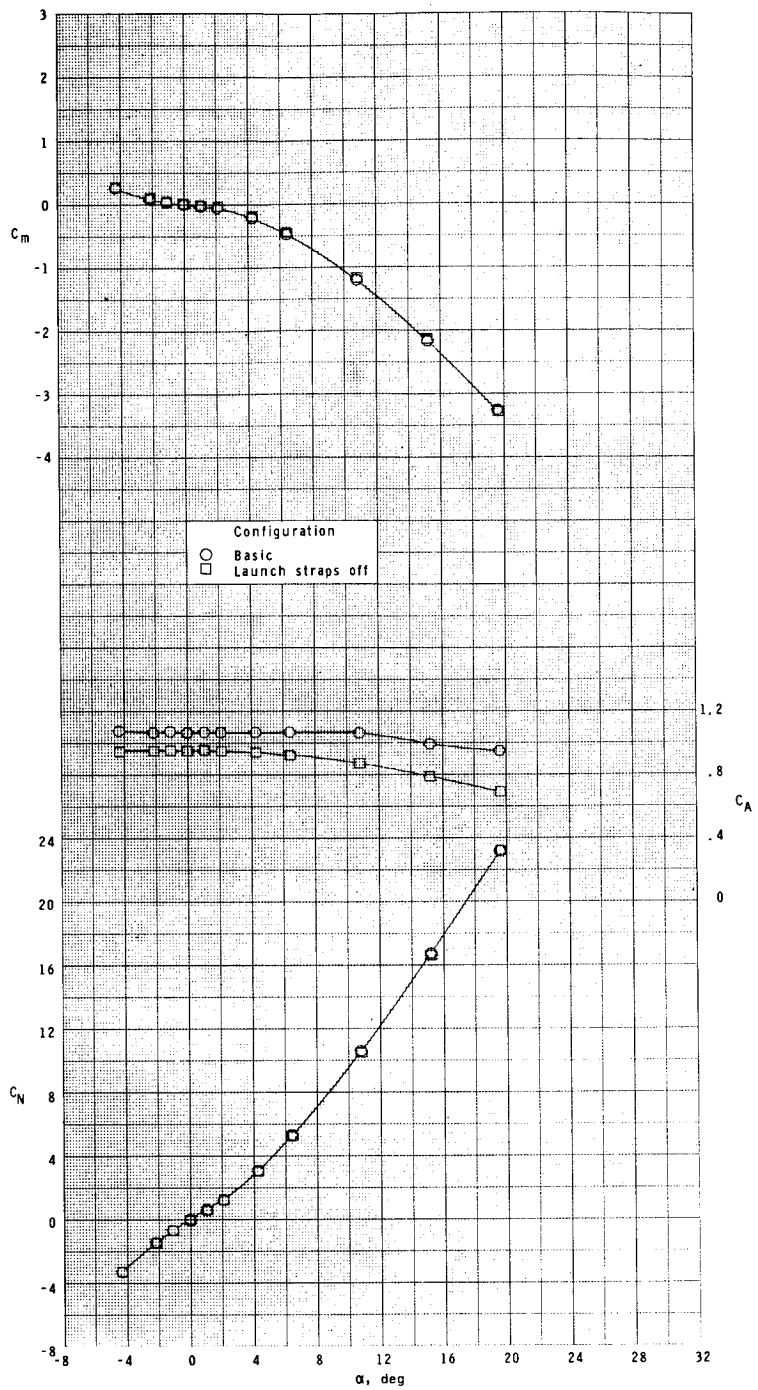

(c) M = 0.80.

Figure 6.- Continued.

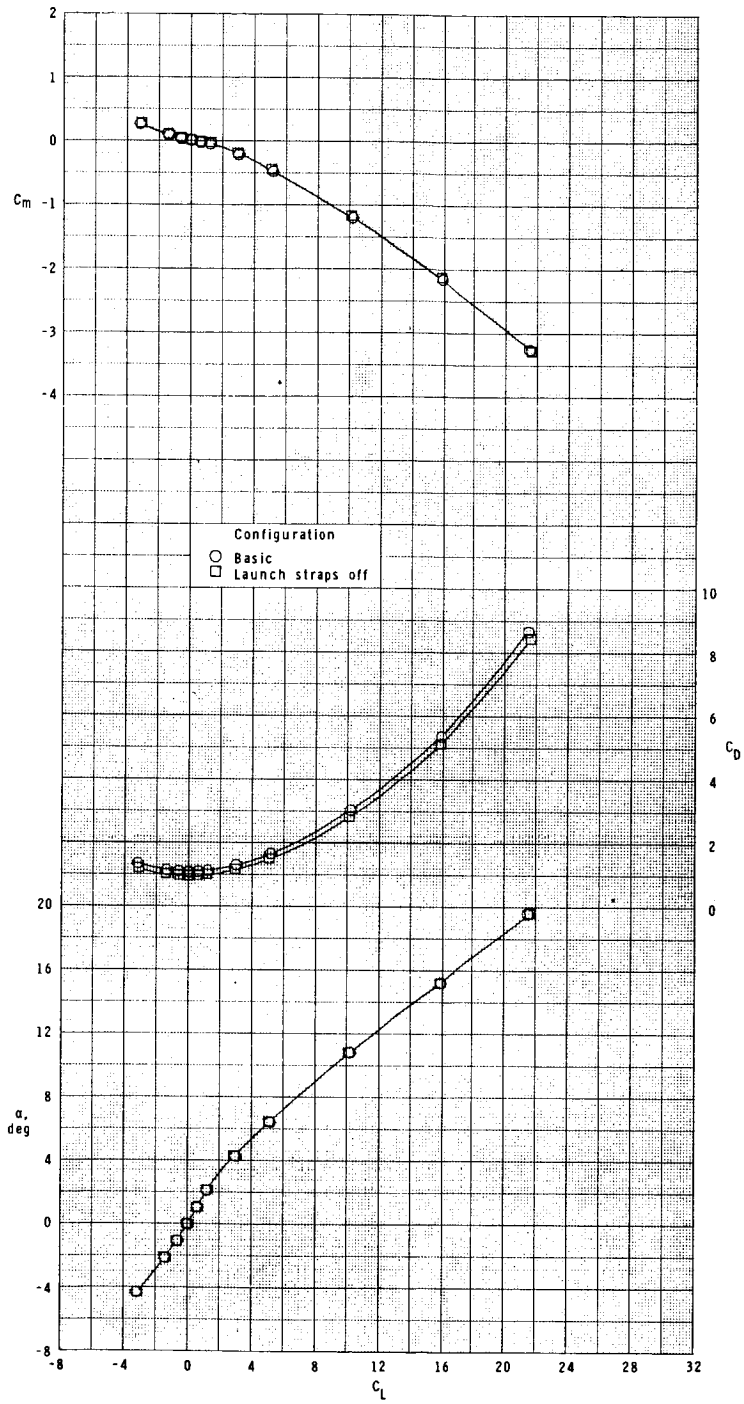

(c) Concluded.

Figure 6.- Continued.

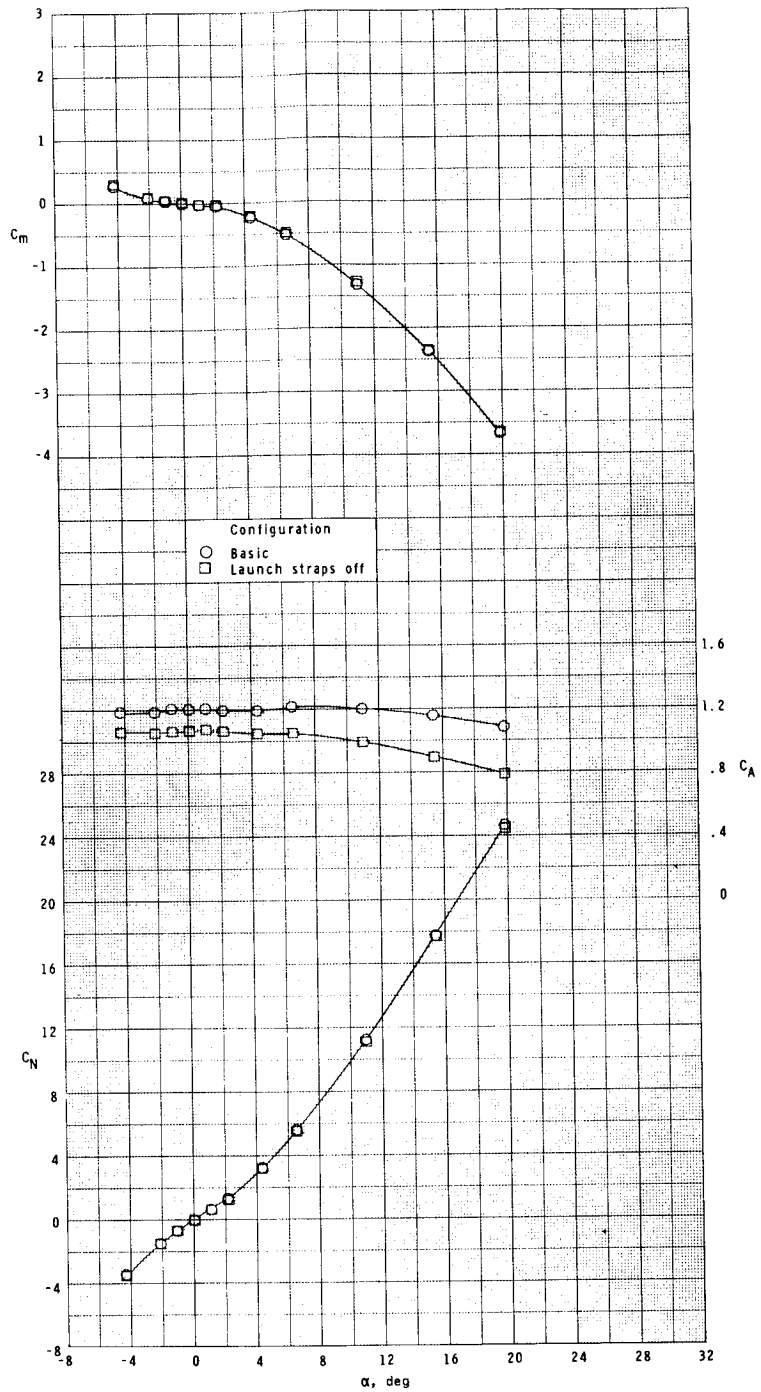

(d) M = 0.90.

Figure 6.- Continued.

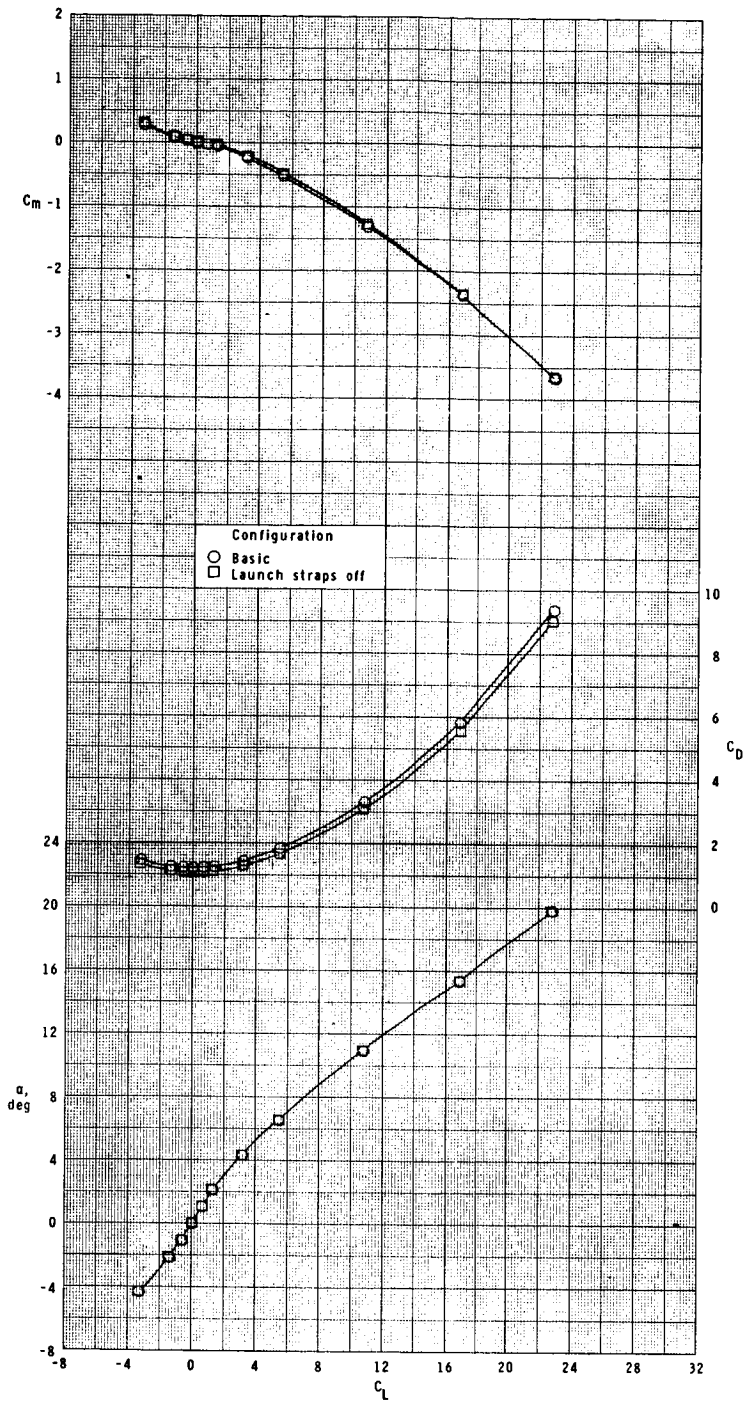

(d) Concluded.

Figure 6.- Continued.

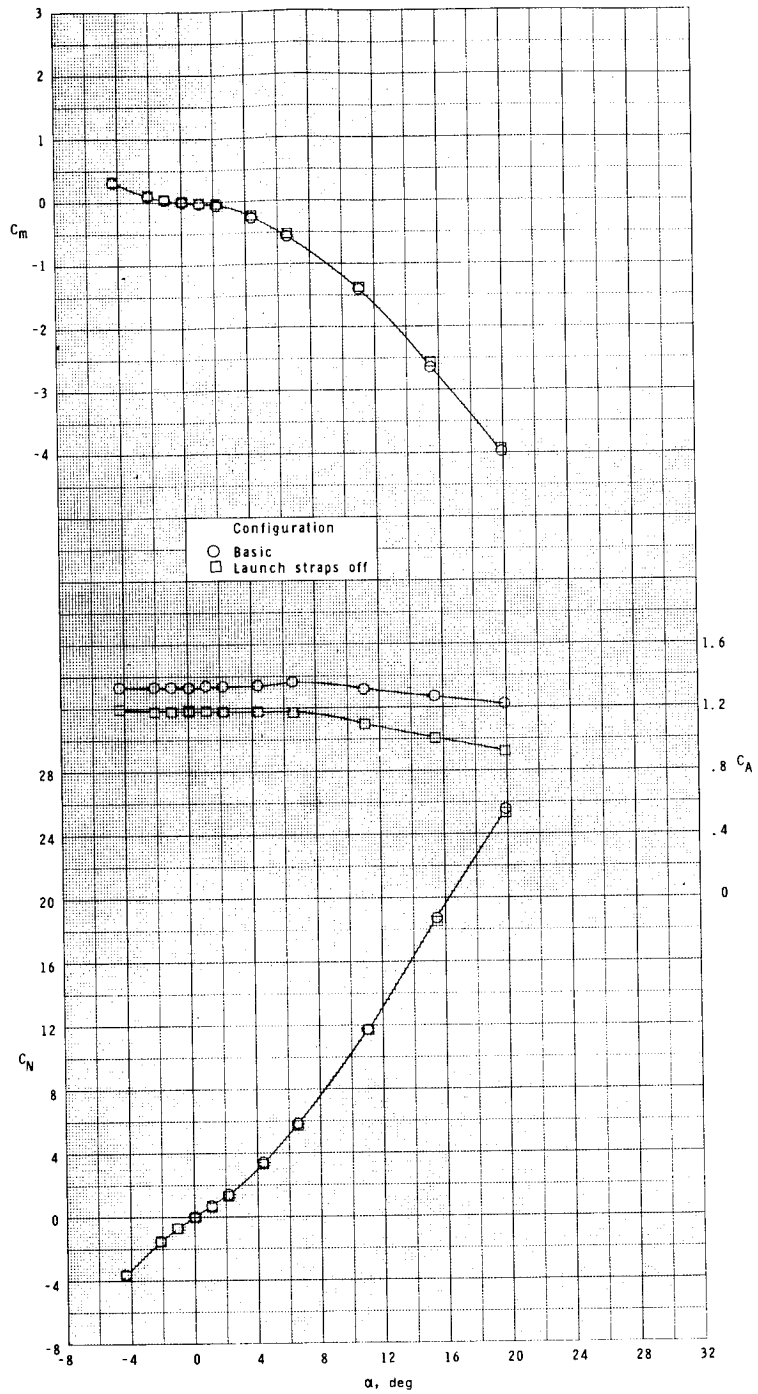

(e) M = 0.95.

Figure 6.- Continued.

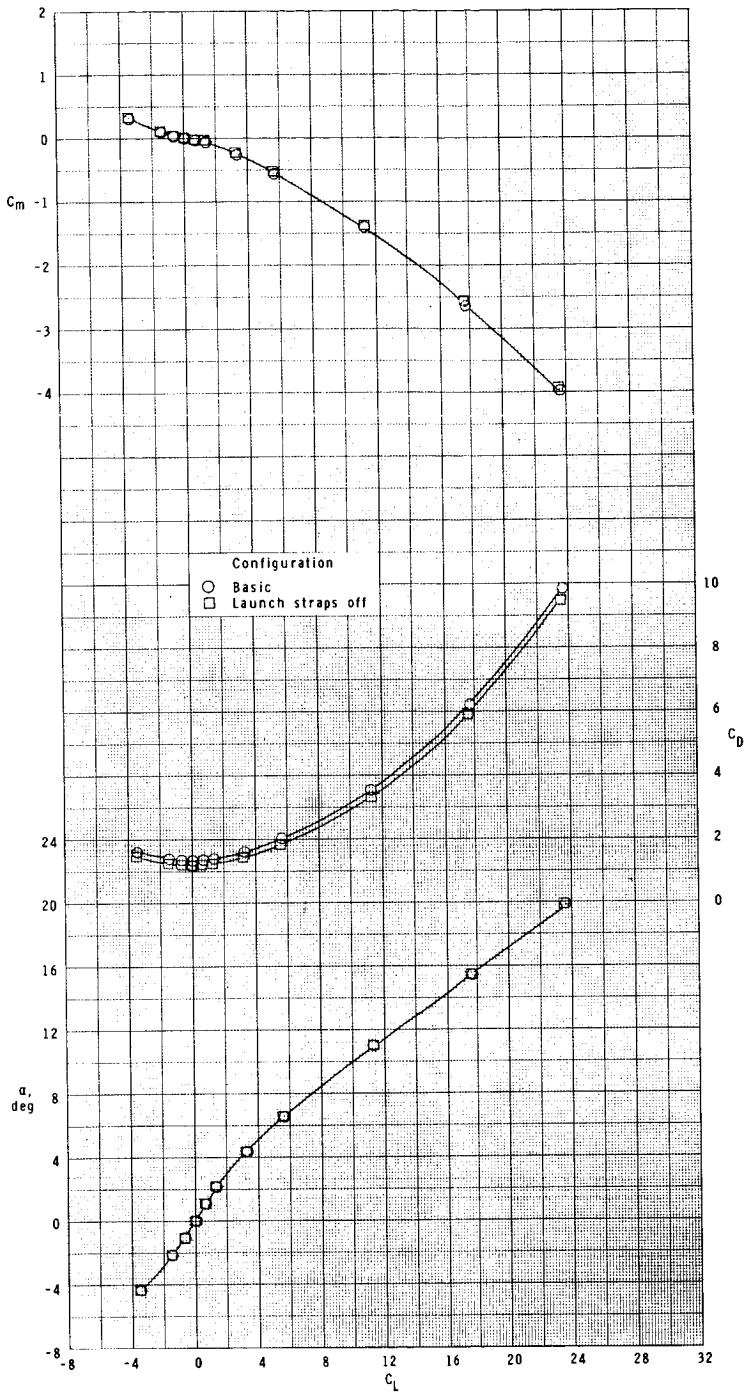

(e) Concluded.

Figure 6.- Continued.

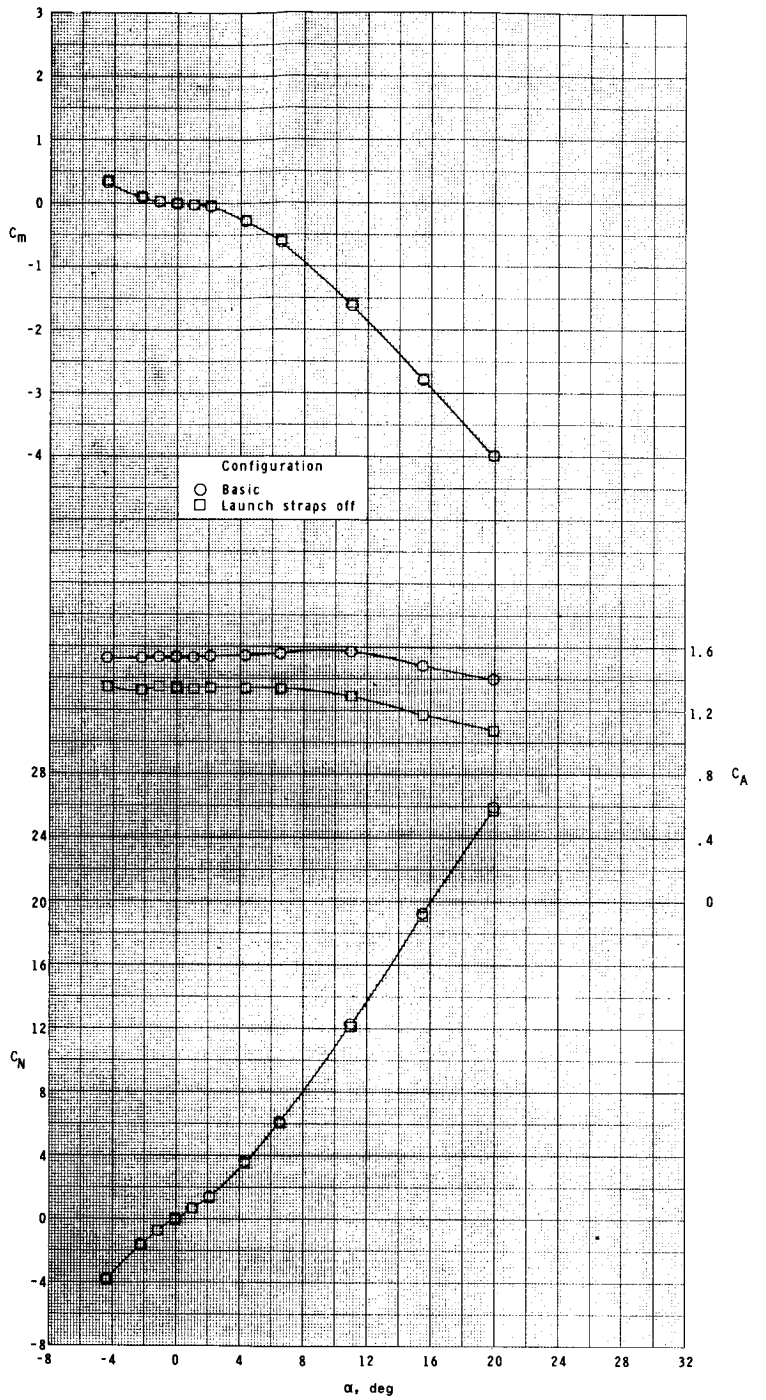

(f) M = 1.00.

Figure 6.- Continued.

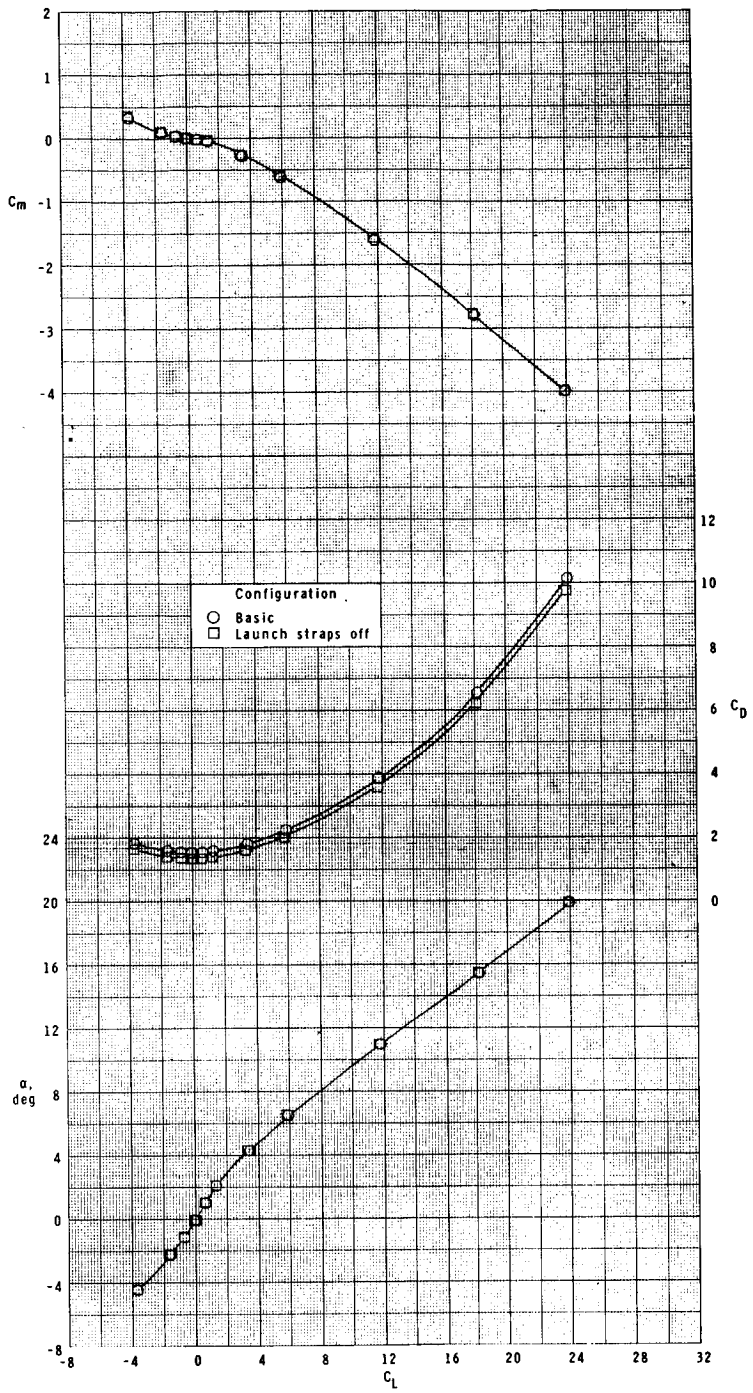

(f) Concluded.

Figure 6.- Continued.

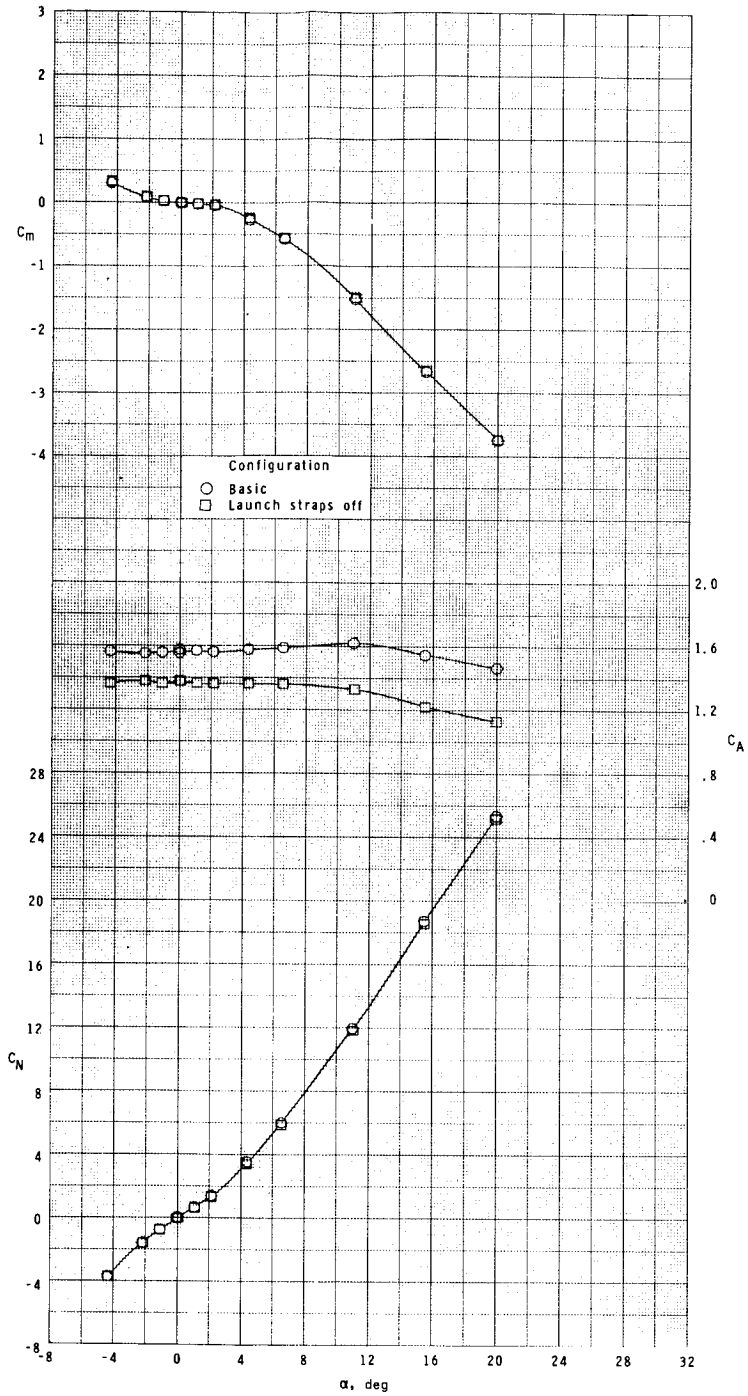

(g) M = 1.03.

Figure 6.- Continued.

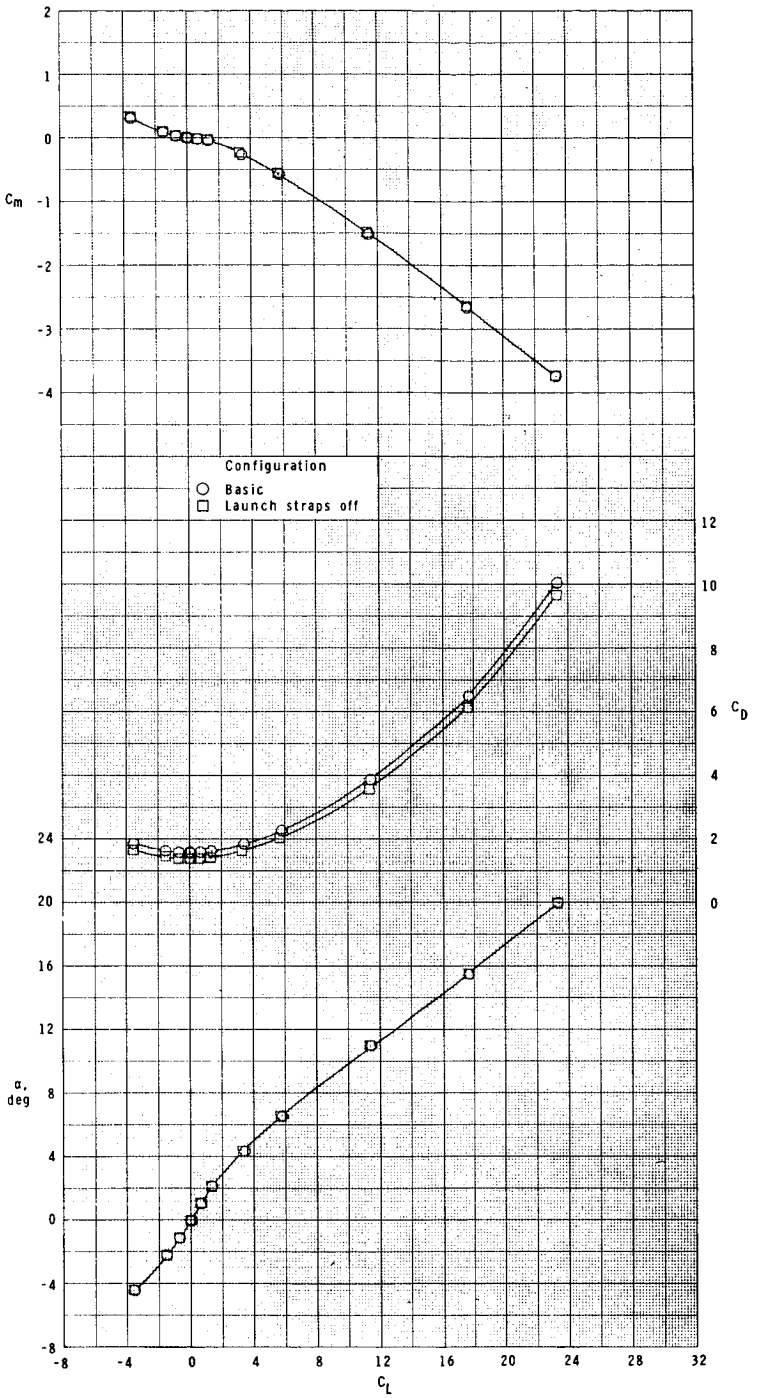

(g) Concluded.

Figure 6.- Continued.

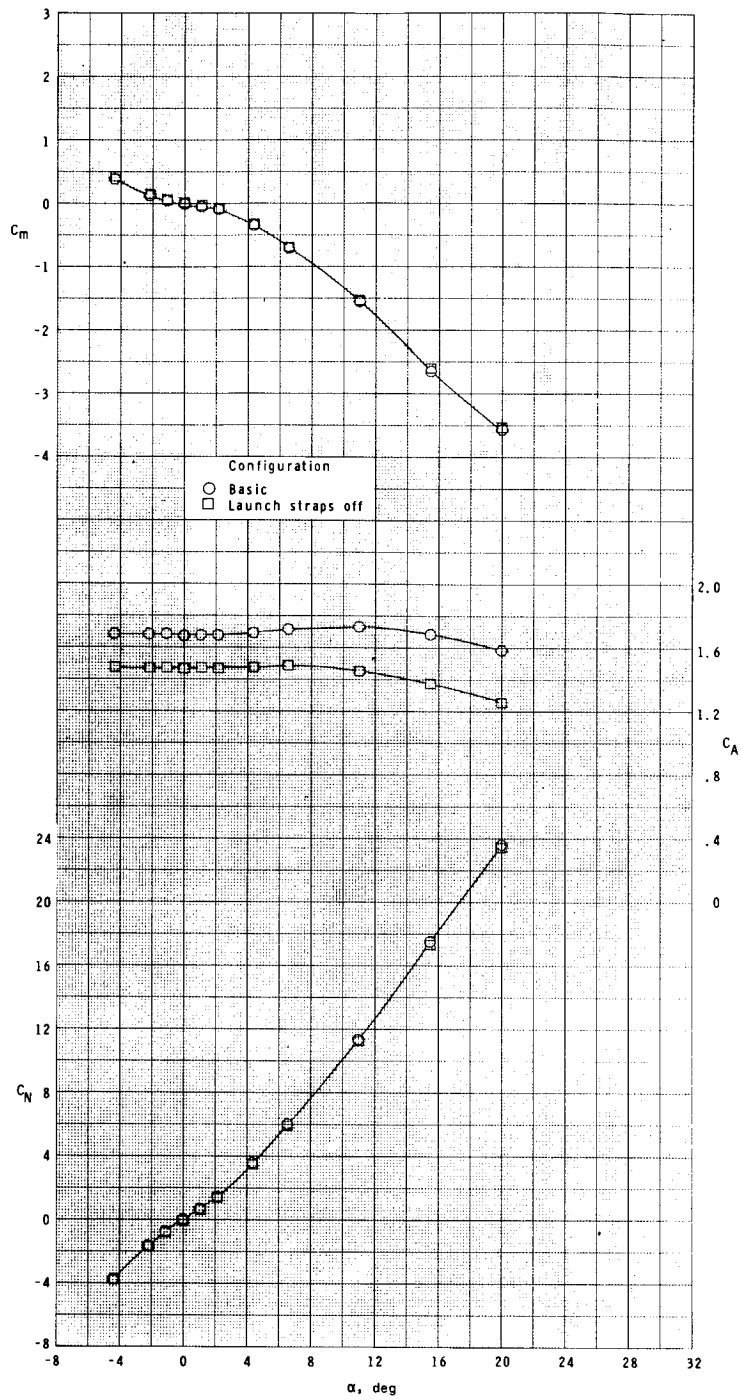

(h) M = 1.20.

Figure 6.- Continued.

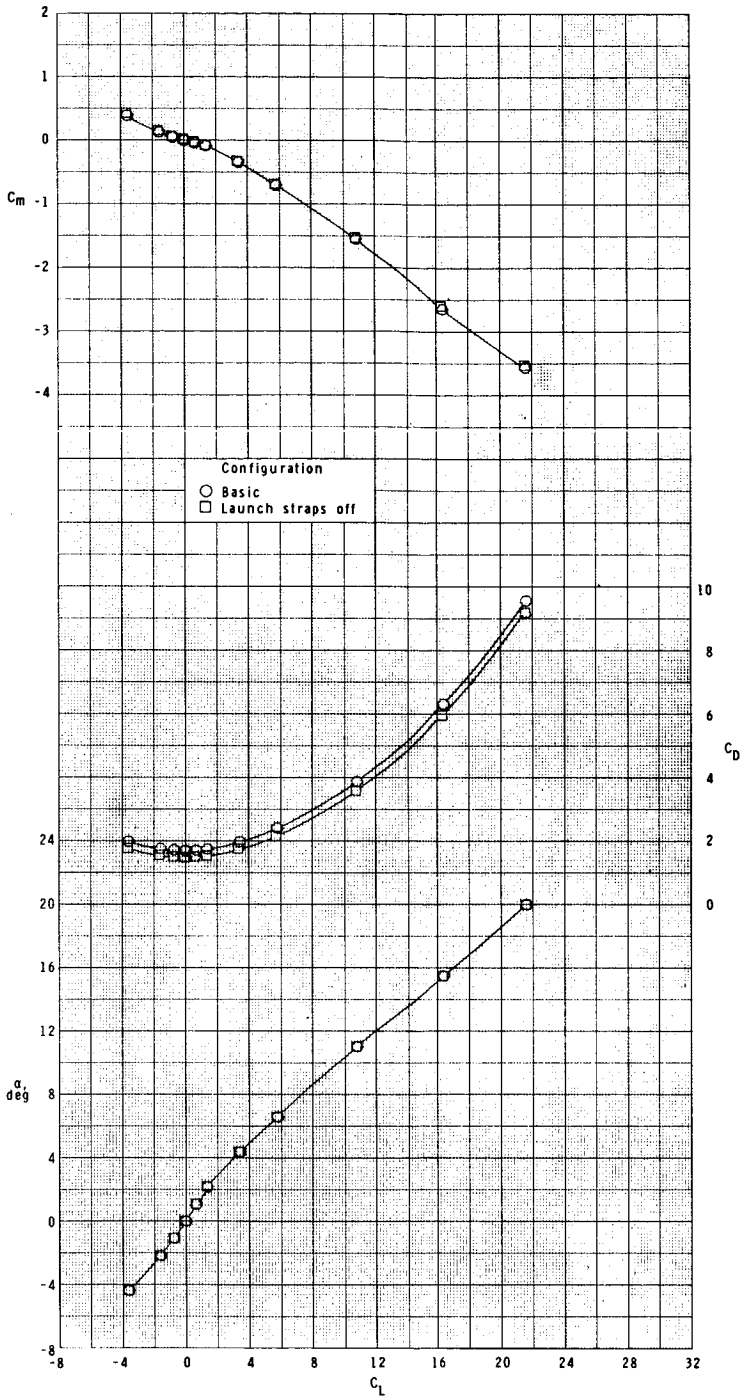

(h) Concluded.

Figure 6.- Continued.

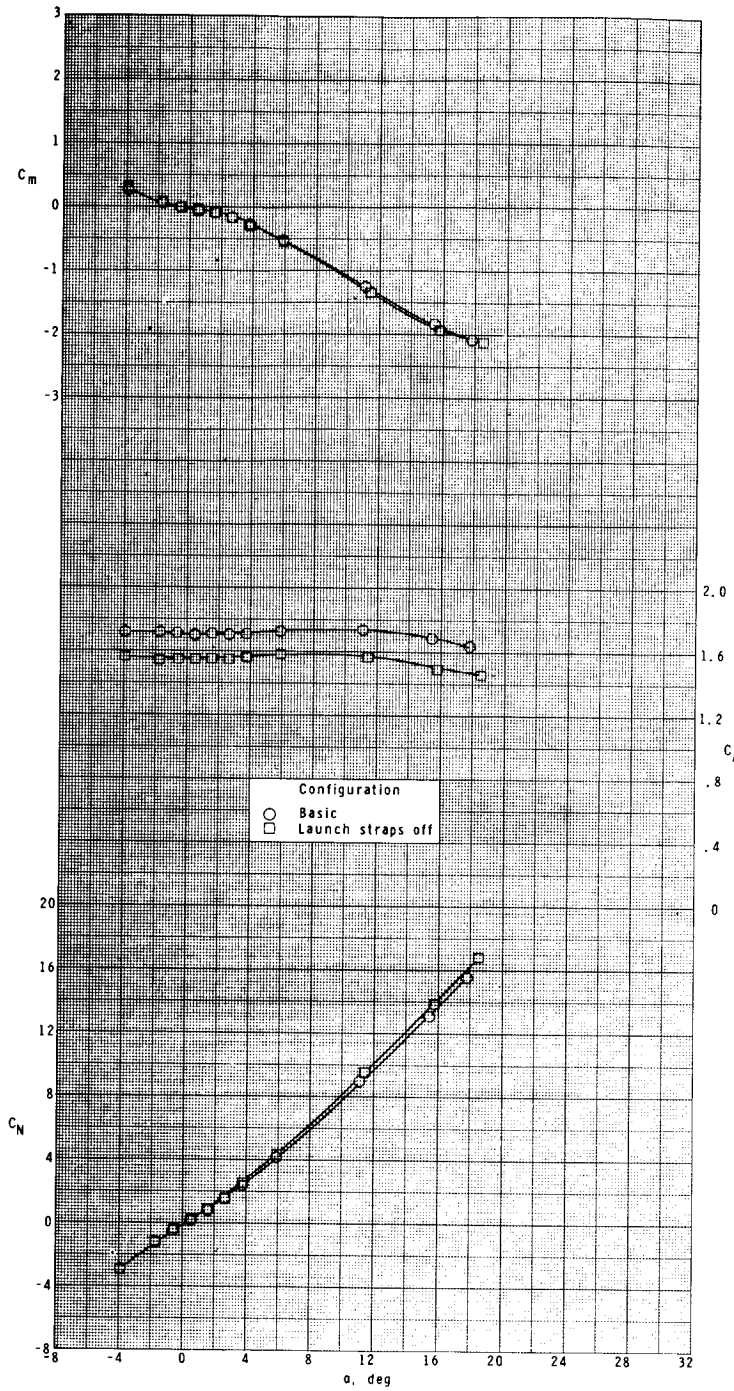

(i) M = 1.75.

Figure 6.- Continued.

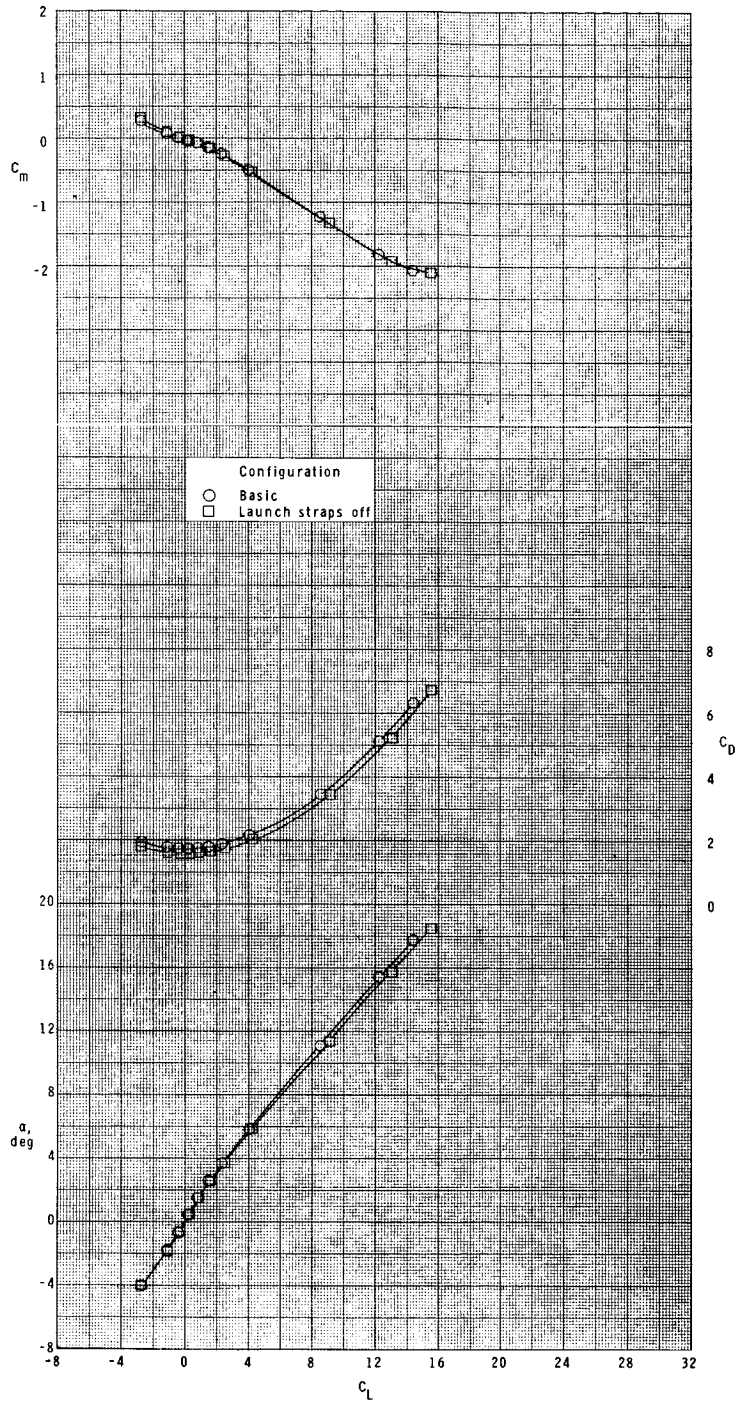

(i) Concluded.

Figure 6.- Continued.

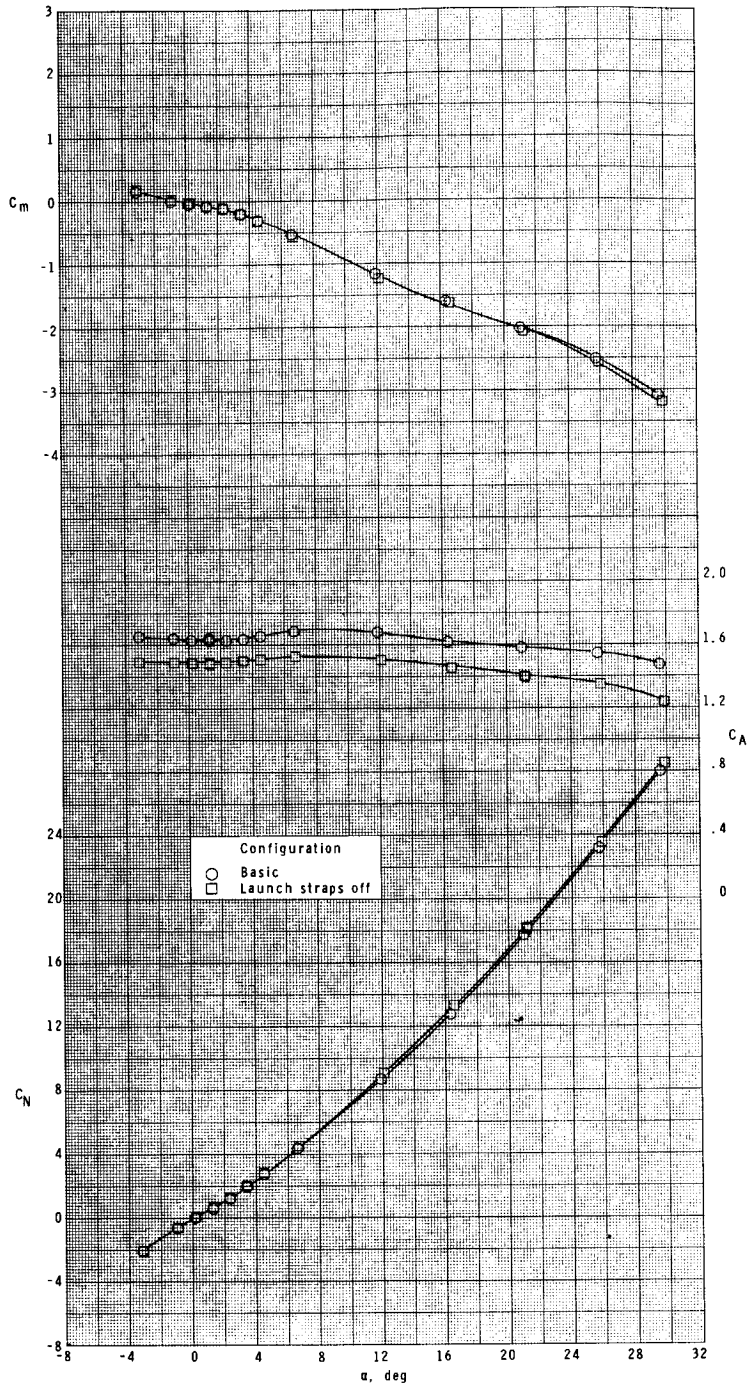

(j) M = 2.10.

Figure 6.- Continued.

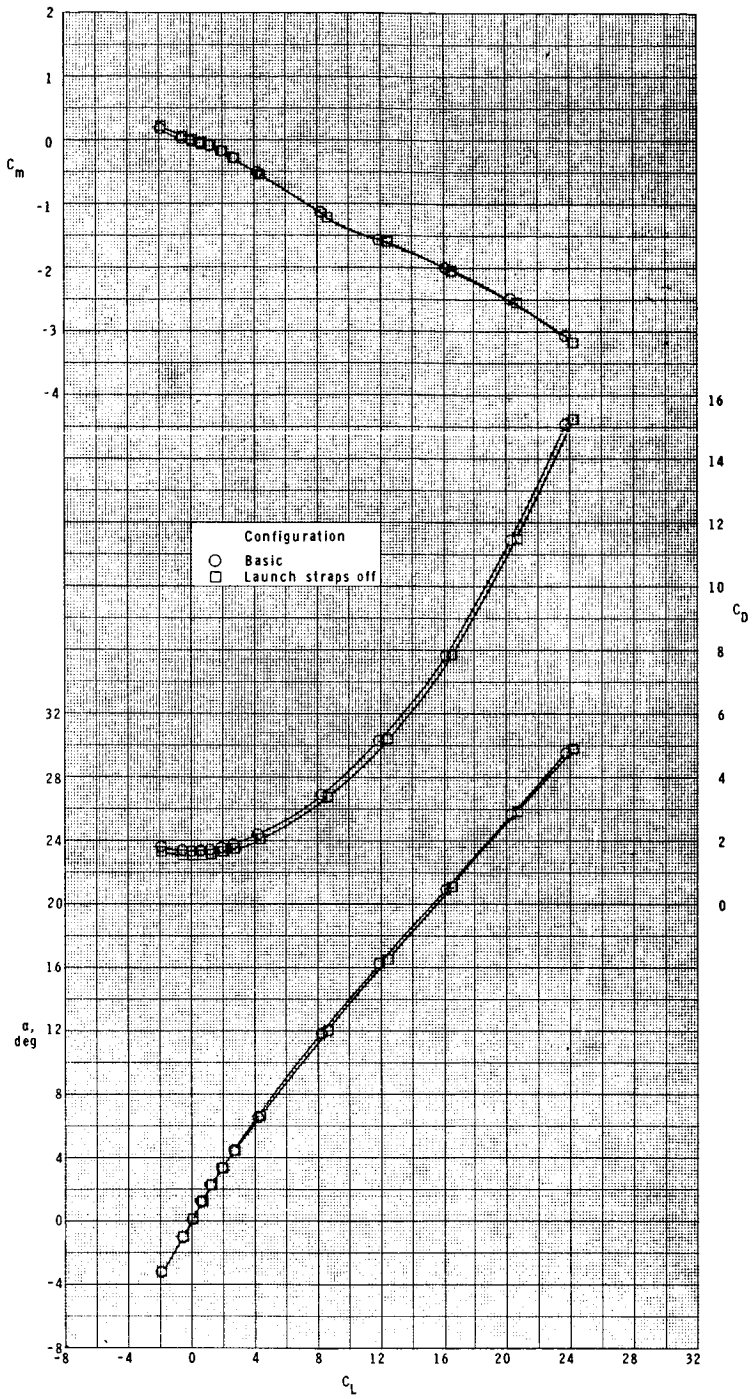

(j) Concluded.

Figure 6.- Continued.

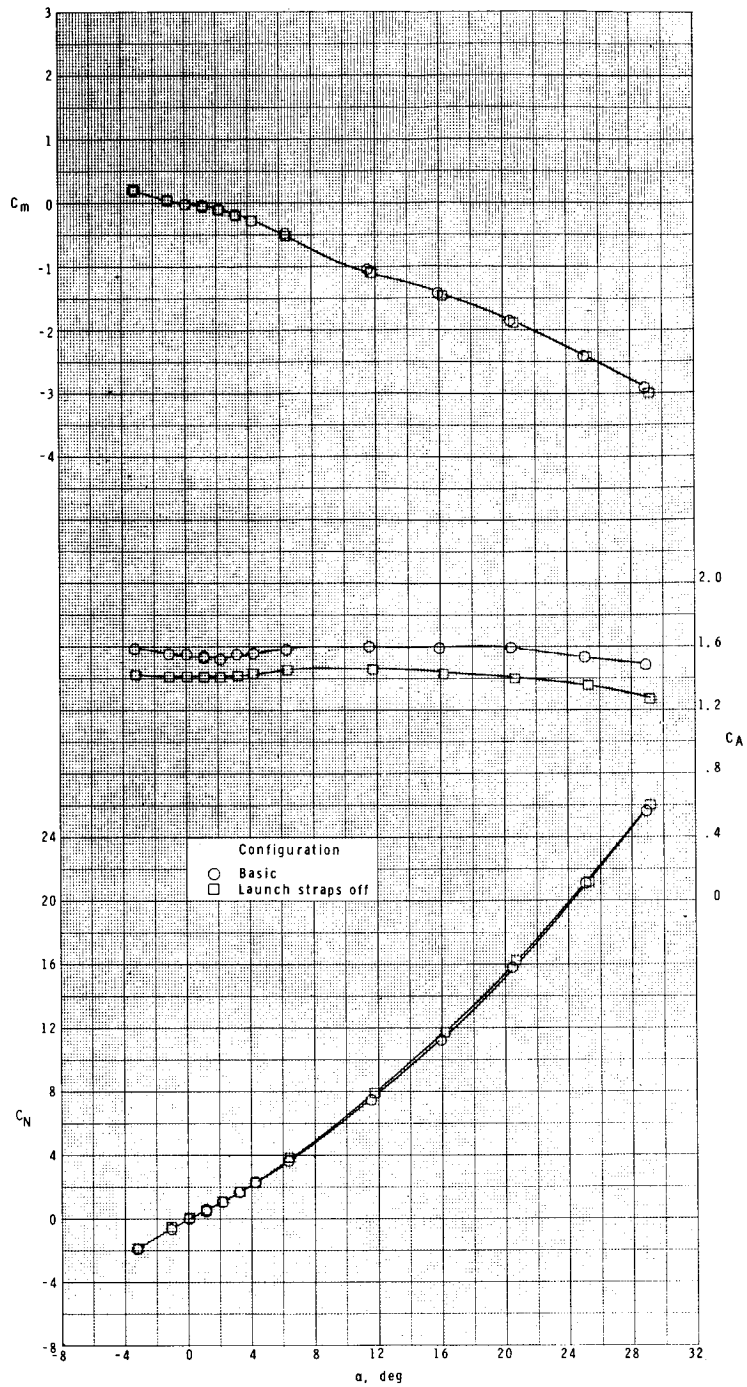

(k) M = 2.50.

Figure 6.- Continued.

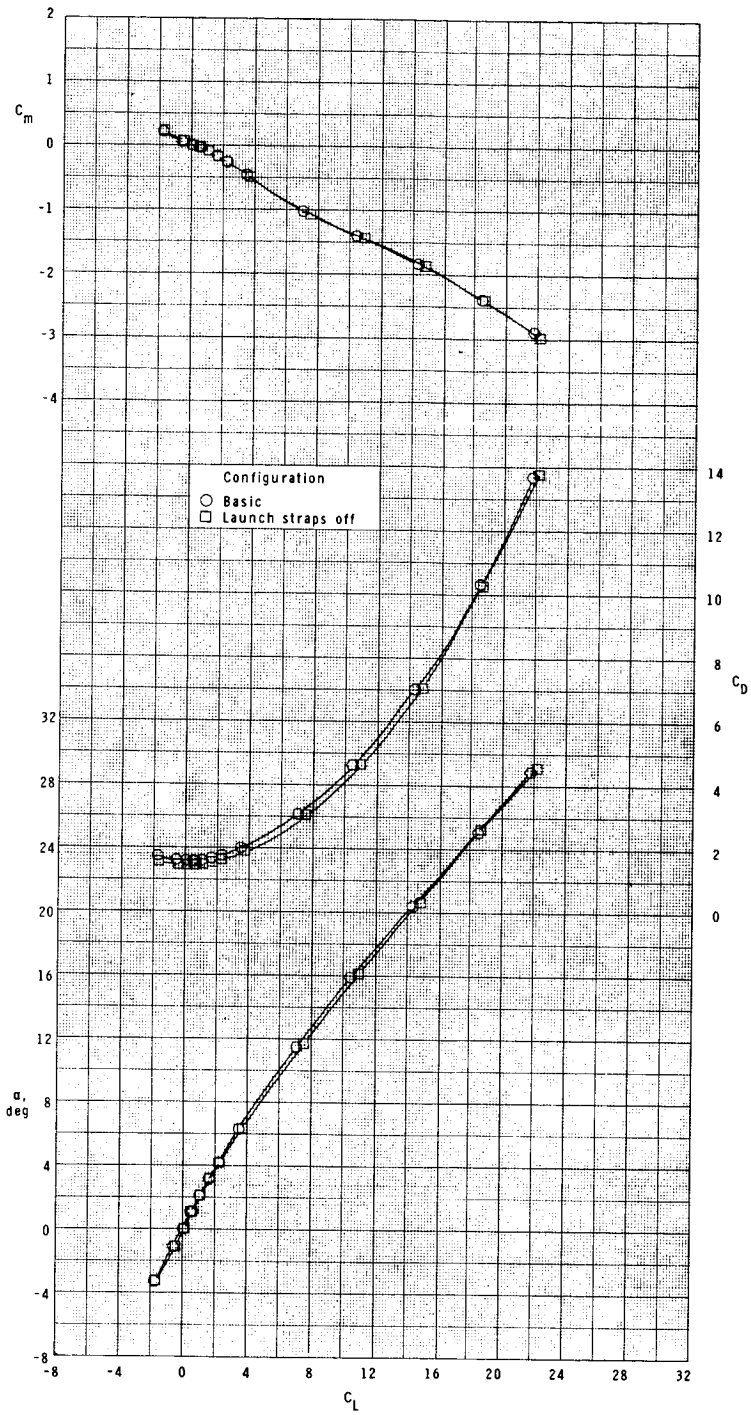

(k) Concluded.

Figure 6.- Continued.

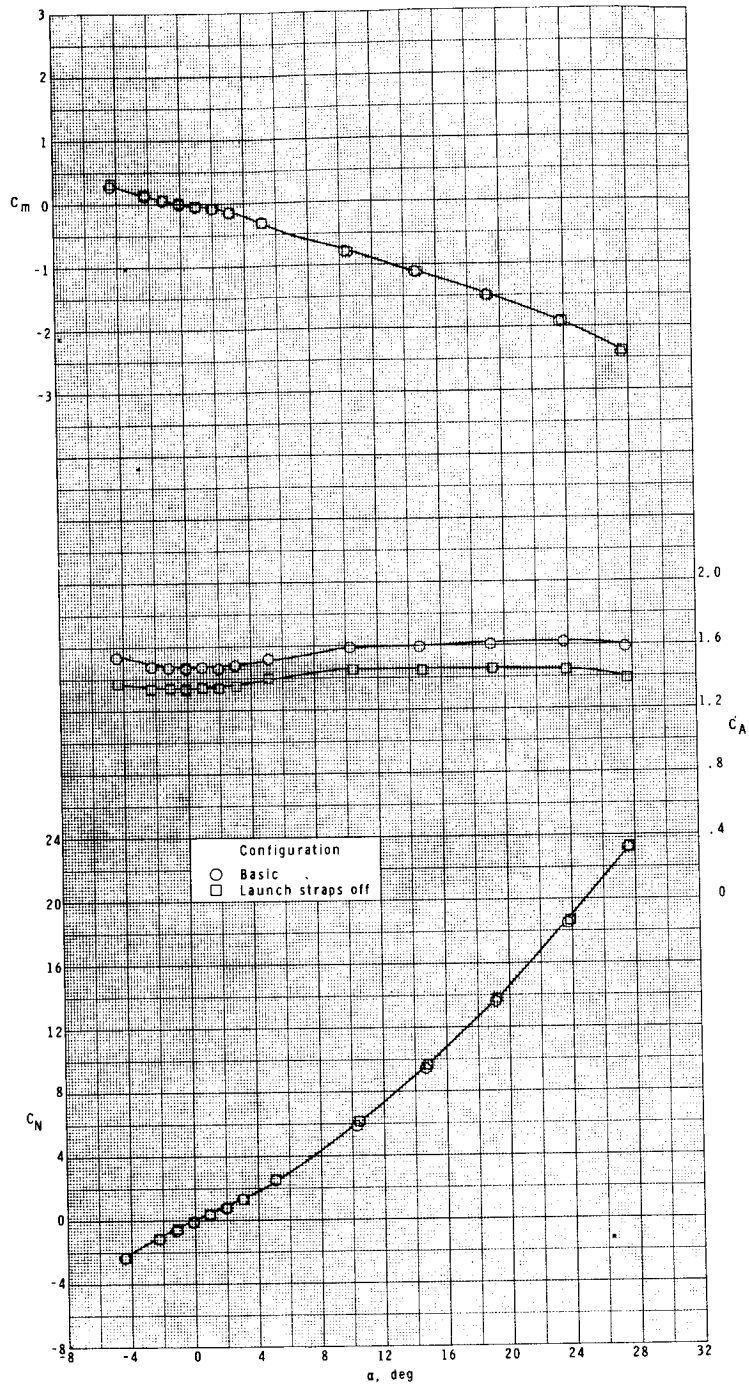

(l) M = 2.86.

Figure 6.- Continued.

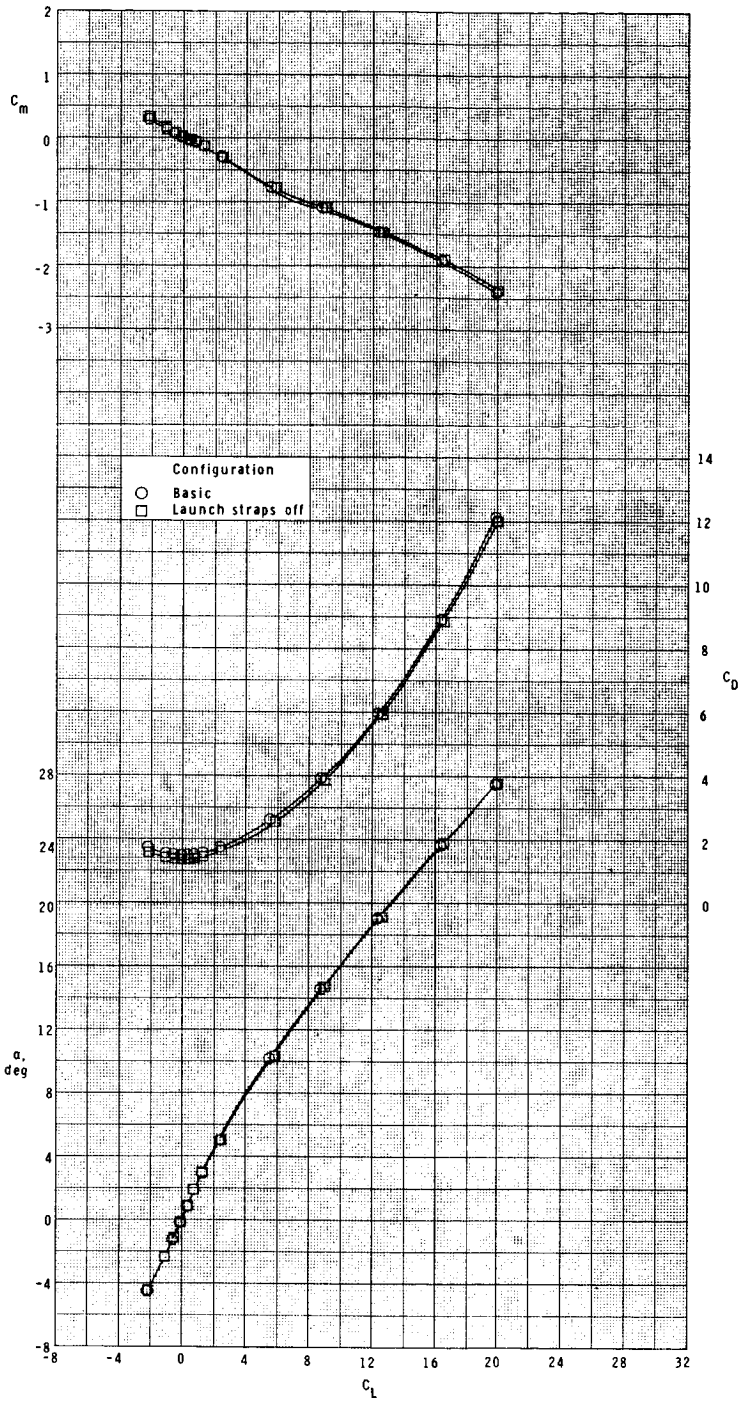

(l) Concluded.

Figure 6.- Continued.

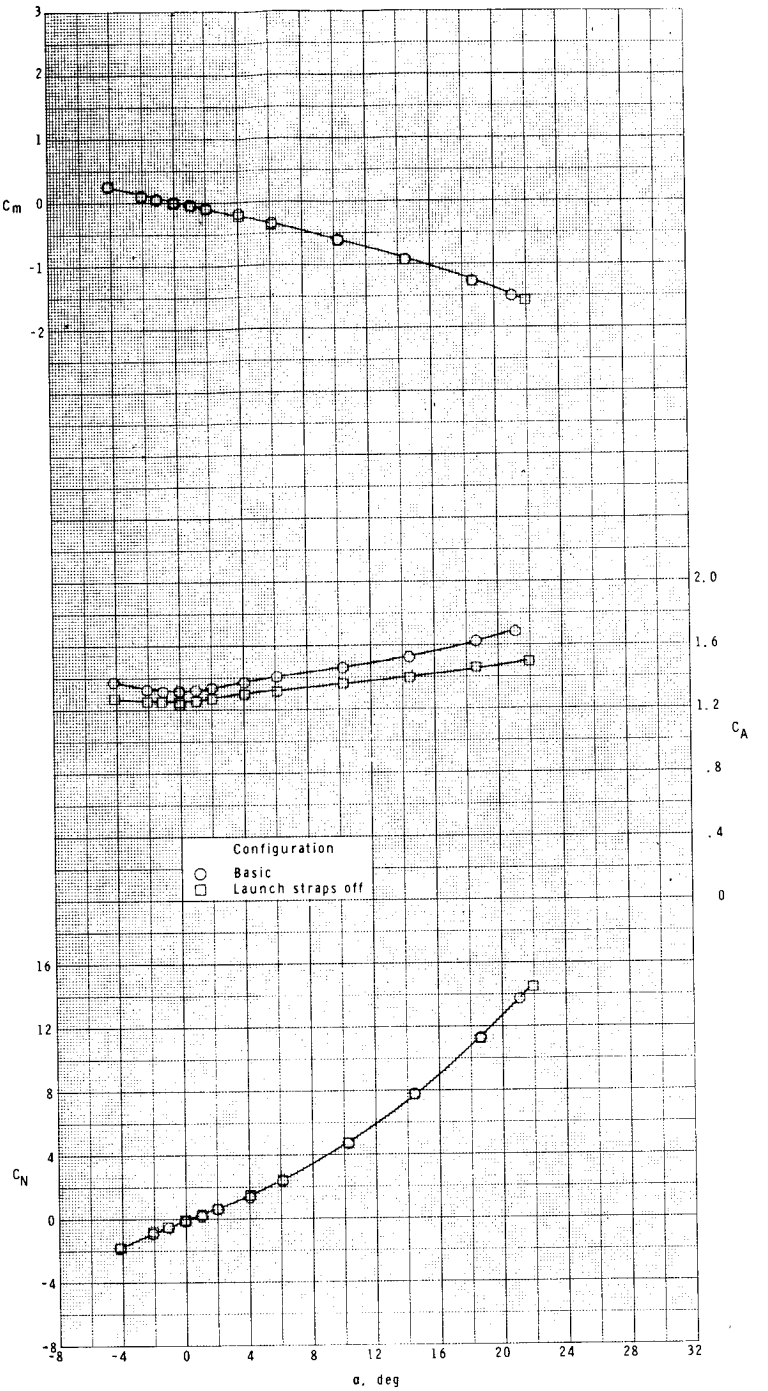

(m) M = 3.95.

Figure 6.- Continued.

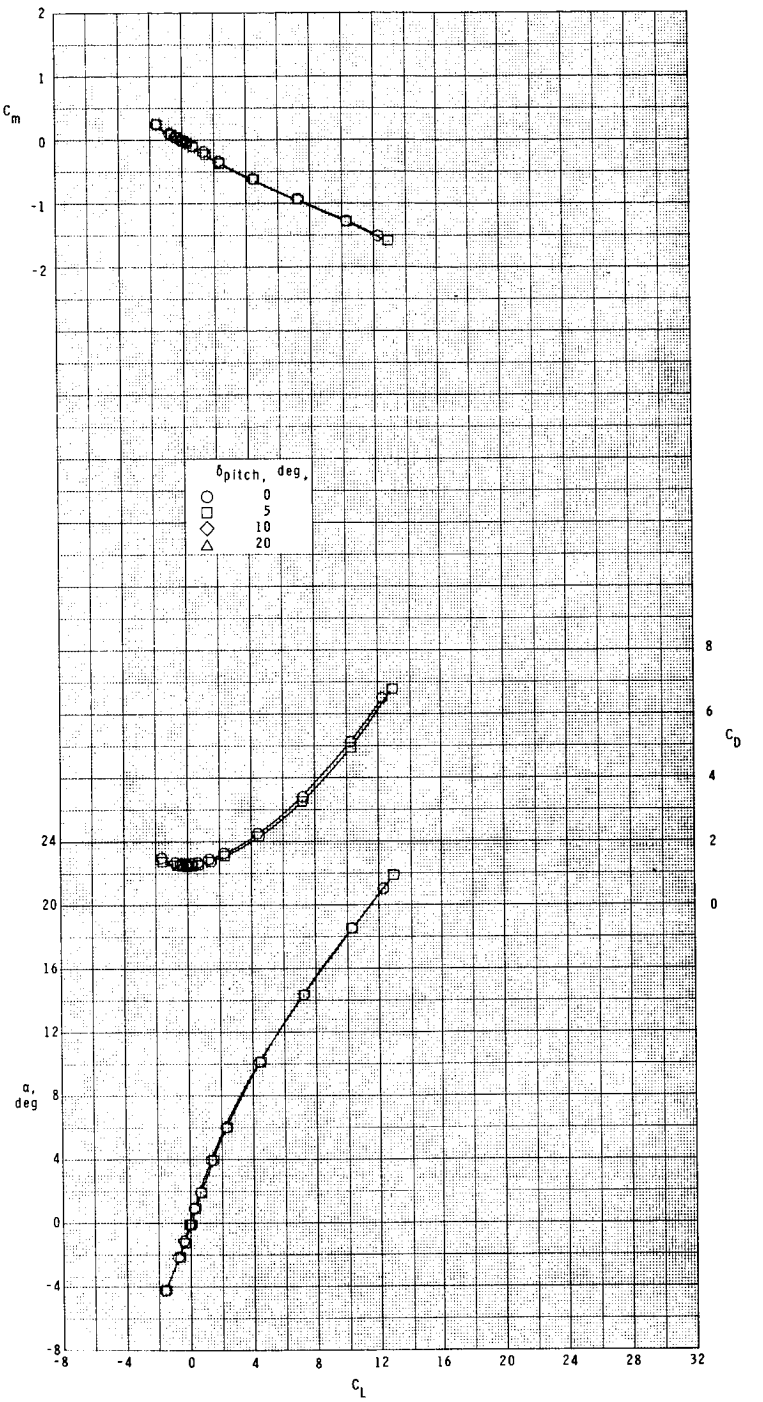

(m) Concluded.

Figure 6.- Continued.

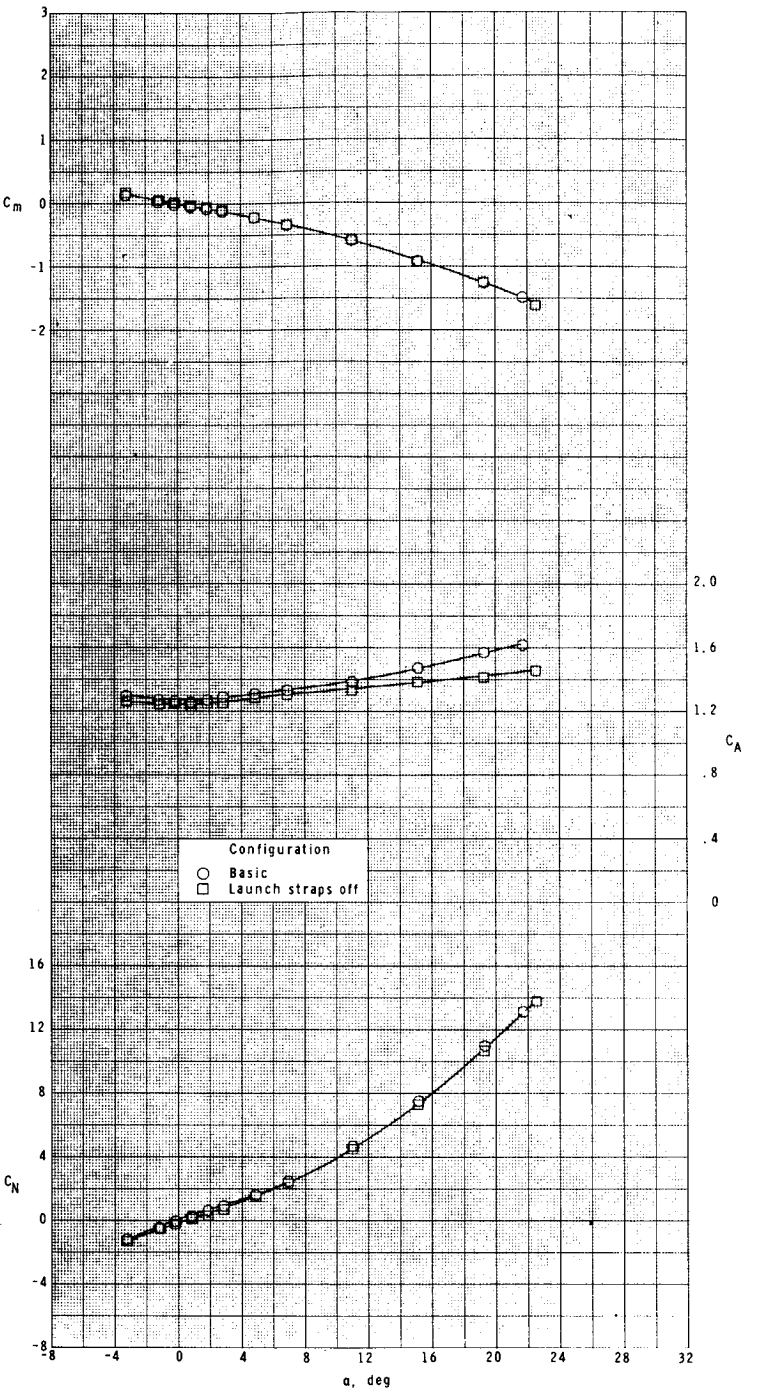

(n) M = 4.63.

Figure 6.- Continued.

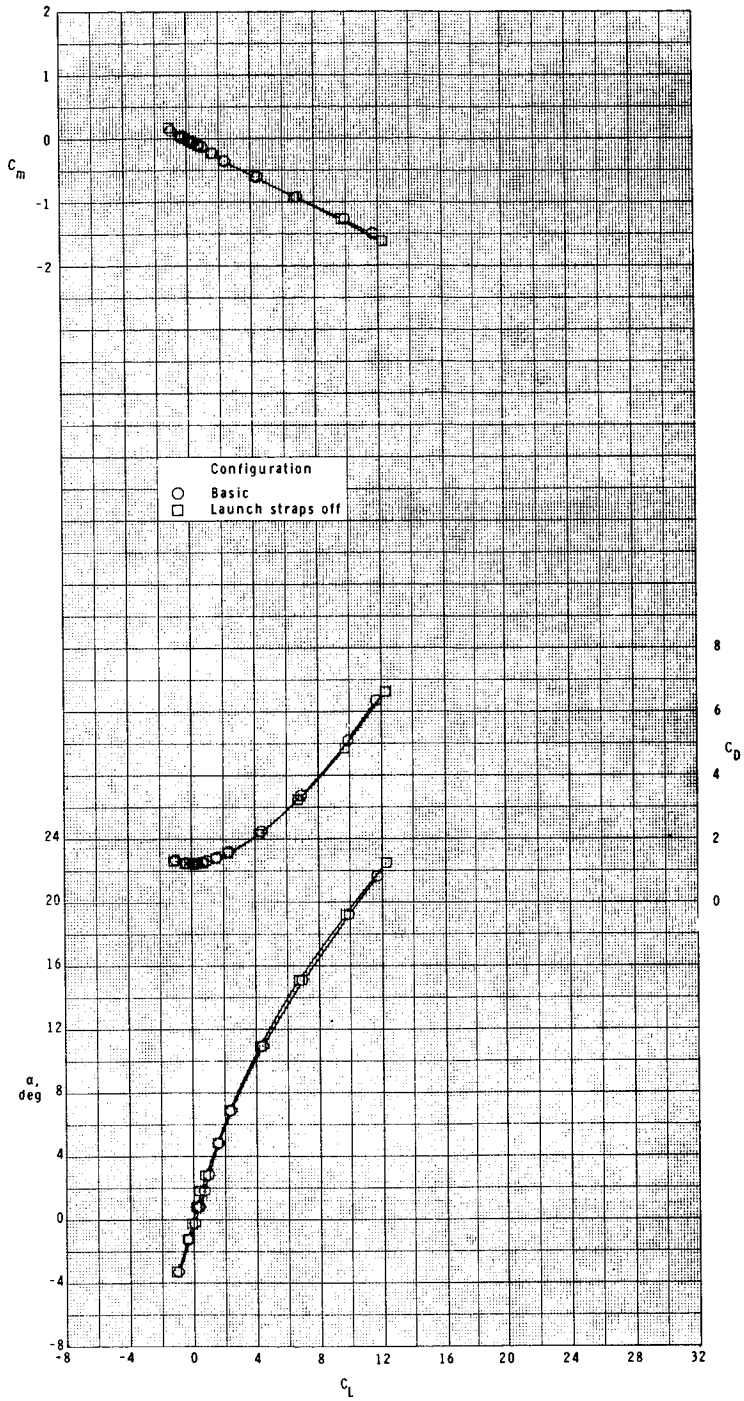

(n) Concluded.

Figure 6.- Concluded.

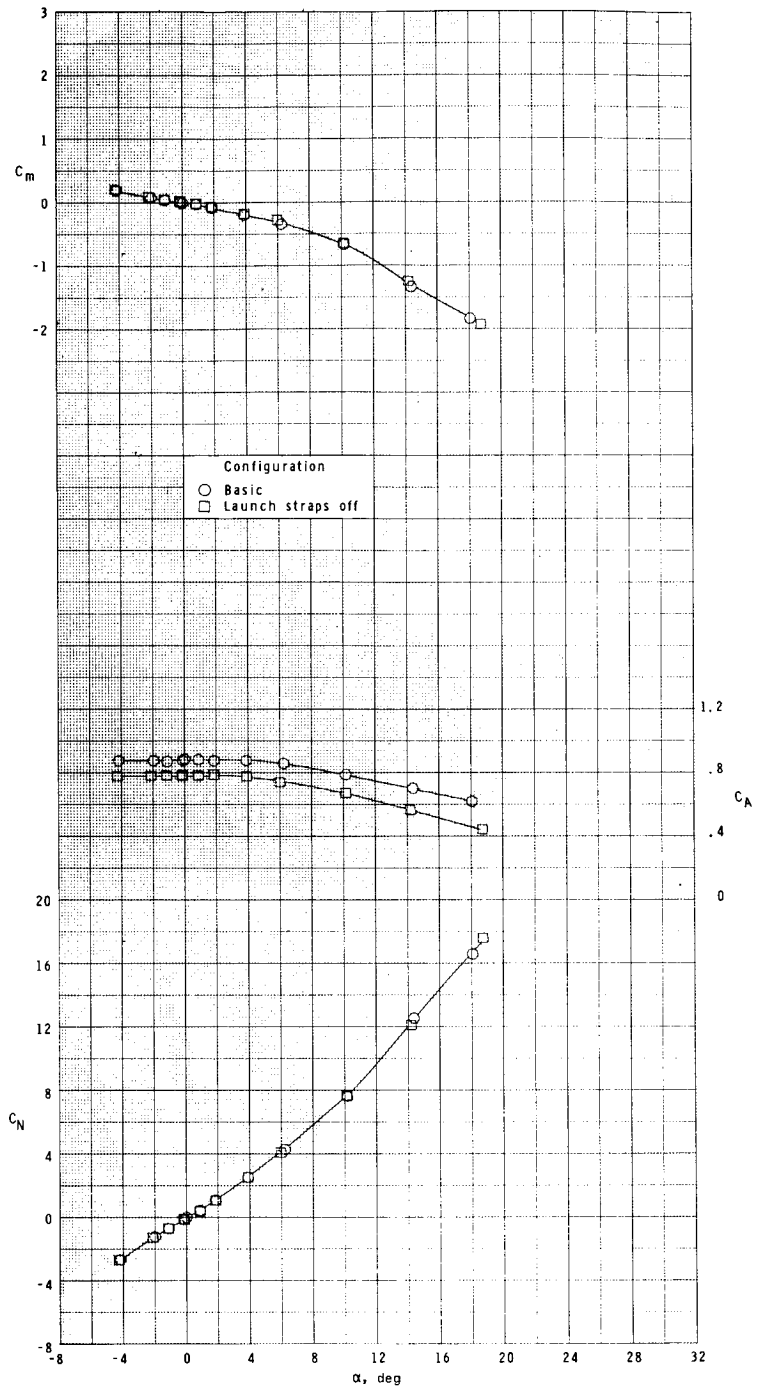

(a) M = 0.20.

Figure 7.- Effect of launch straps on the longitudinal characteristics. $\phi = -45^{o}$.

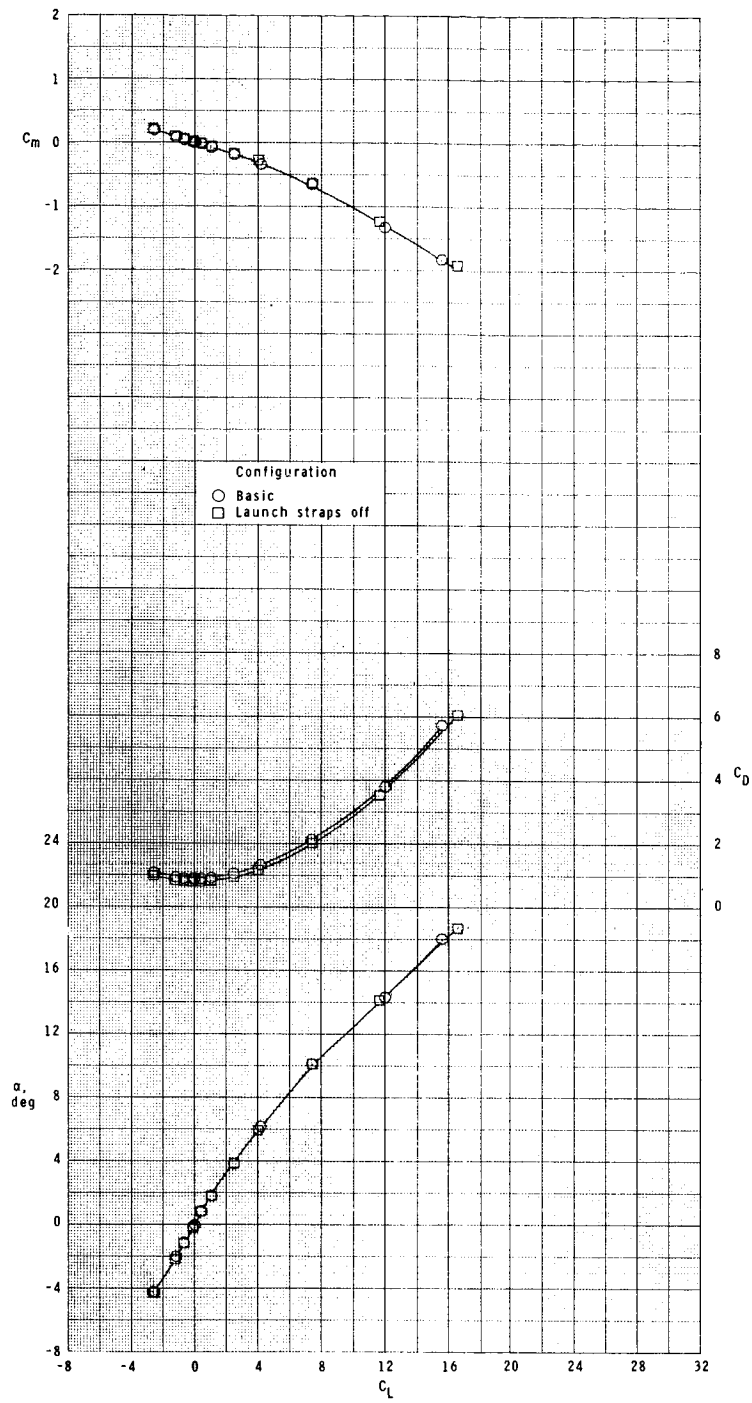

(a) Concluded.

Figure 7.- Continued.

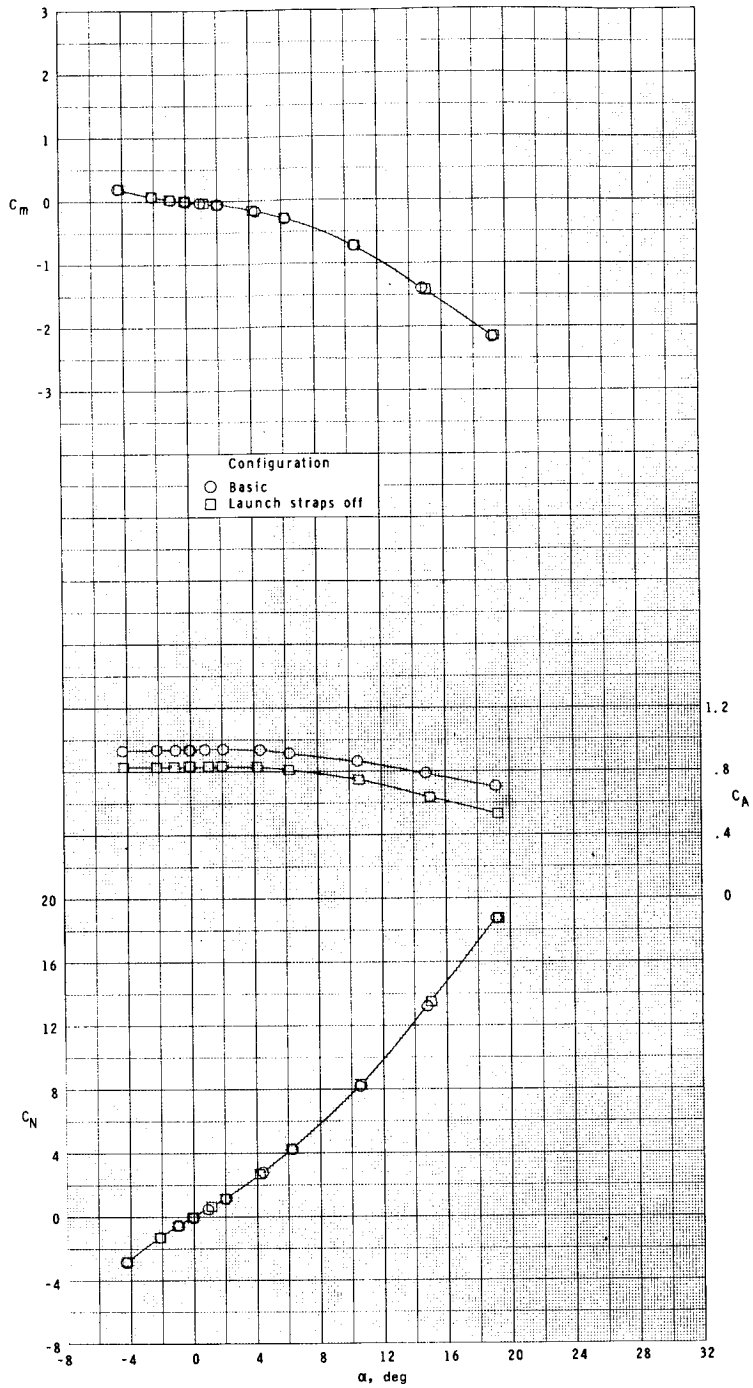

(b) M = 0.60.

Figure 7.- Continued.

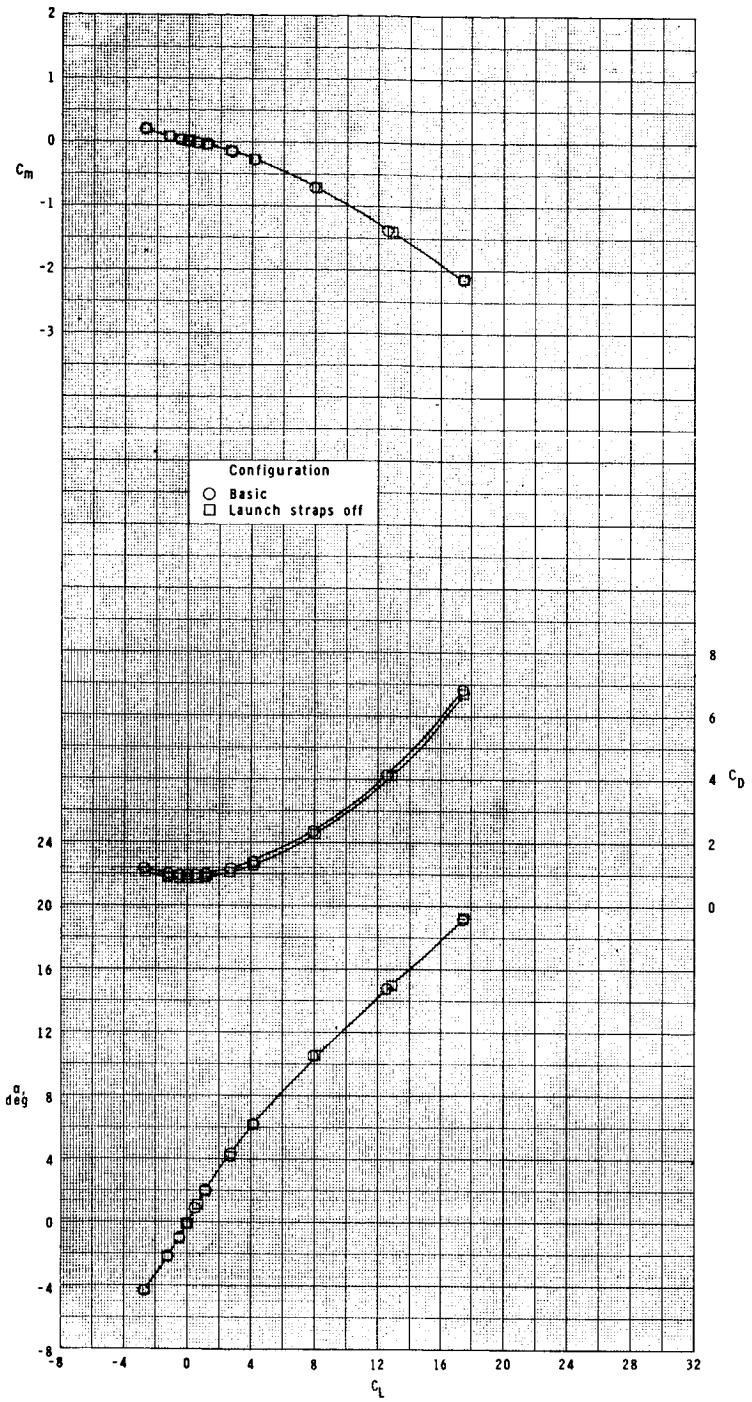

(b) Concluded.

Figure 7.- Continued.

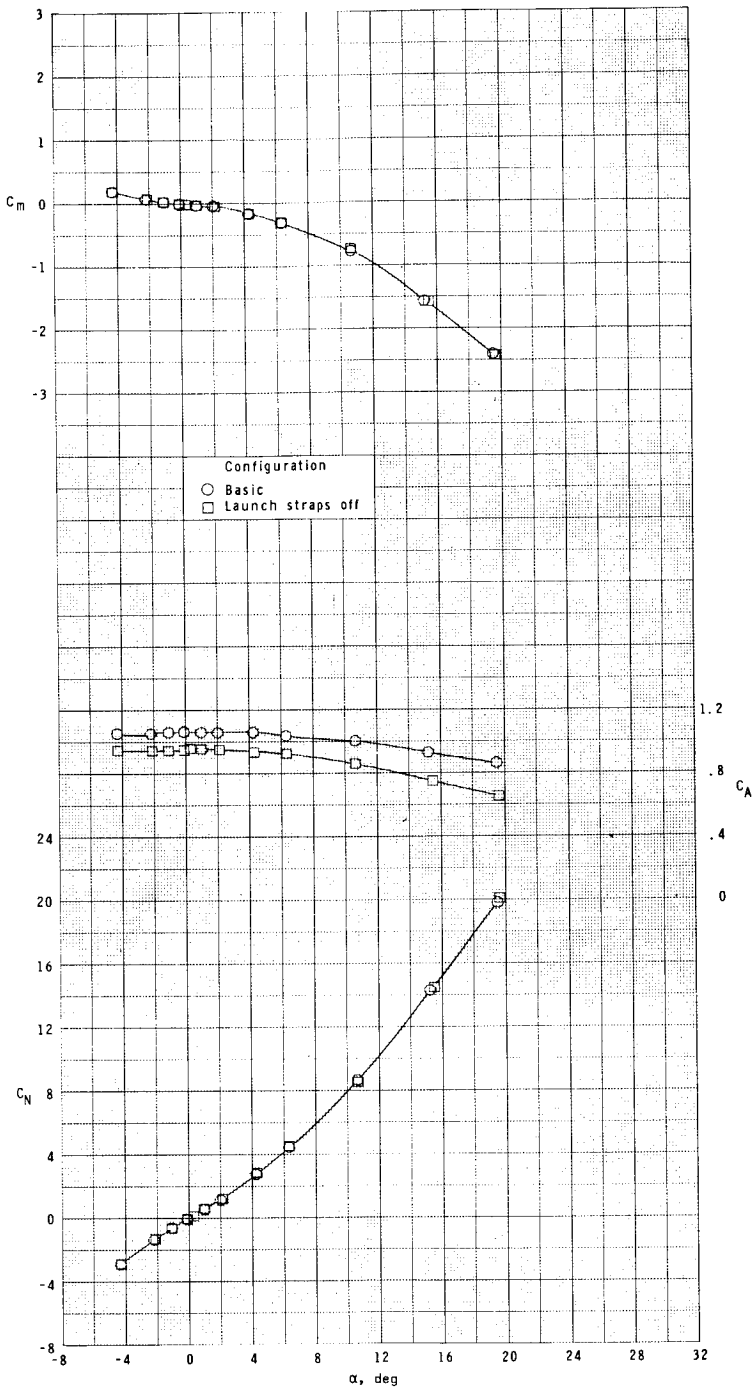

(c) M = 0.80.

Figure 7.- Continued.

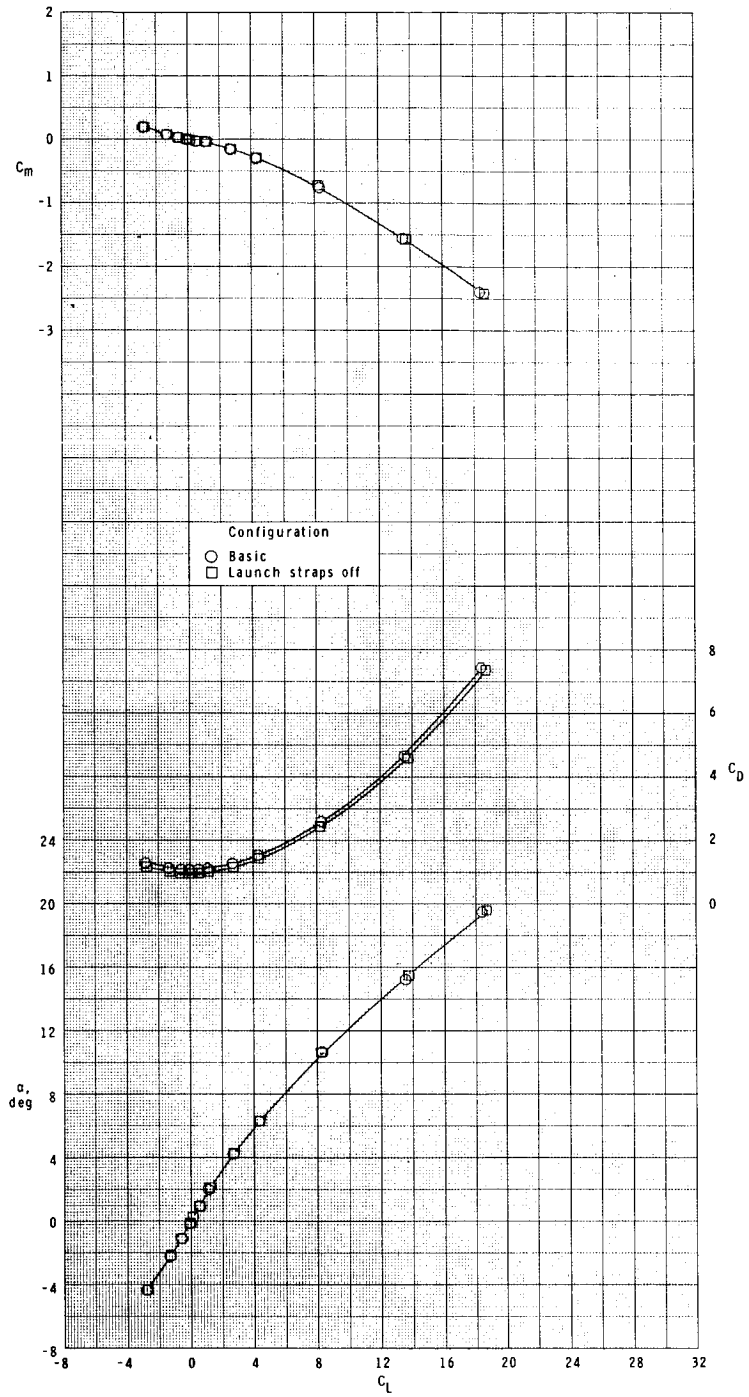

(c) Concluded.

Figure 7.- Continued.

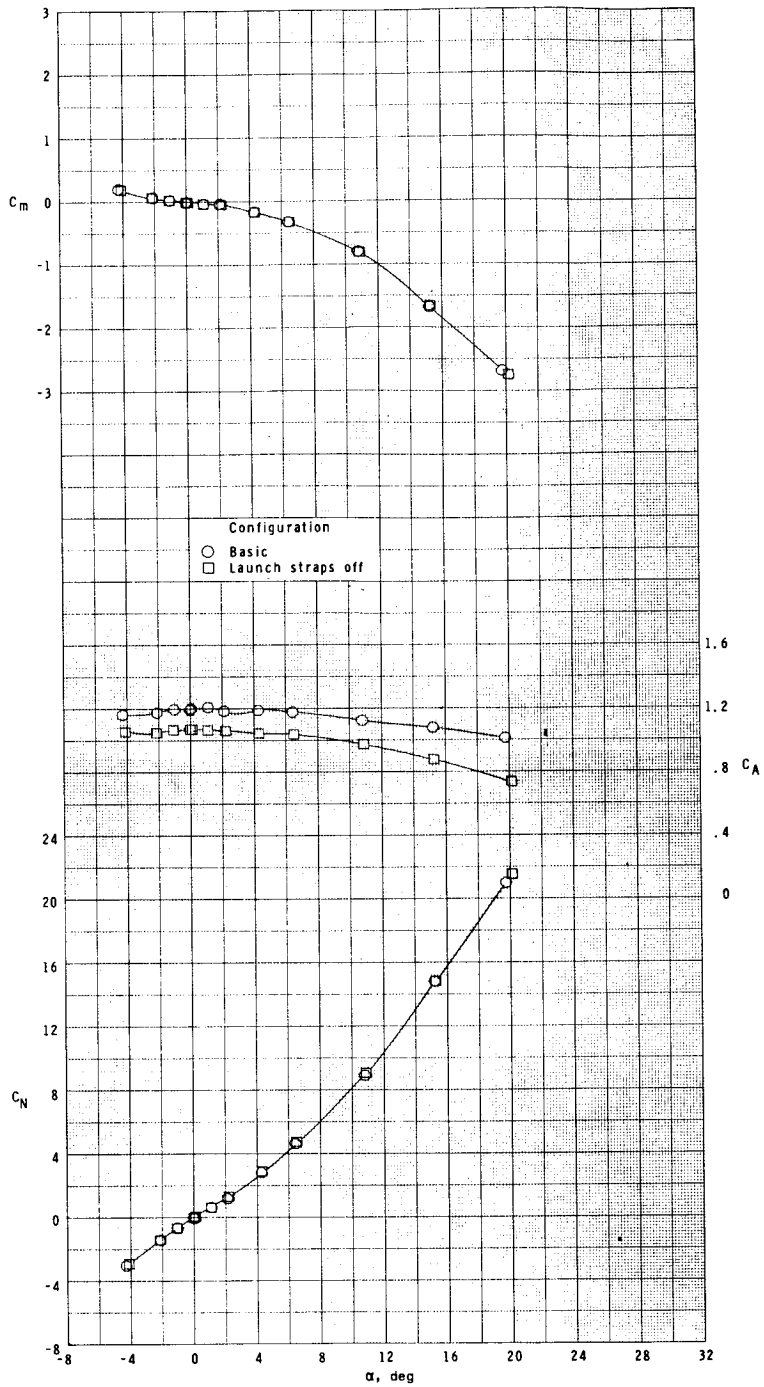

(d) M = 0.90.

Figure 7.- Continued.

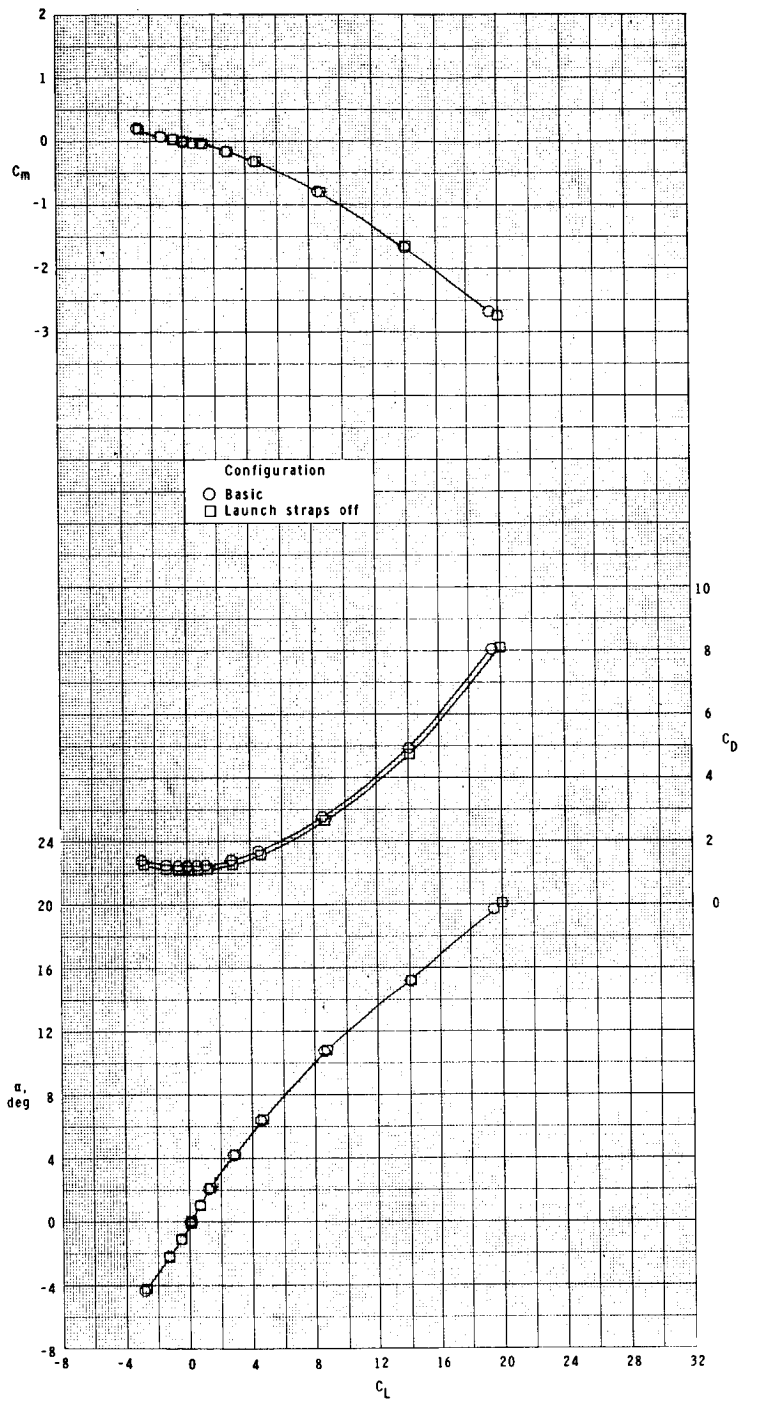

(d) Concluded.

Figure 7.- Continued.

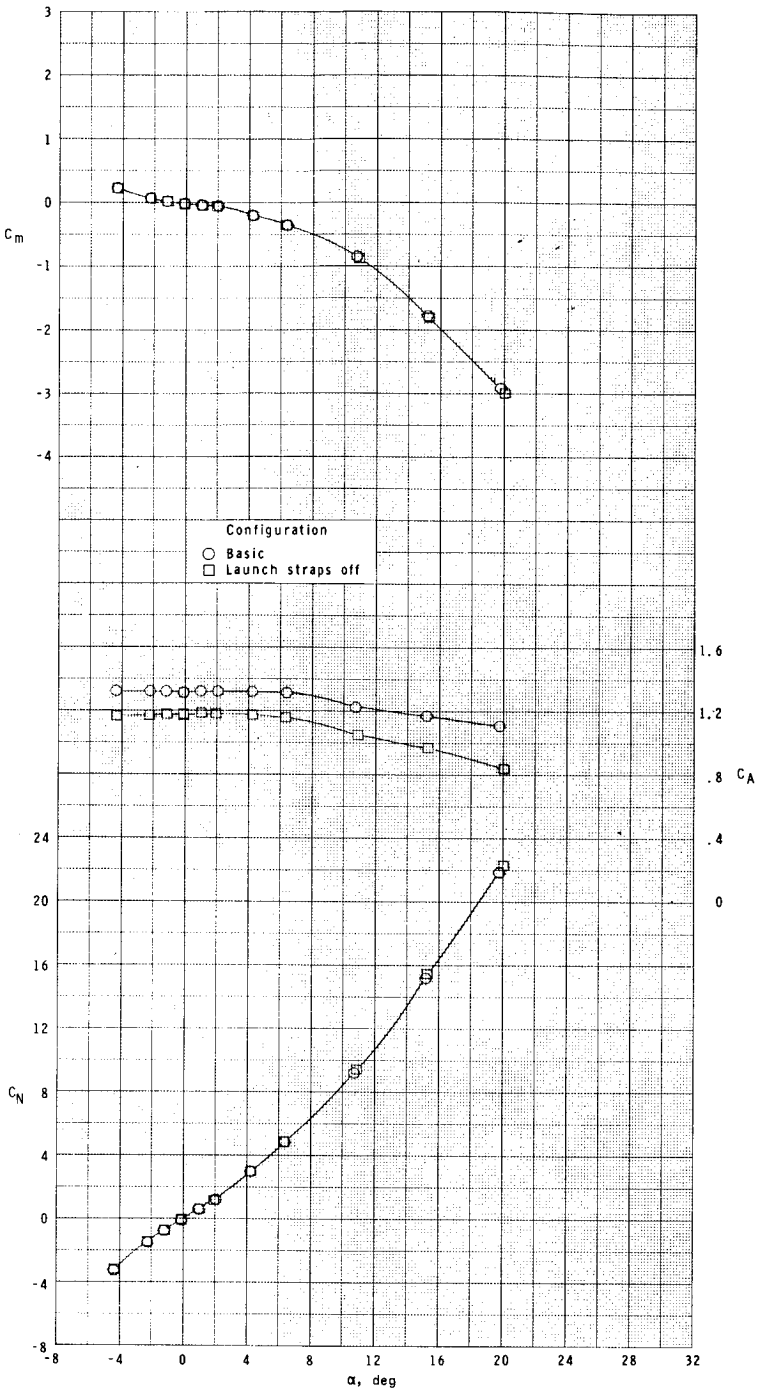

(e) M = 0.95.

Figure 7.- Continued.

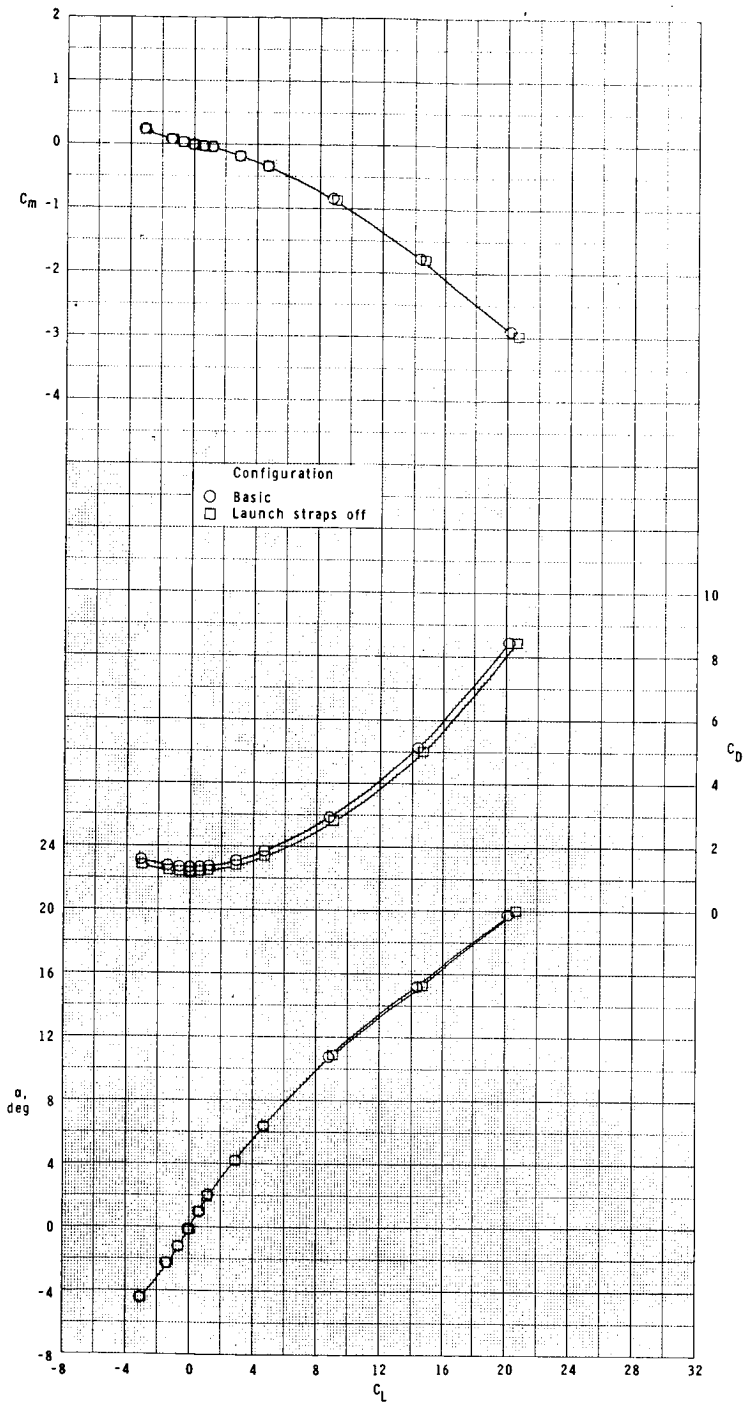

(e) Concluded.

Figure 7.- Continued.

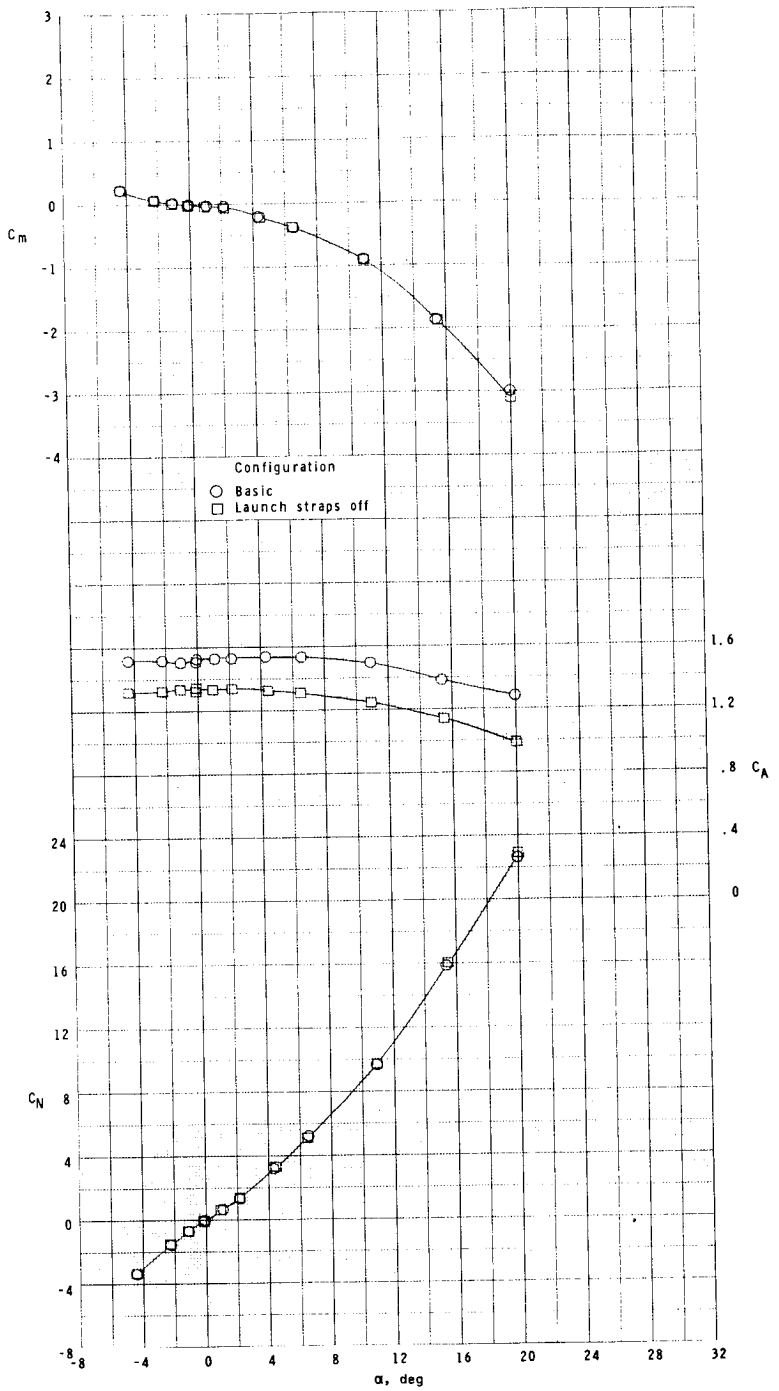

(f) M = 1.00.

Figure 7.- Continued.

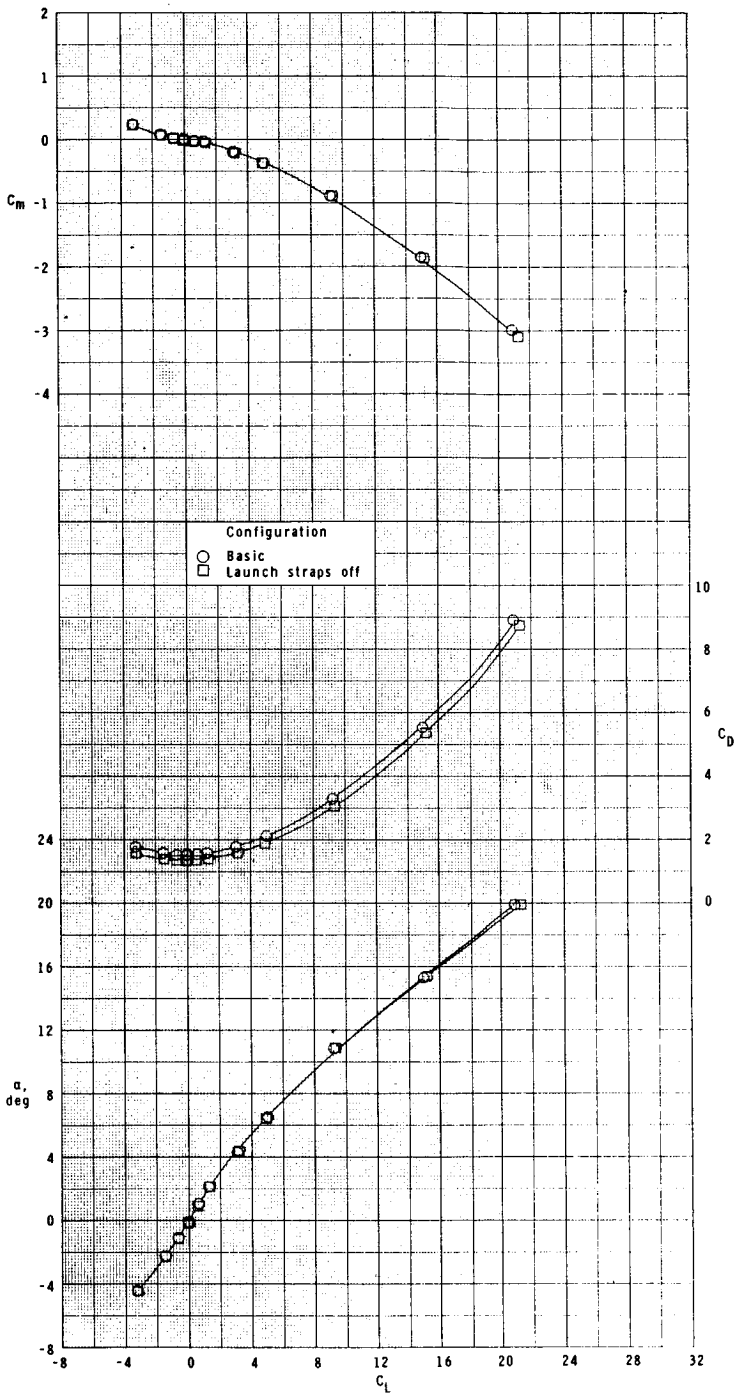

(f) Concluded.

Figure 7.- Continued.

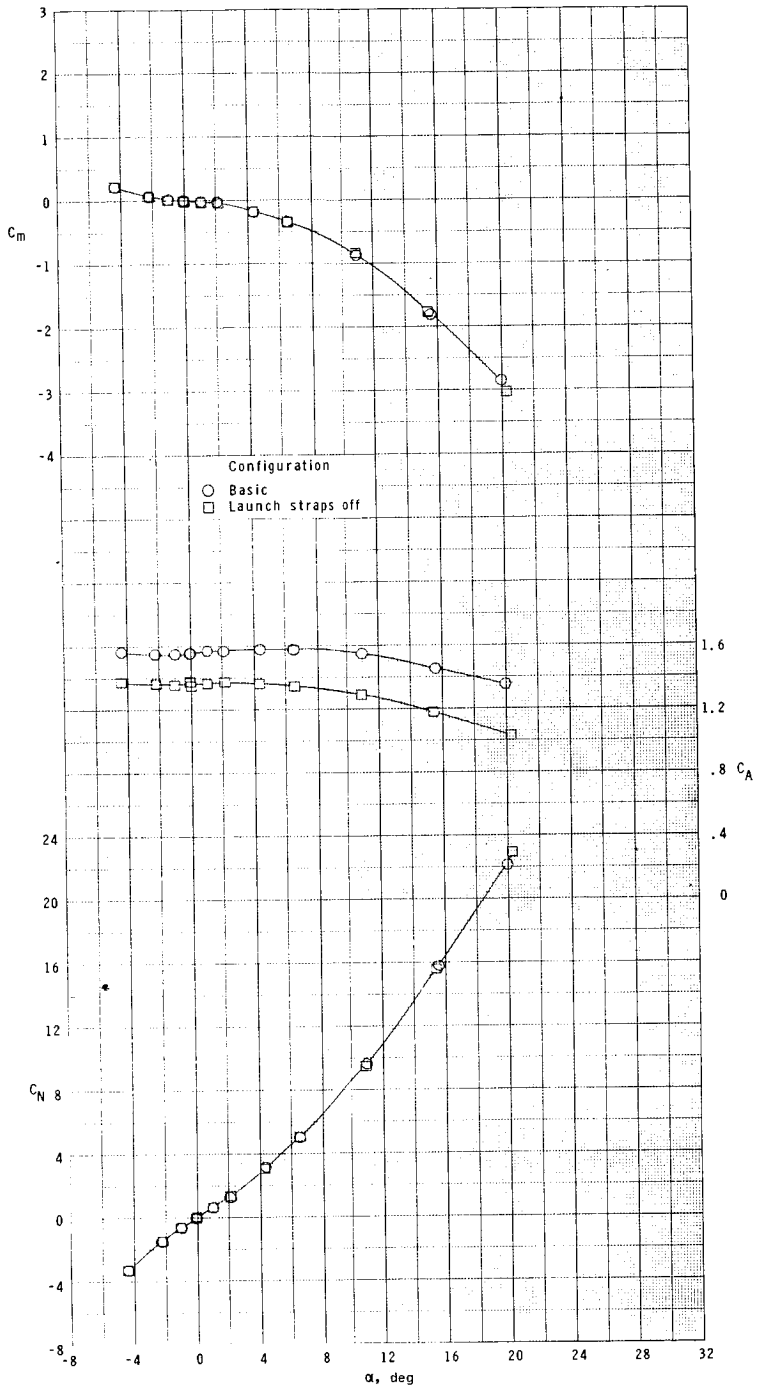

(g) M = 1.03.

Figure 7.- Continued.

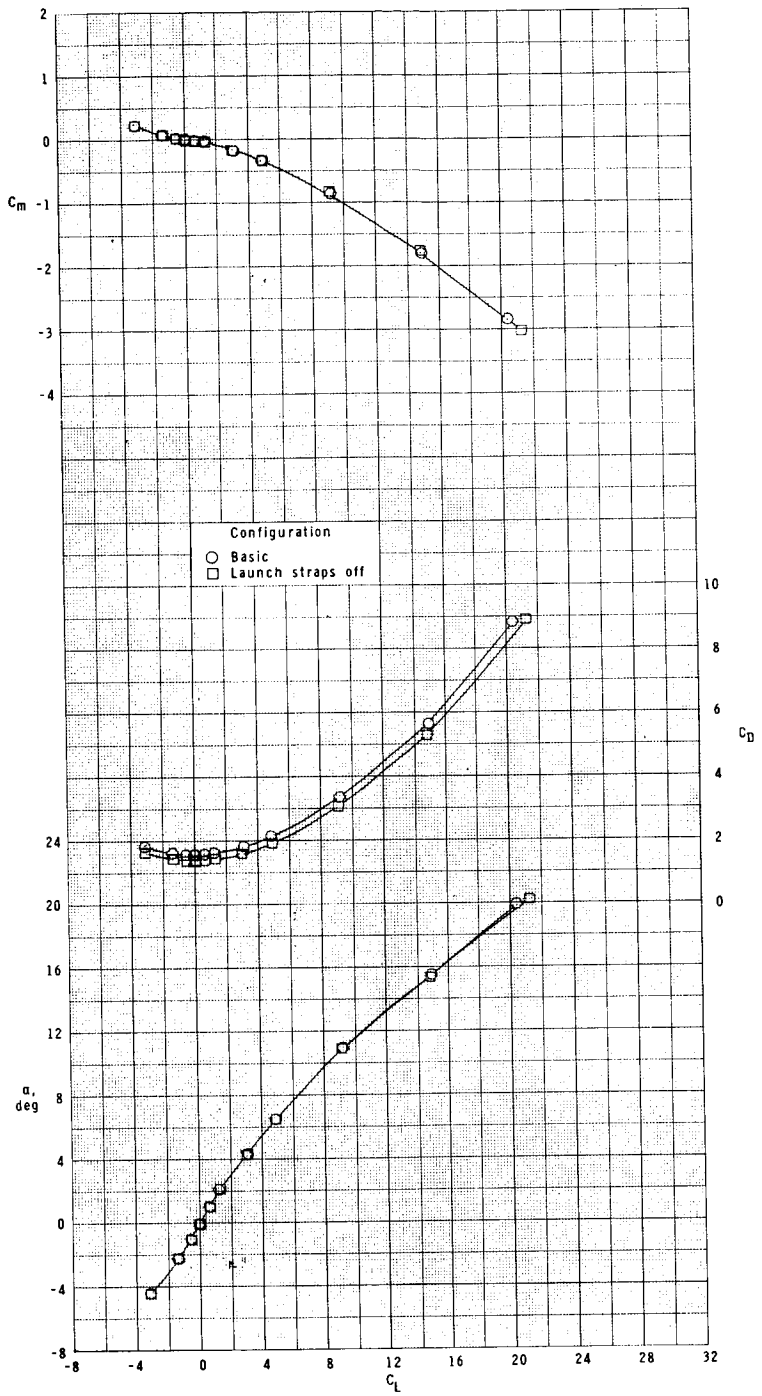

(g) Concluded.

Figure 7.- Continued.

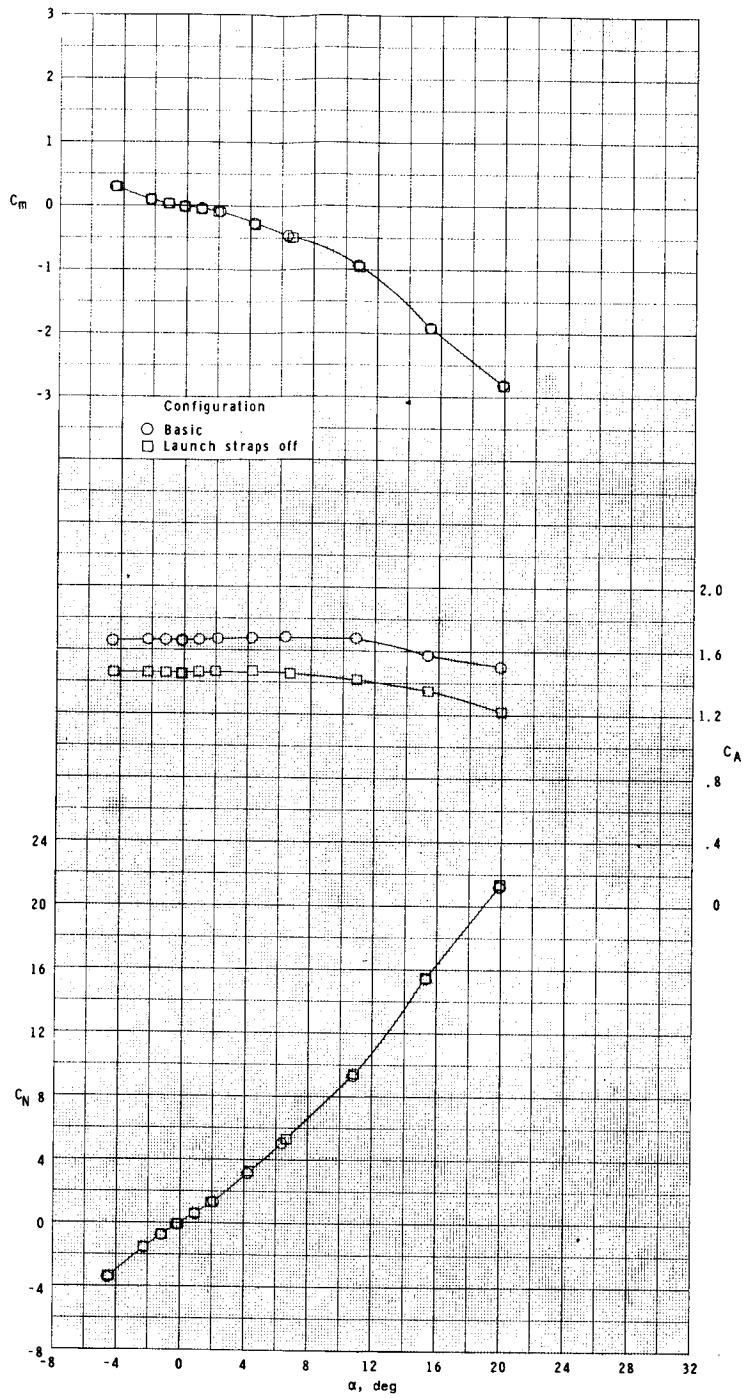

(h) M = 1.20.

Figure 7.- Continued.

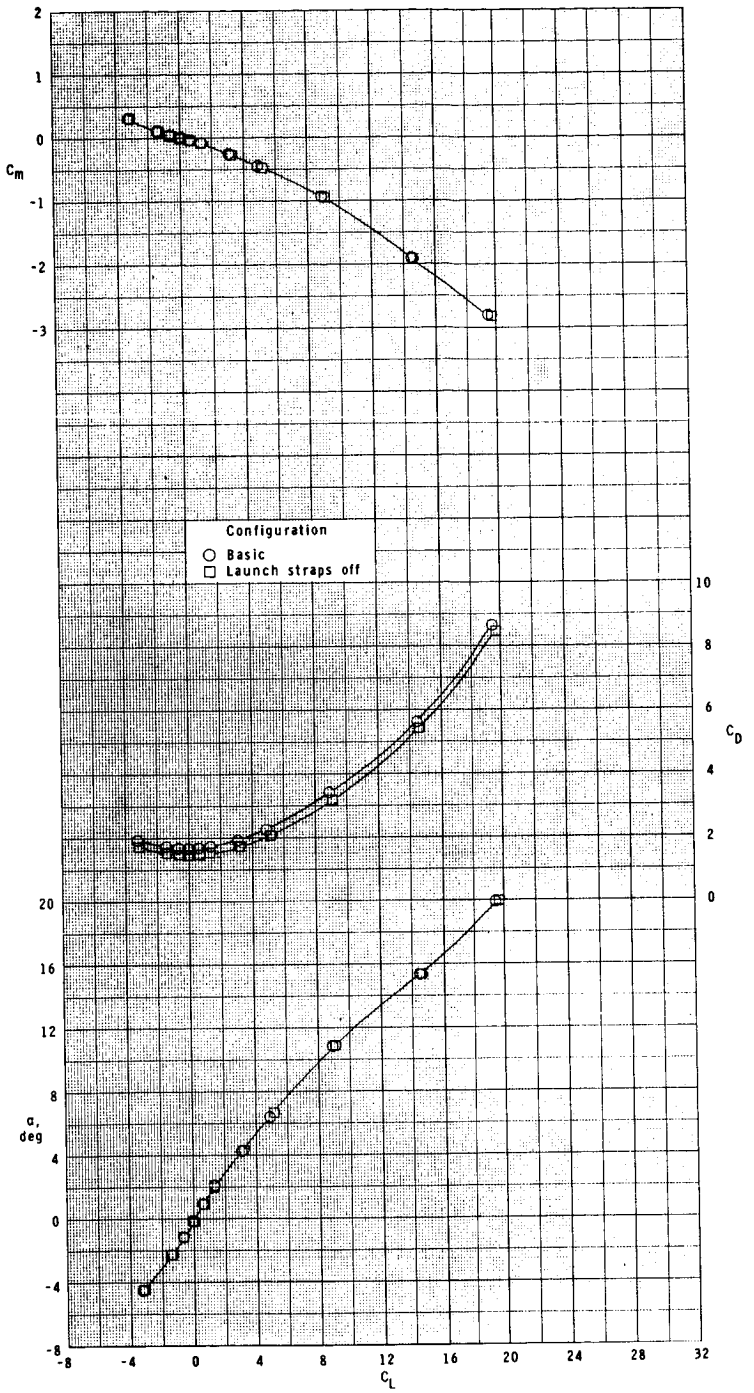

(h) Concluded.

Figure 7.- Continued.

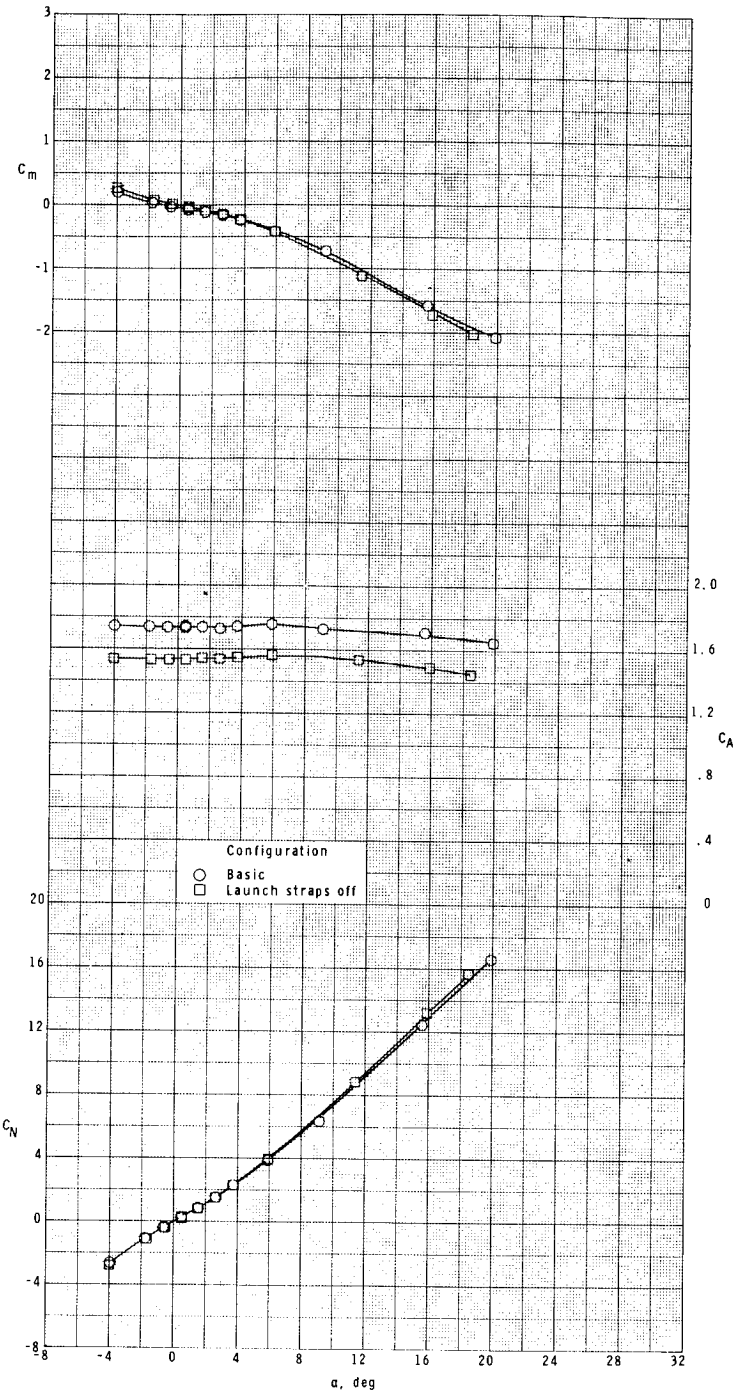

(i) M = 1.75.

Figure 7.- Continued.

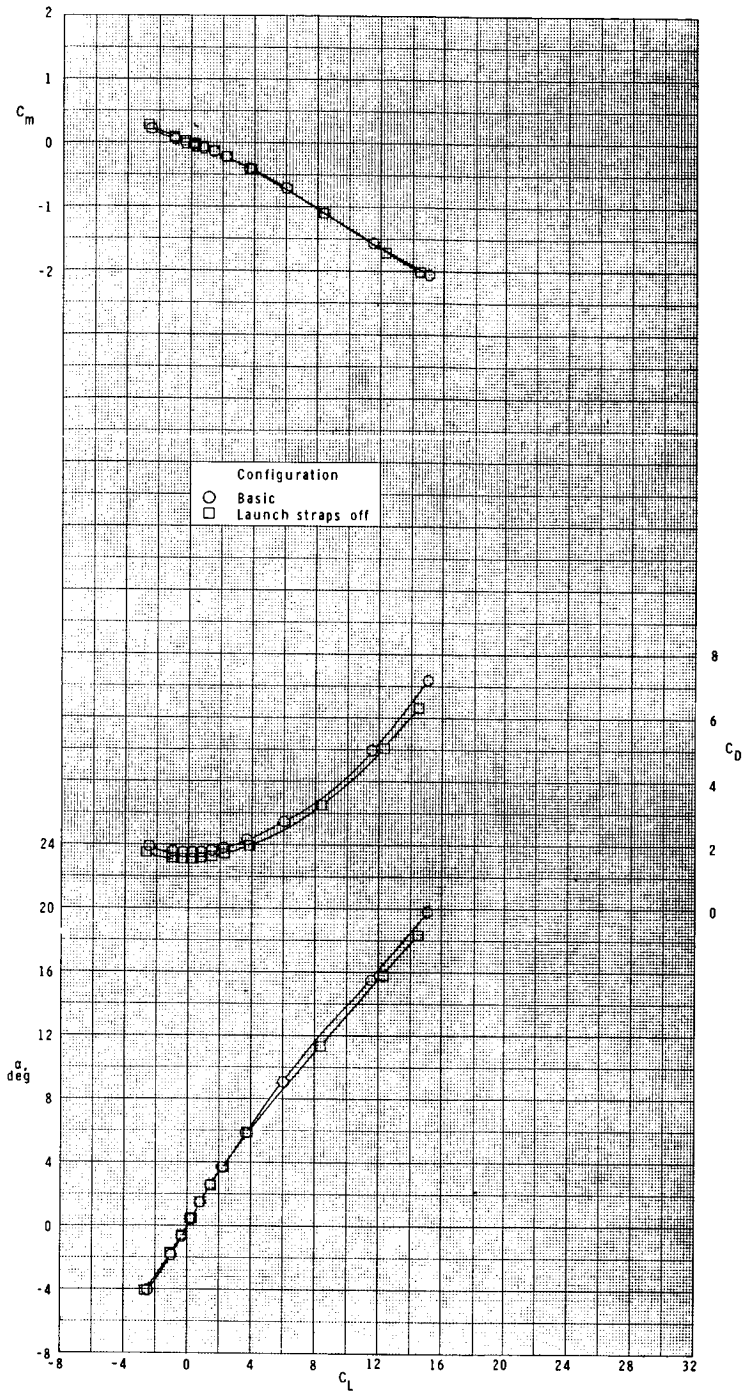

(i) Concluded.

Figure 7.- Continued.

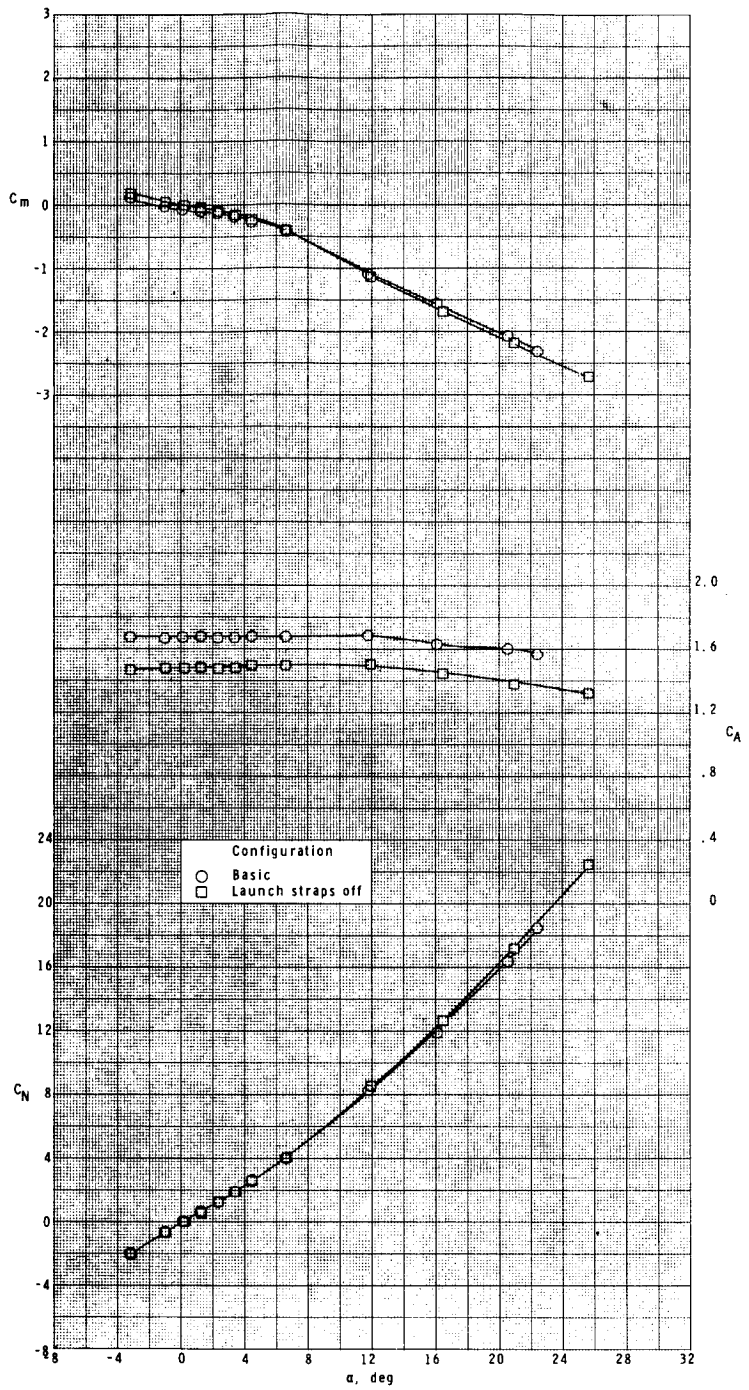

(j) M = 2.10.

Figure 7.- Continued.

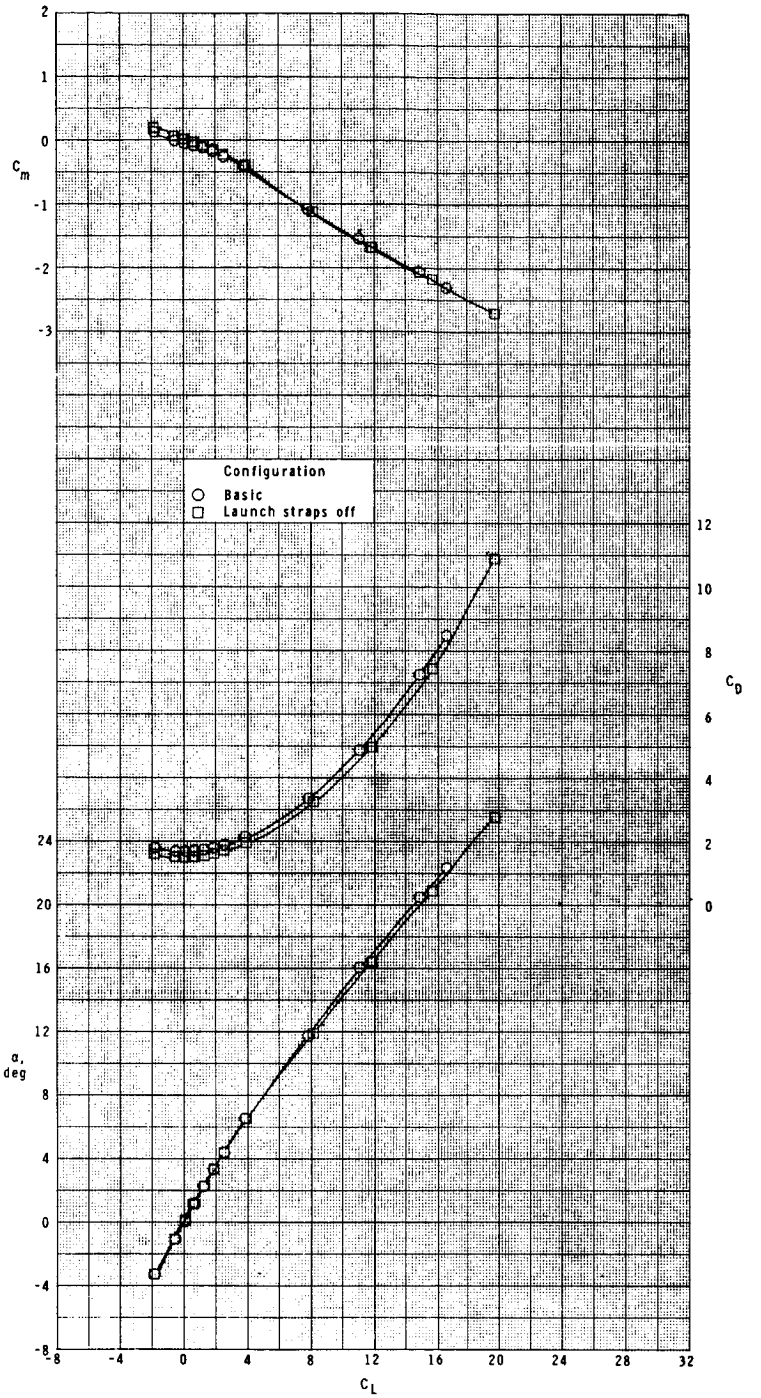

(j) Concluded.

Figure 7.- Continued.

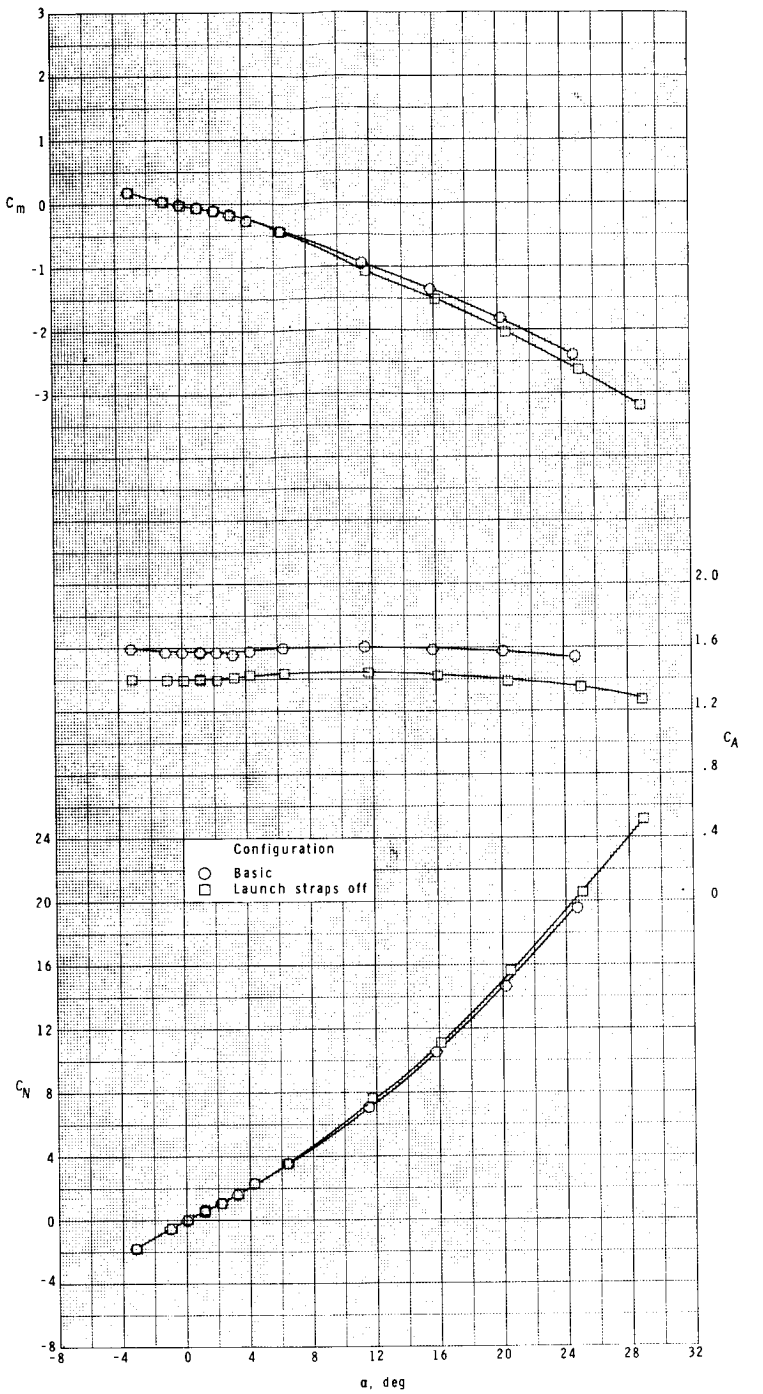

(k) M = 2.50.

Figure 7.- Continued.

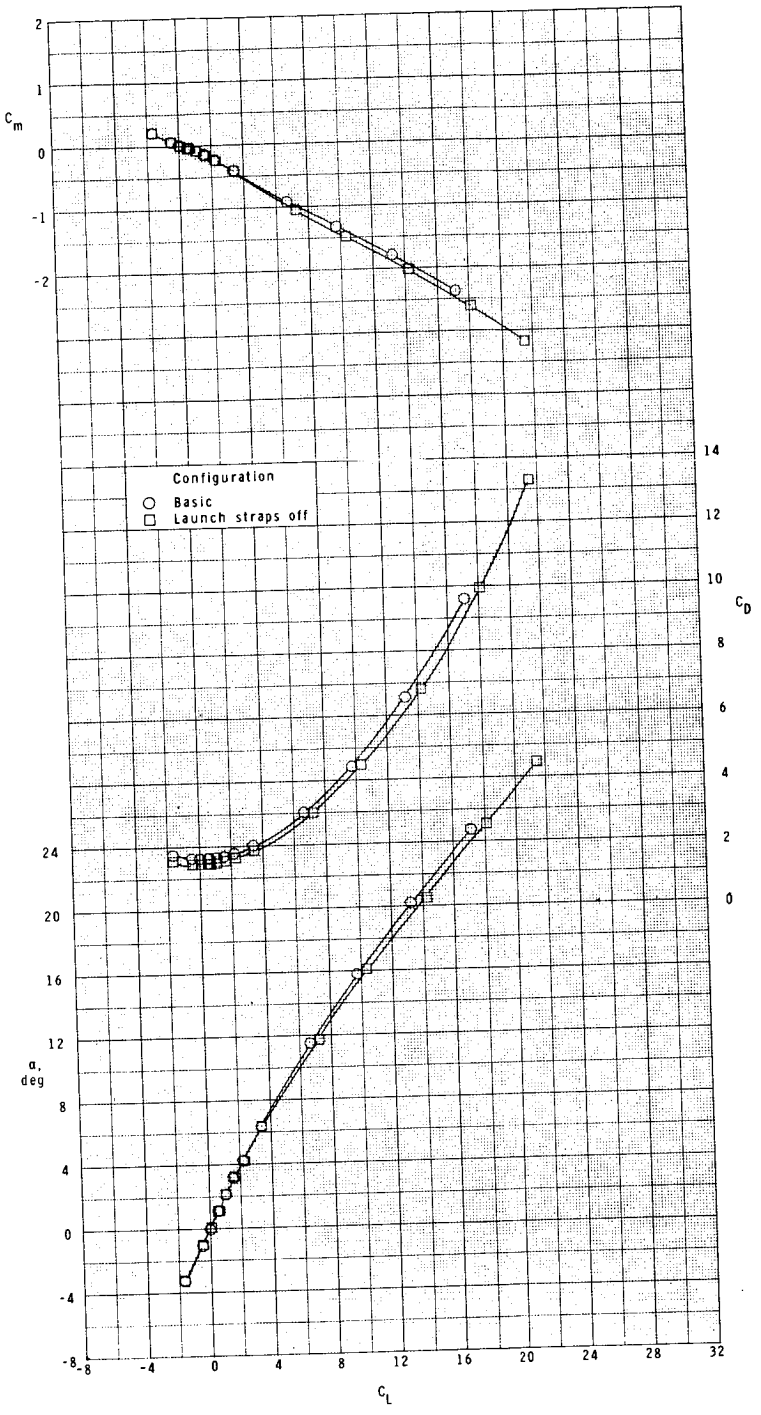

(k) Concluded.

Figure 7.- Continued.

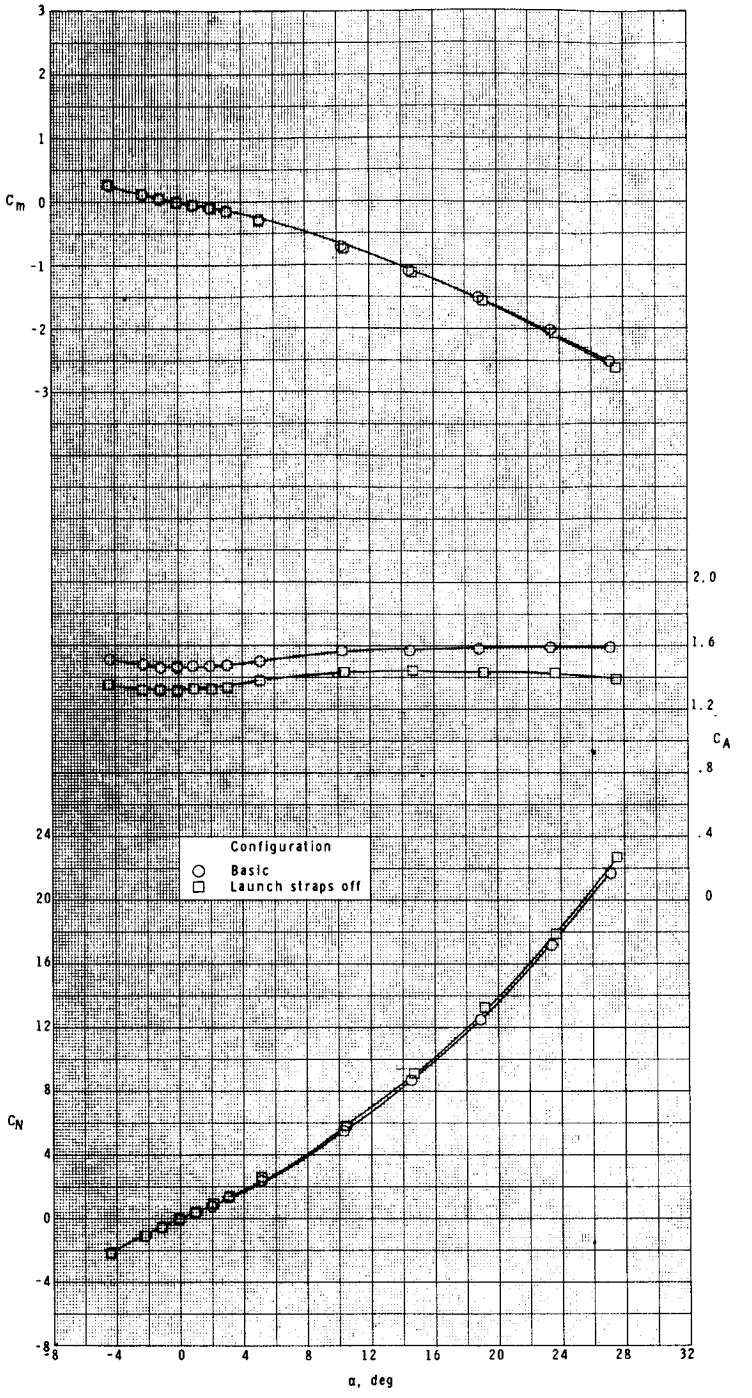

(l) M = 2.86.

Figure 7.- Continued.

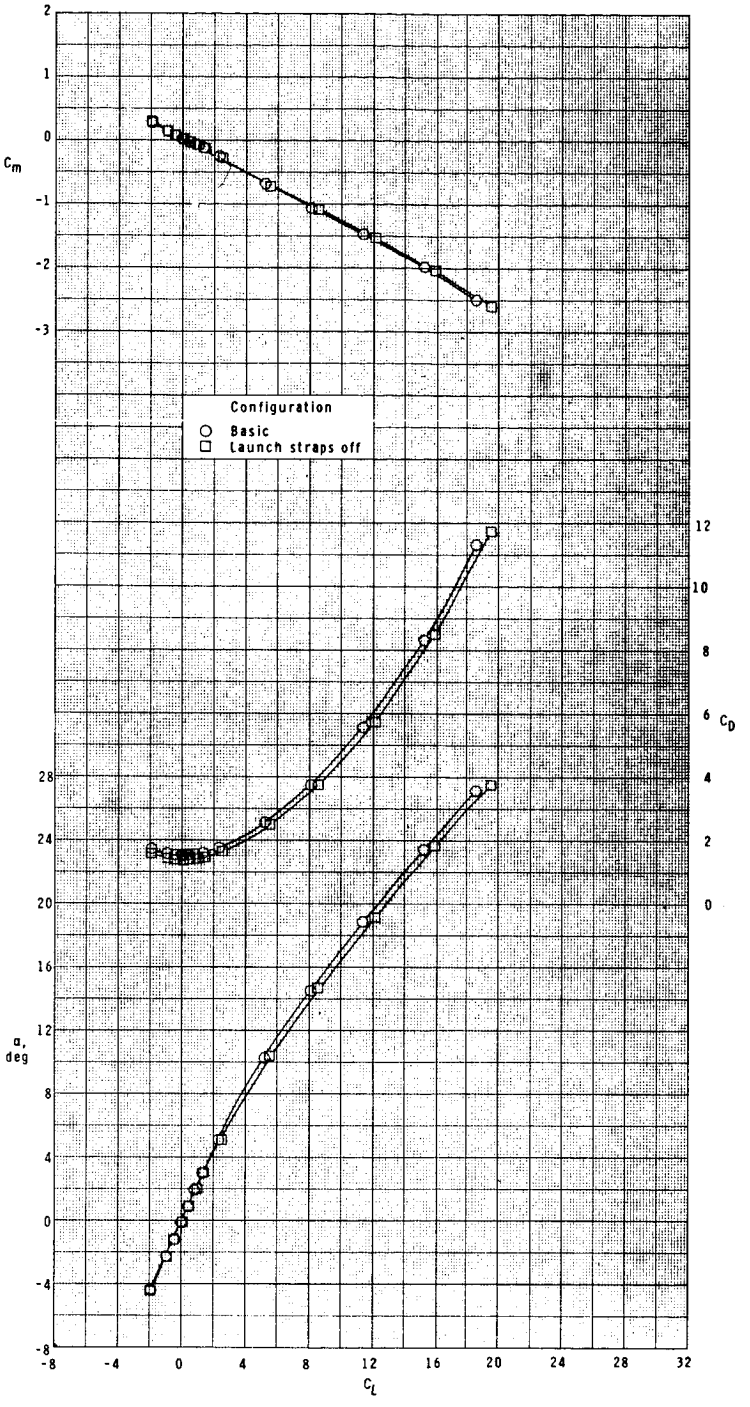

(l) Concluded.

Figure 7.- Continued.

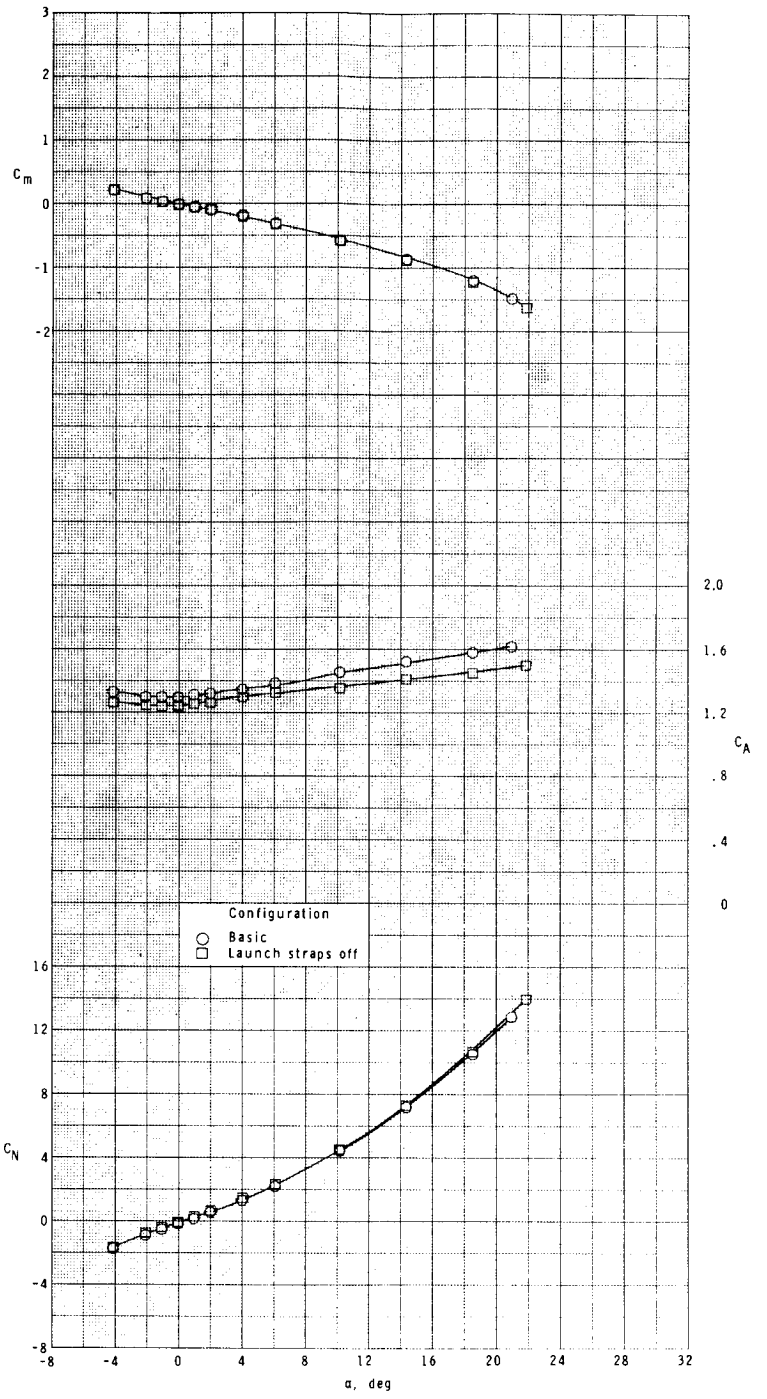

(m) M = 3.95.

Figure 7.- Continued.

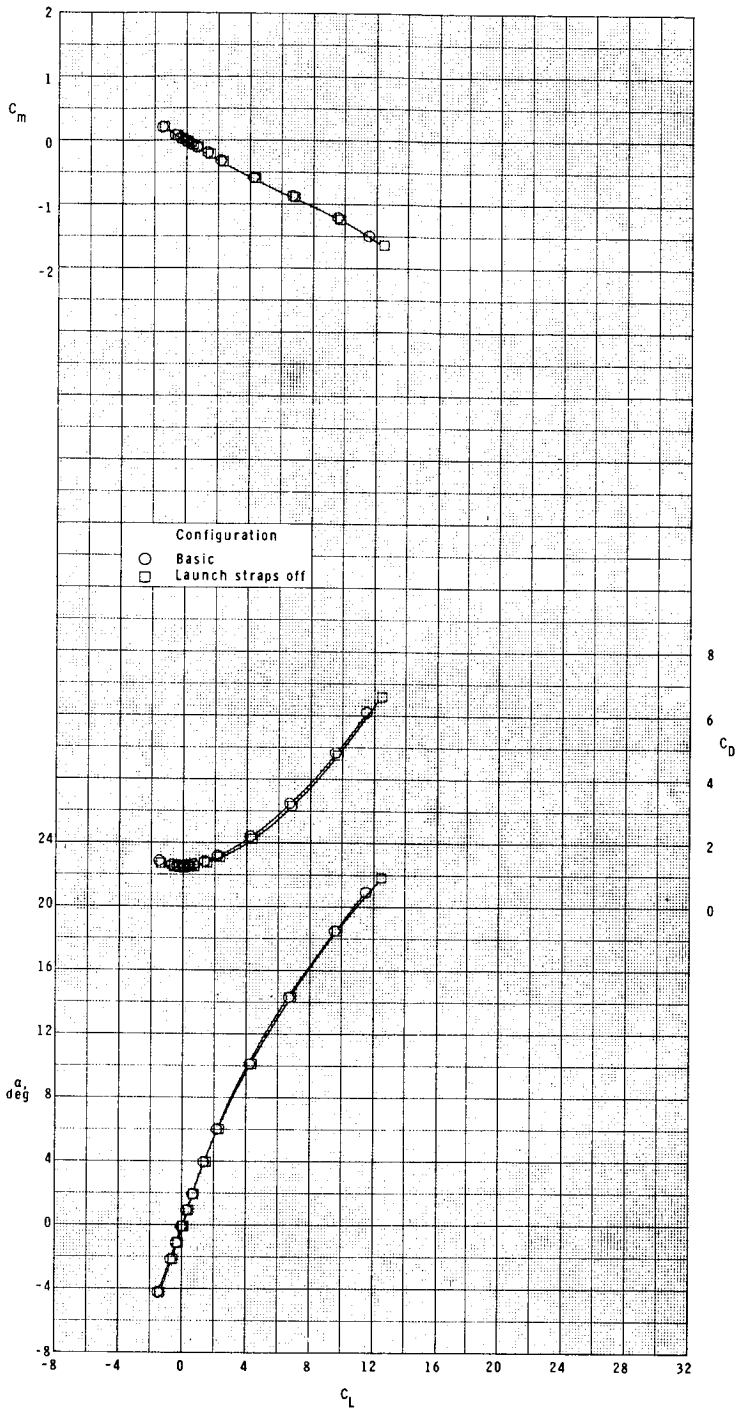

(m) Concluded.

Figure 7.- Continued.

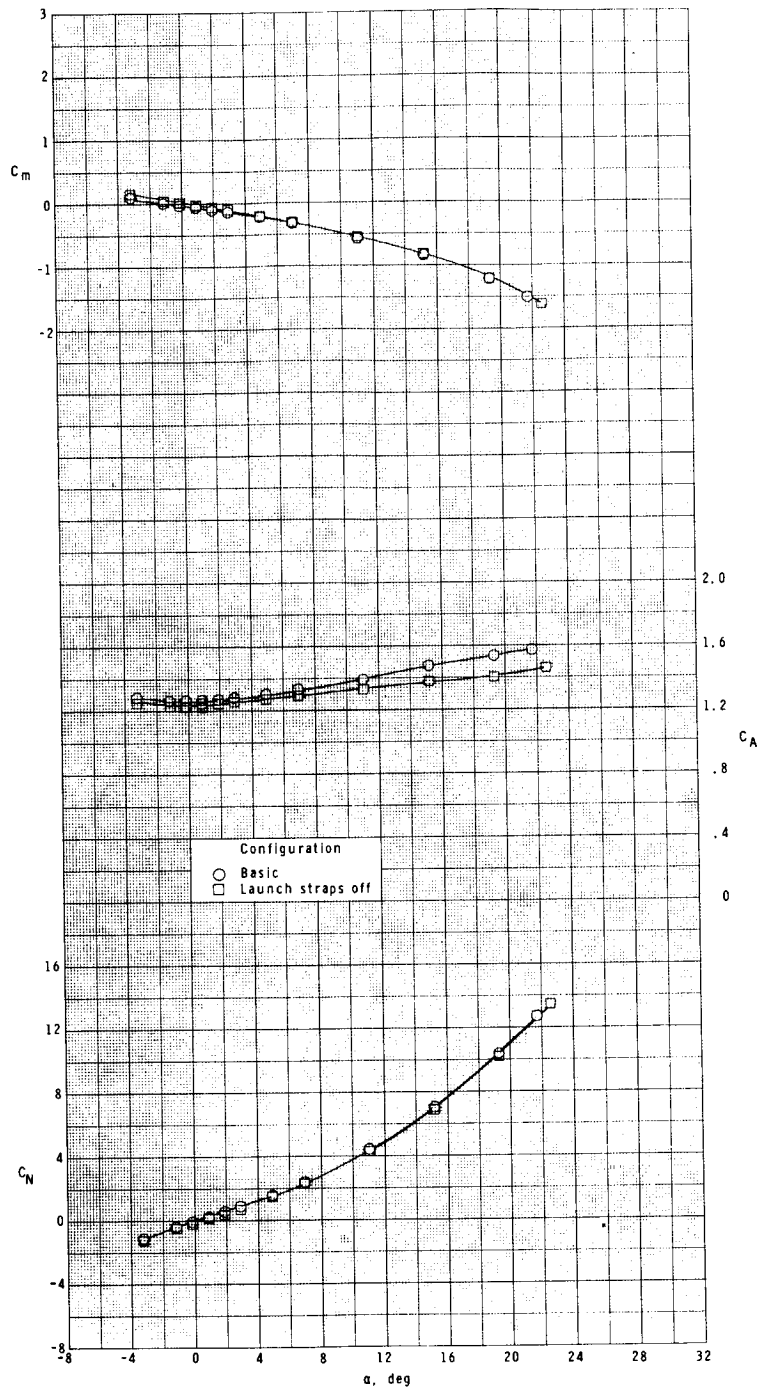

(n) M = 4.63.

Figure 7.- Continued.

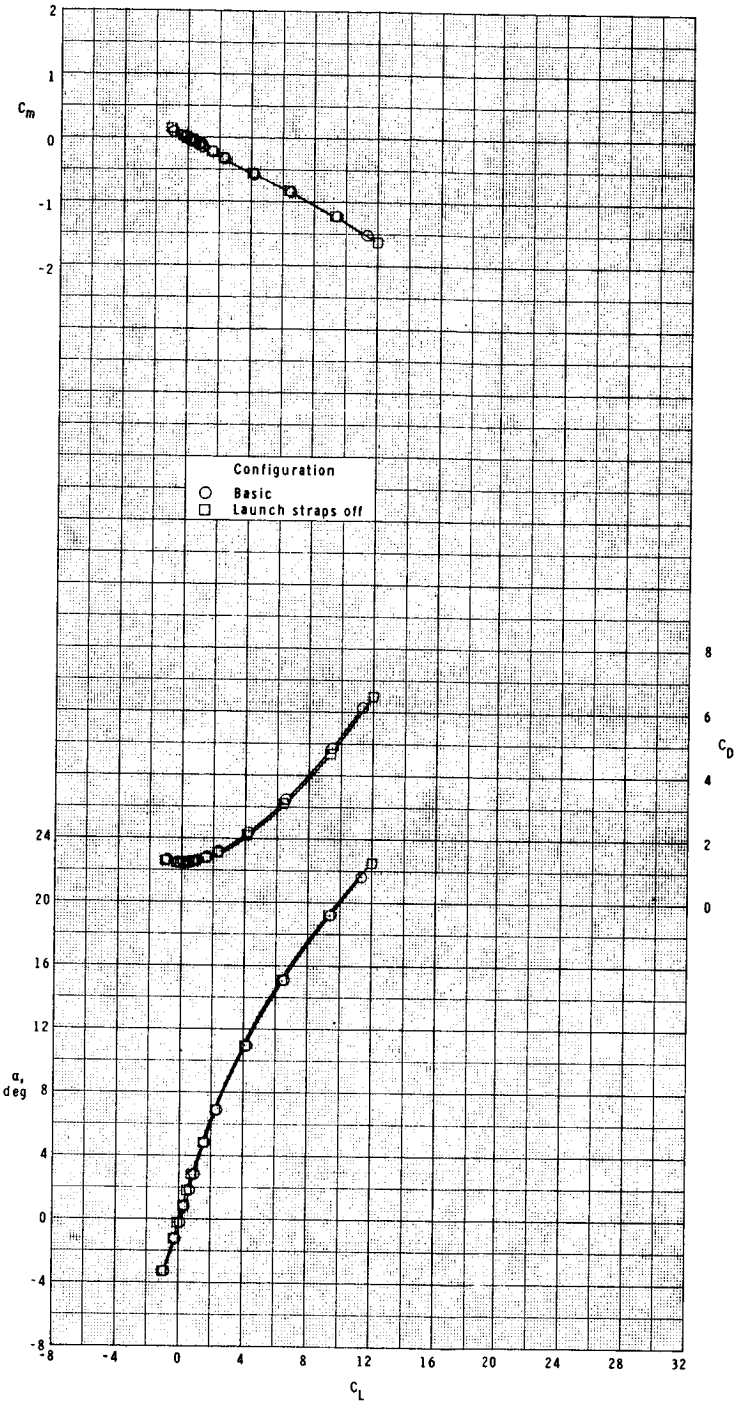

(n) Concluded.

Figure 7.- Concluded.

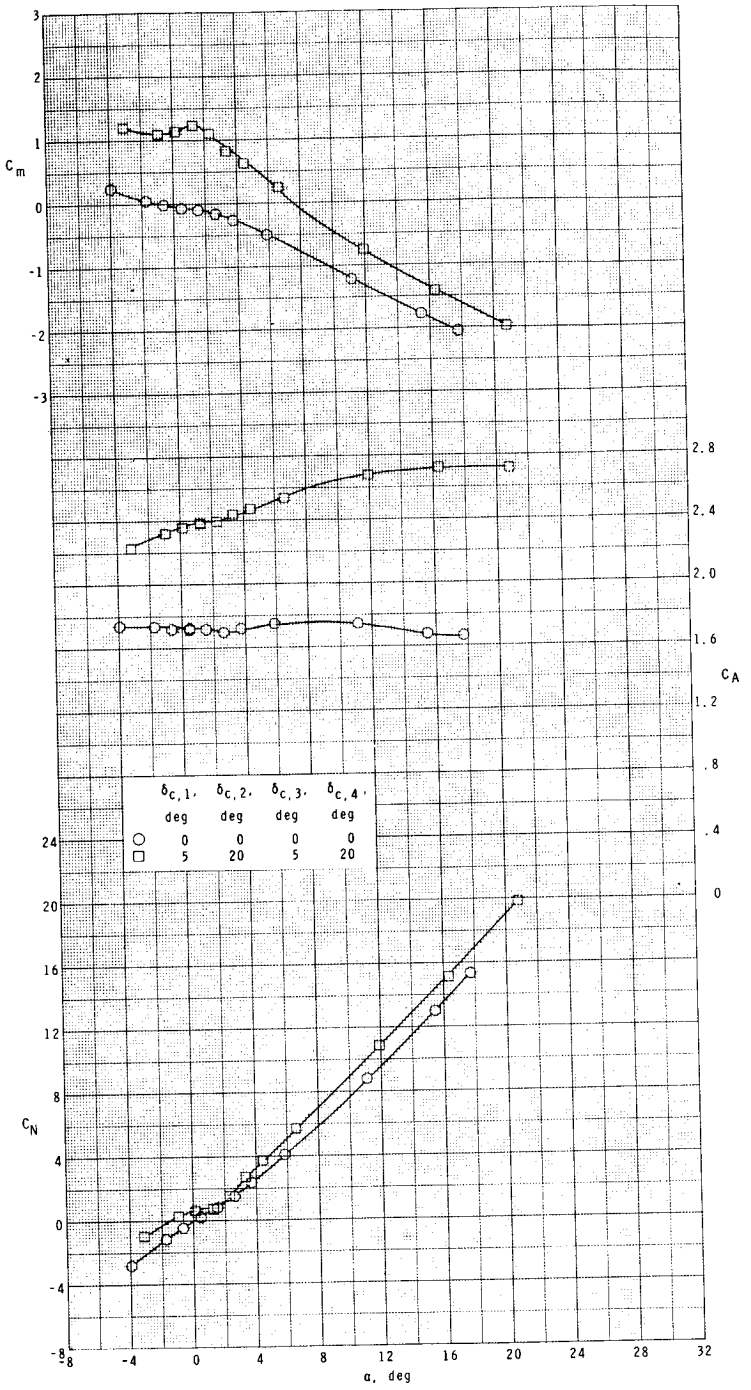

(a) M = 1.75.

Figure 8.- Control effectiveness for pitch-yaw maneuver. $\phi = -14.04^{o}$.

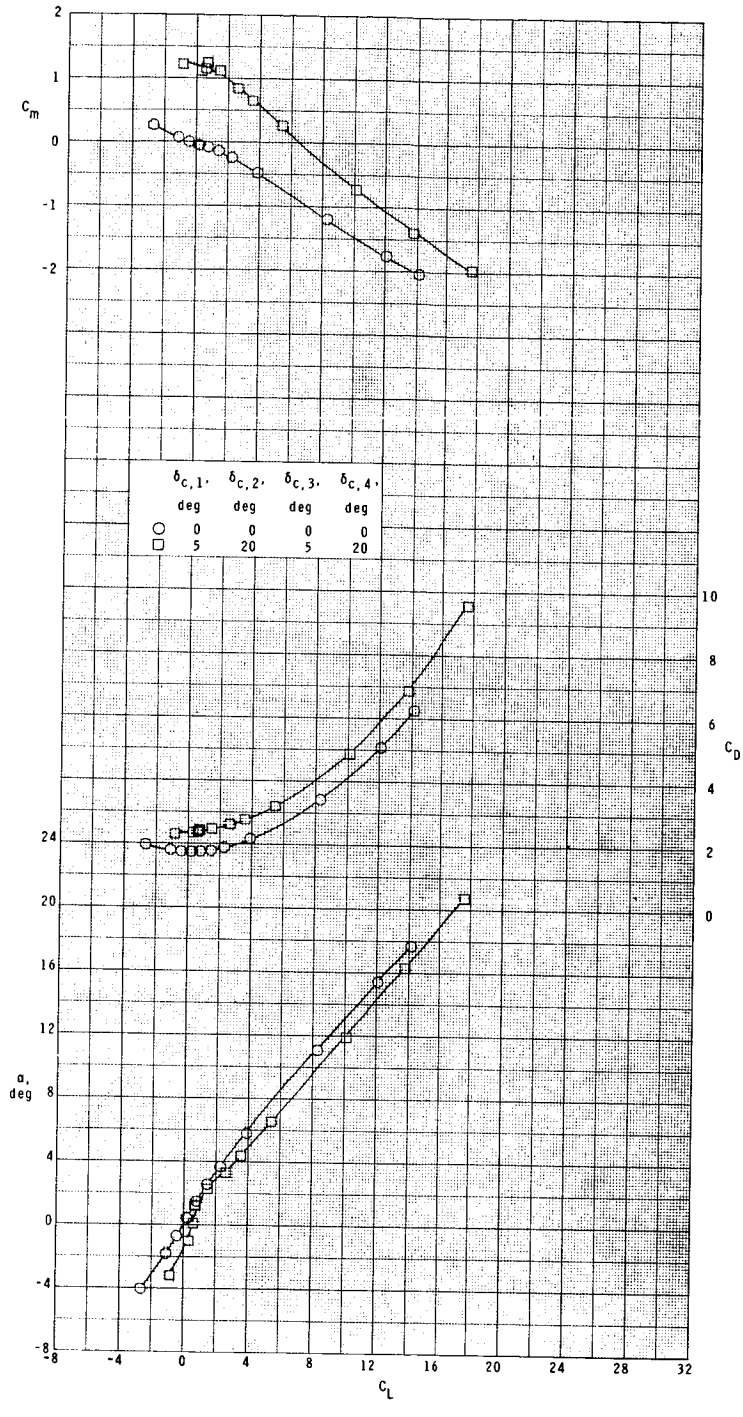

(a) Concluded.

Figure 8.- Continued.

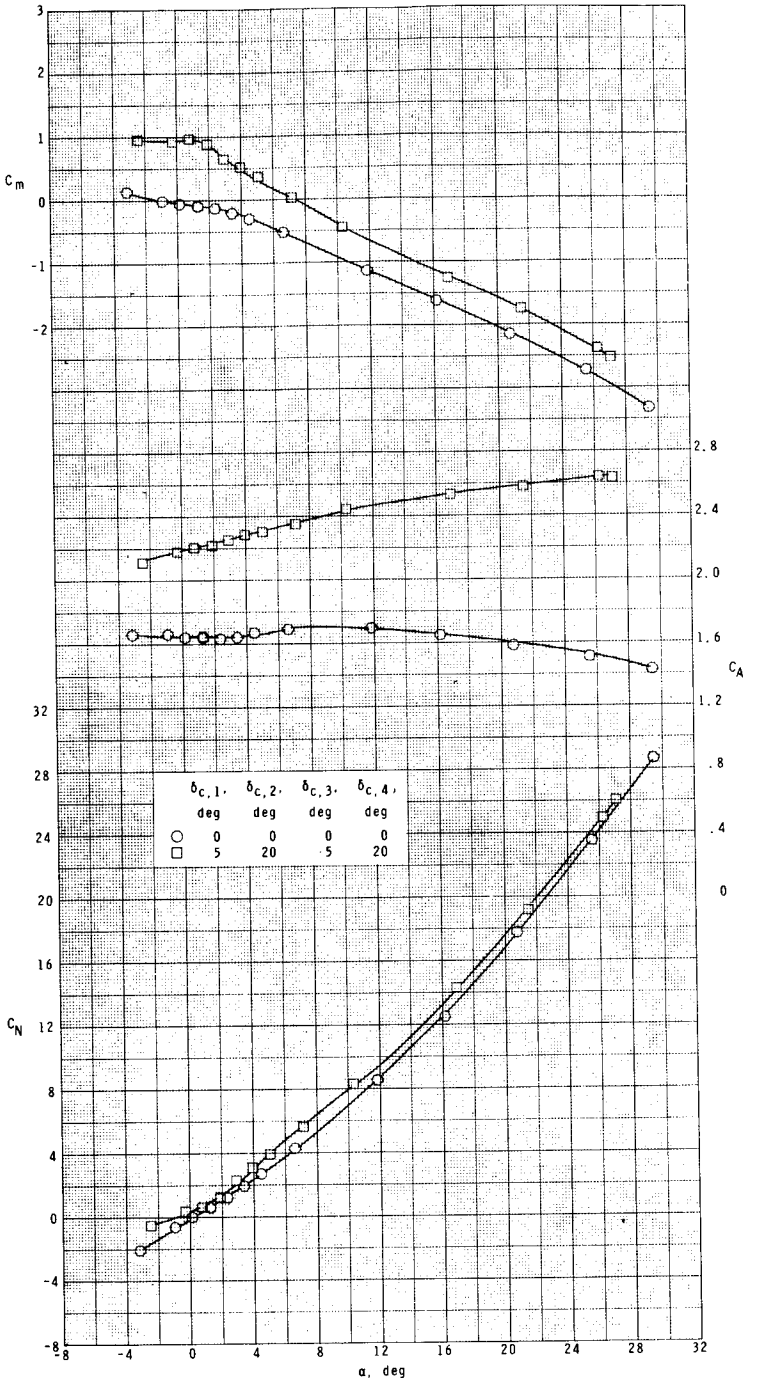

(b) M = 2.10.

Figure 8.- Continued.

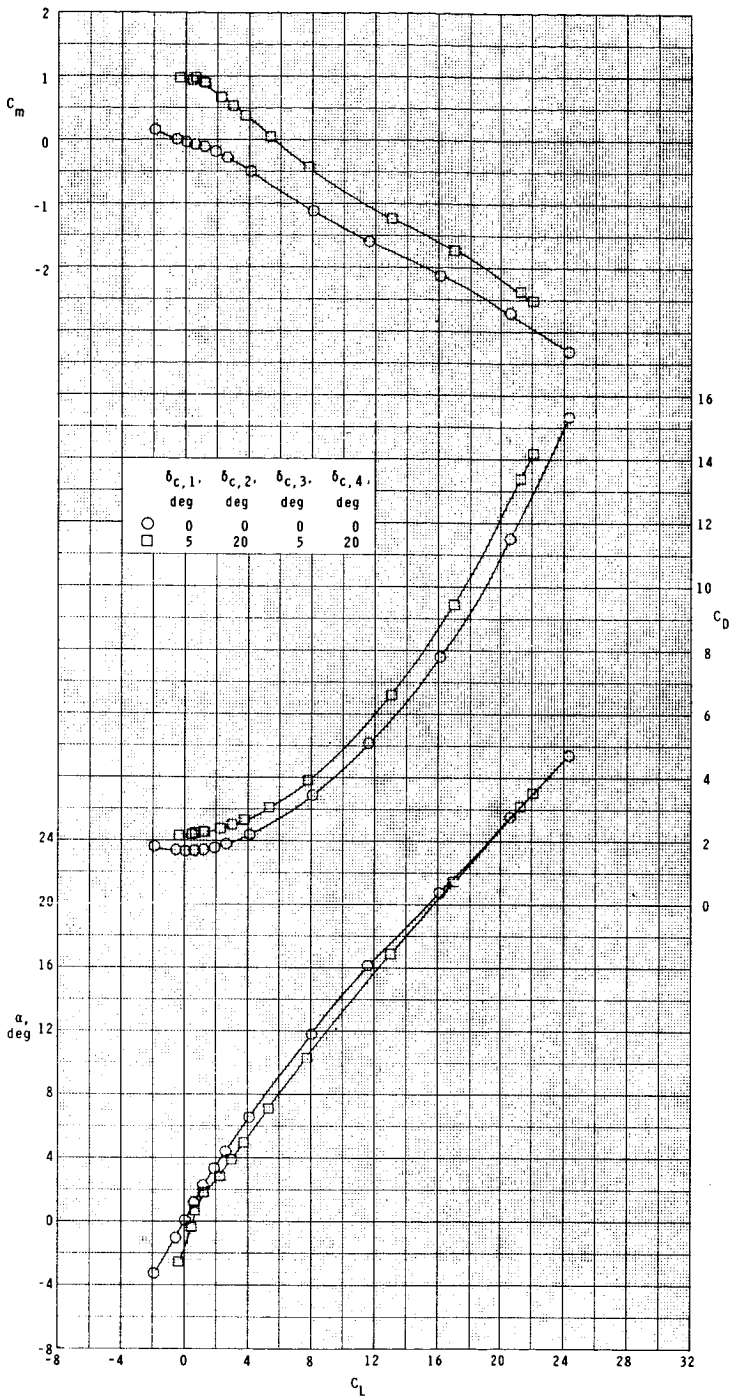

(b) Concluded.

Figure 8.- Continued.

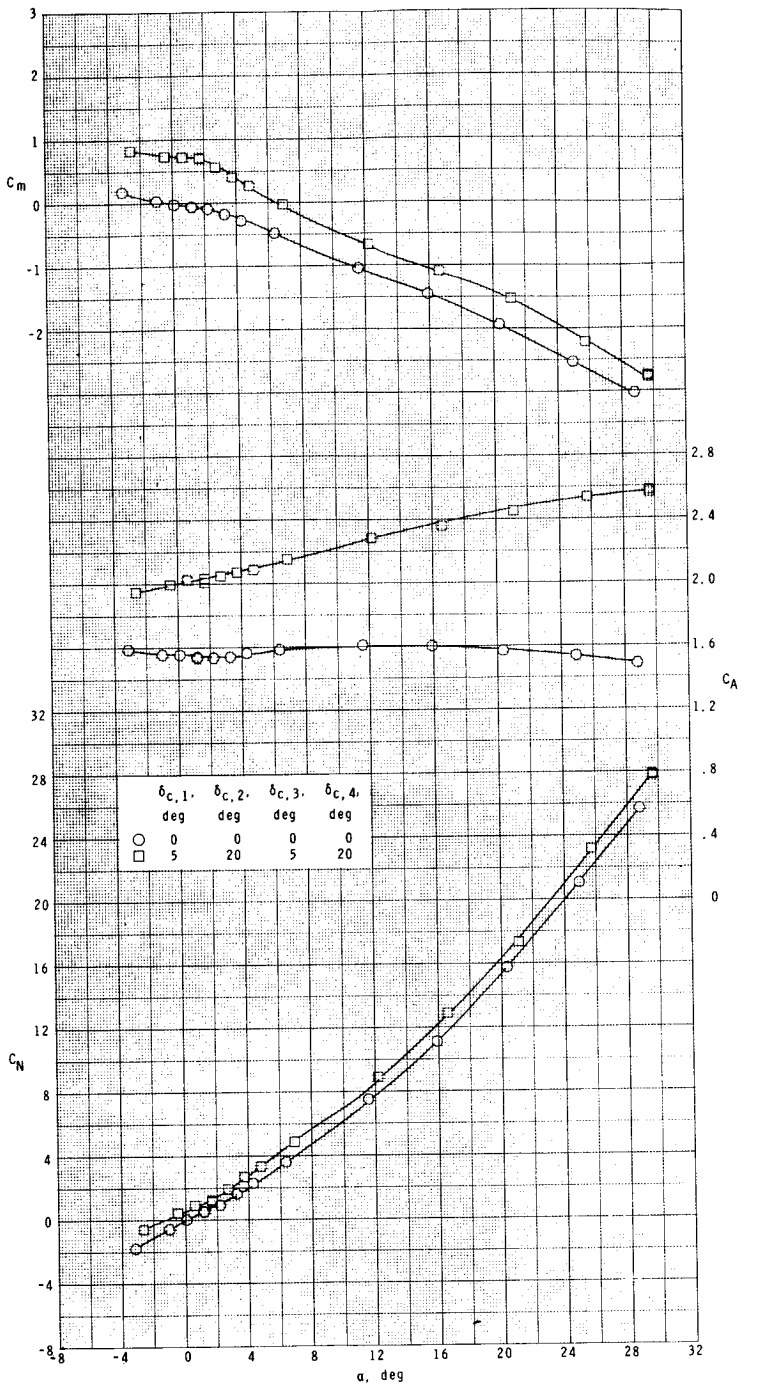

(c) M = 2.50.

Figure 8.- Continued.

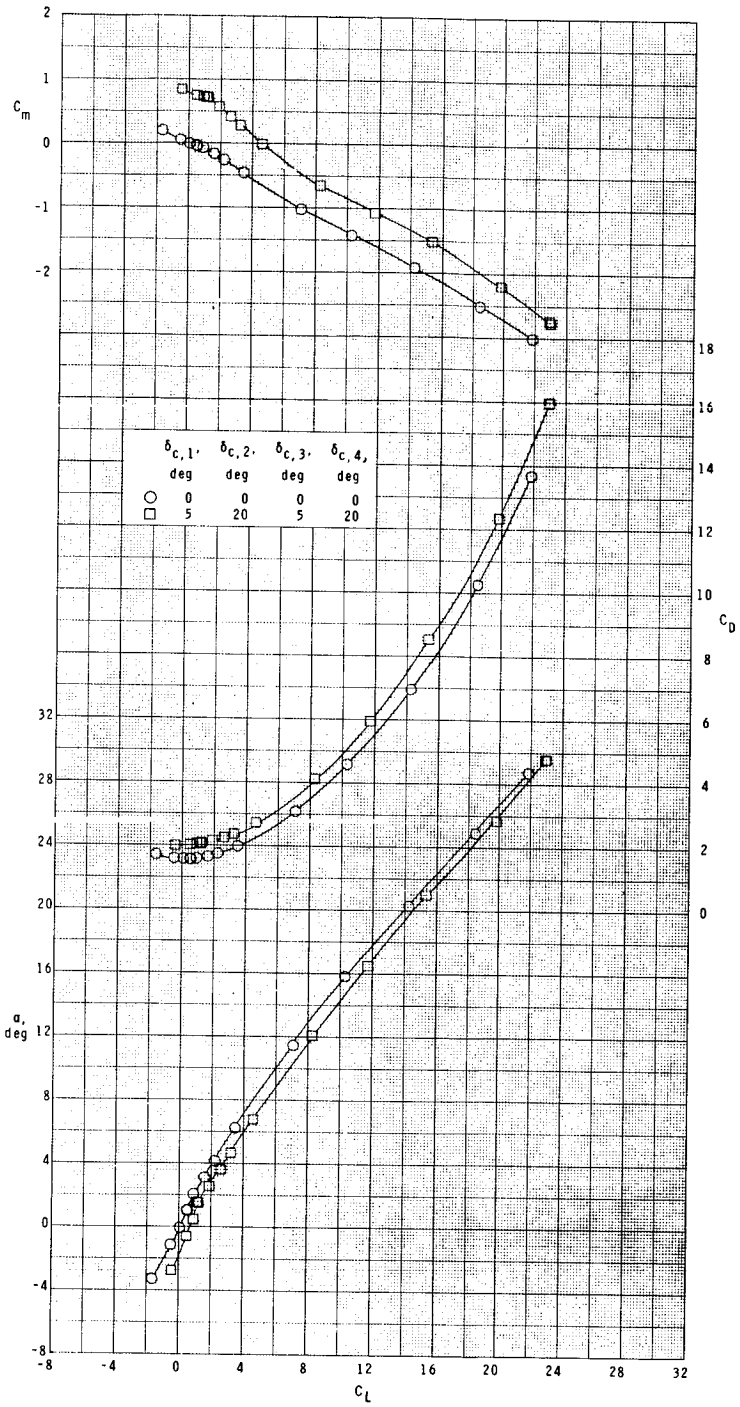

(c) Concluded.

Figure 8.- Continued.

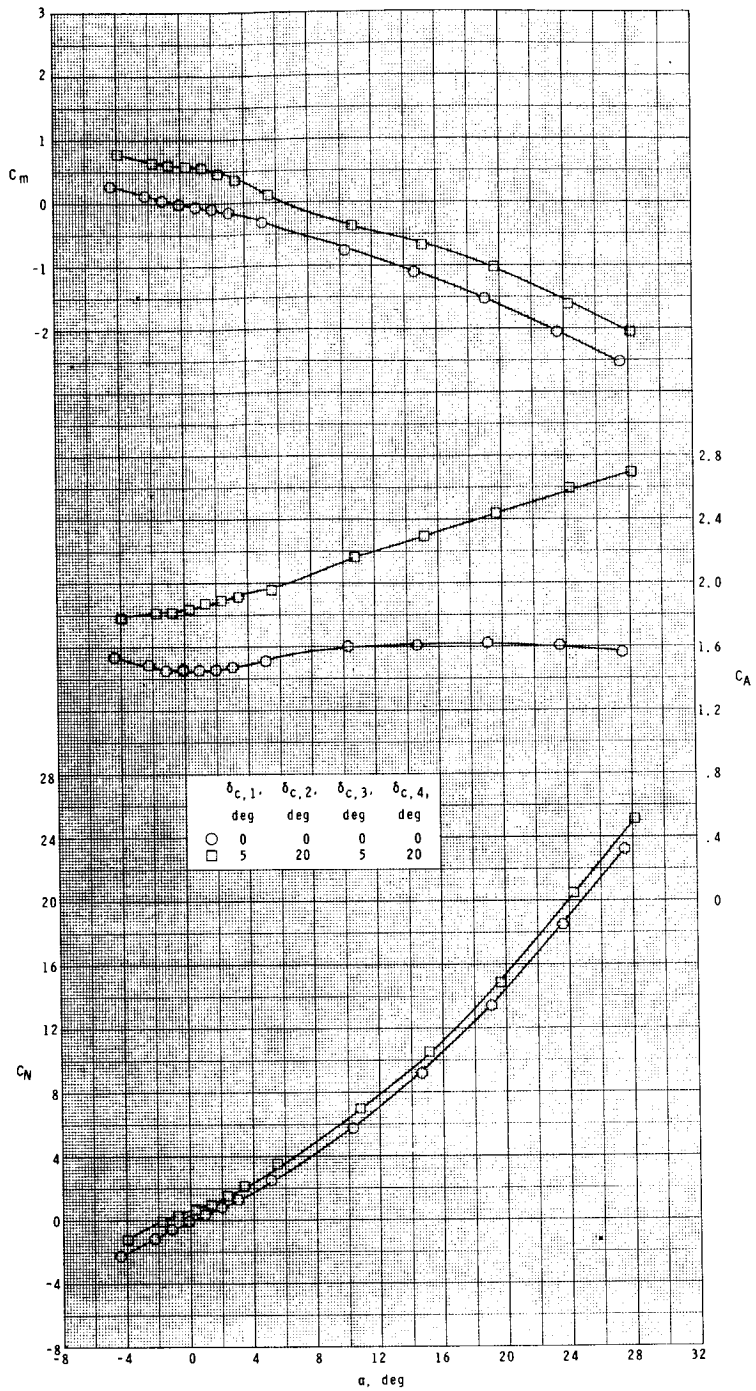

(d) M = 2.86.

Figure 8.- Continued.

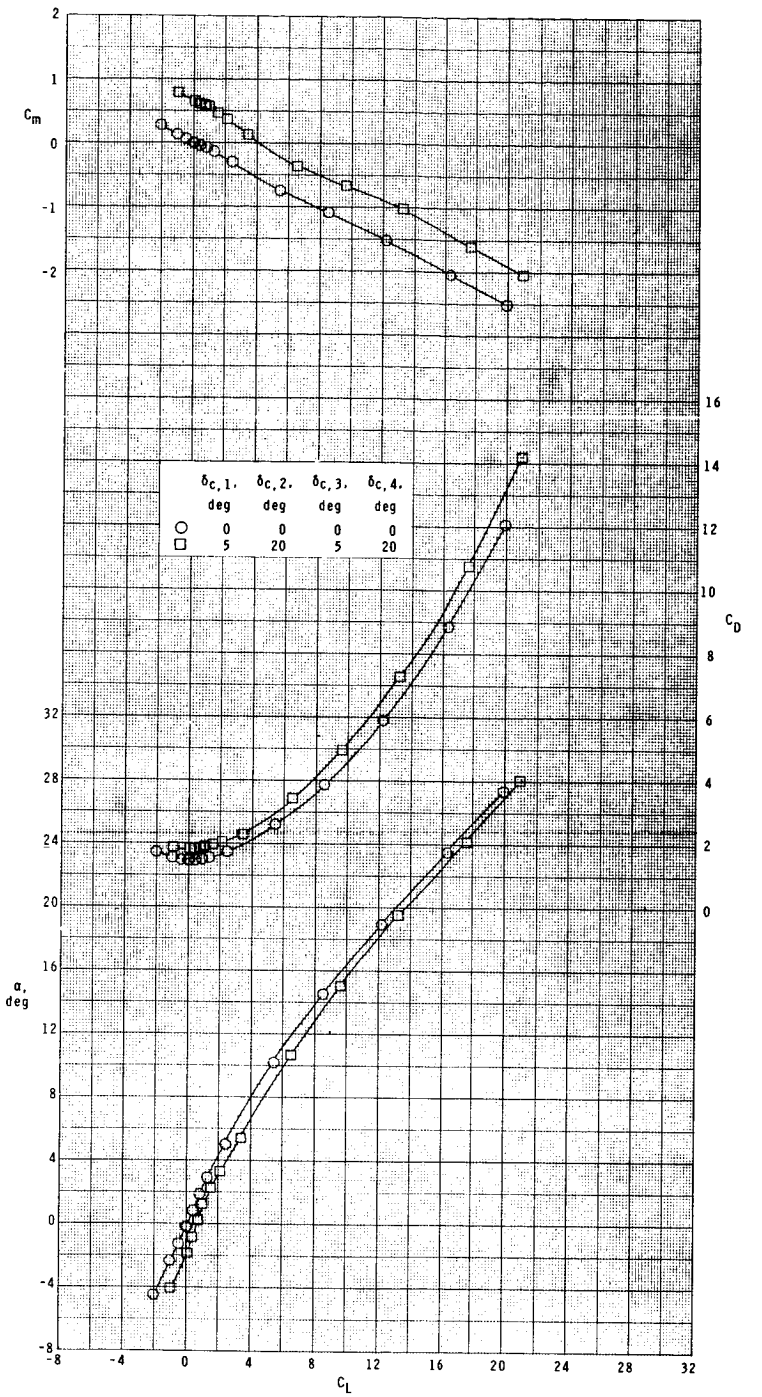

(d) Concluded.

Figure 8.- Continued.

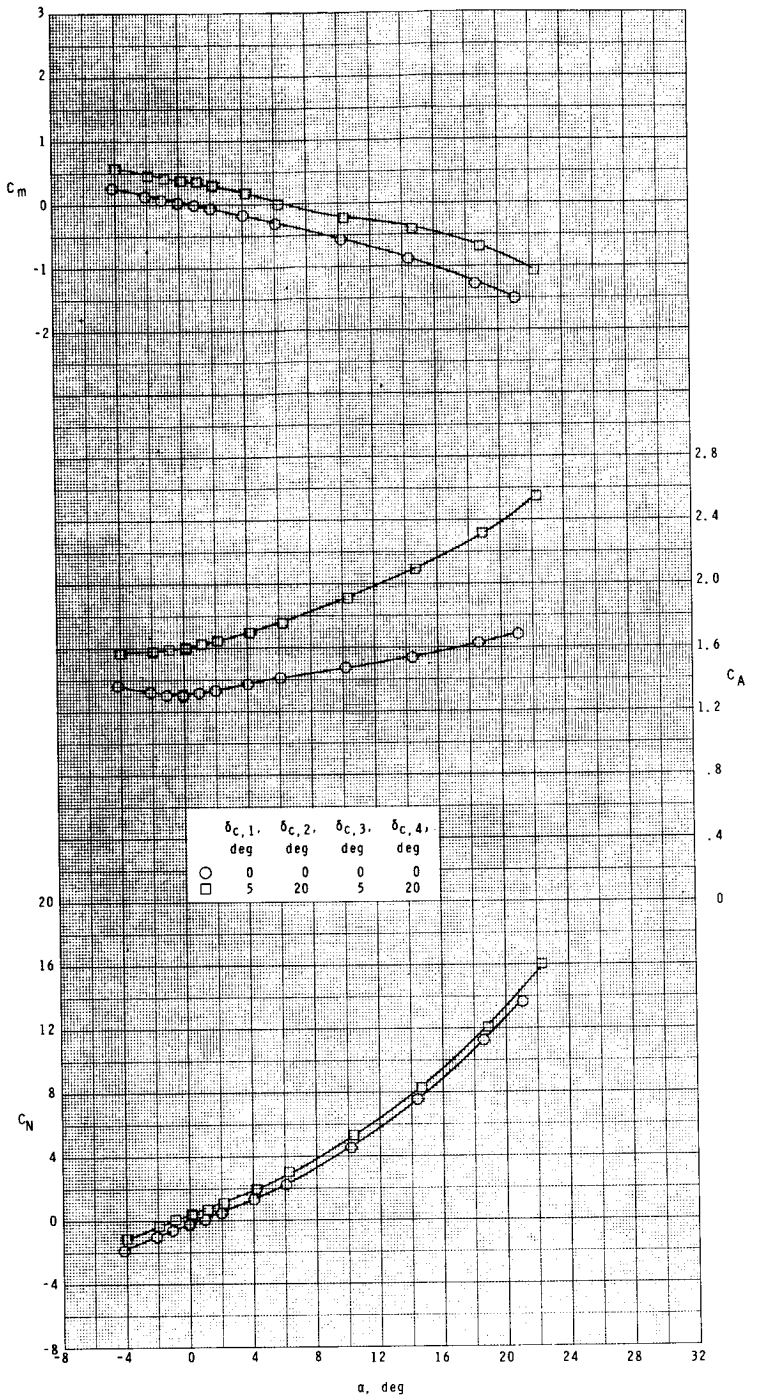

(e) M = 3.95.

Figure 8.- Continued.

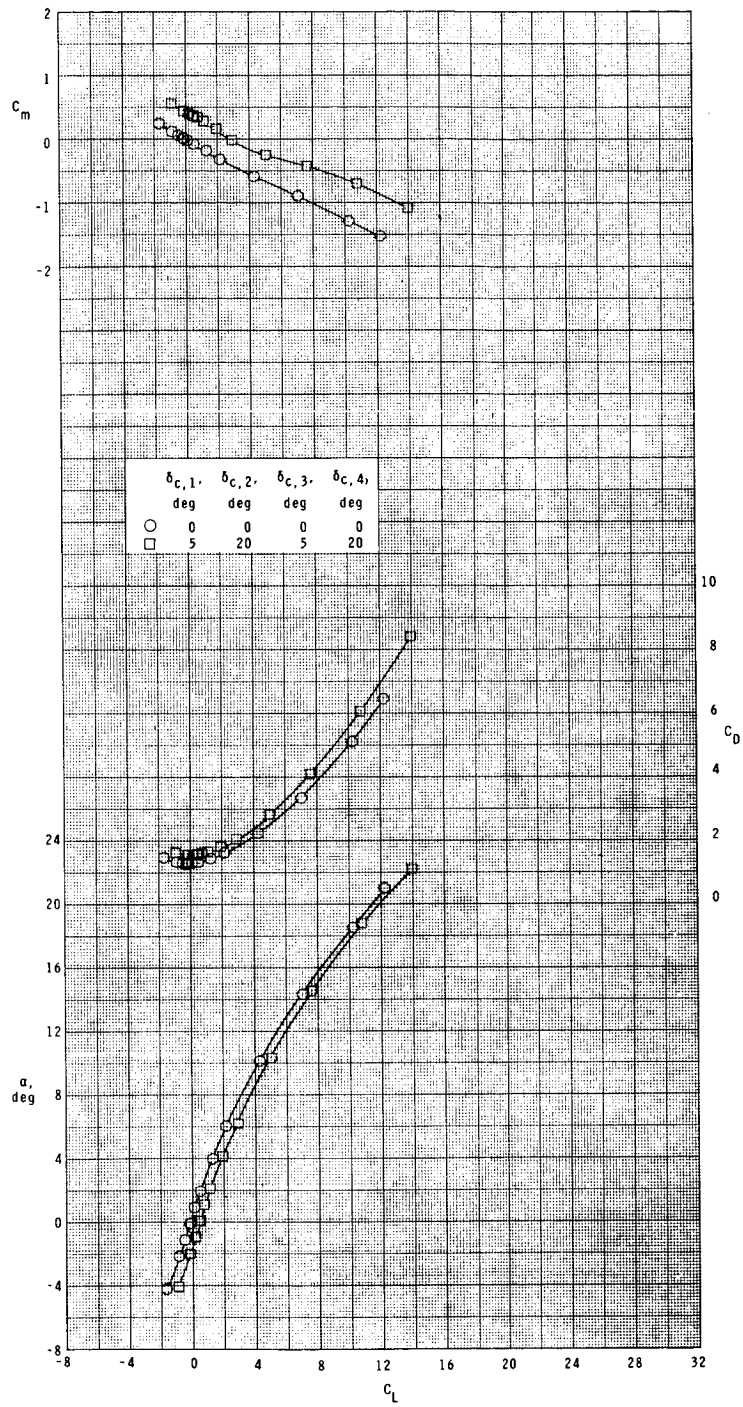

(e) Concluded.

Figure 8.- Continued.

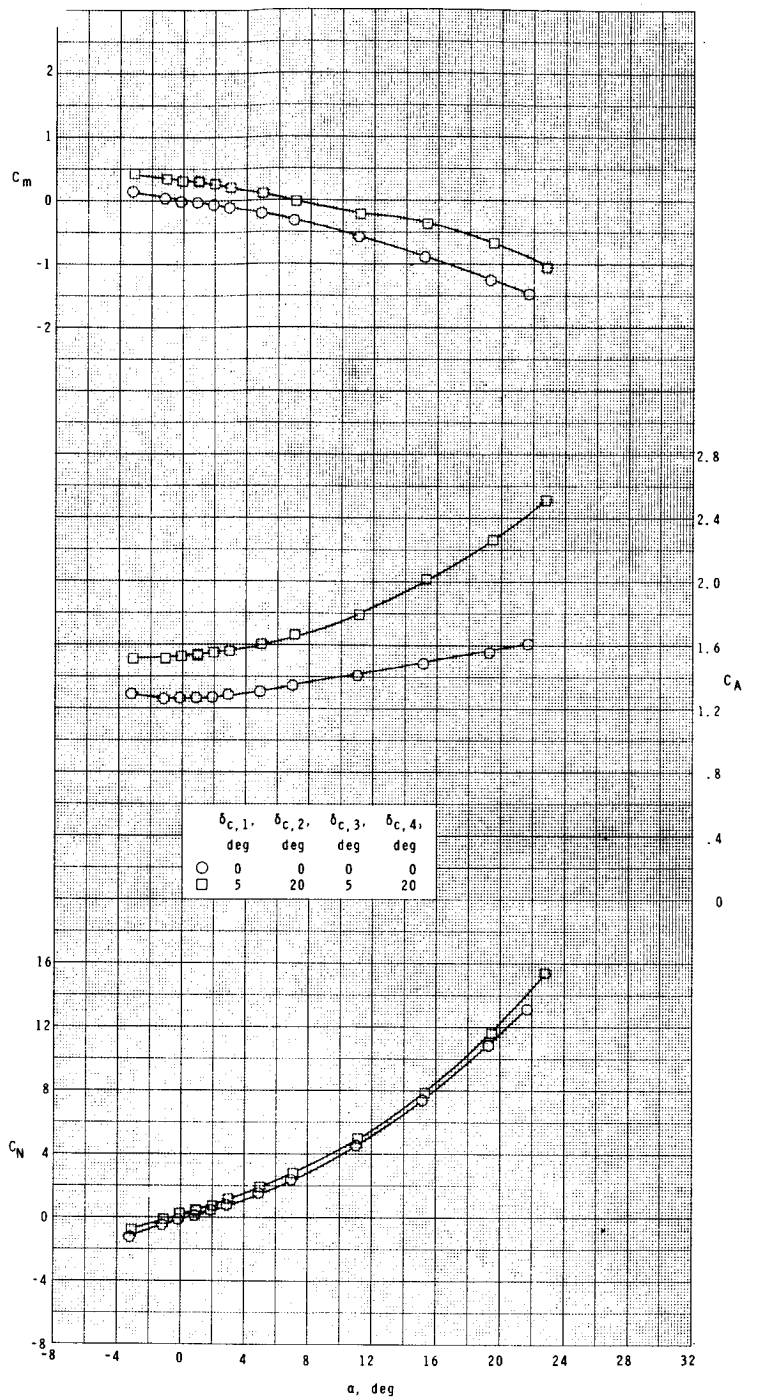

(f) M = 4.63.

Figure 8.- Continued.

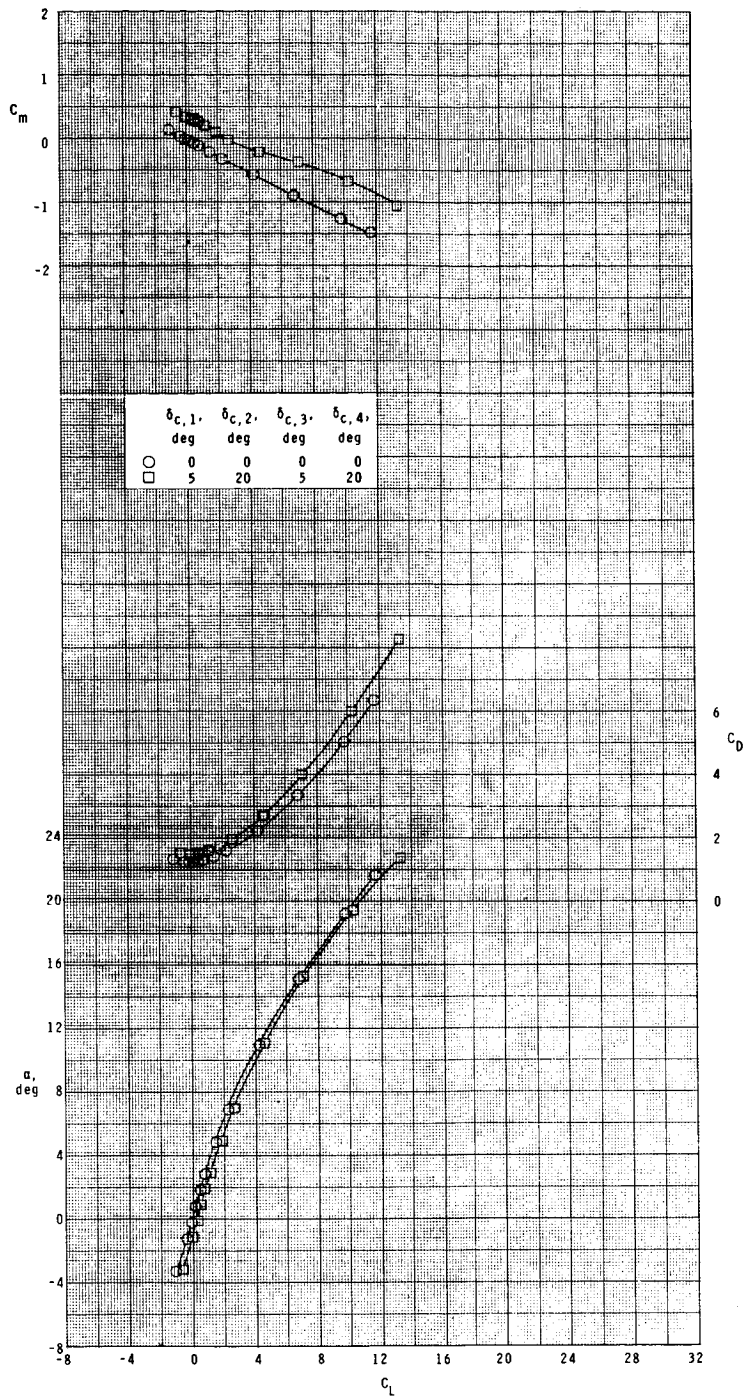

(f) Concluded.

Figure 8.- Concluded.

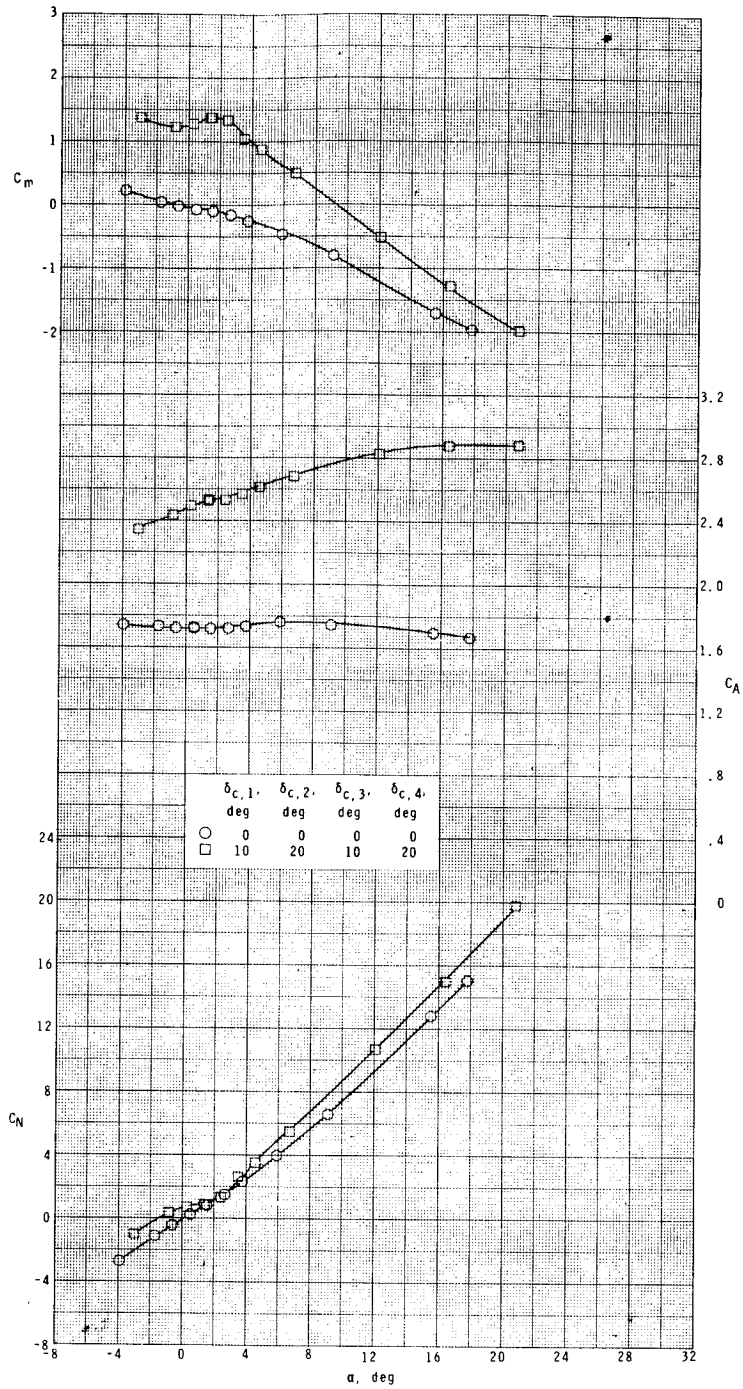

(a) M = 1.75.

Figure 9.- Control effectiveness for pitch-yaw maneuver. $\phi = -26.57^{o}$.

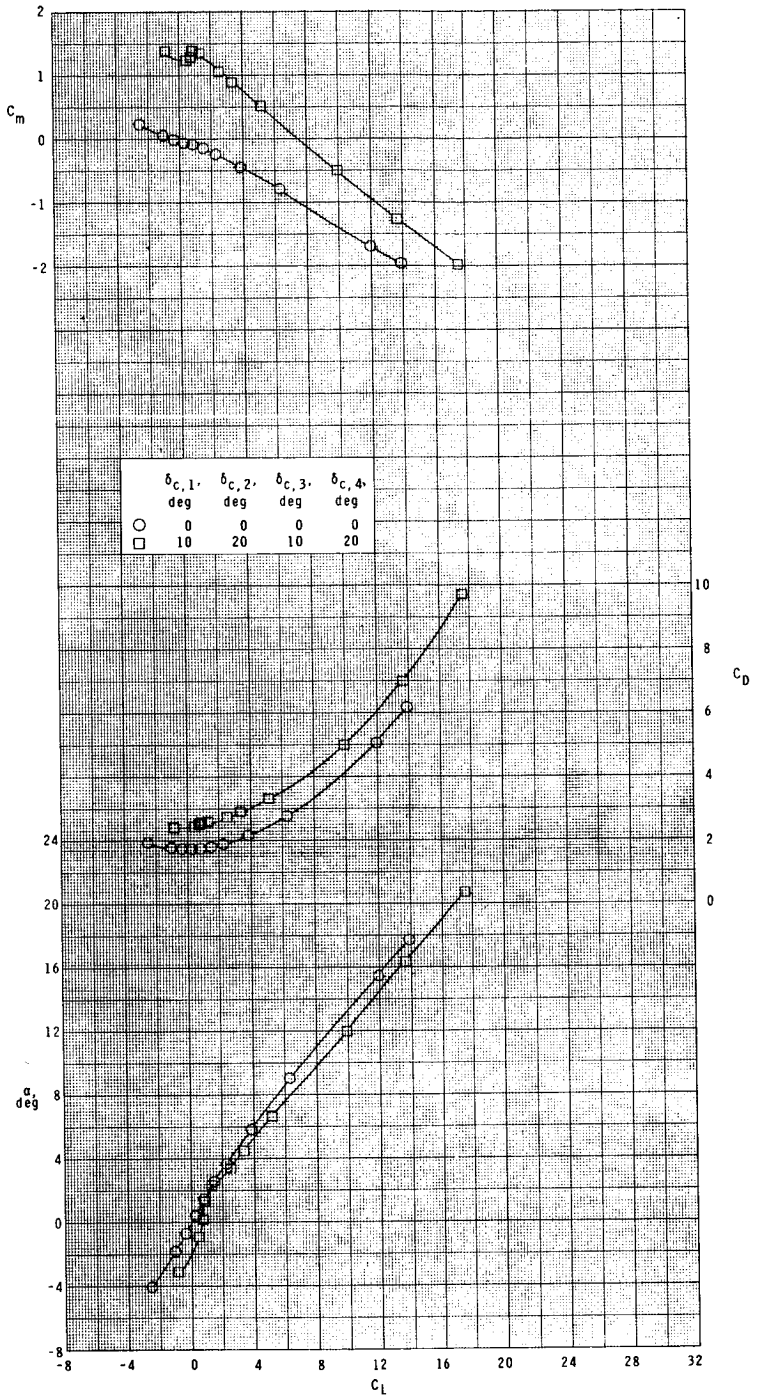

(a) Concluded.

Figure 9.- Continued.

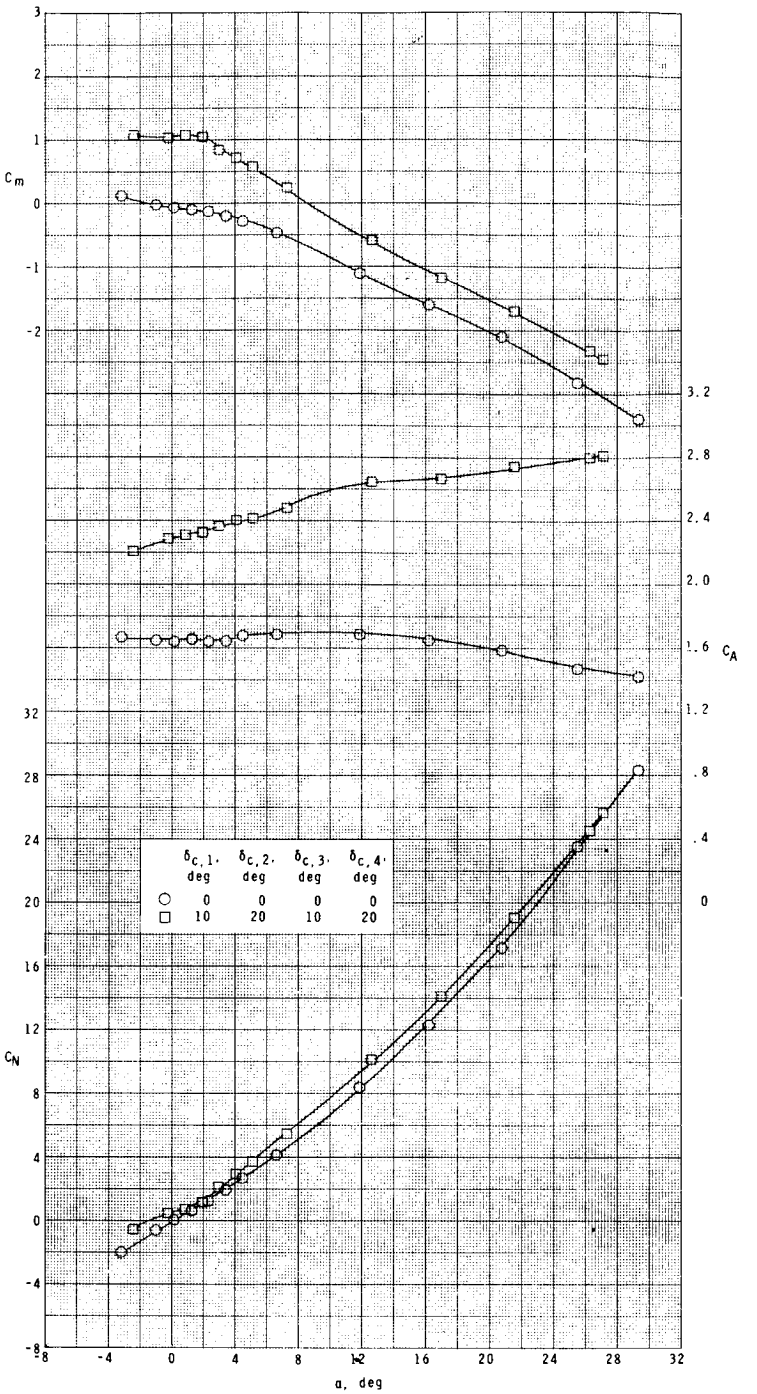

(b) M = 2.10.

Figure 9.- Continued.

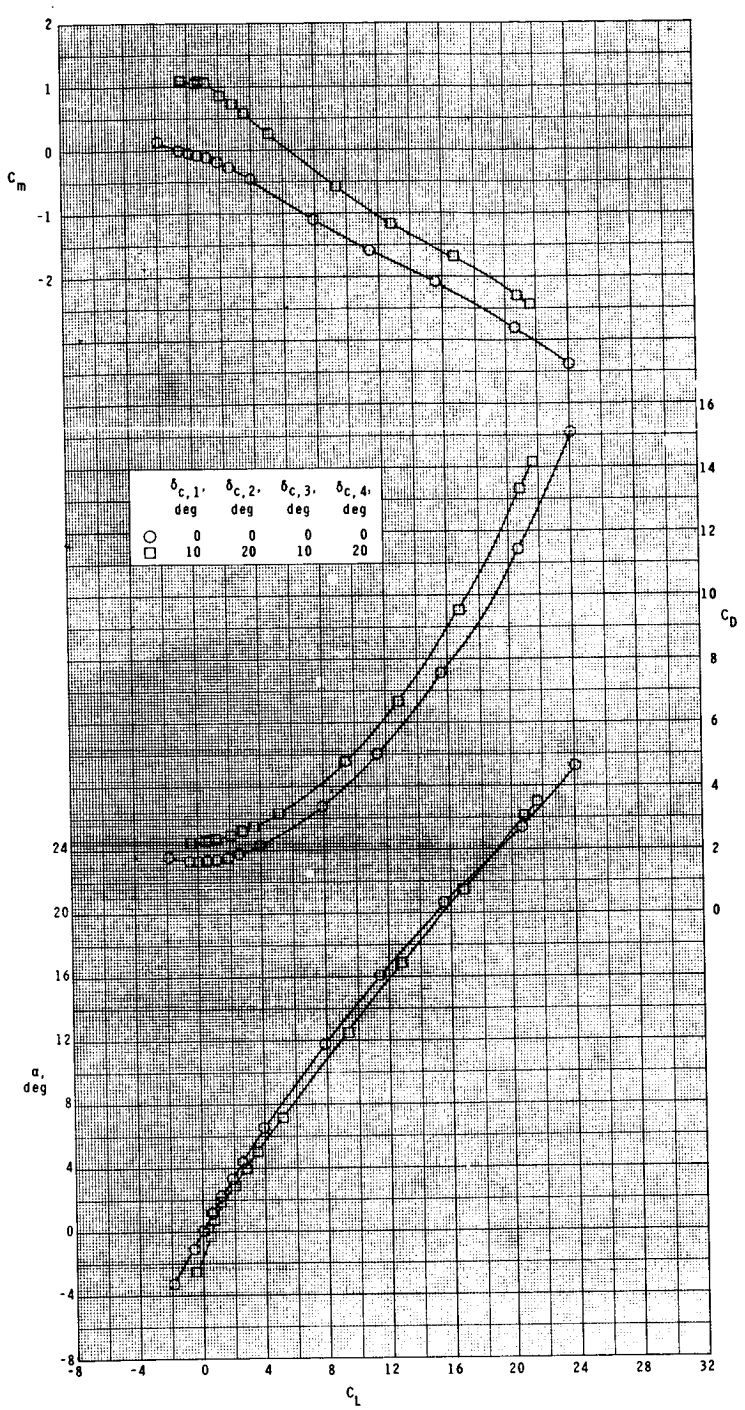

(b) Concluded.

Figure 9.- Continued.

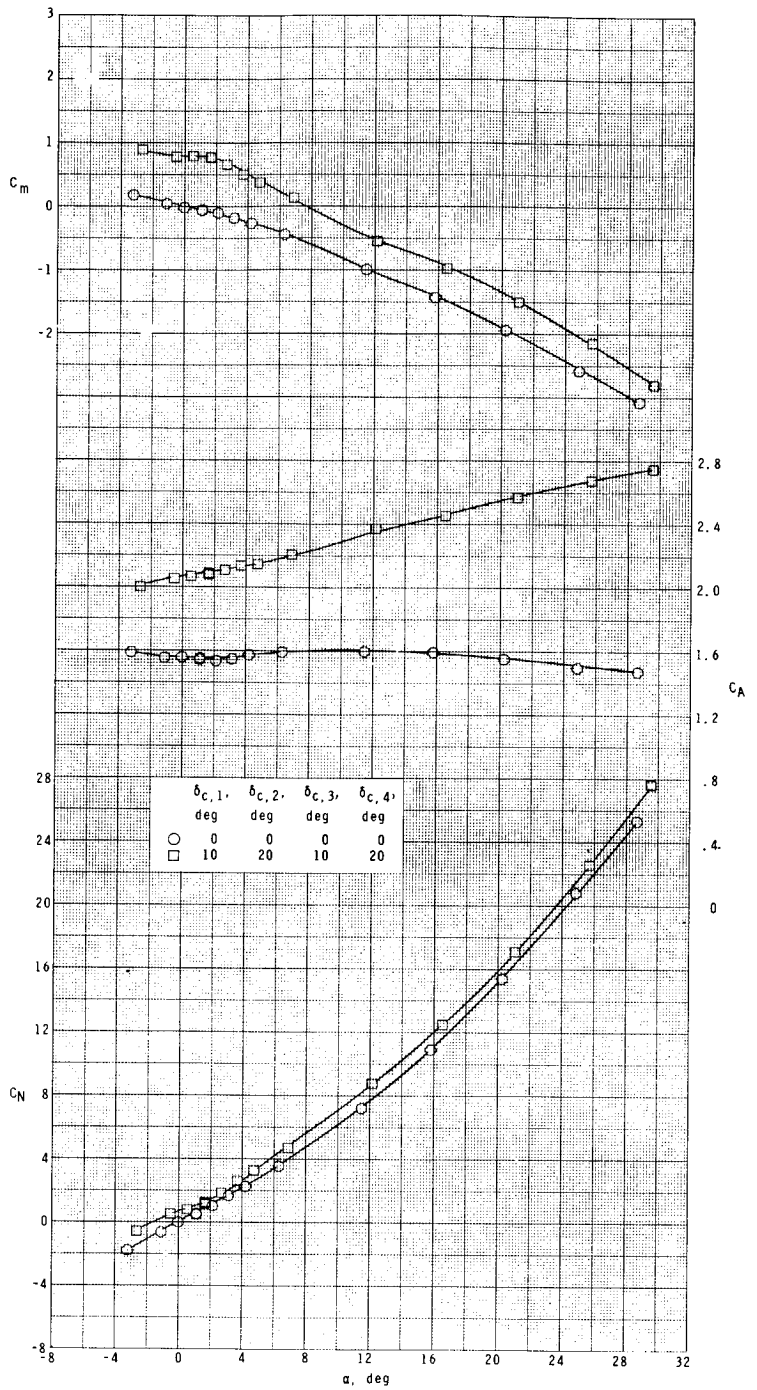

(c) M = 2.50.

Figure 9.- Continued.

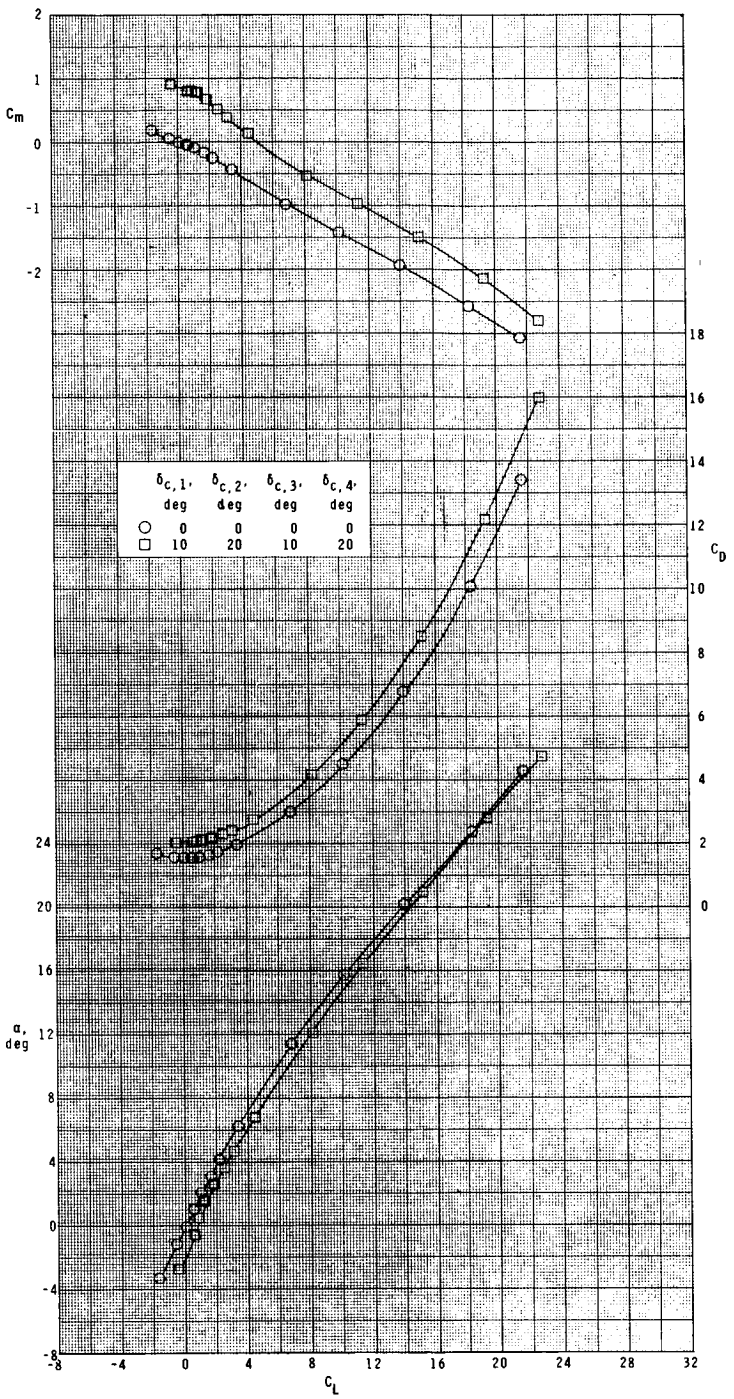

(c) Concluded.

Figure 9.- Continued.

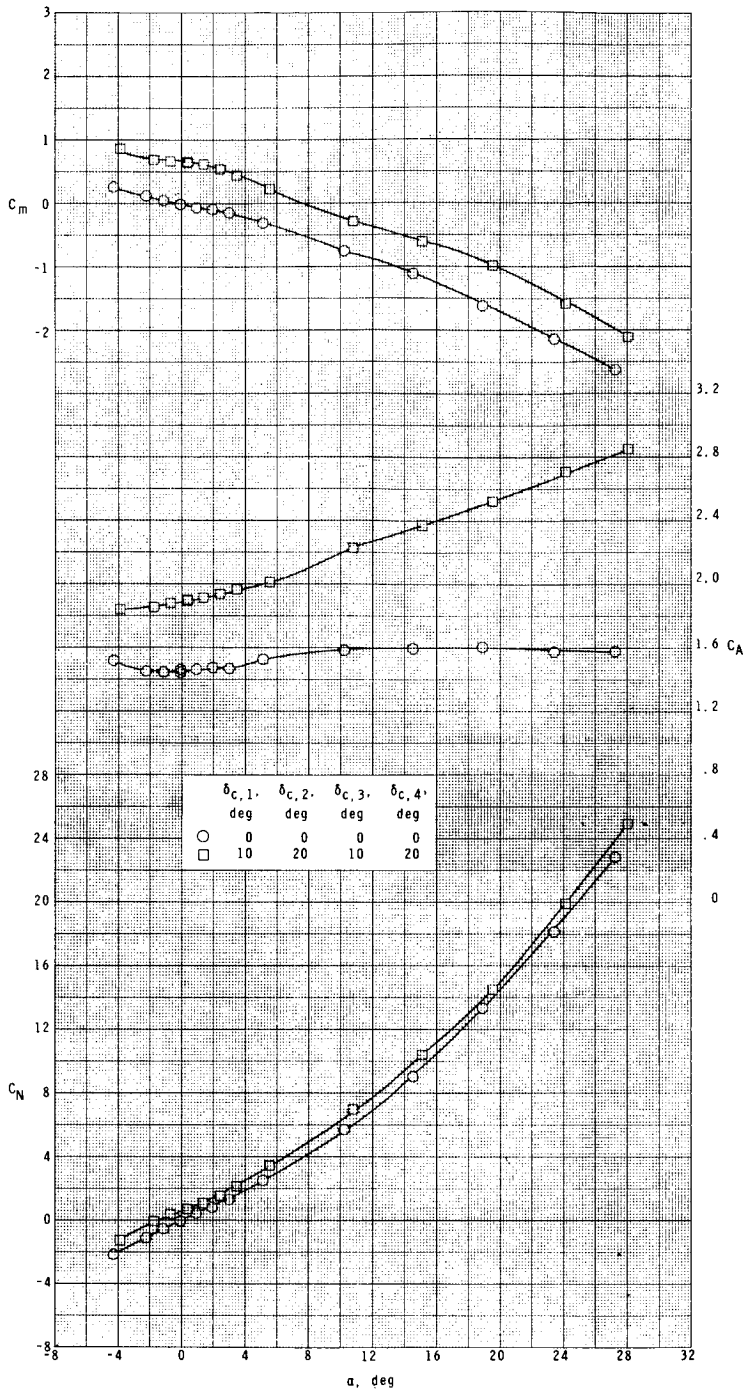

(d) M = 2.86.

Figure 9.- Continued.

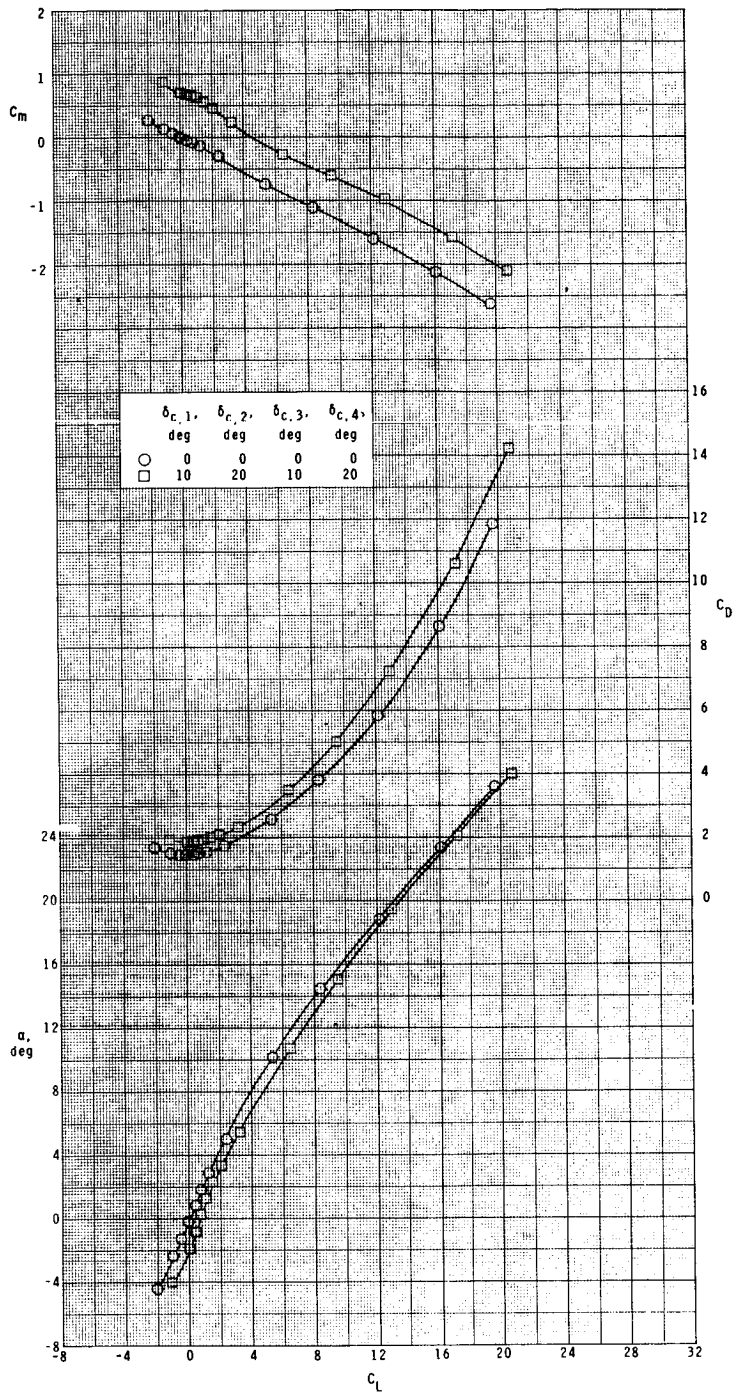

(d) Concluded.

Figure 9.- Continued.

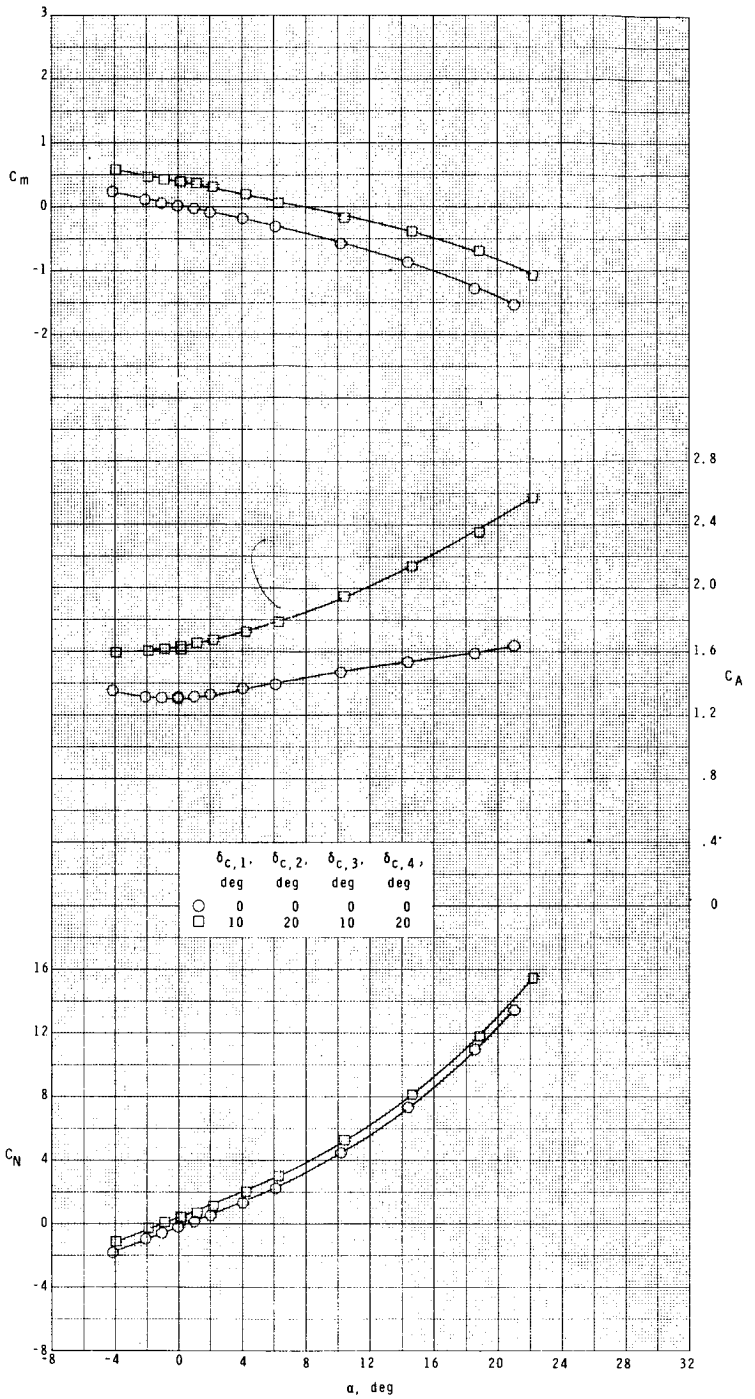

(e) M = 3.95.

Figure 9.- Continued.

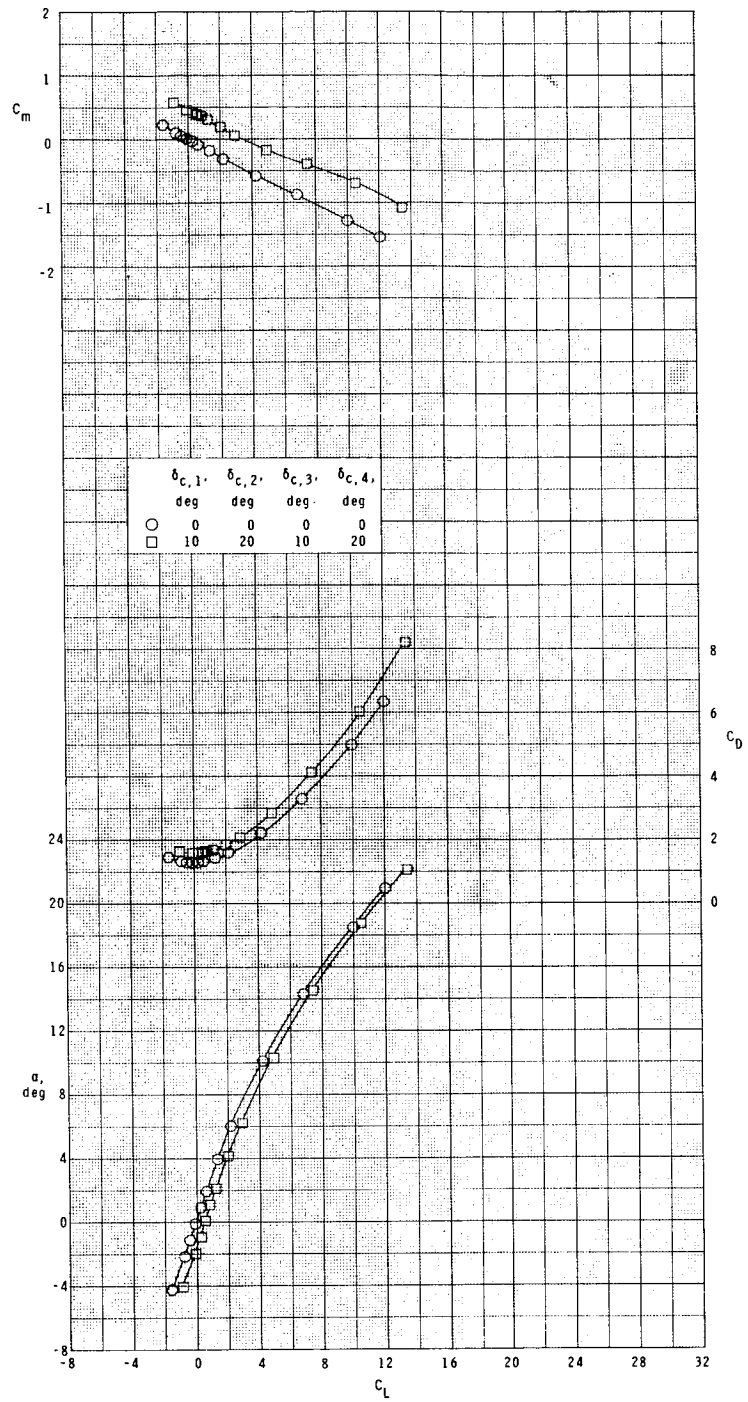

(e) Concluded.

Figure 9.- Continued.

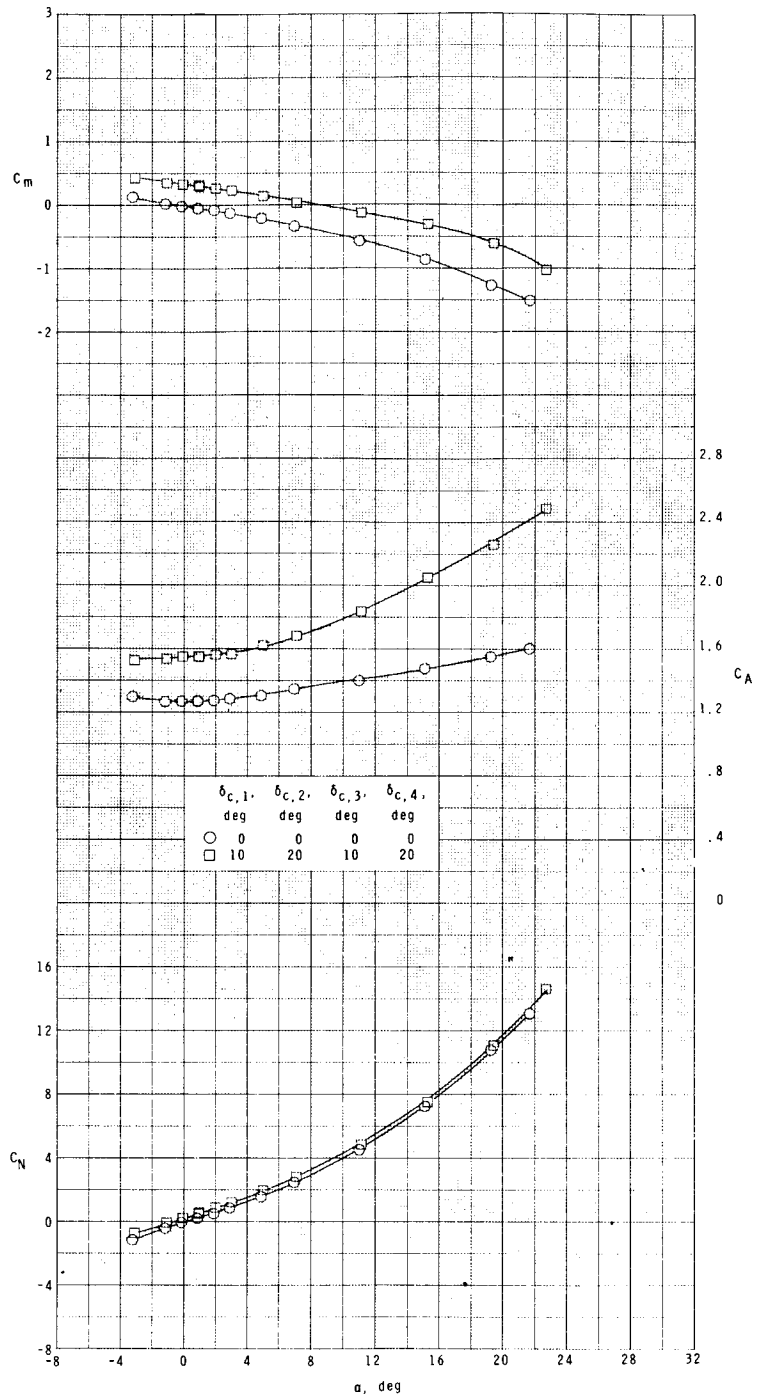

(f) M = 4.63.

Figure 9.- Continued.

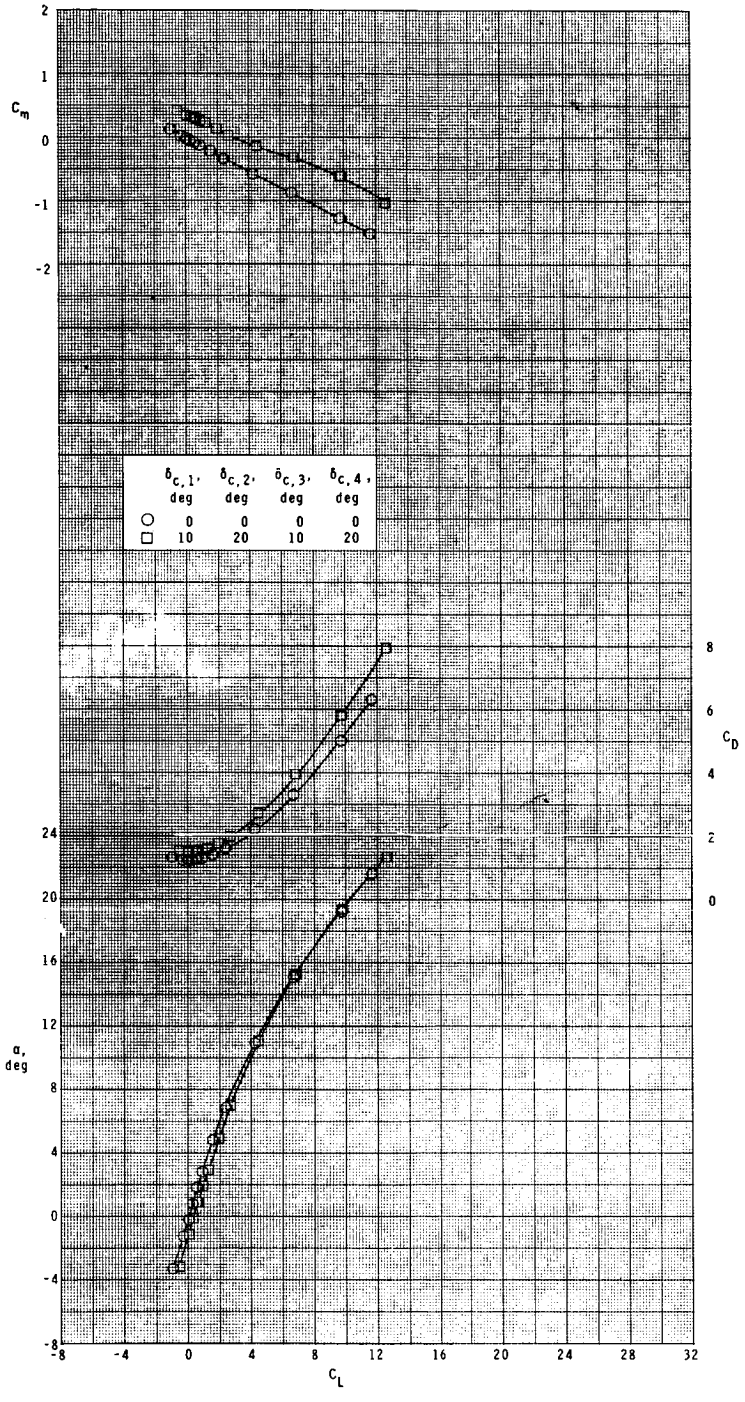

(f) Concluded.

Figure 9.- Concluded.

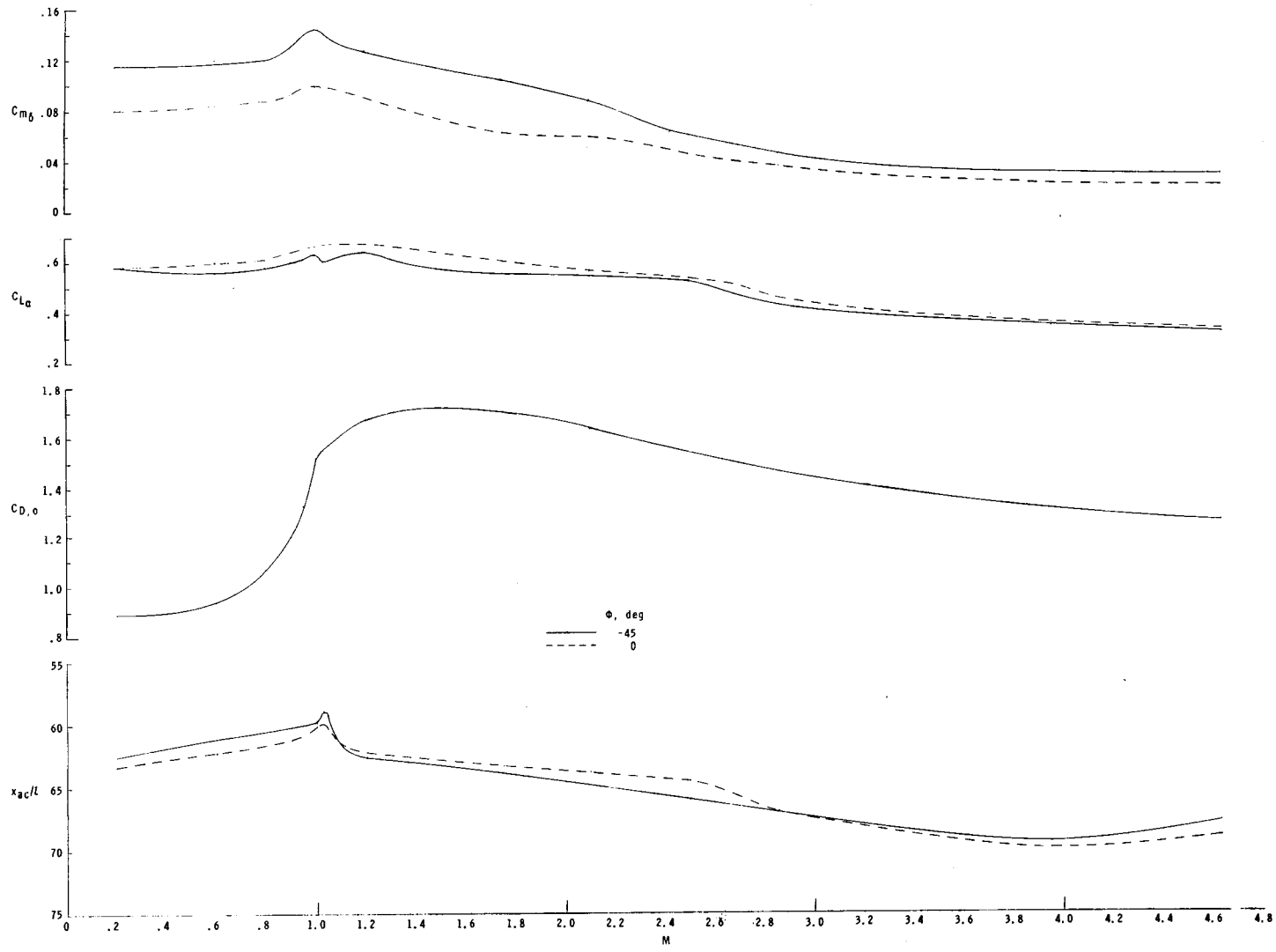

(a) C_{m_δ}, C_{L_α}, $C_{D,o}$, and x_{ac}/l as a function of Mach number.

Figure 10.- Summary of longitudinal aerodynamic characteristics.

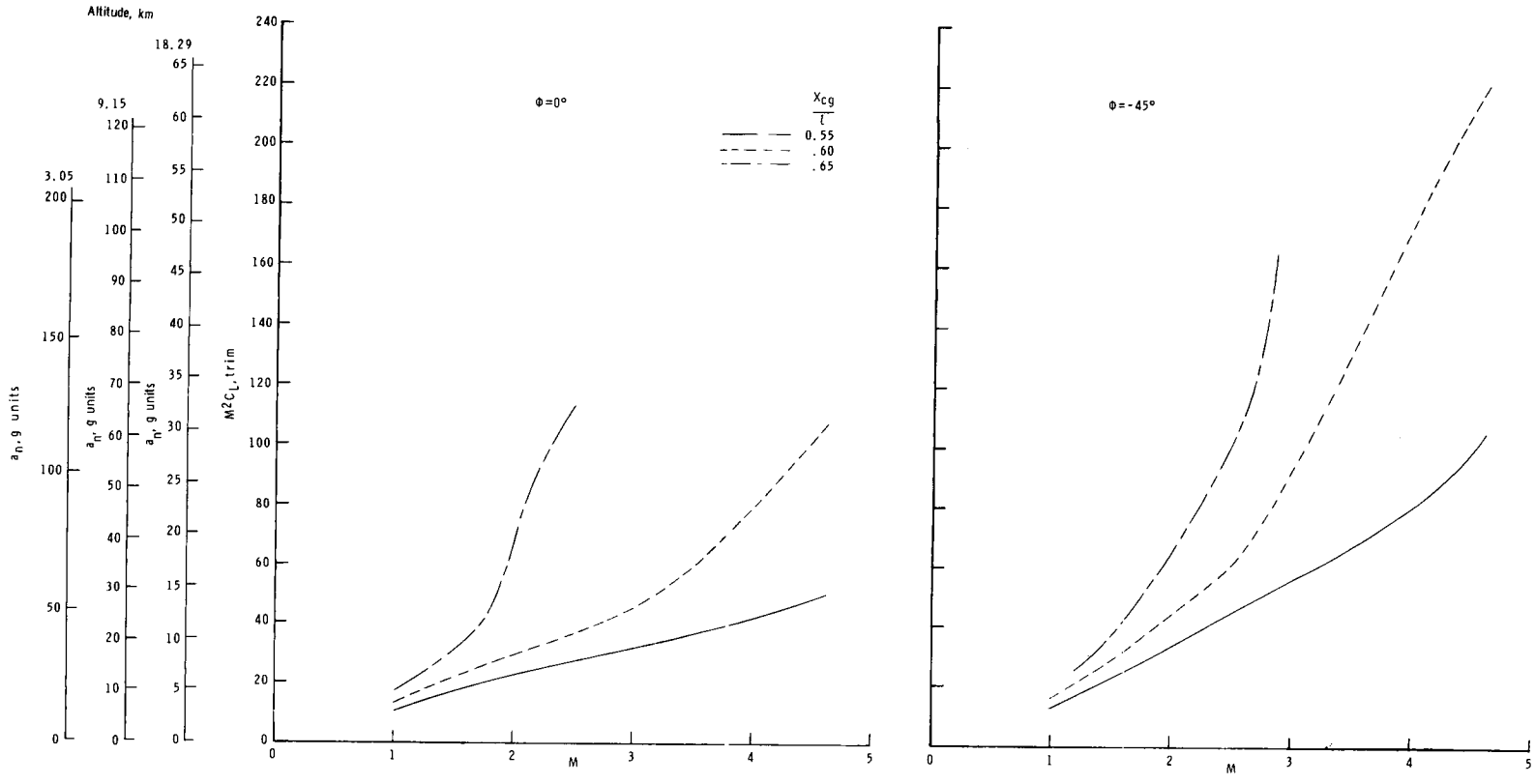

(b) Variation of a_n with Mach number for various center-of-gravity locations. $\delta_{pitch} = 20^o$.

Figure 10.- Concluded.

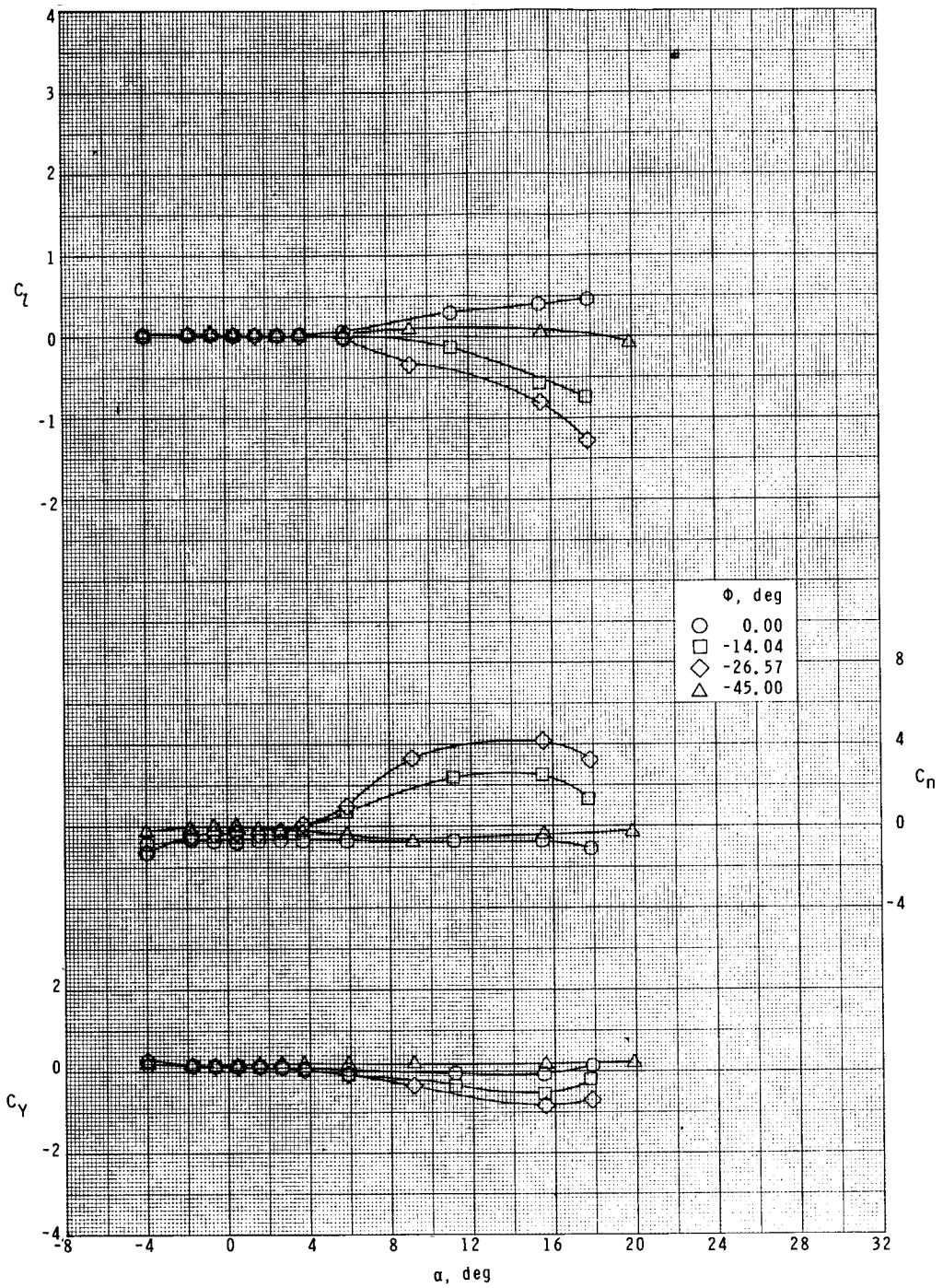

(a) M = 1.75.

Figure 11.- Effect of model roll orientation on lateral characteristics.

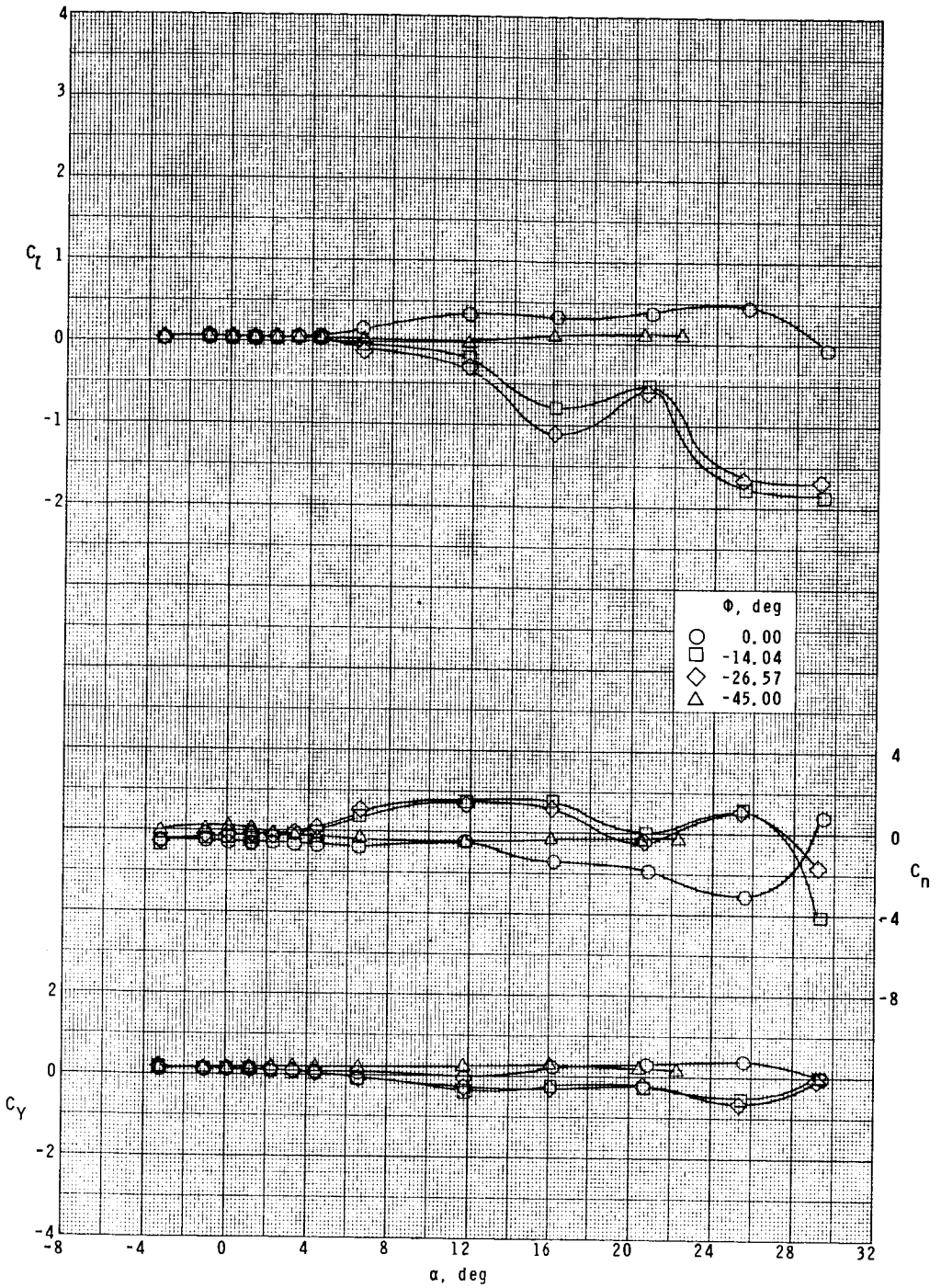

(b) M = 2.10.

Figure 11.- Continued.

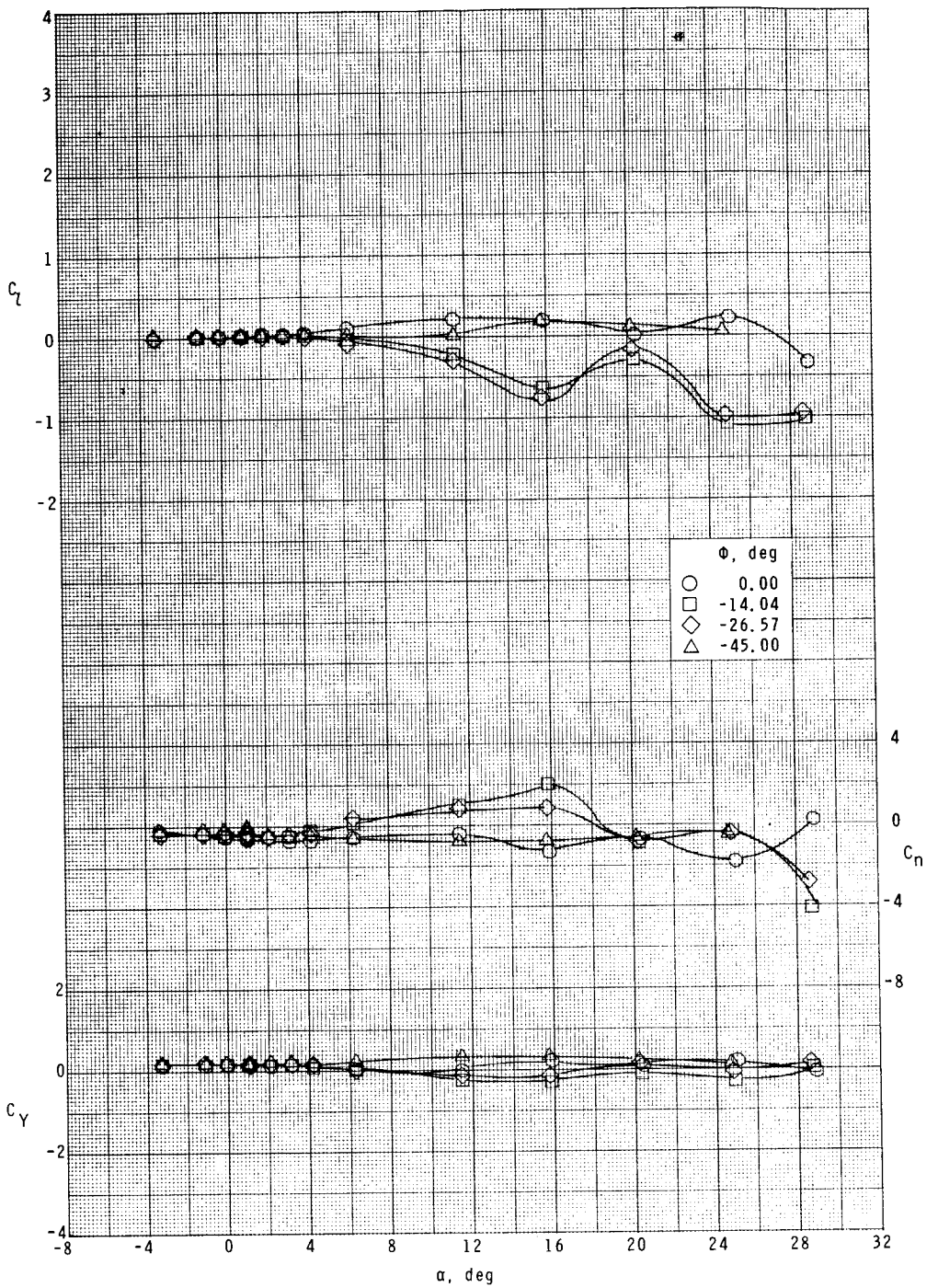

(c) M = 2.50.

Figure 11.- Continued.

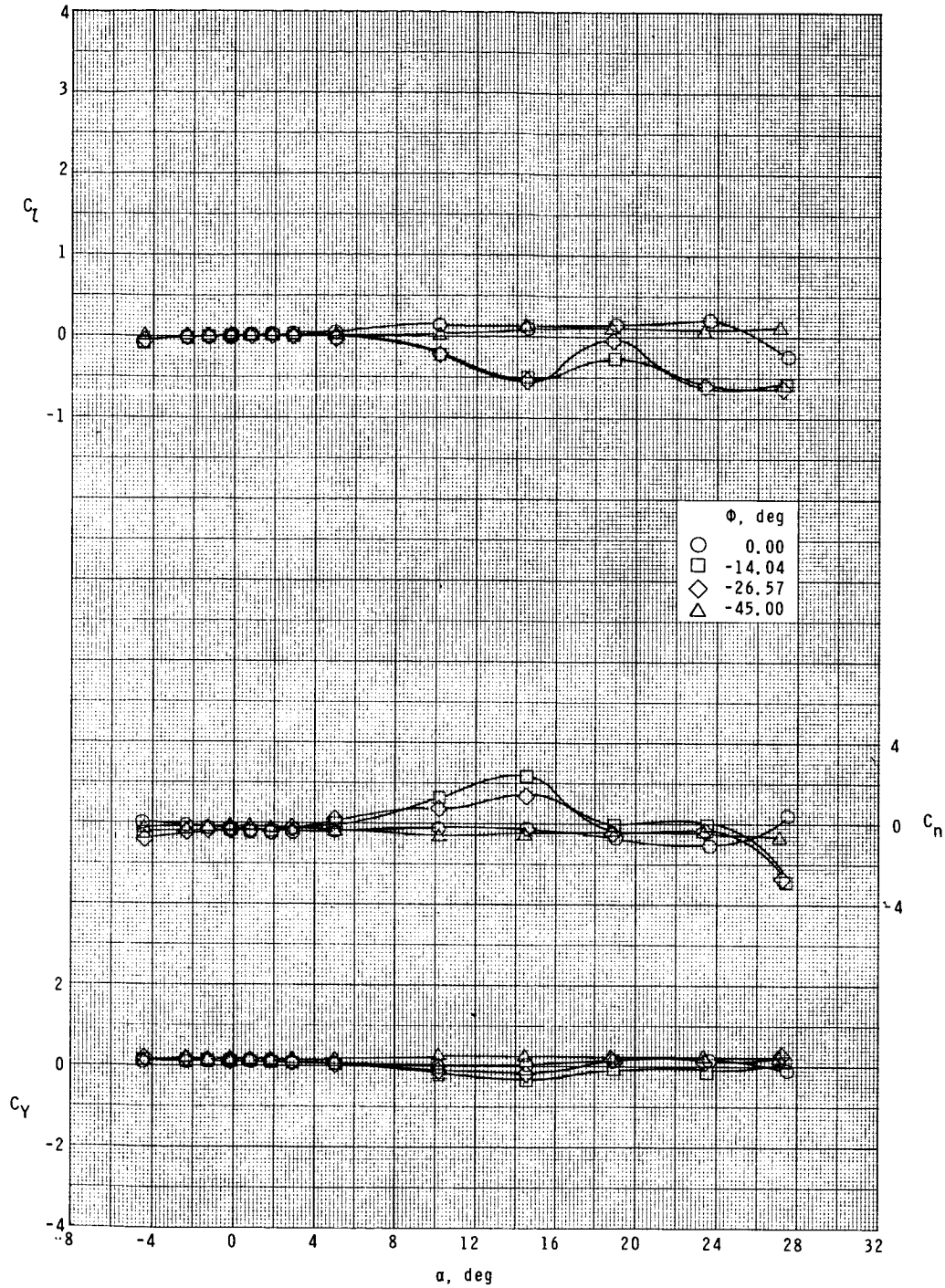

(d) M = 2.86.

Figure 11.- Continued.

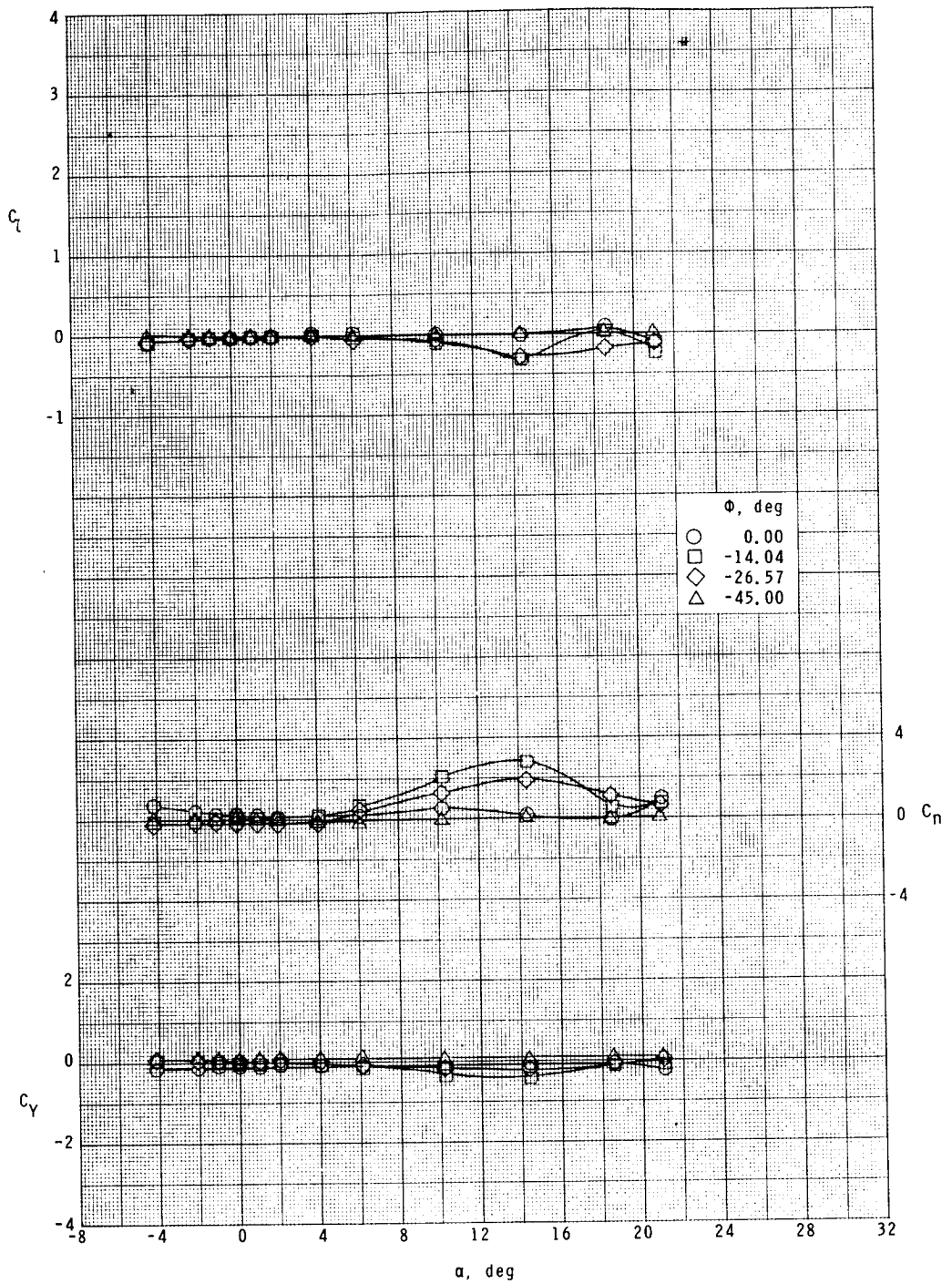

(e) M = 3.95.

Figure 11.- Continued.

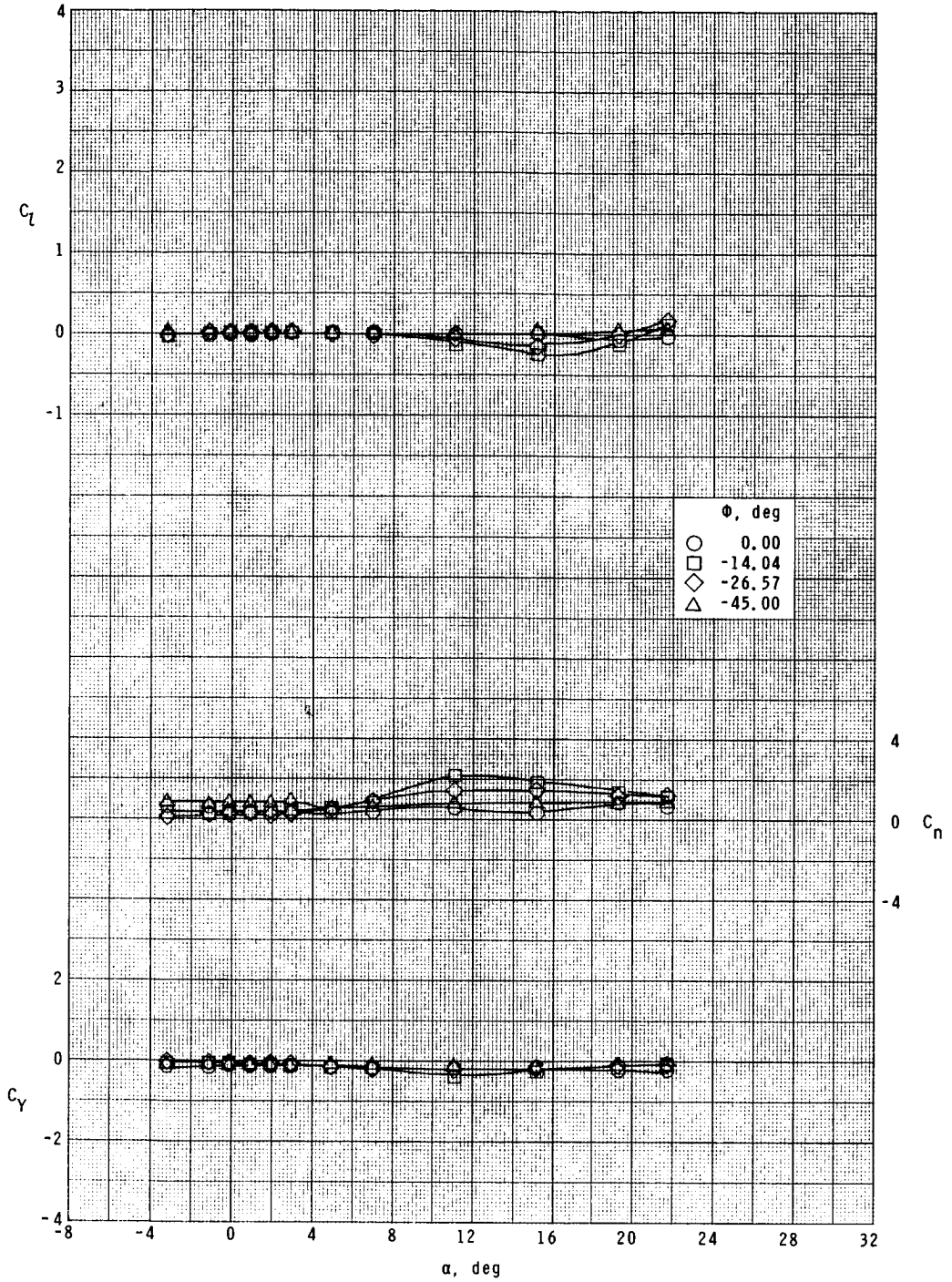

(f) M = 4.63.

Figure 11.- Concluded.

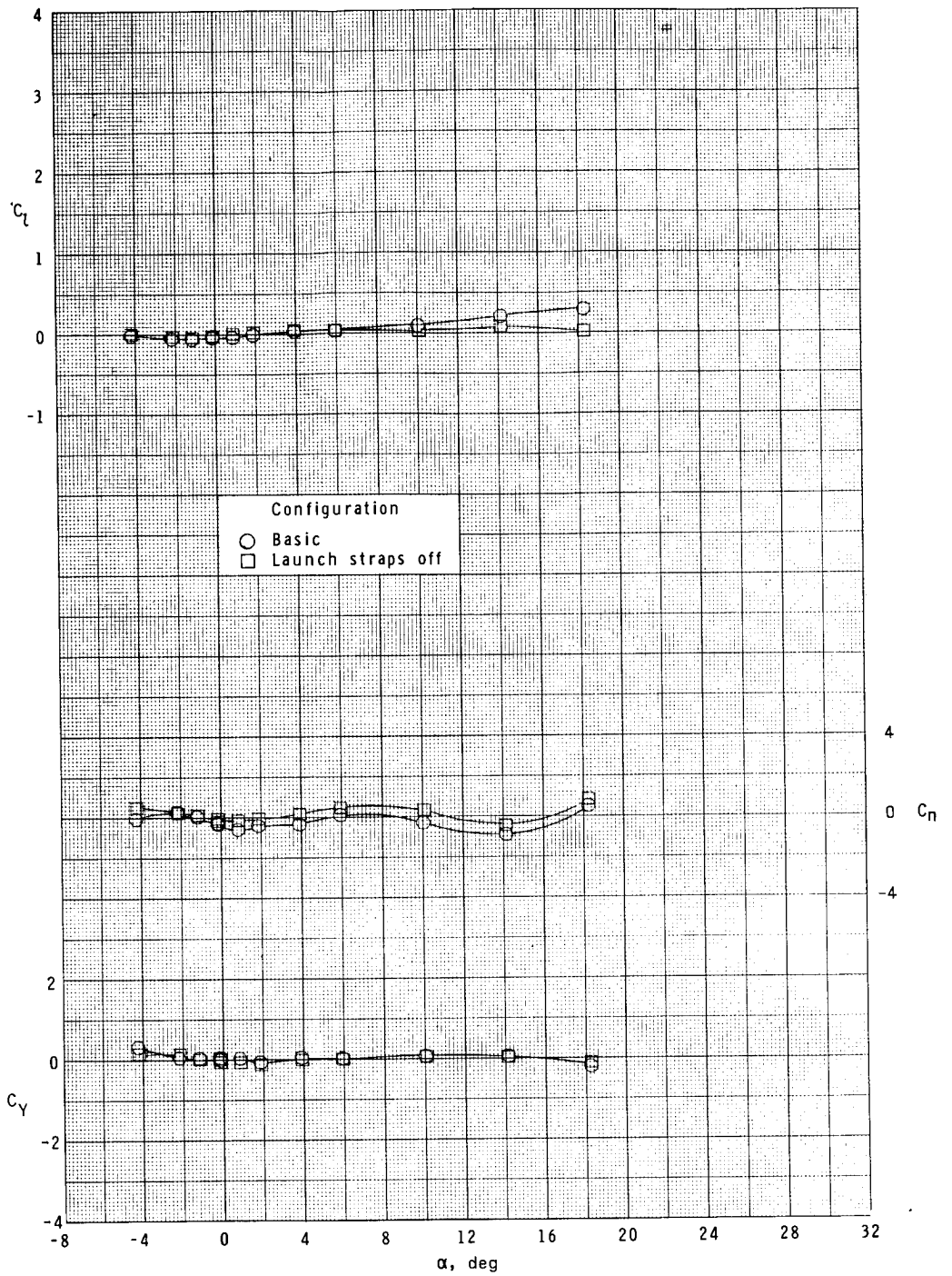

(a) M = 0.20.

Figure 12.- Effect of launch straps on lateral characteristics. $\phi = 0^o$.

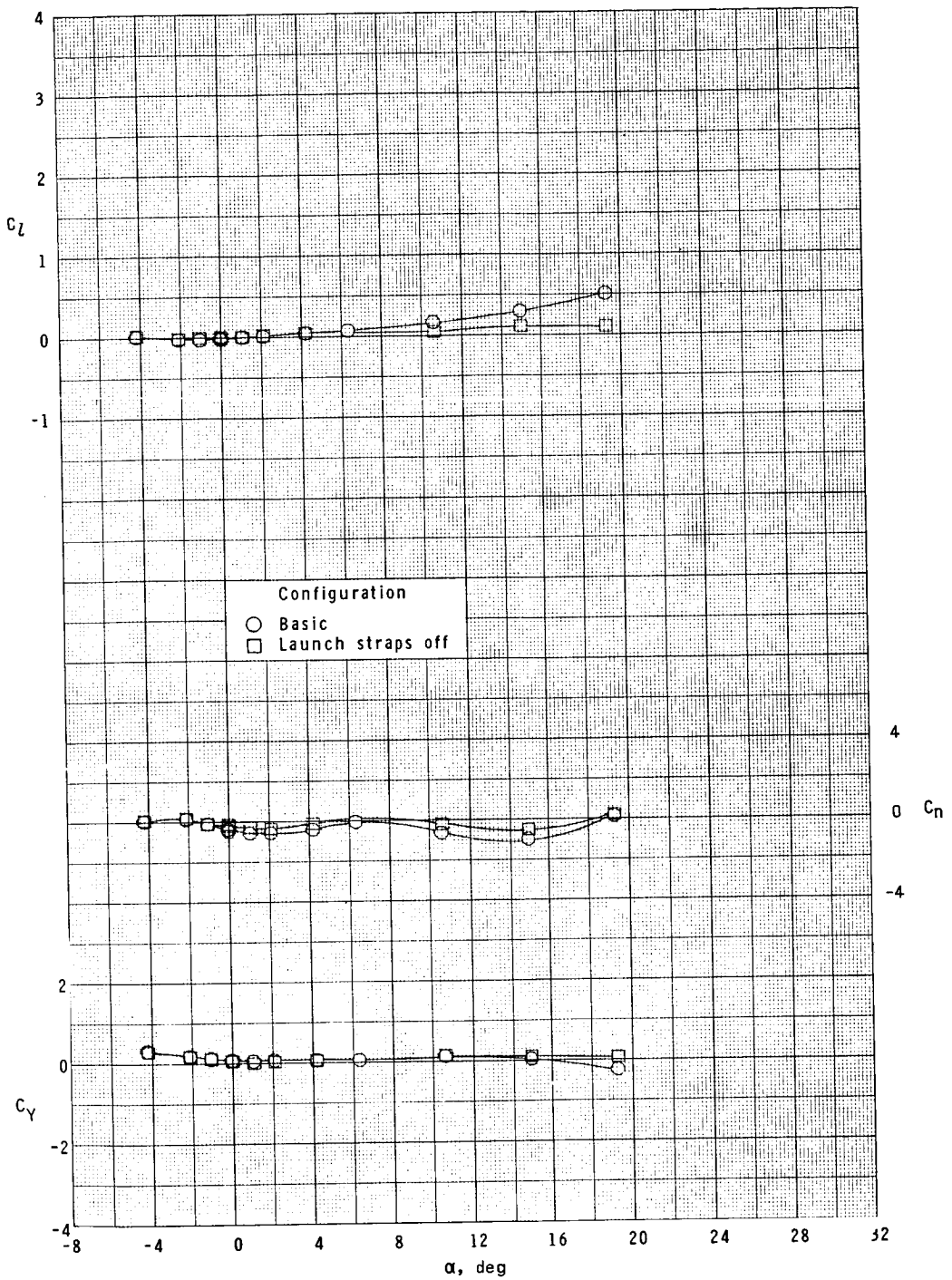

(b) M = 0.60.

Figure 12.- Continued.

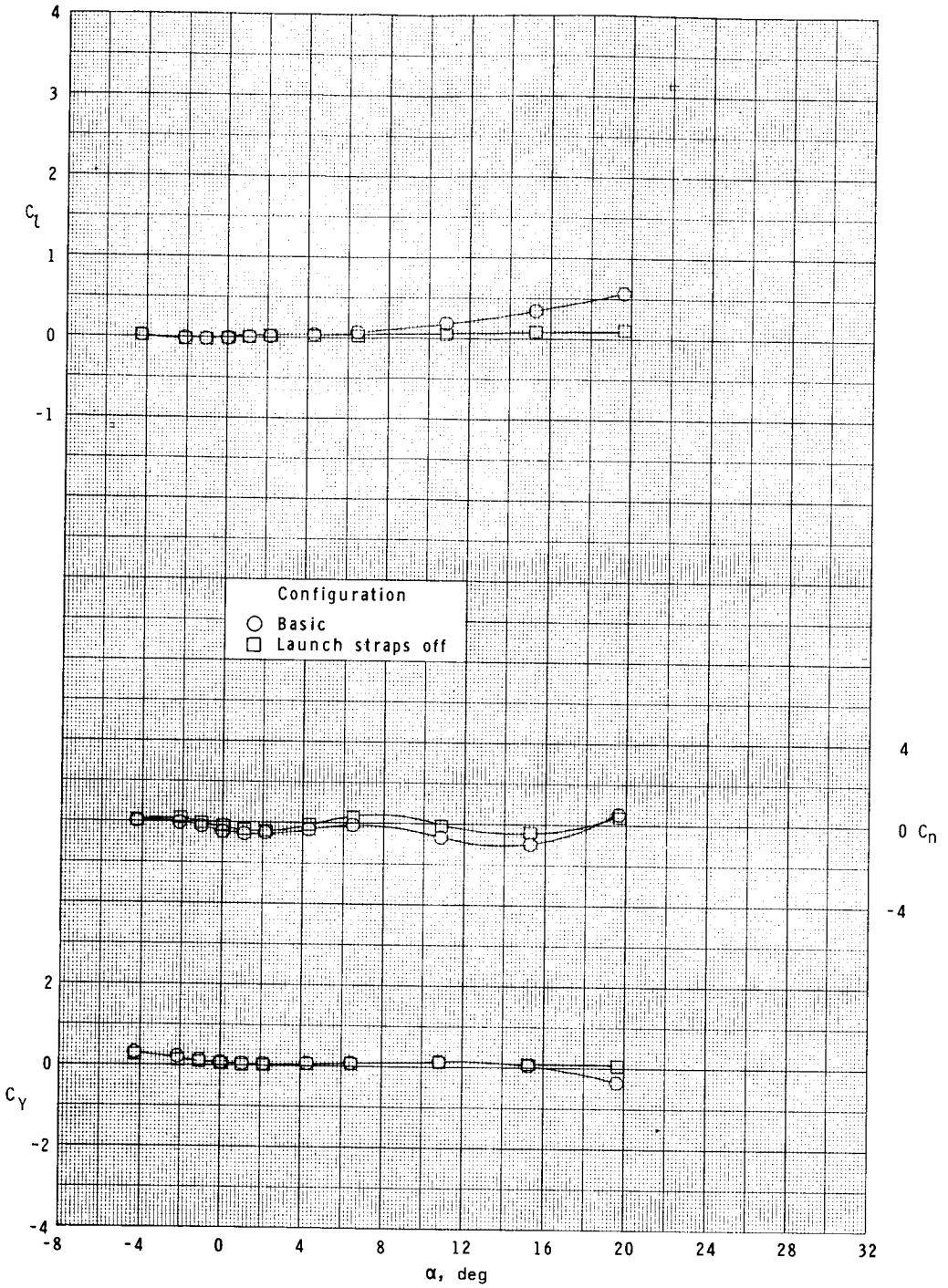

(c) M = 0.80.

Figure 12.- Continued.

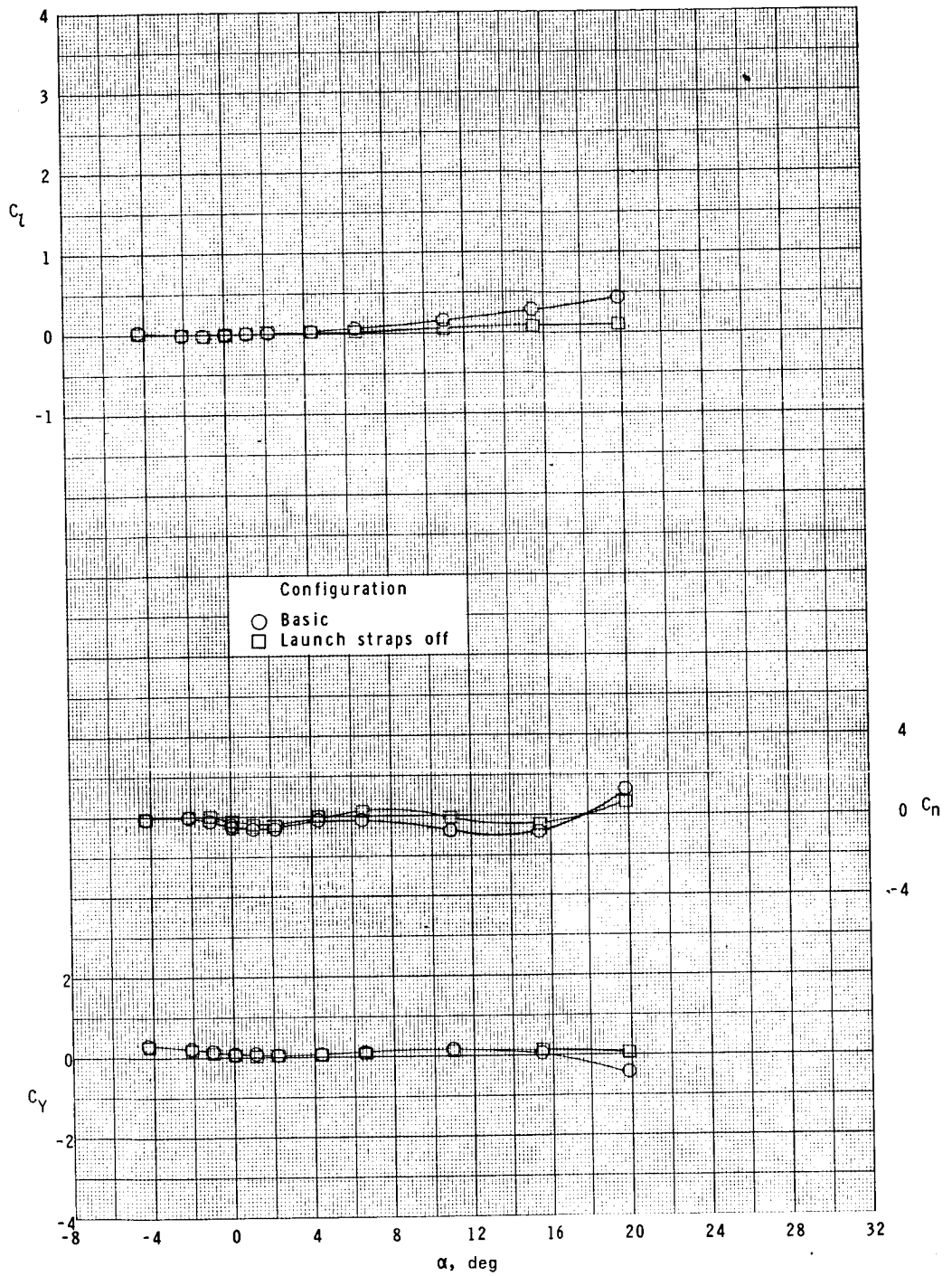

(d) M = 0.90.

Figure 12.- Continued.

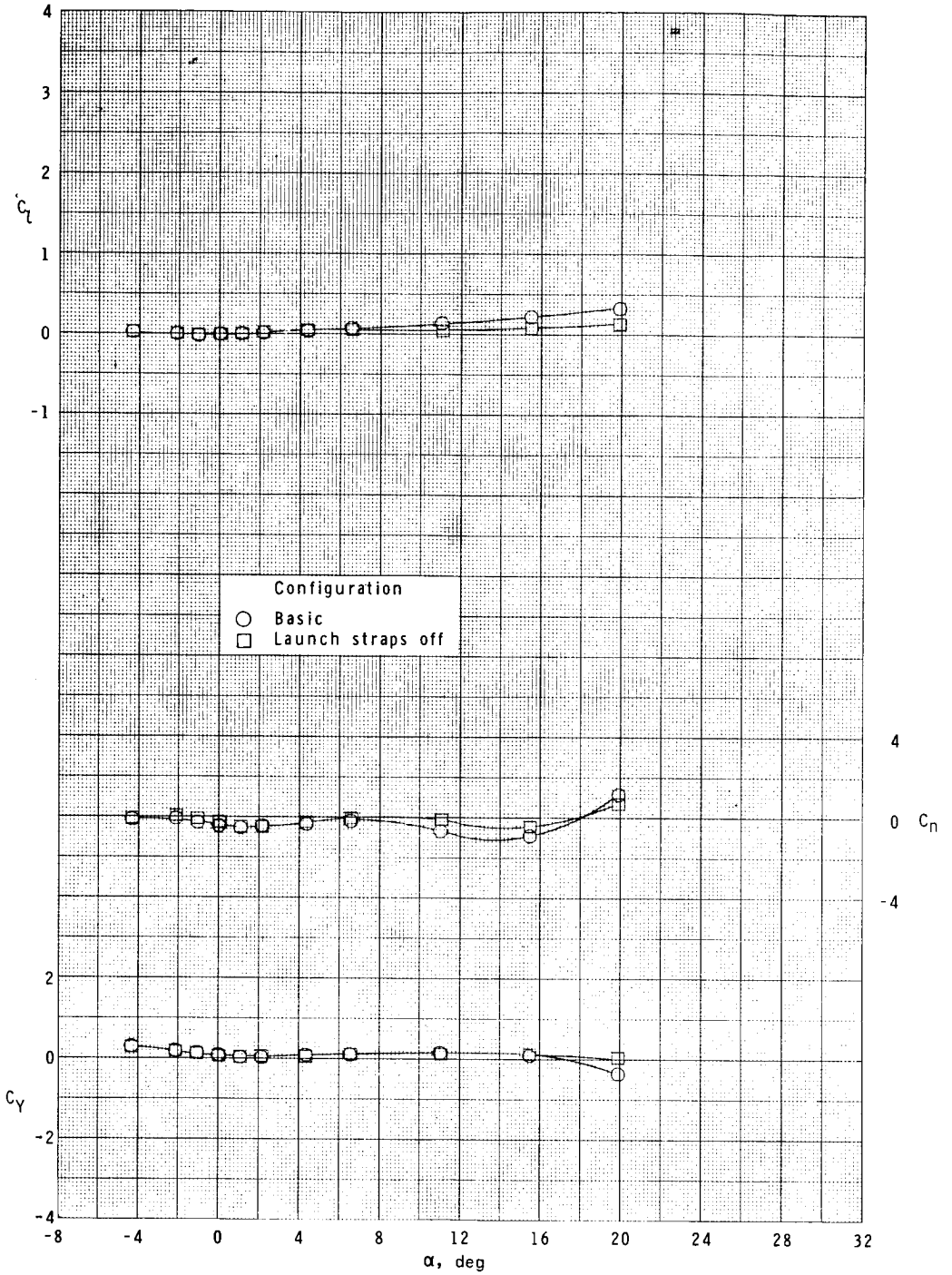

(e) M = 0.95.

Figure 12.- Continued.

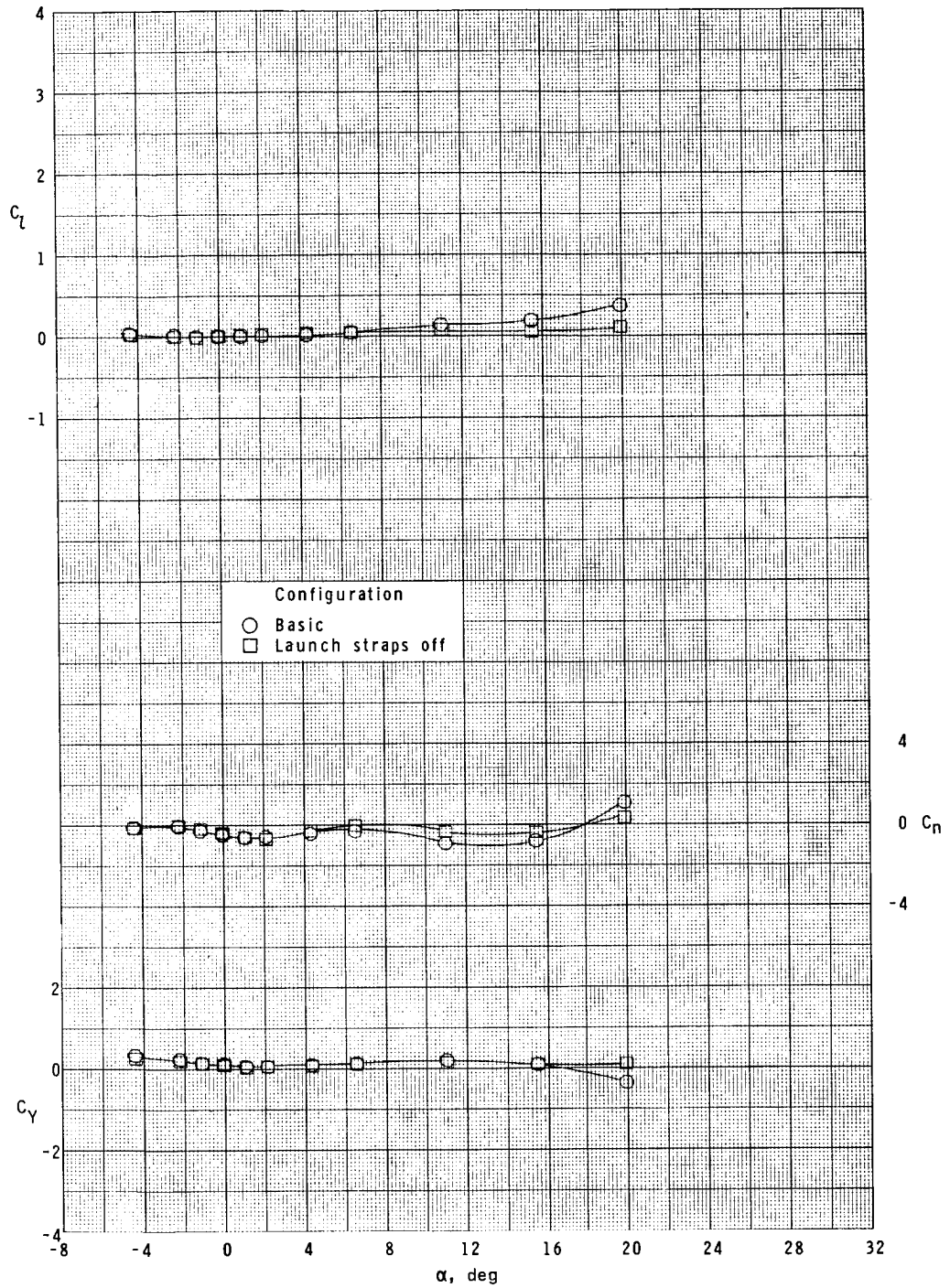

(f) M = 1.00.

Figure 12.- Continued.

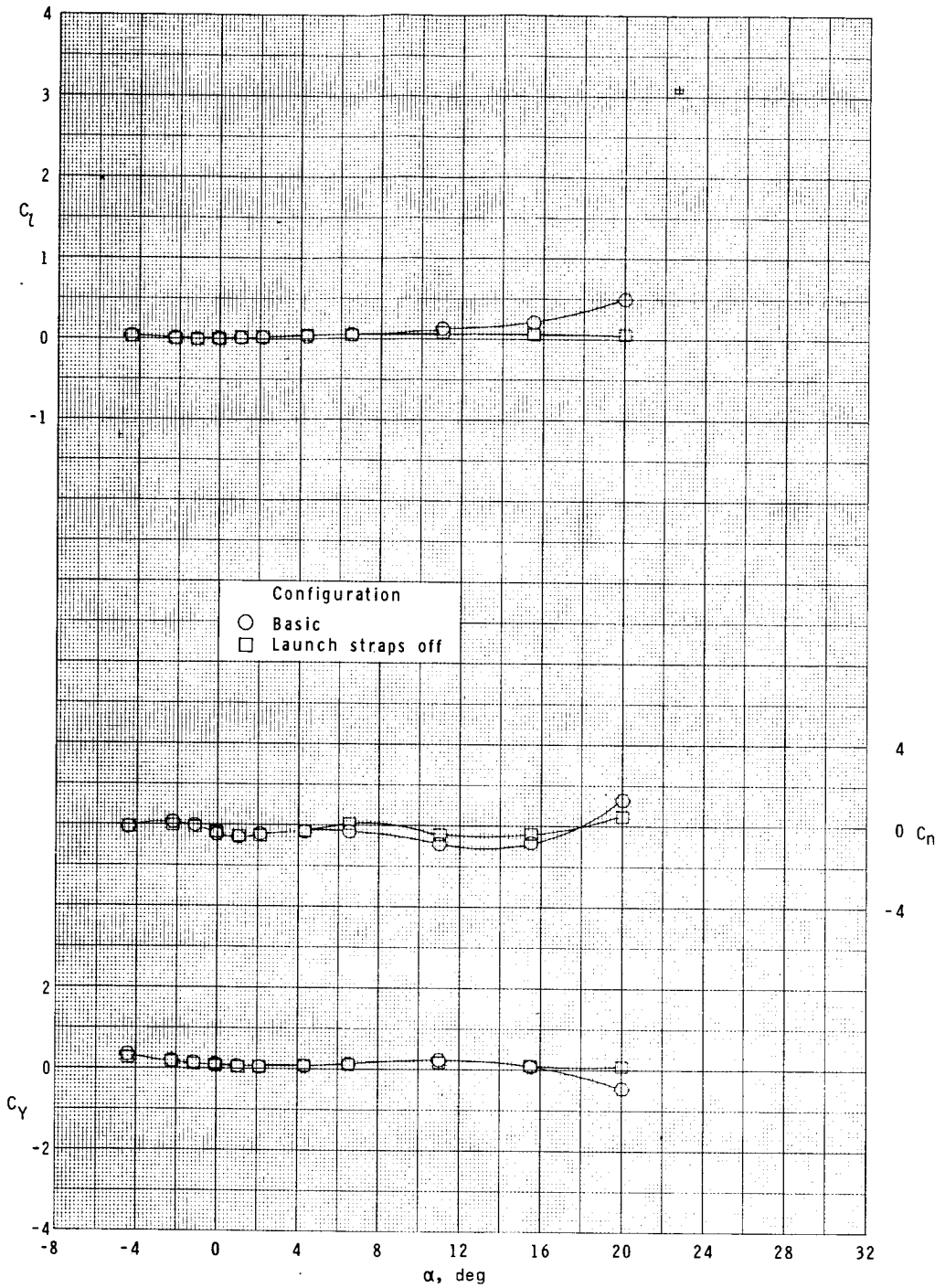

(g) M = 1.03.

Figure 12.- Continued.

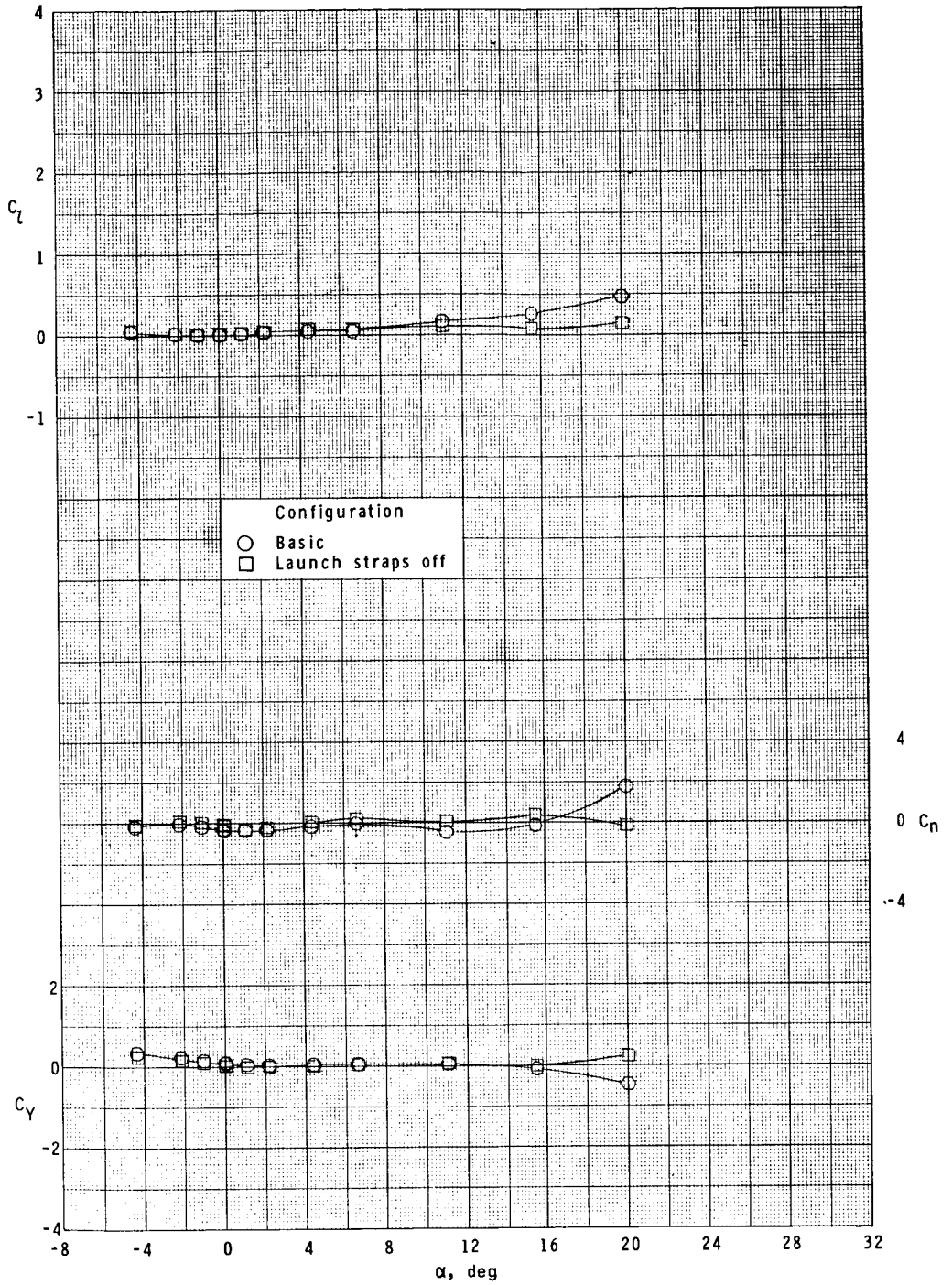

(h) M = 1.20.

Figure 12.- Continued.

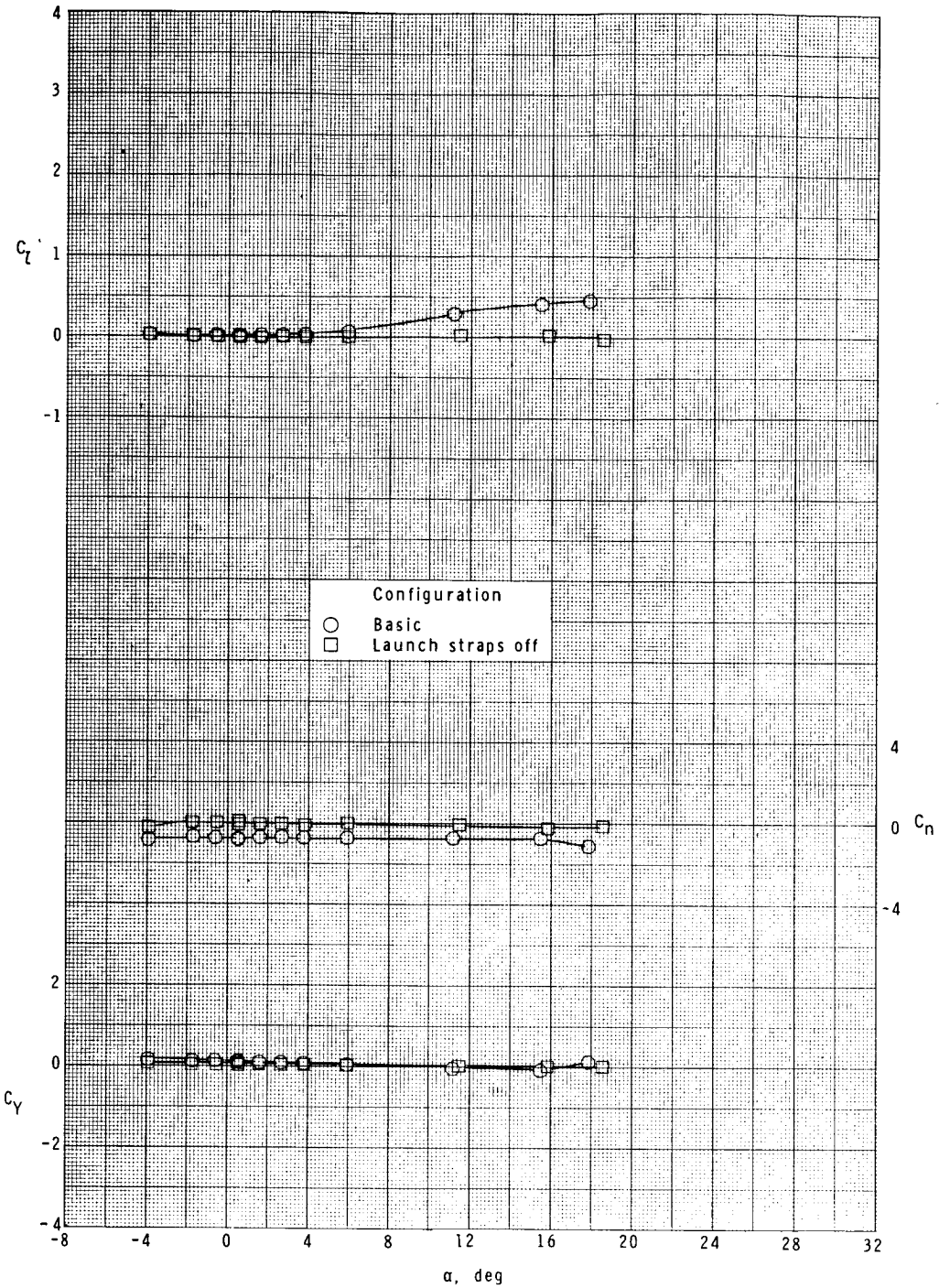

(i) M = 1.75.

Figure 12.- Effect of launch straps. $\phi = 0^{o}$.

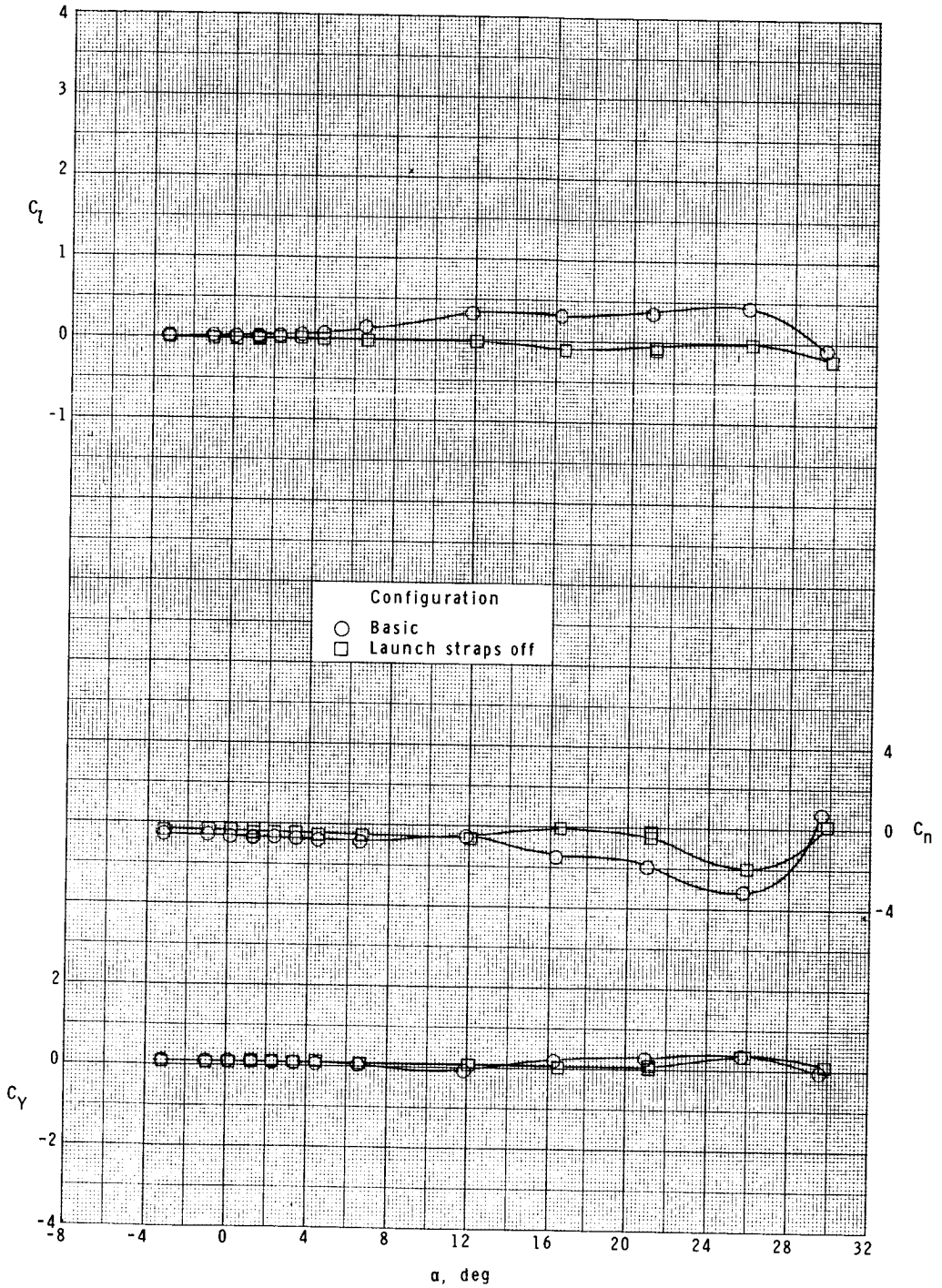

(j) M = 2.10.

Figure 12.- Continued.

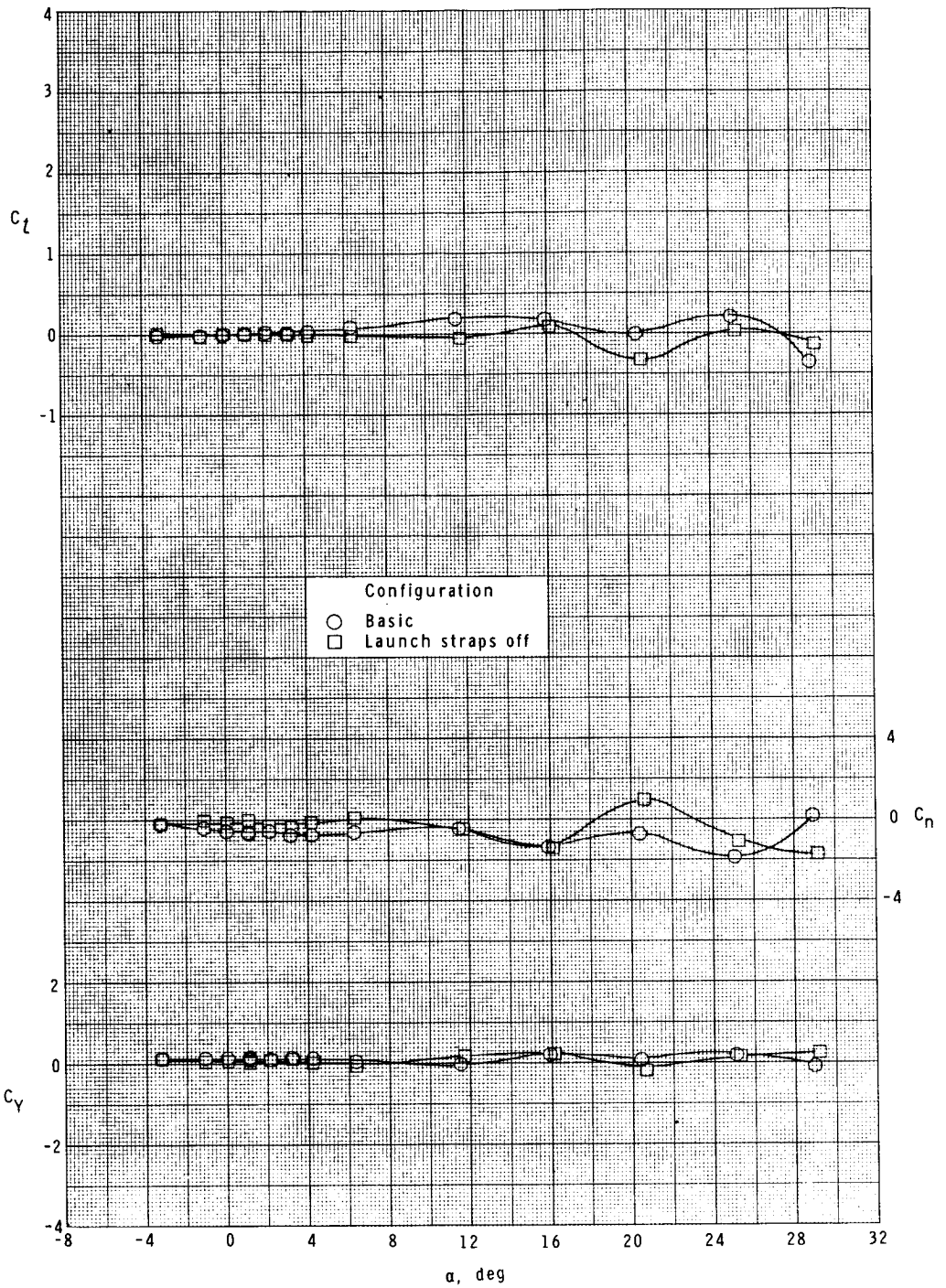

(k) M = 2.50.

Figure 12.- Continued.

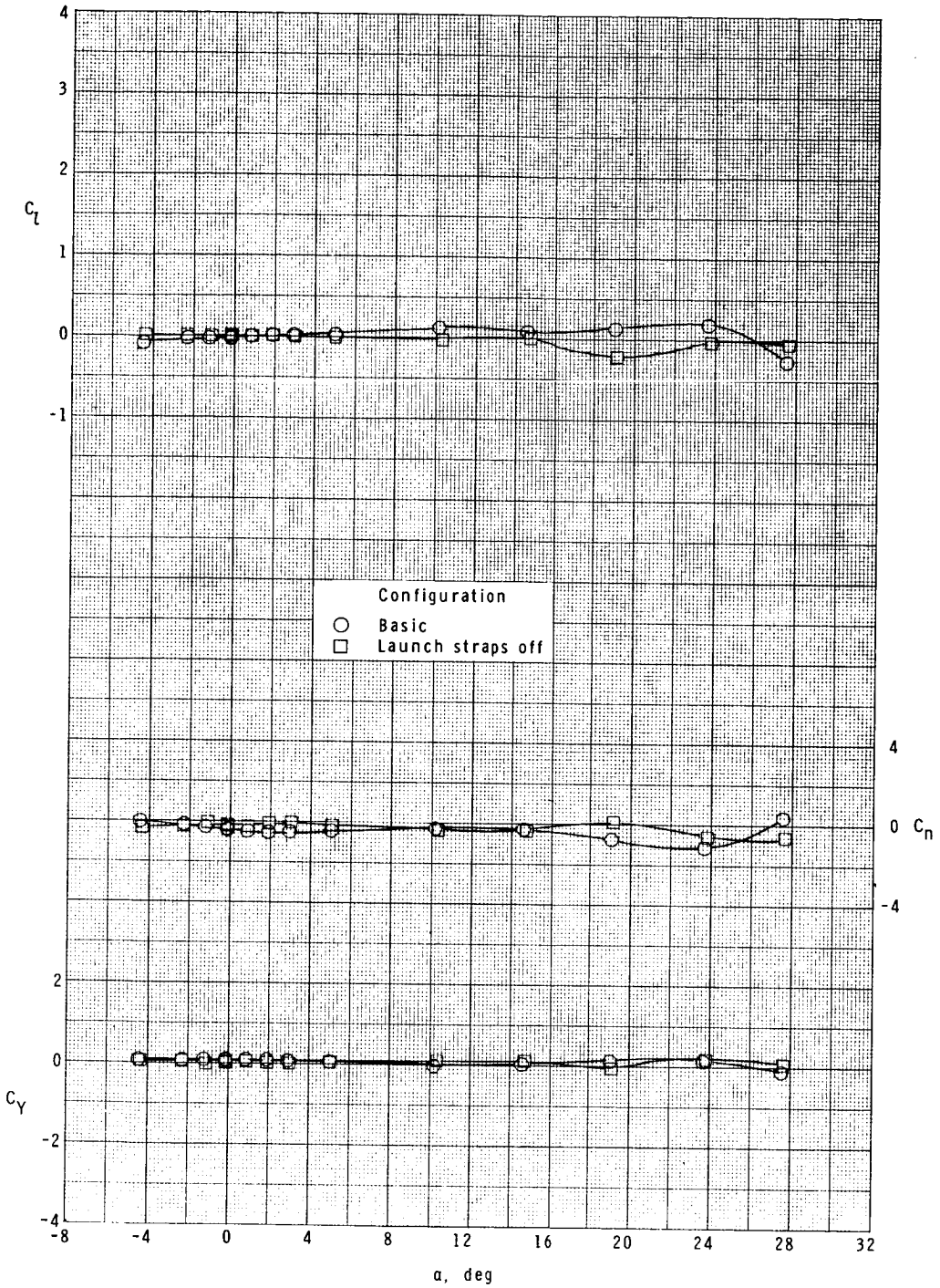

(l) M = 2.86.

Figure 12.- Continued.

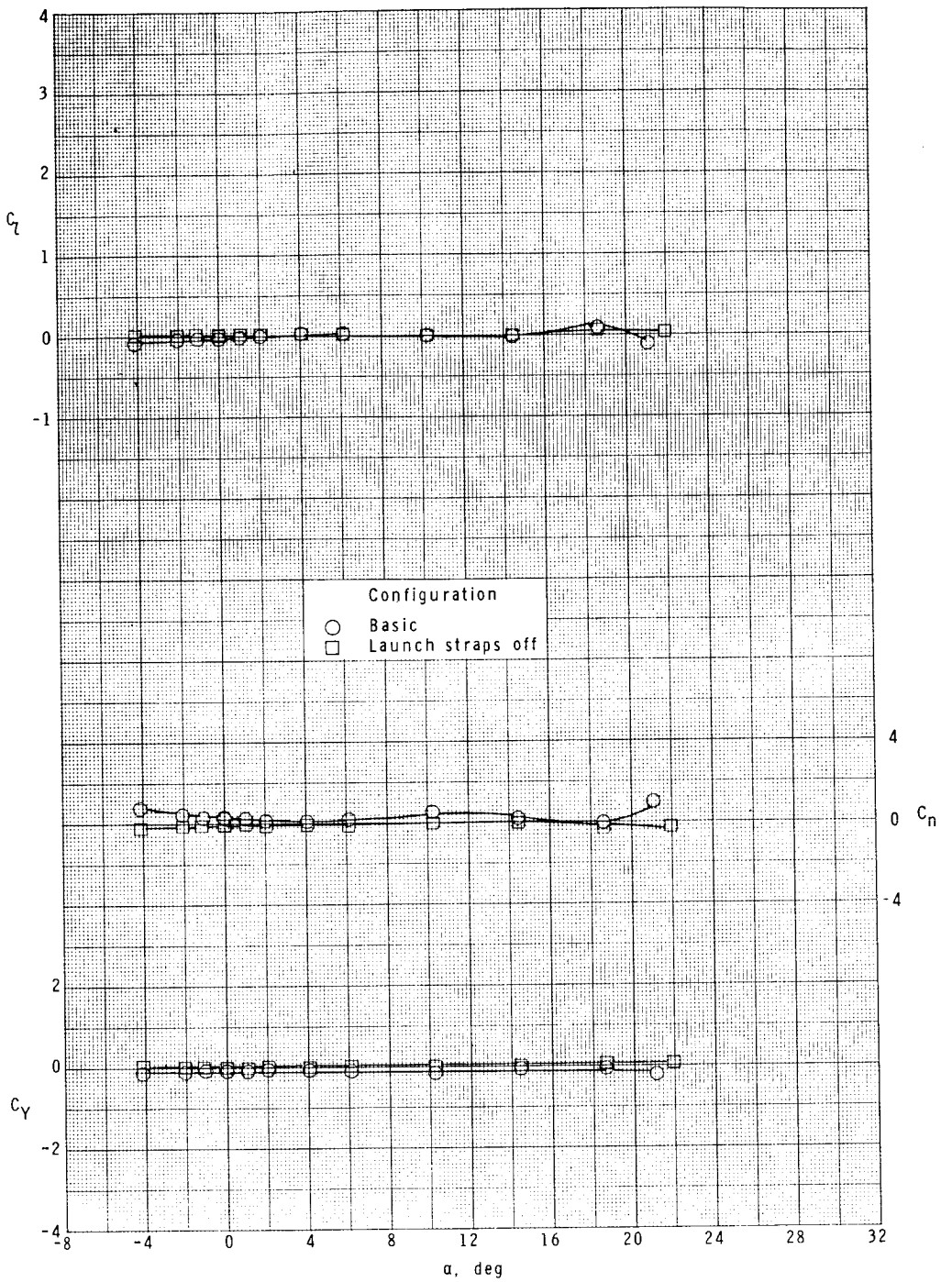

(m) M = 3.95.

Figure 12.- Continued.

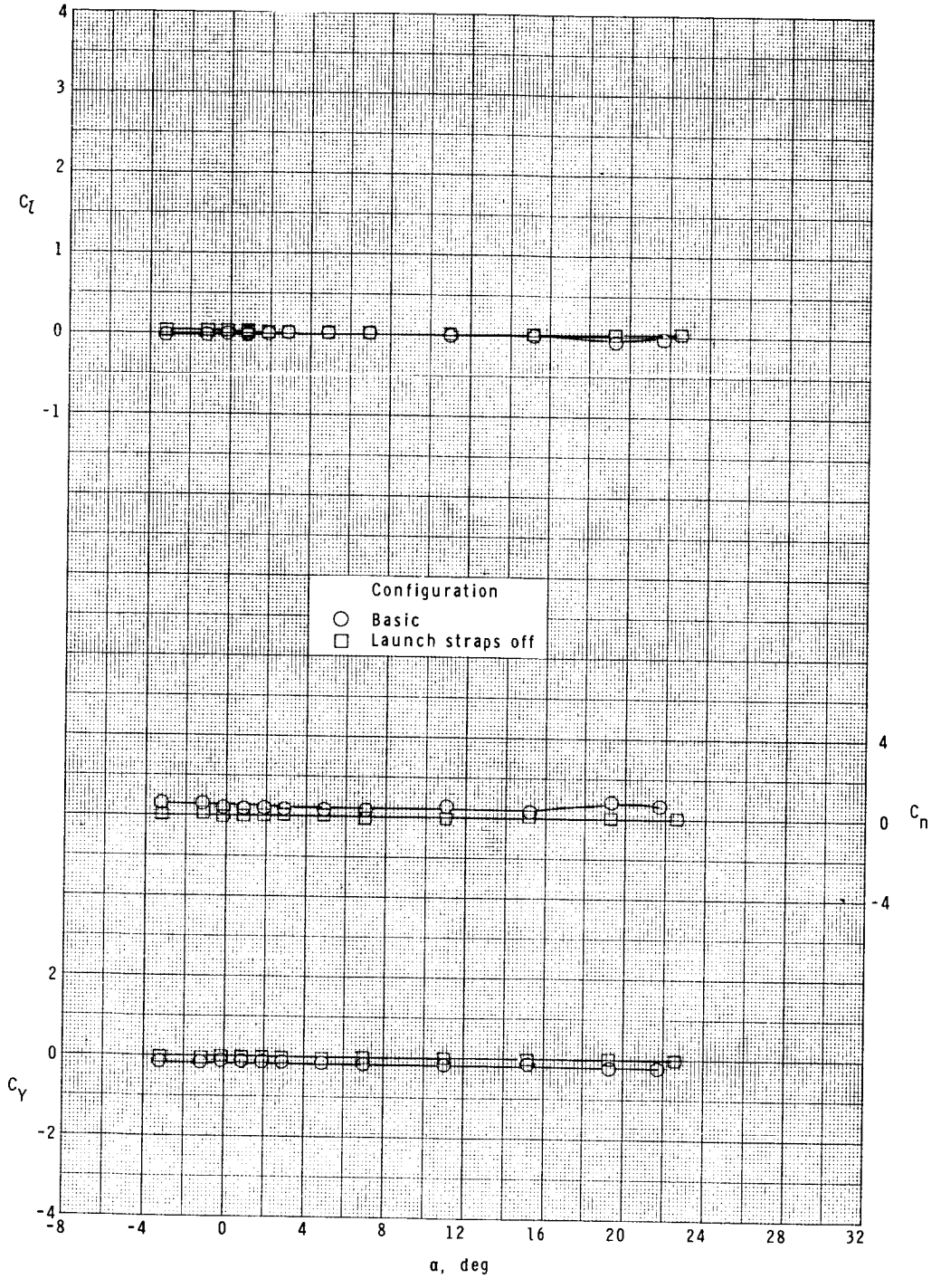

(n) M = 4.63.

Figure 12.- Concluded.

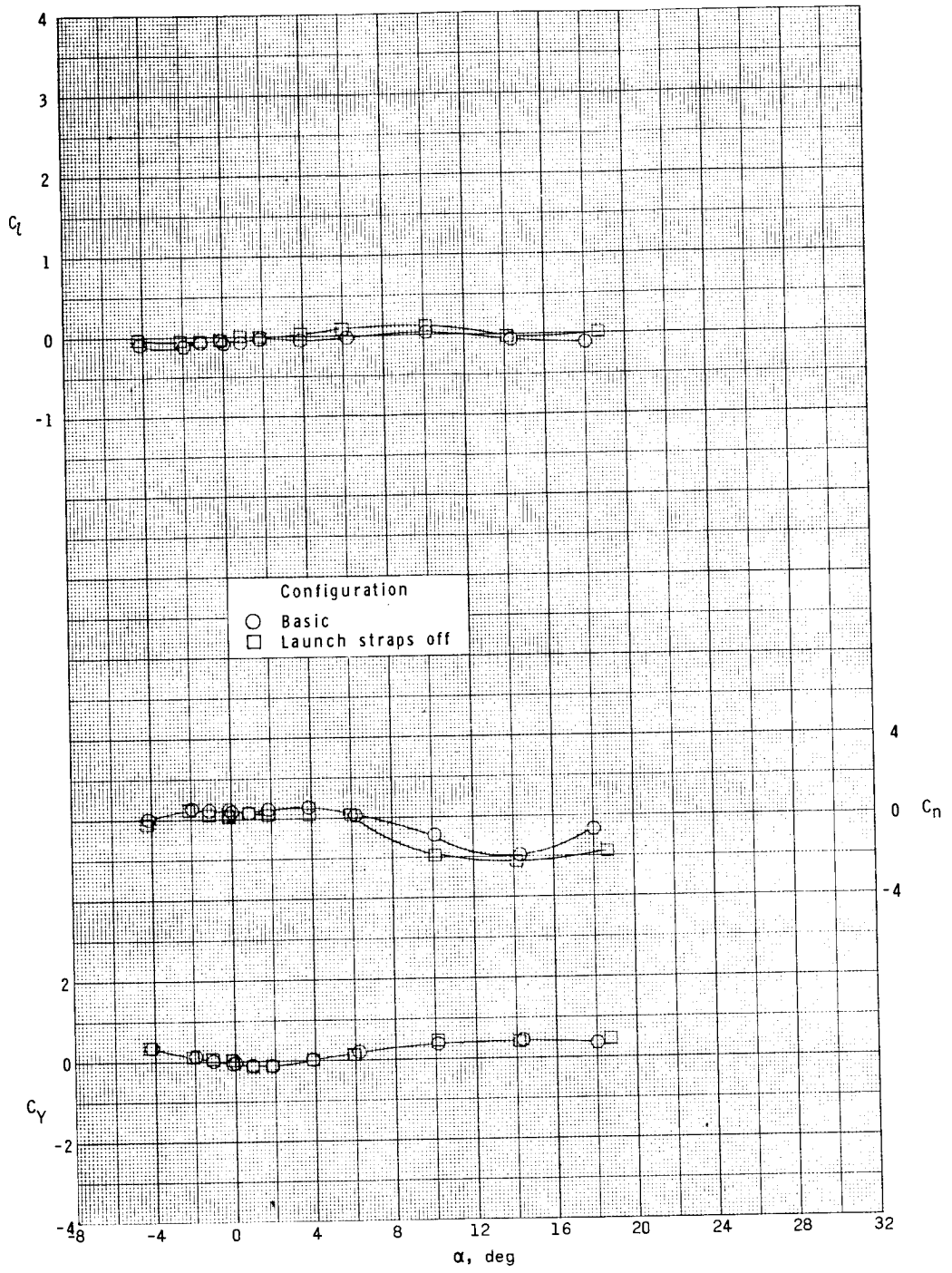

(a) M = 0.20.

Figure 13.- Effect of launch straps on lateral characteristics. $\phi = -45^{o}$.

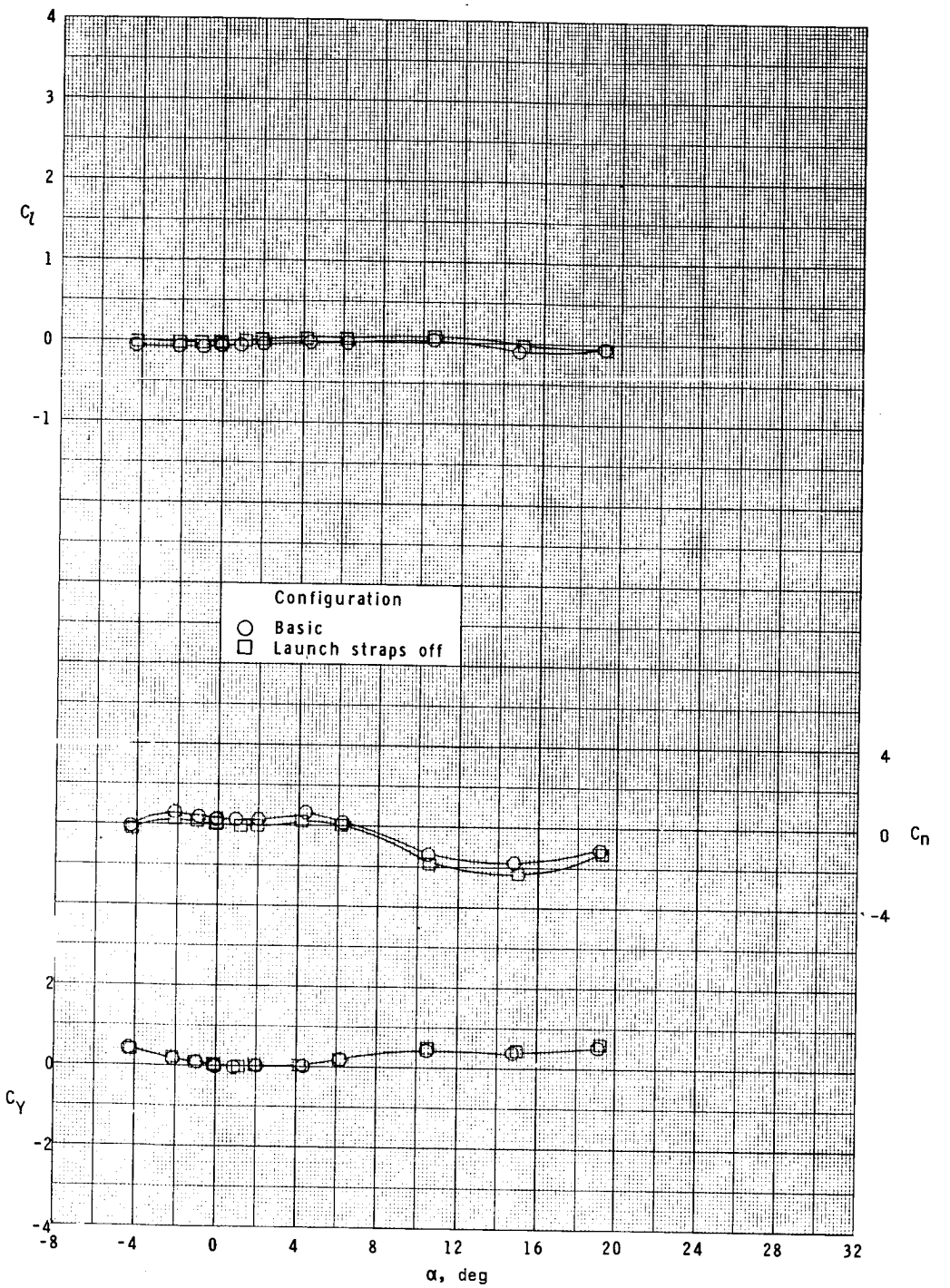

(b) $M = 0.60$.

Figure 13.- Continued.

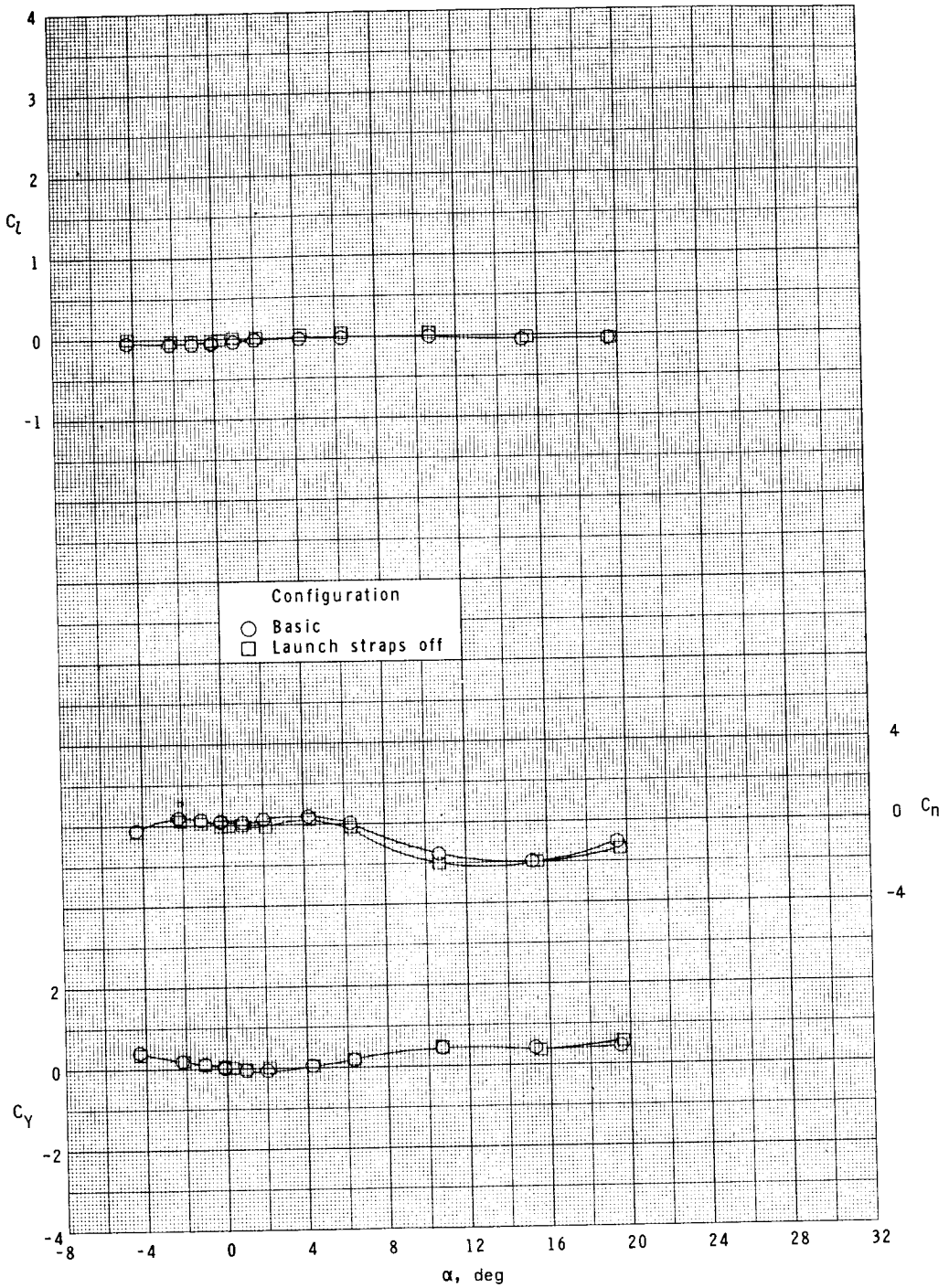

(c) M = 0.80.

Figure 13.- Continued.

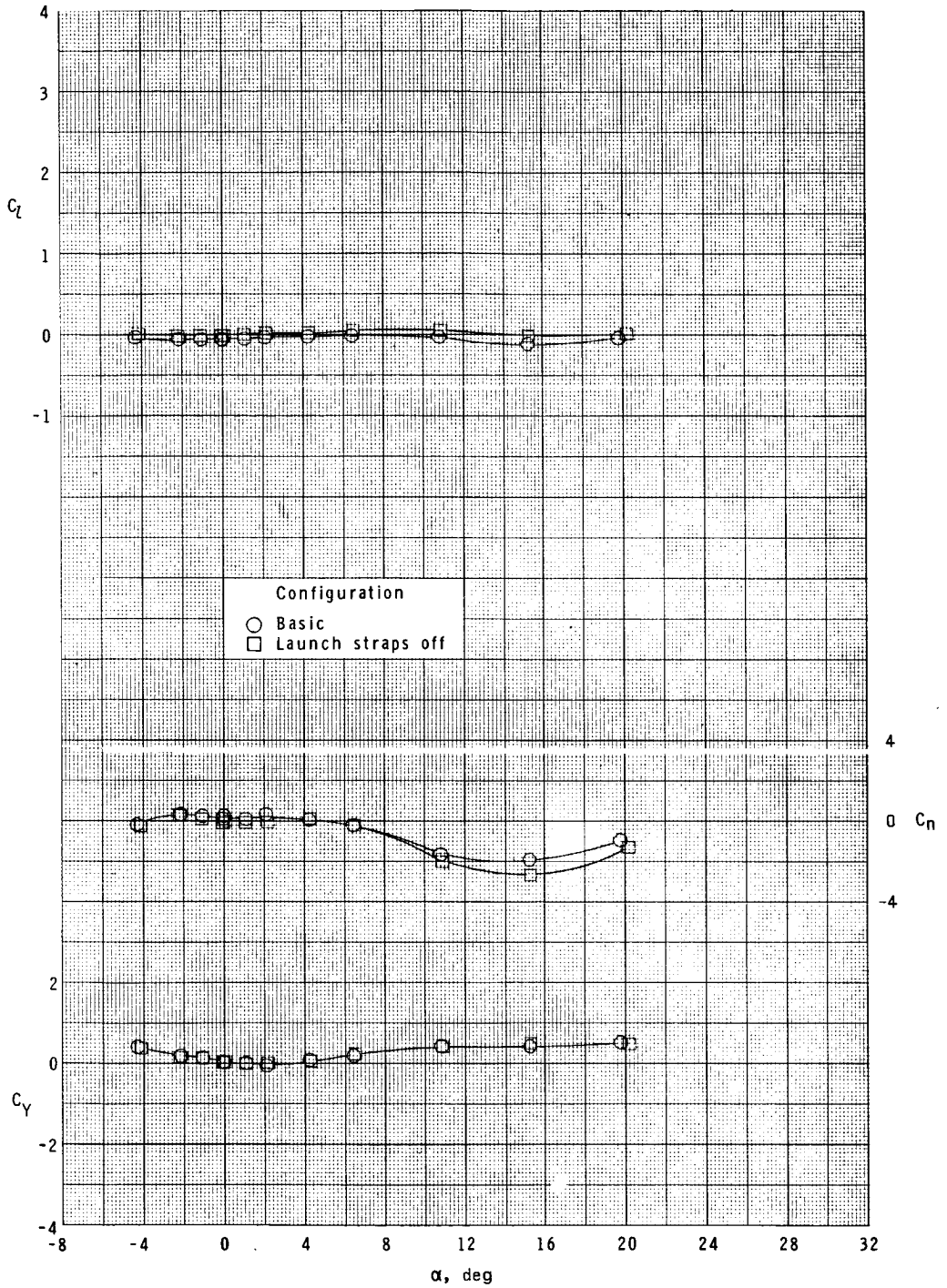

(d) M = 0.90.

Figure 13.- Continued.

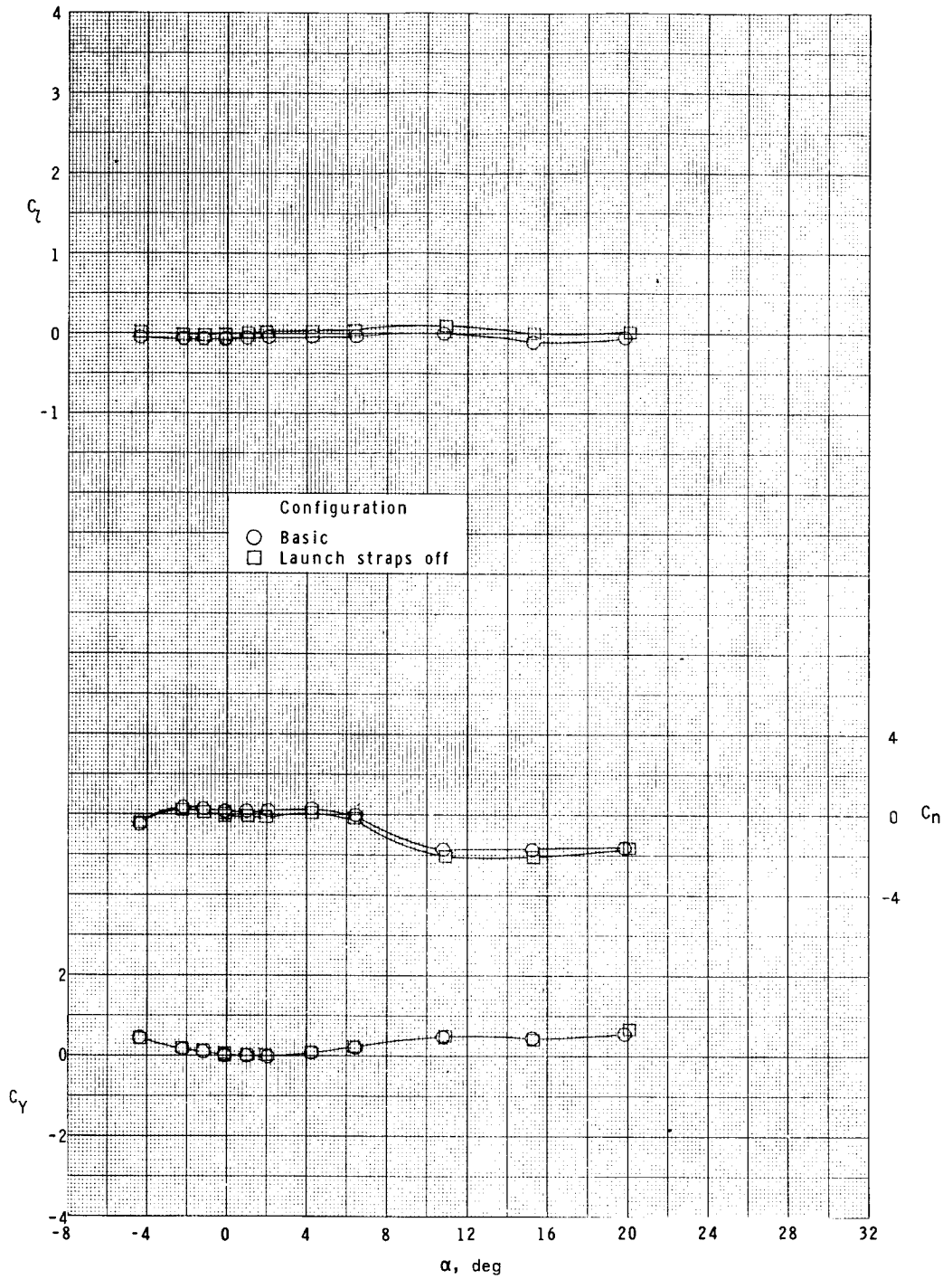

(e) M = 0.95.

Figure 13.- Continued.

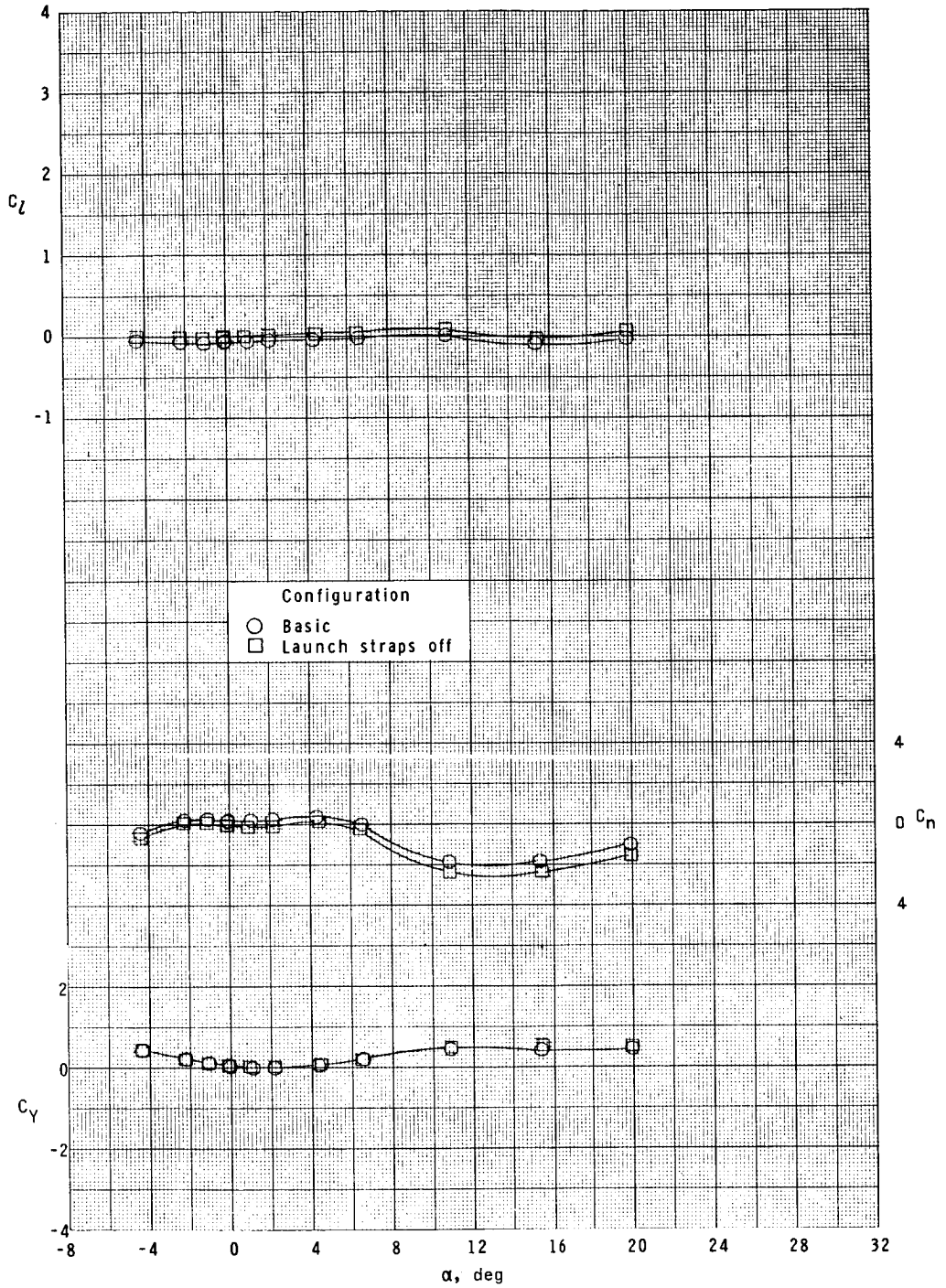

(f) M = 1.00.

Figure 13.- Continued.

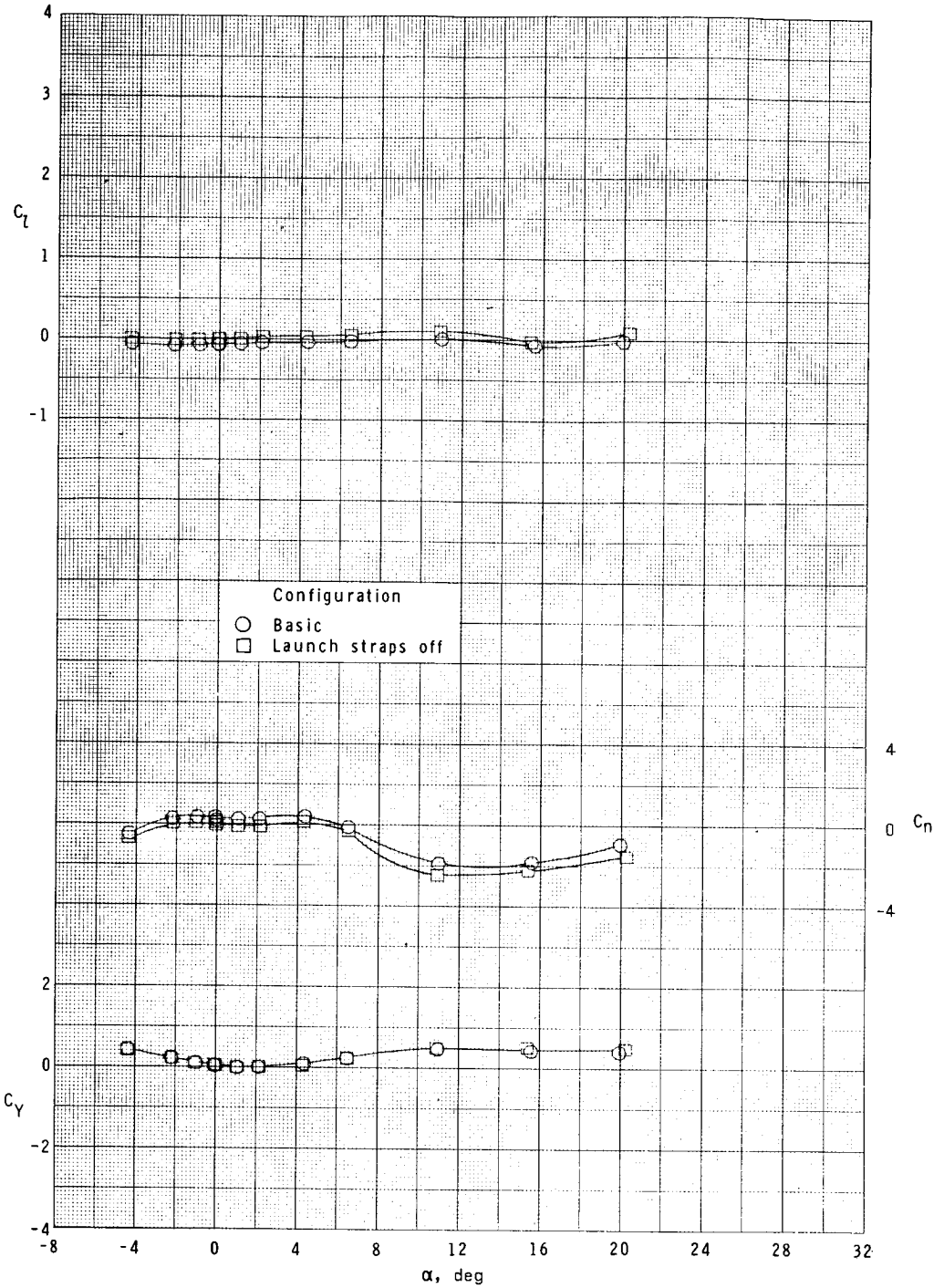

(g) M = 1.03.

Figure 13.- Continued.

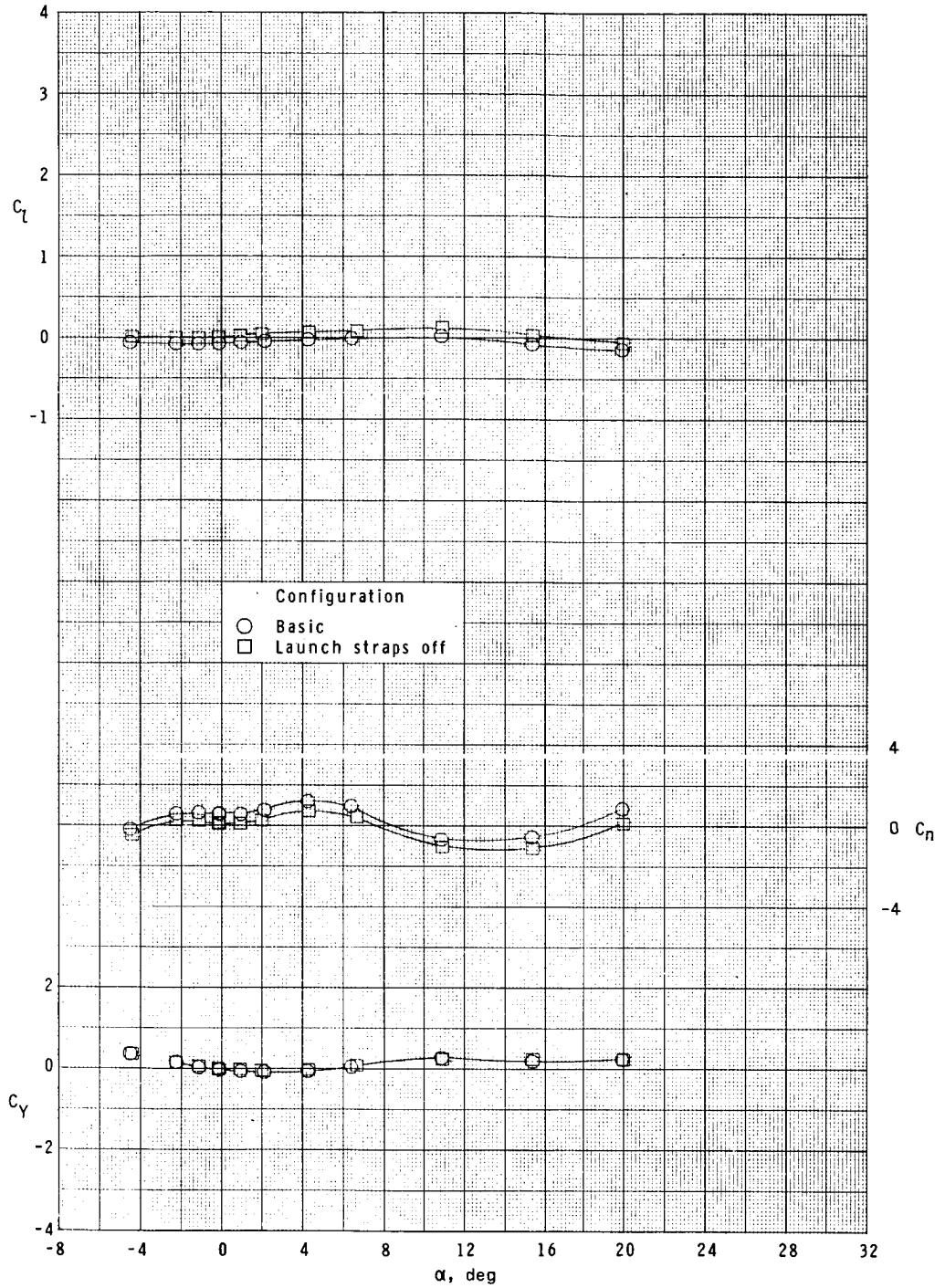

(h) M = 1.20.

Figure 13.- Continued.

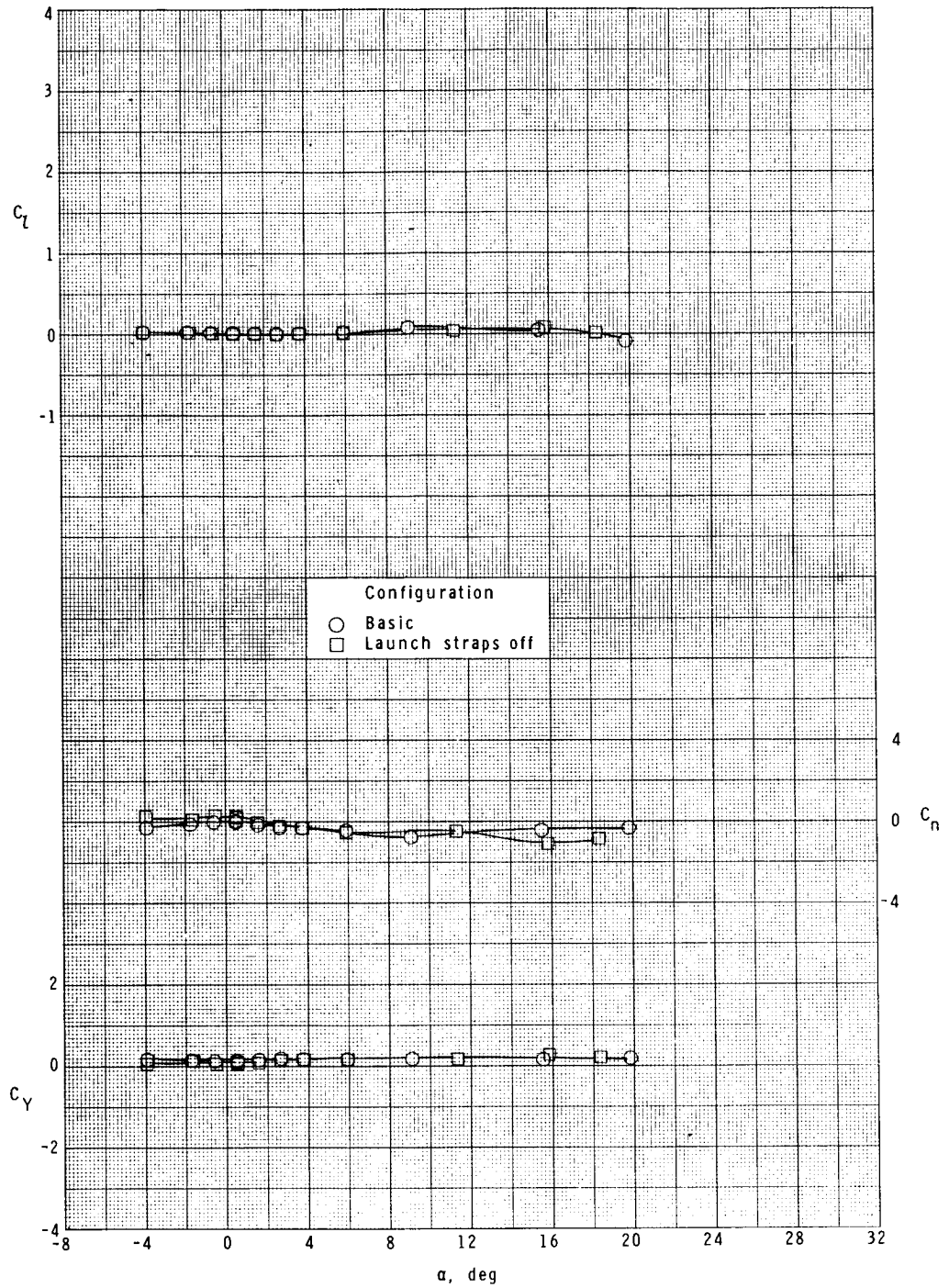

(i) M = 1.75.

Figure 13.- Continued.

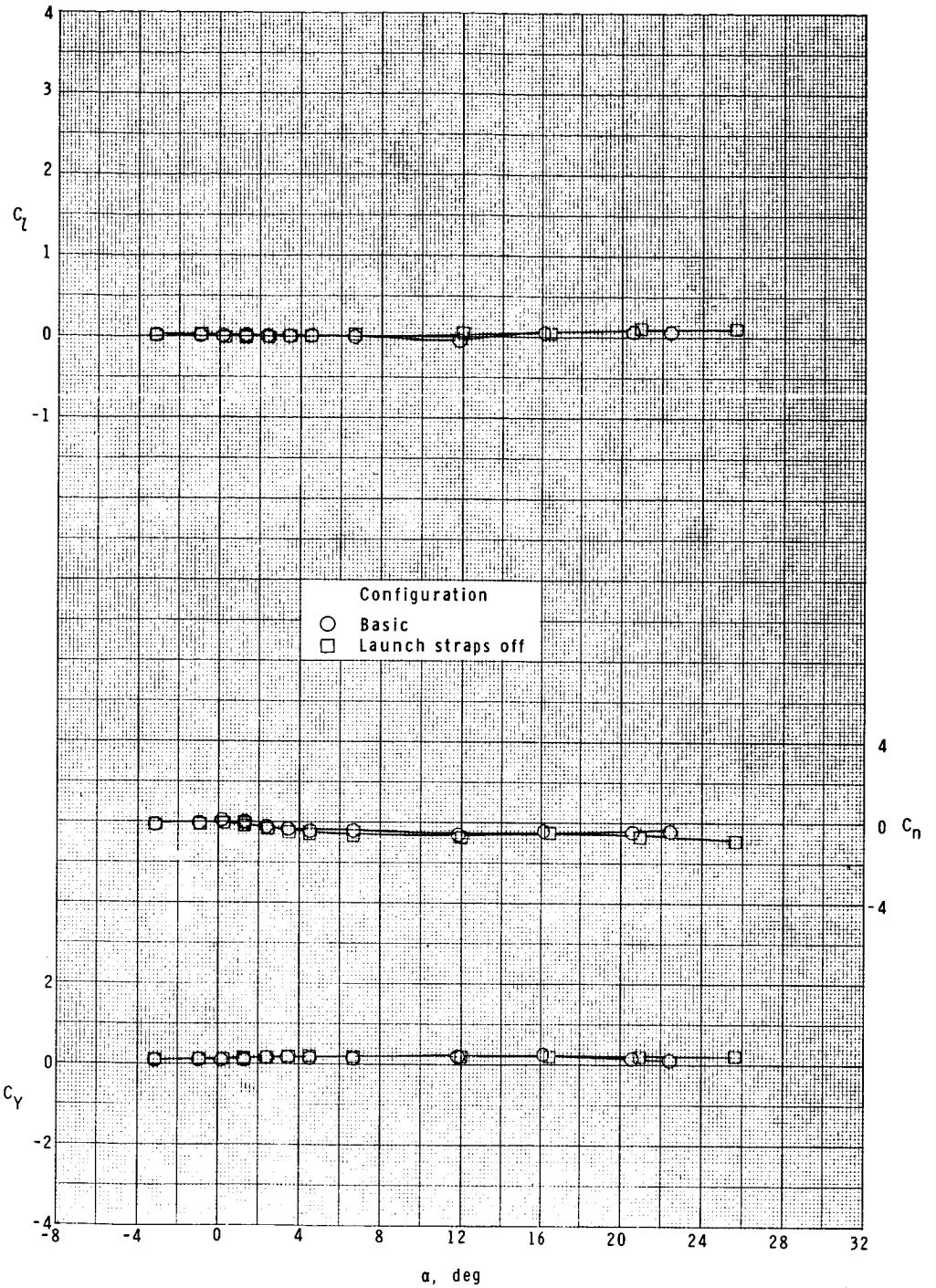

(j) M = 2.10.

Figure 13.- Continued.

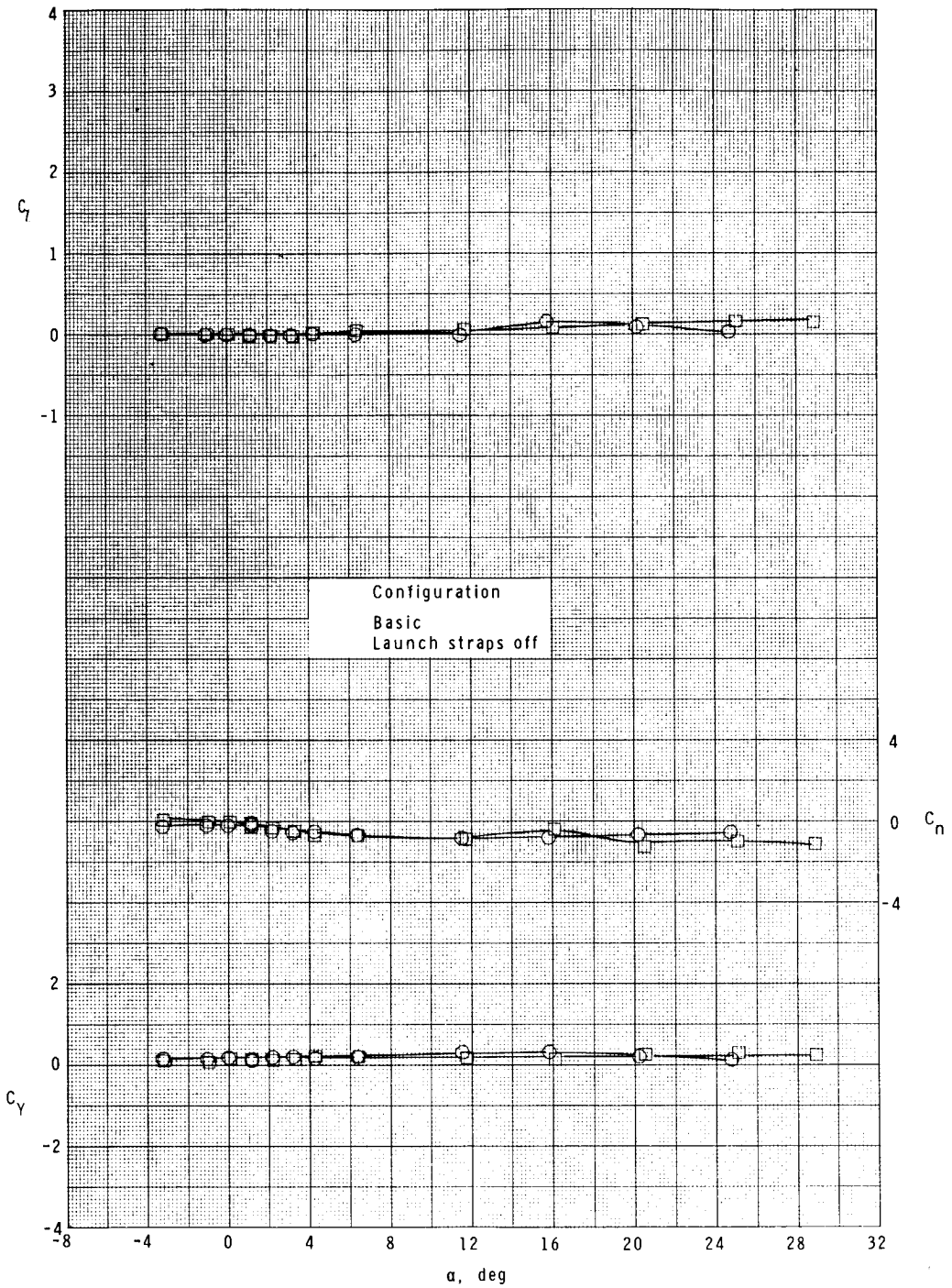

(k) M = 2.50.

Figure 13.- Continued.

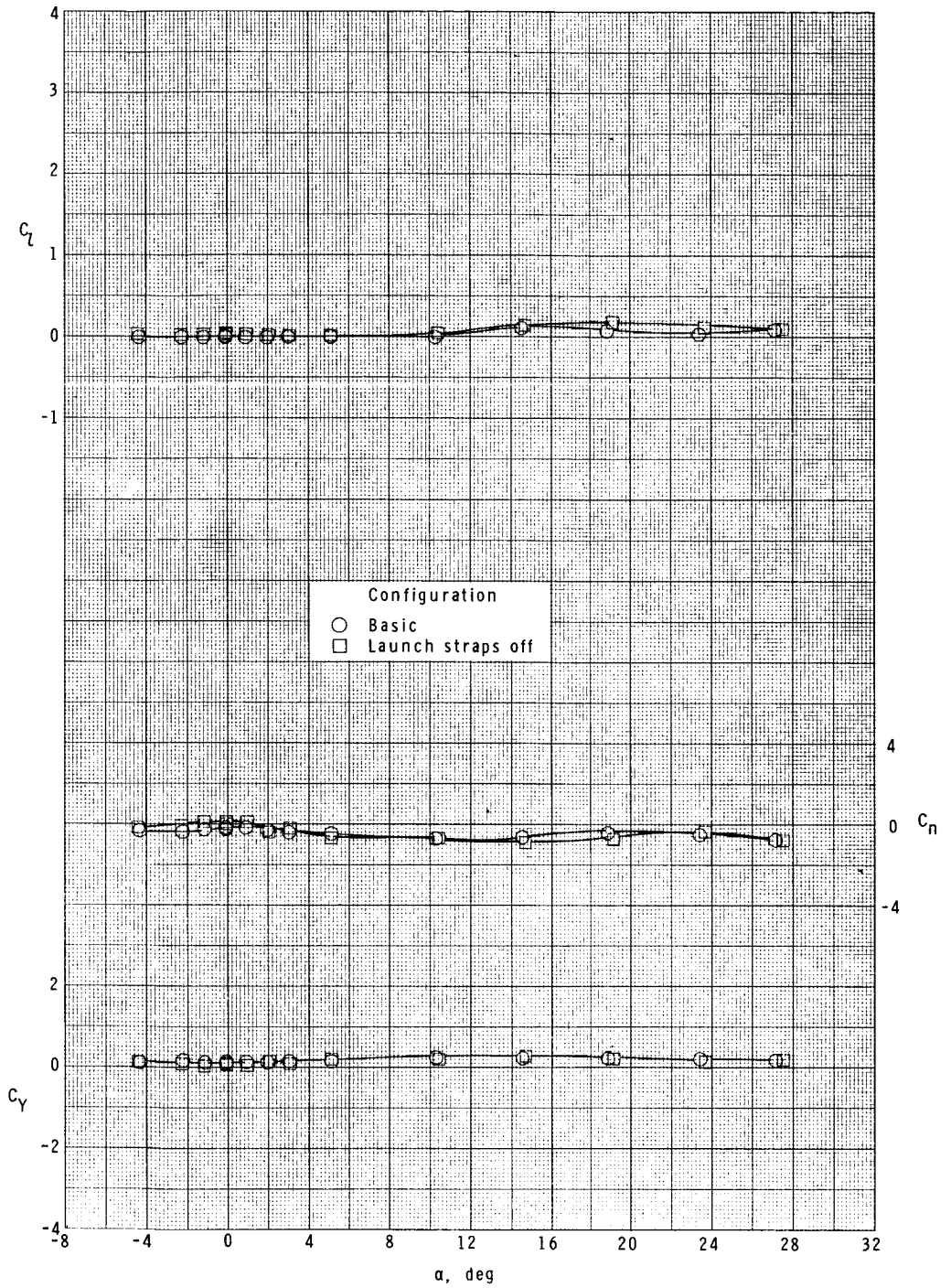

(l) M = 2.86.

Figure 13.- Continued.

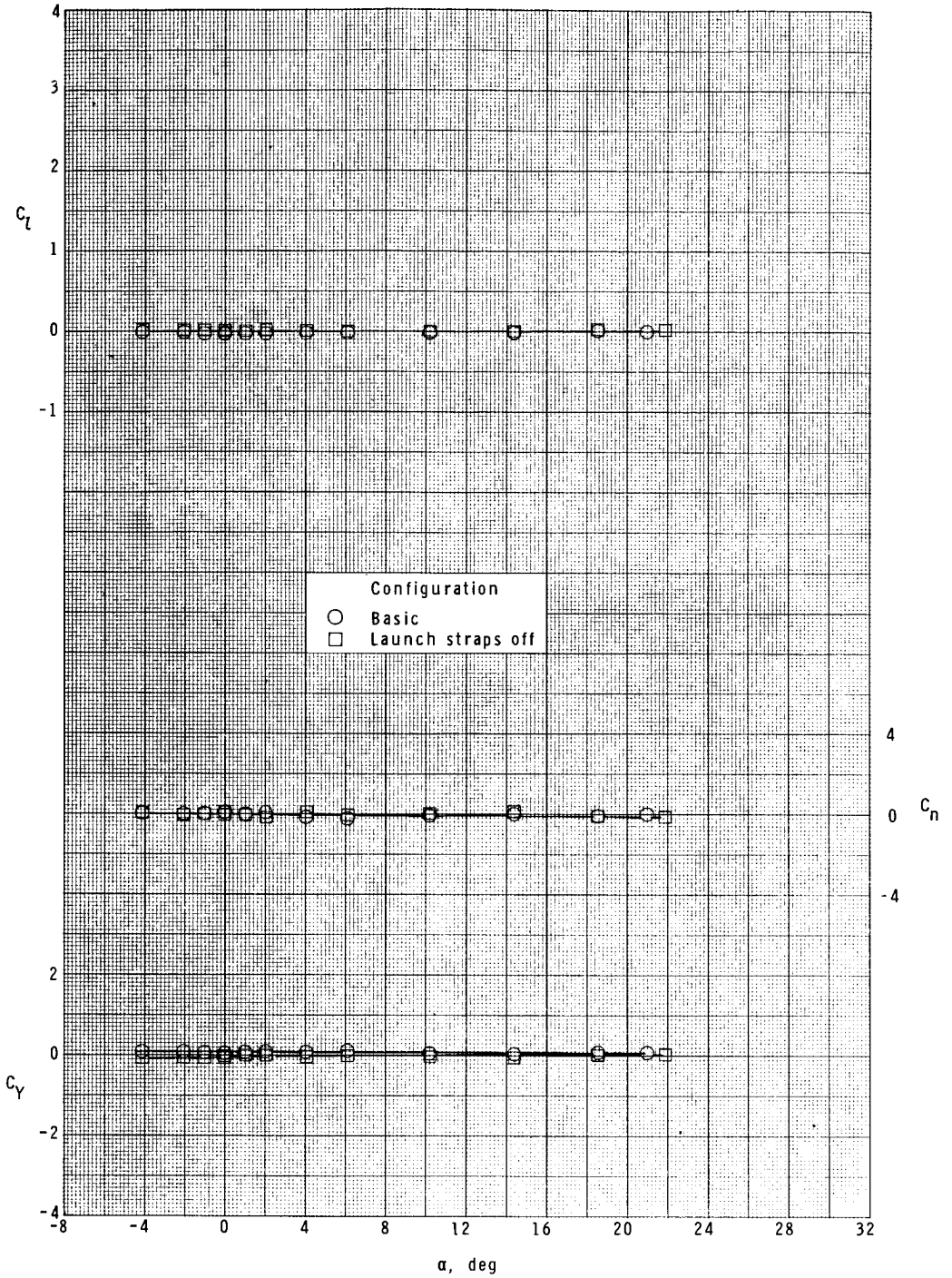

(m) M = 3.95.

Figure 13.- Continued.

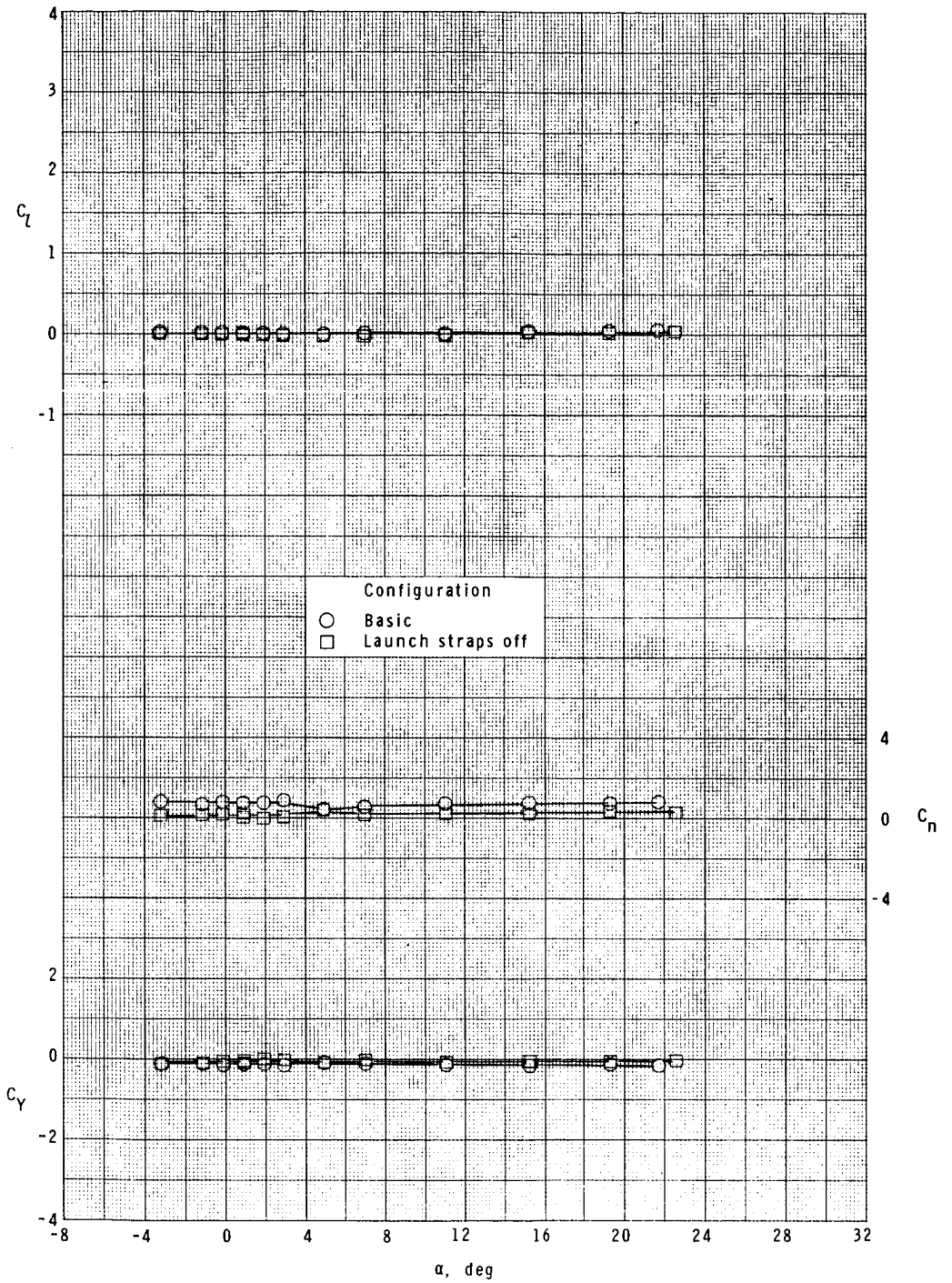

(n) M = 4.63.

Figure 13.- Concluded.

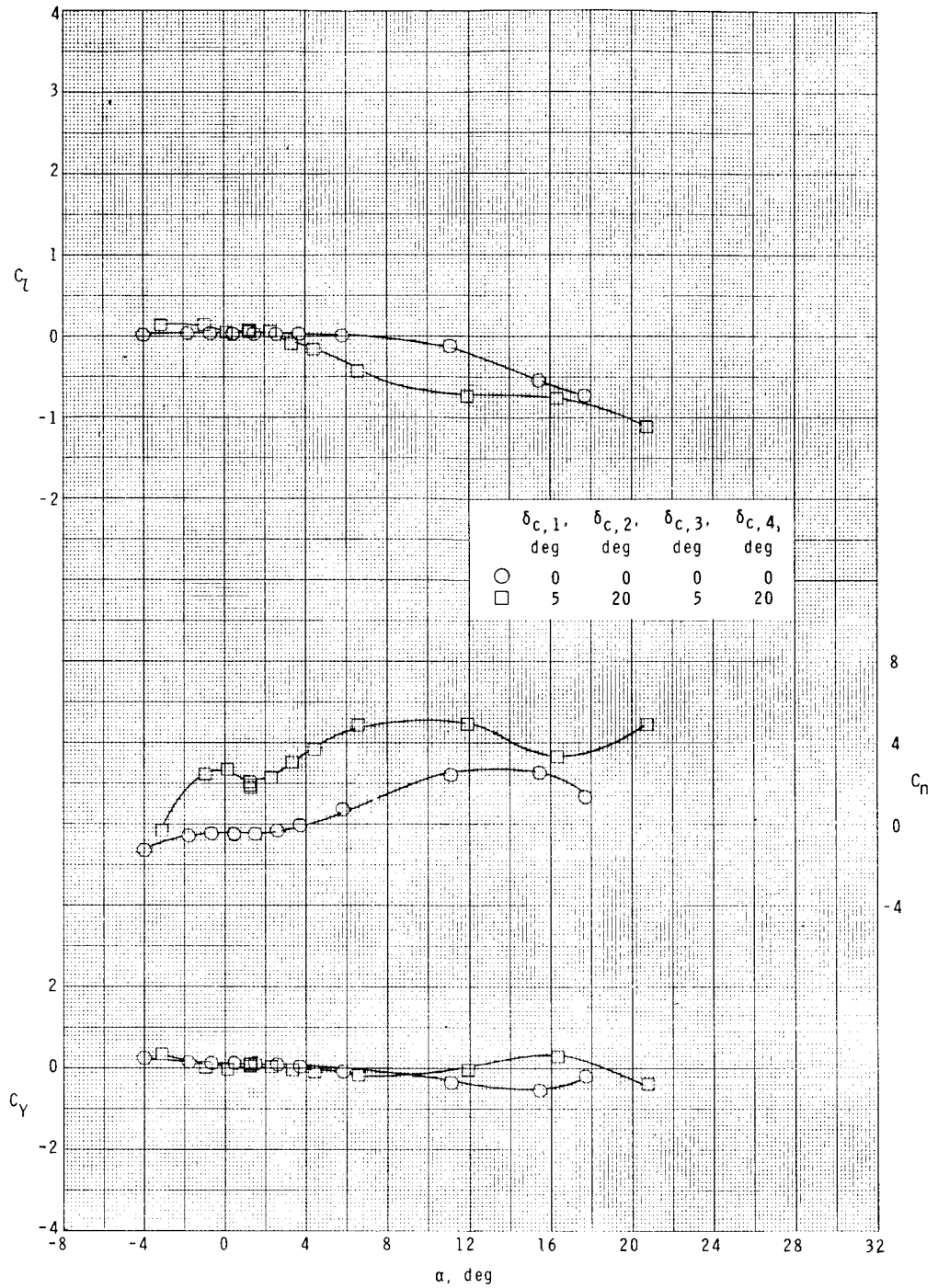

(a) M = 1.75.

Figure 14.- Effect of pitch-yaw control on lateral characteristics. $\phi = -14.04^{o}$.

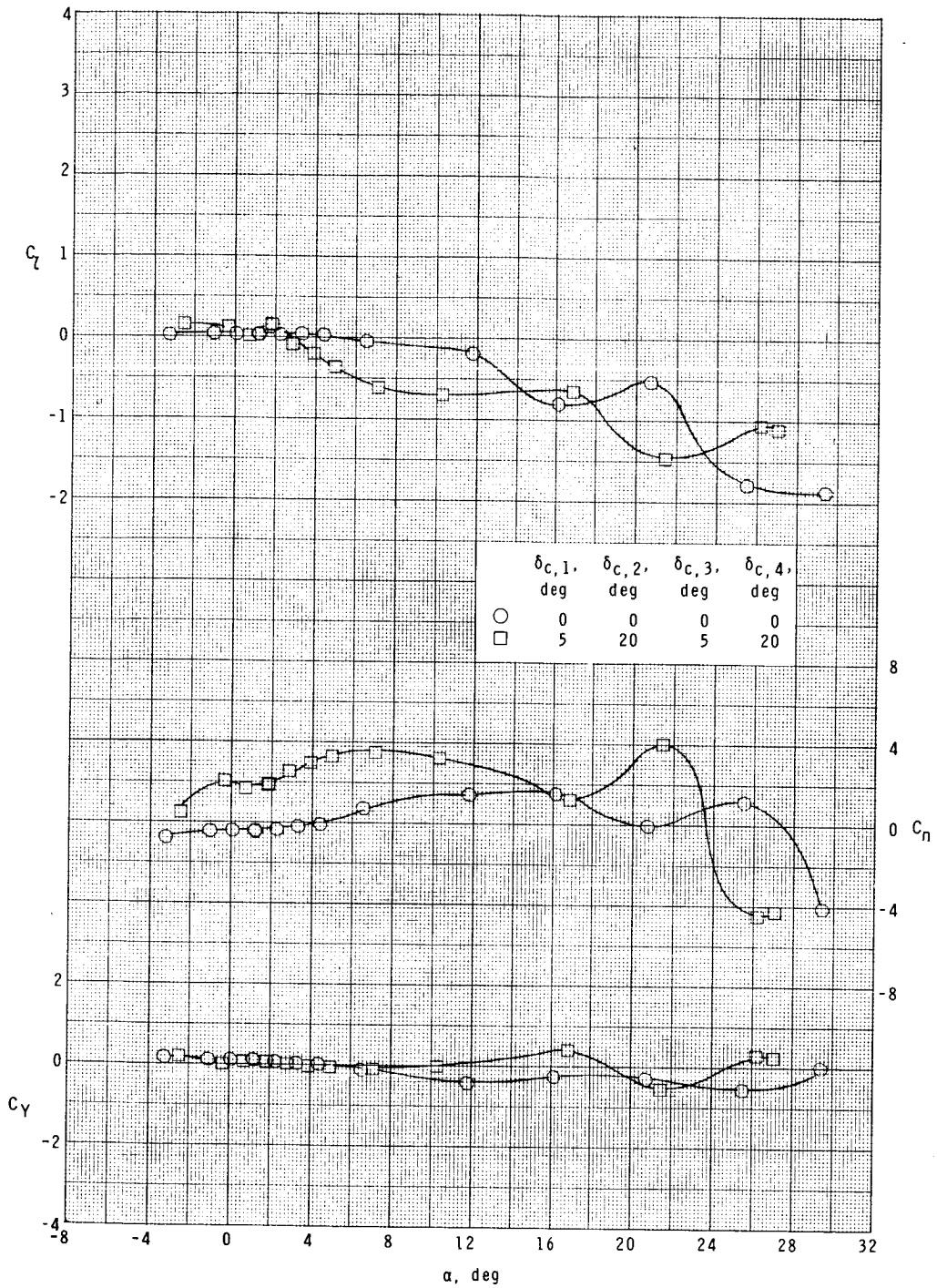

(b) M = 2.10.

Figure 14.- Continued.

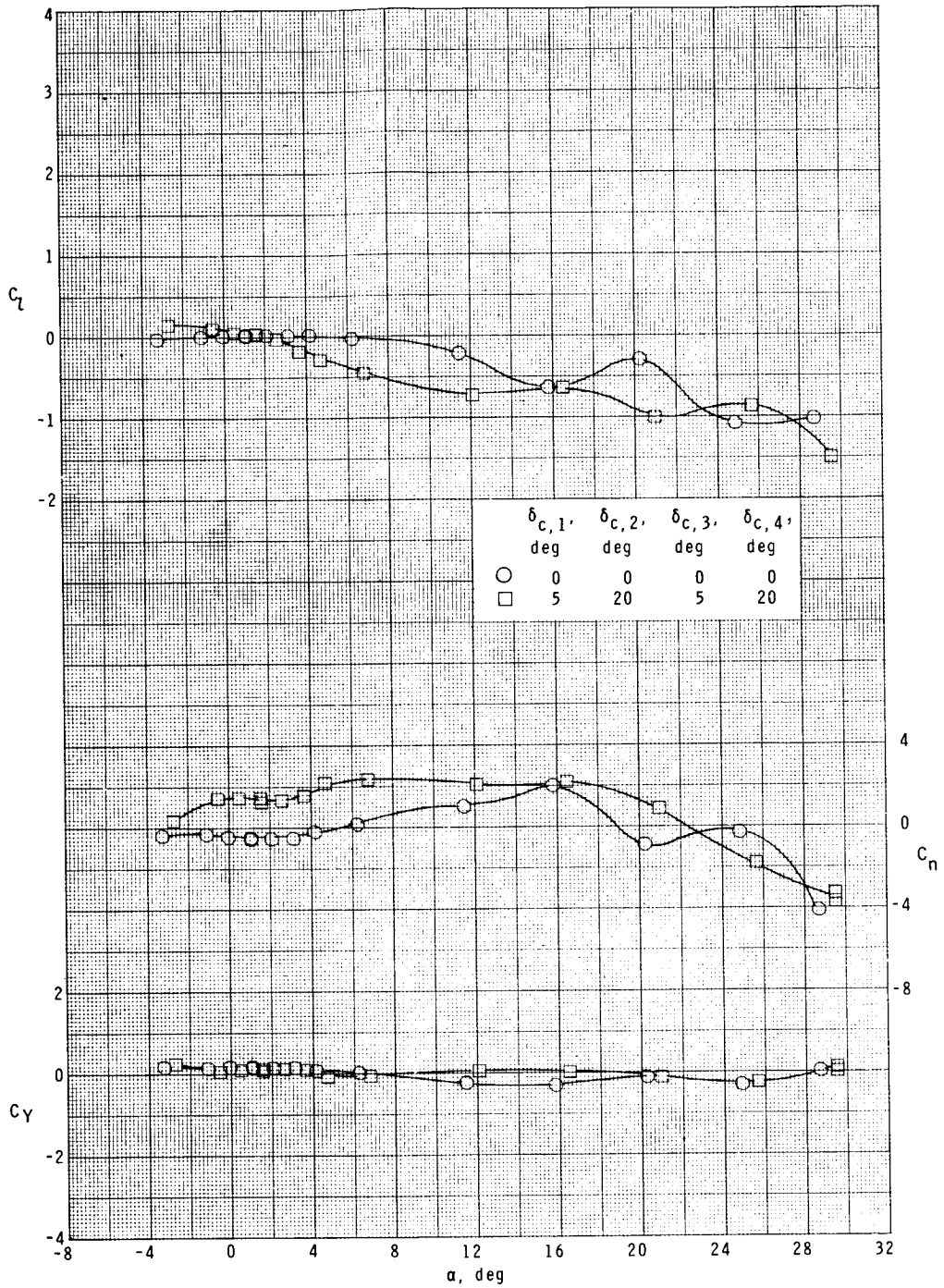

(c) M = 2.50.

Figure 14.- Continued.

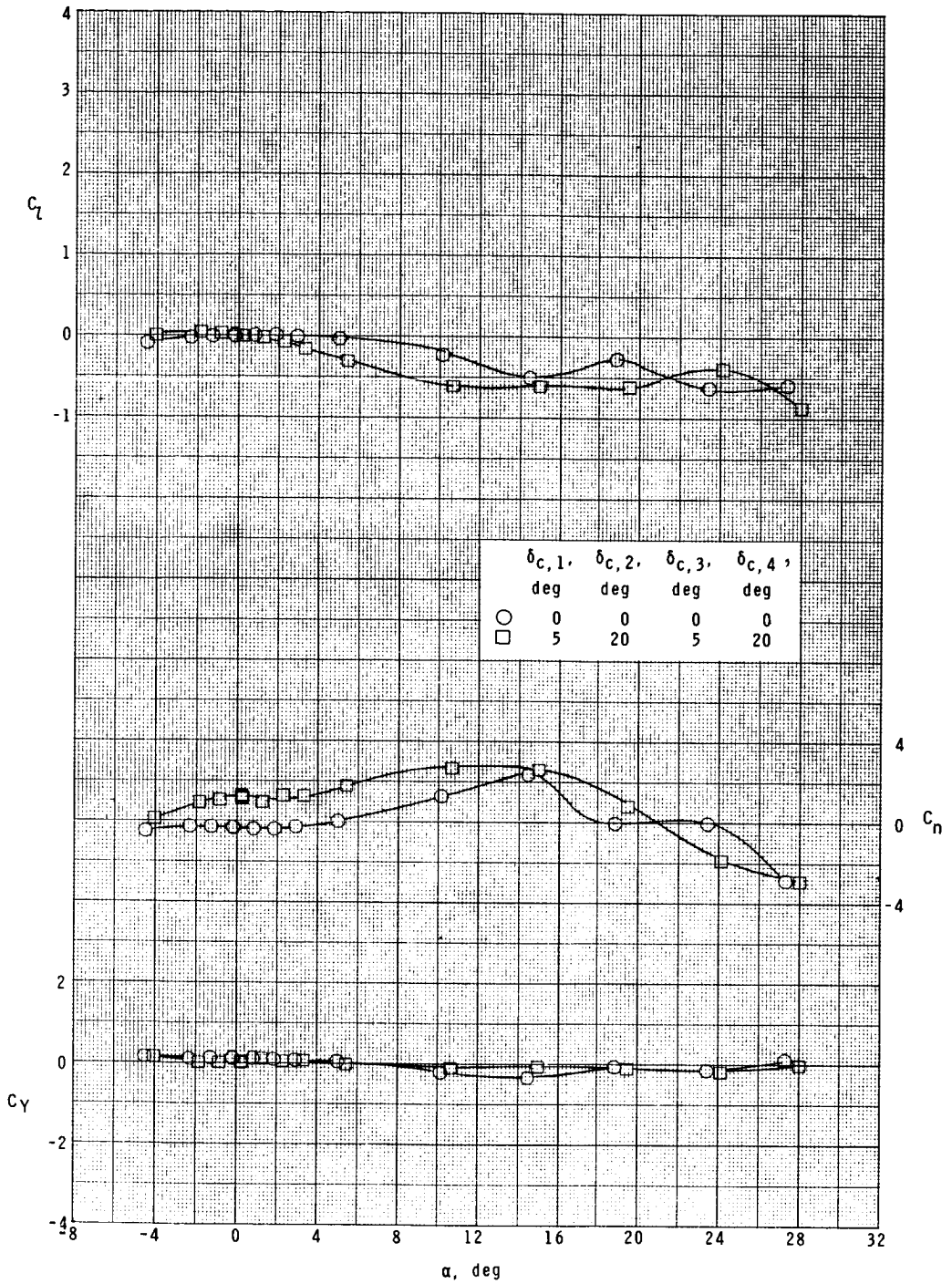

(d) M = 2.86.

Figure 14.- Continued.

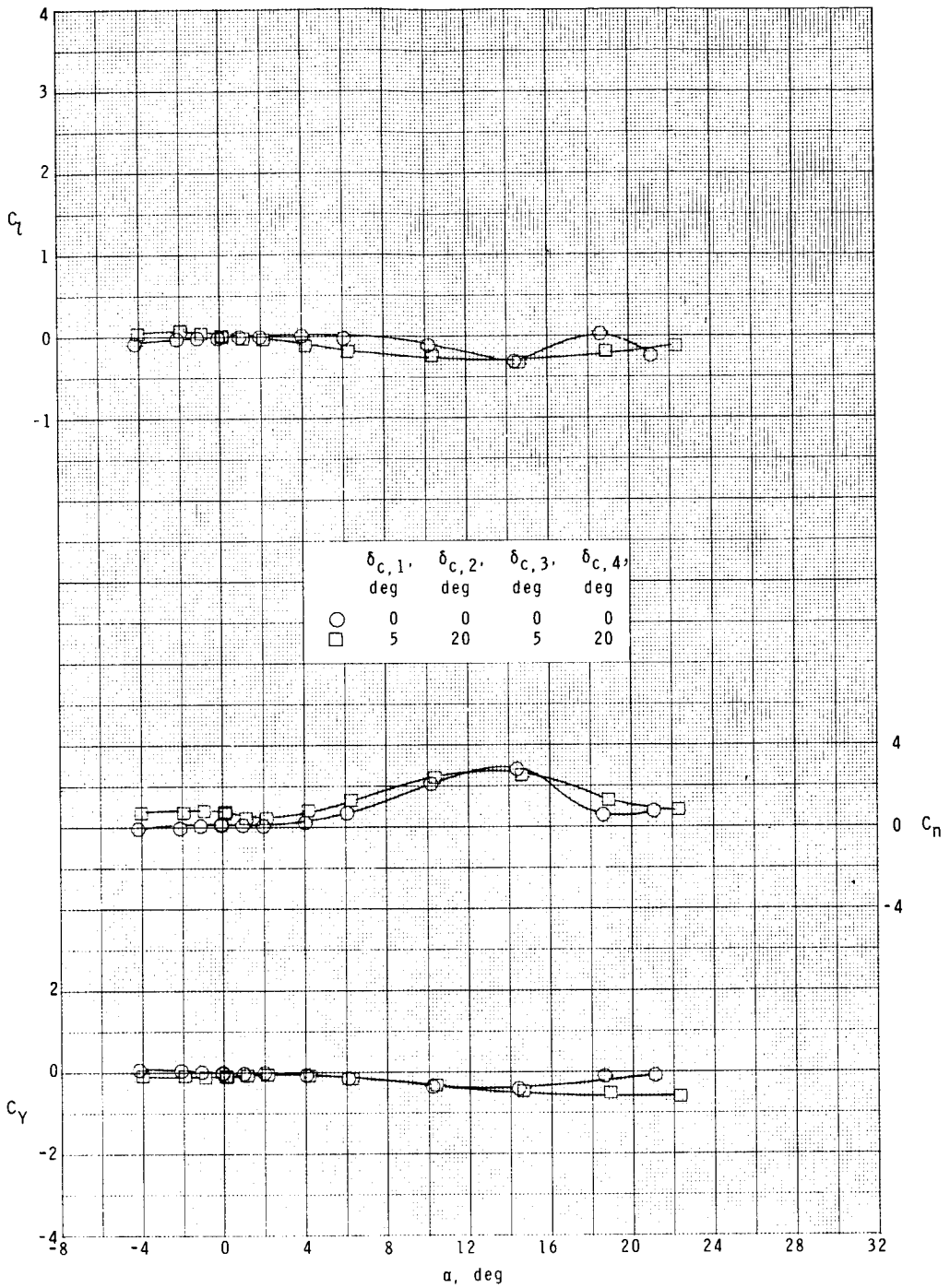

(e) M = 3.95.

Figure 14.- Continued.

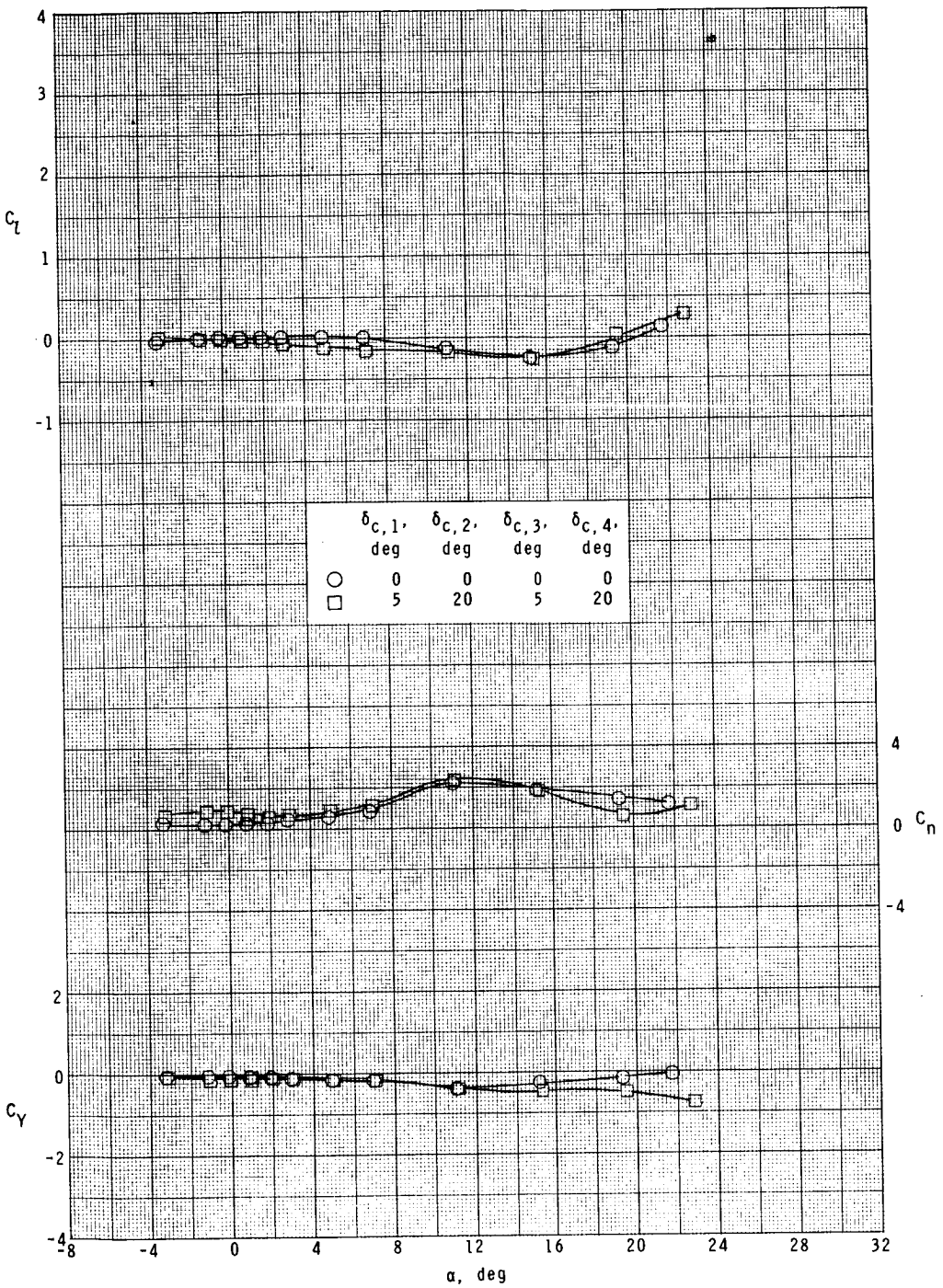

(f) M = 4.63.

Figure 14.- Concluded.

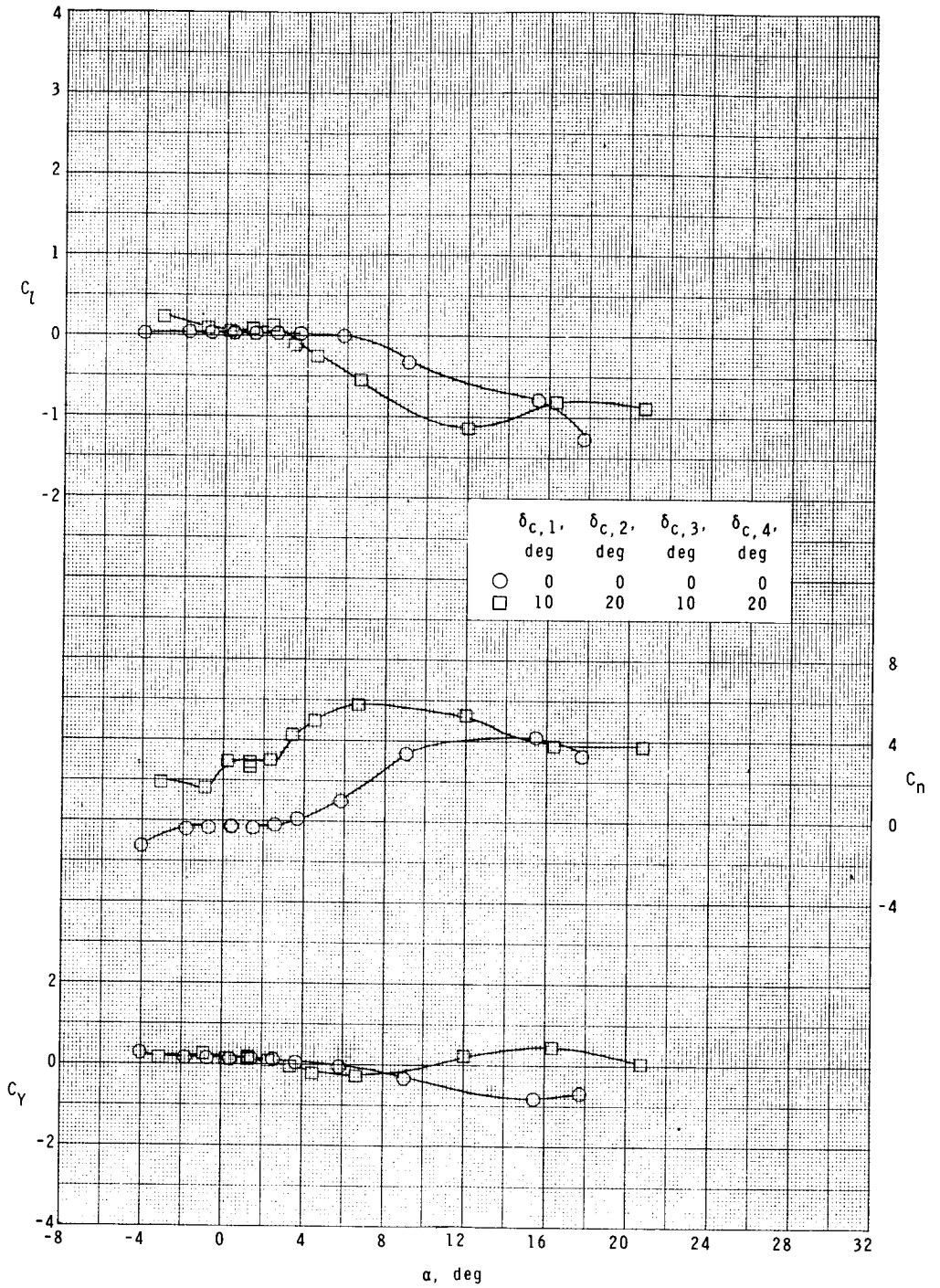

(a) M = 1.75.

Figure 15.- Effect of pitch-yaw control on the lateral characteristics. $\phi = -26.57^{o}$.

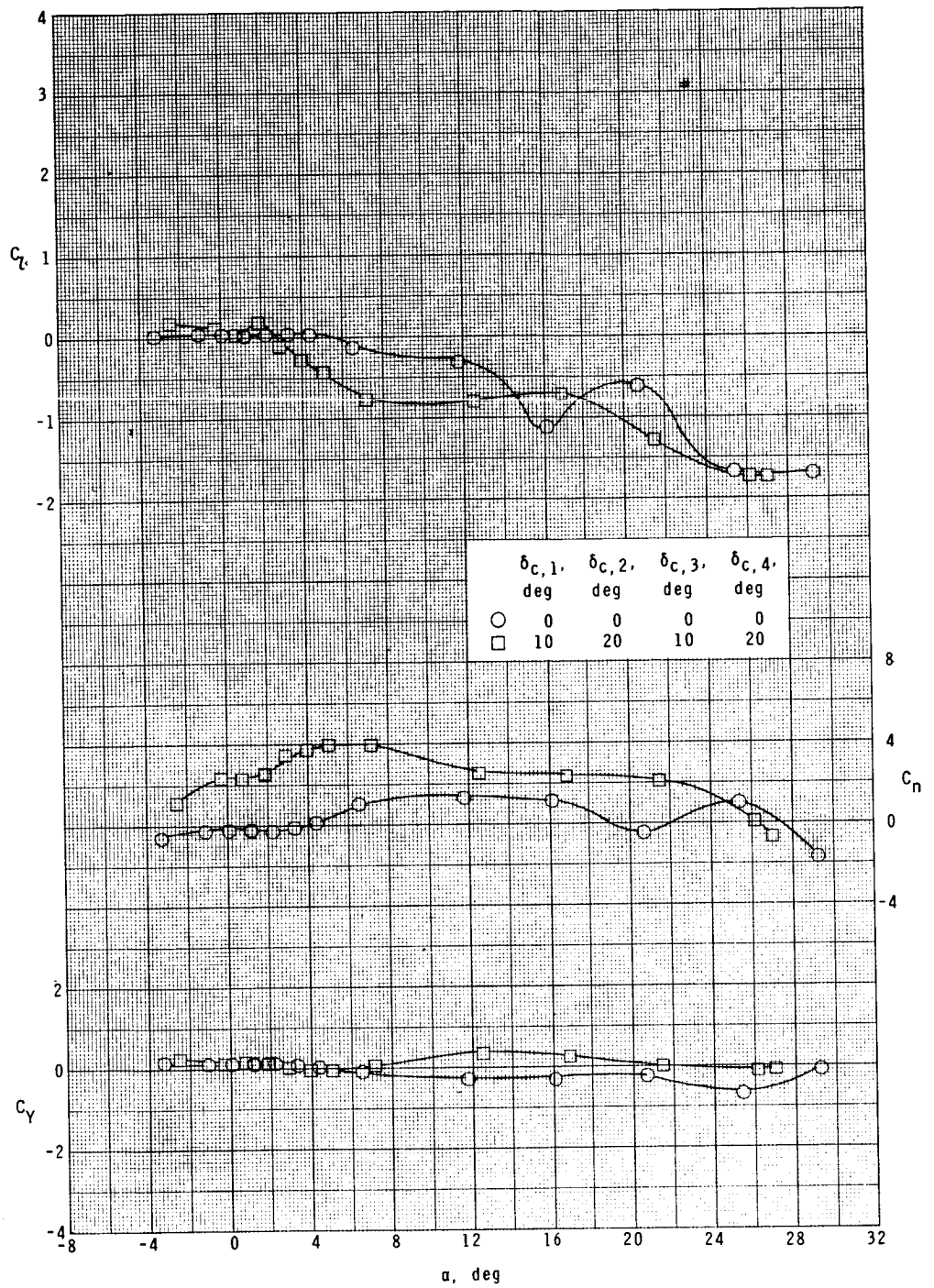

(b) M = 2.10.

Figure 15.- Continued.

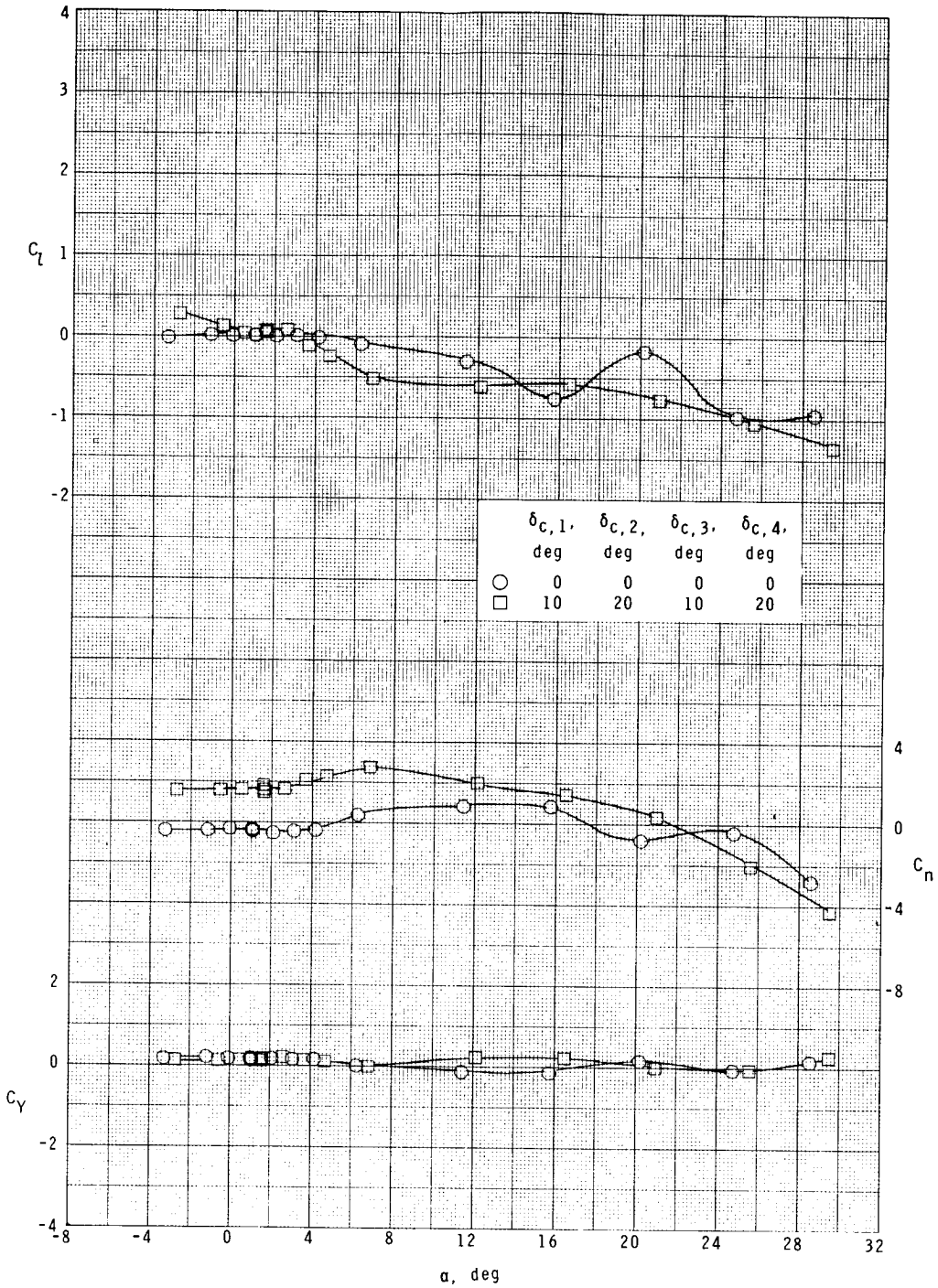

(c) M = 2.50.

Figure 15.- Continued.

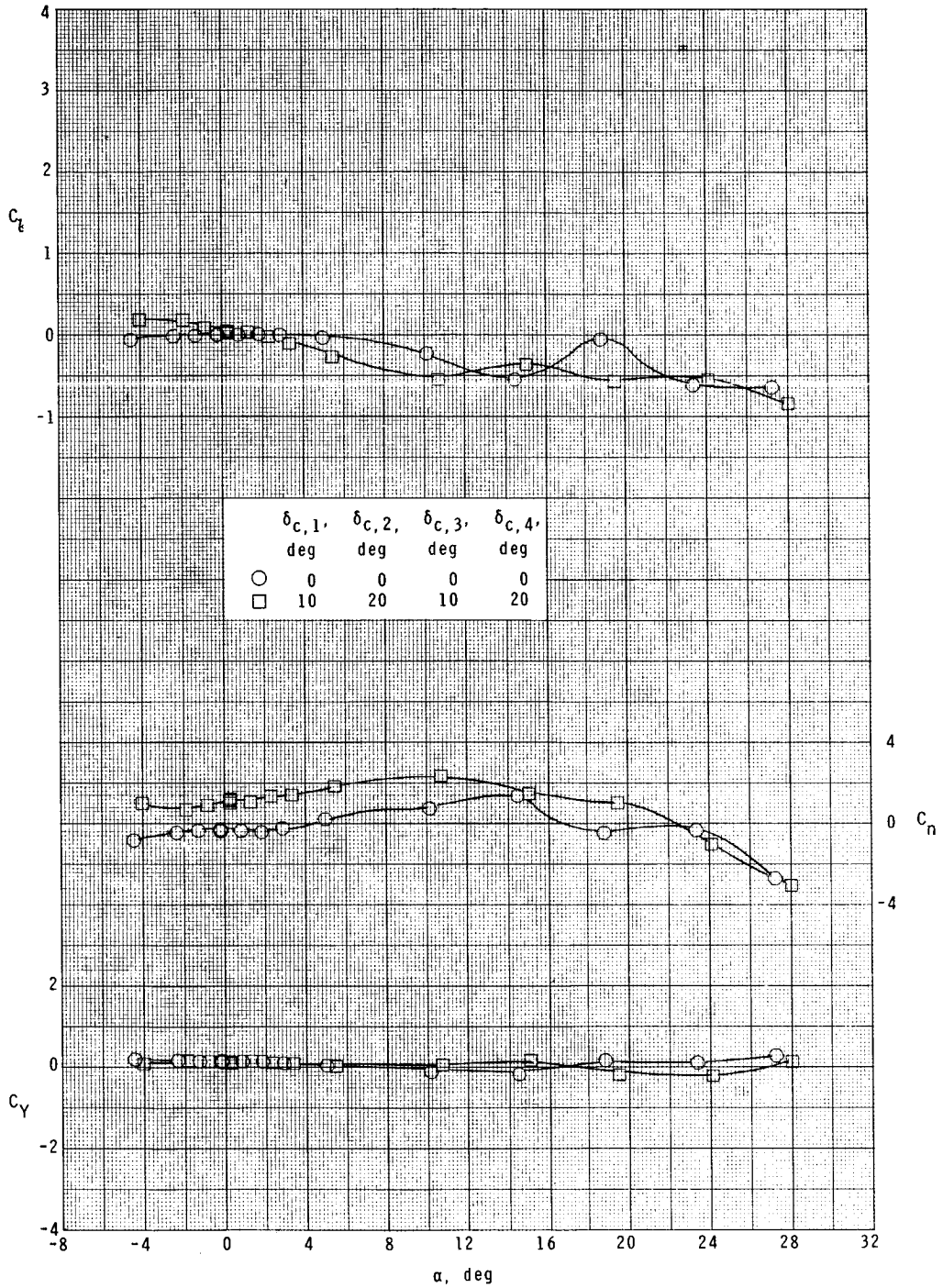

(d) M = 2.86.

Figure 15.- Continued.

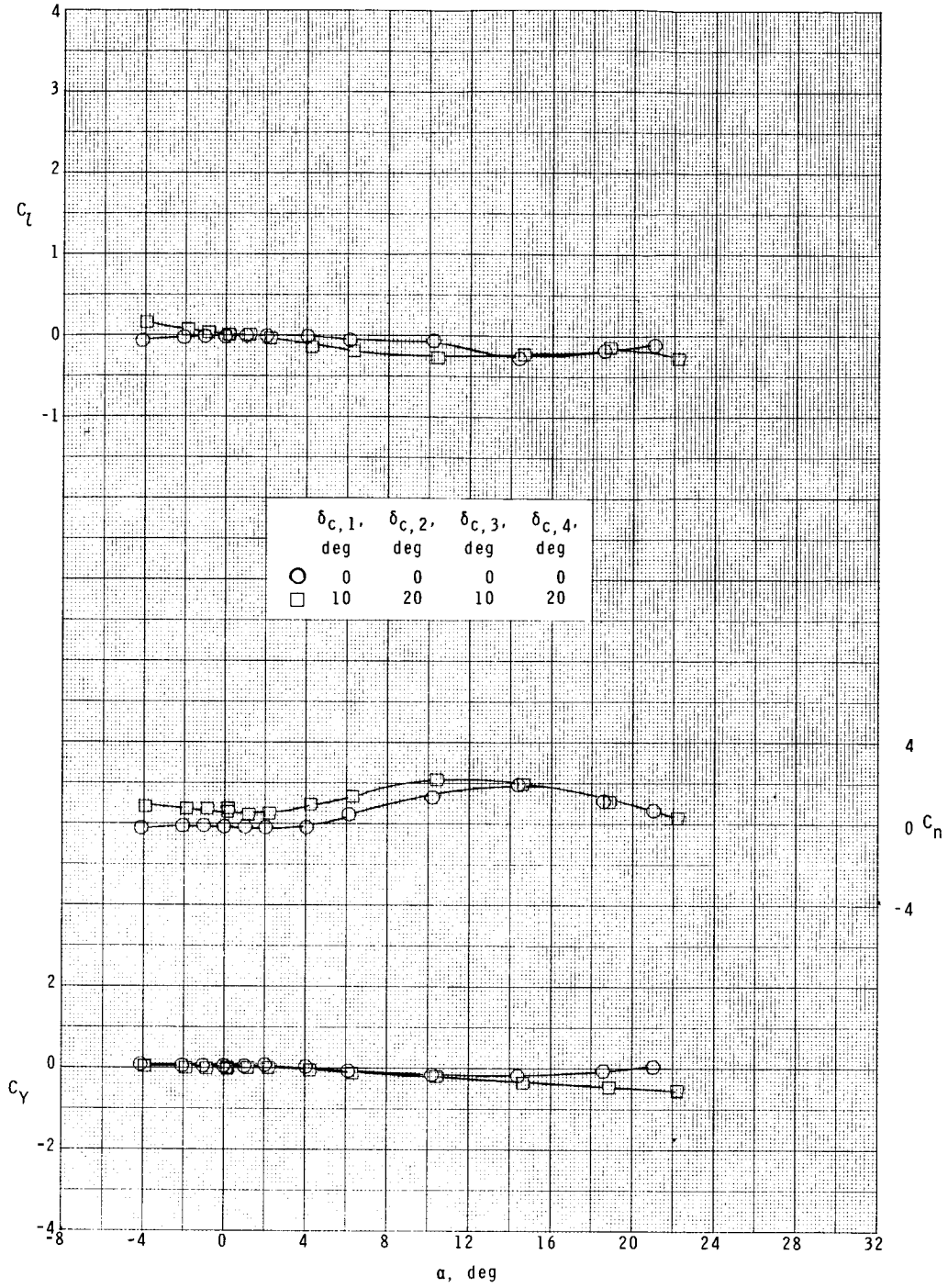

(e) M = 3.95.

Figure 15.- Continued.

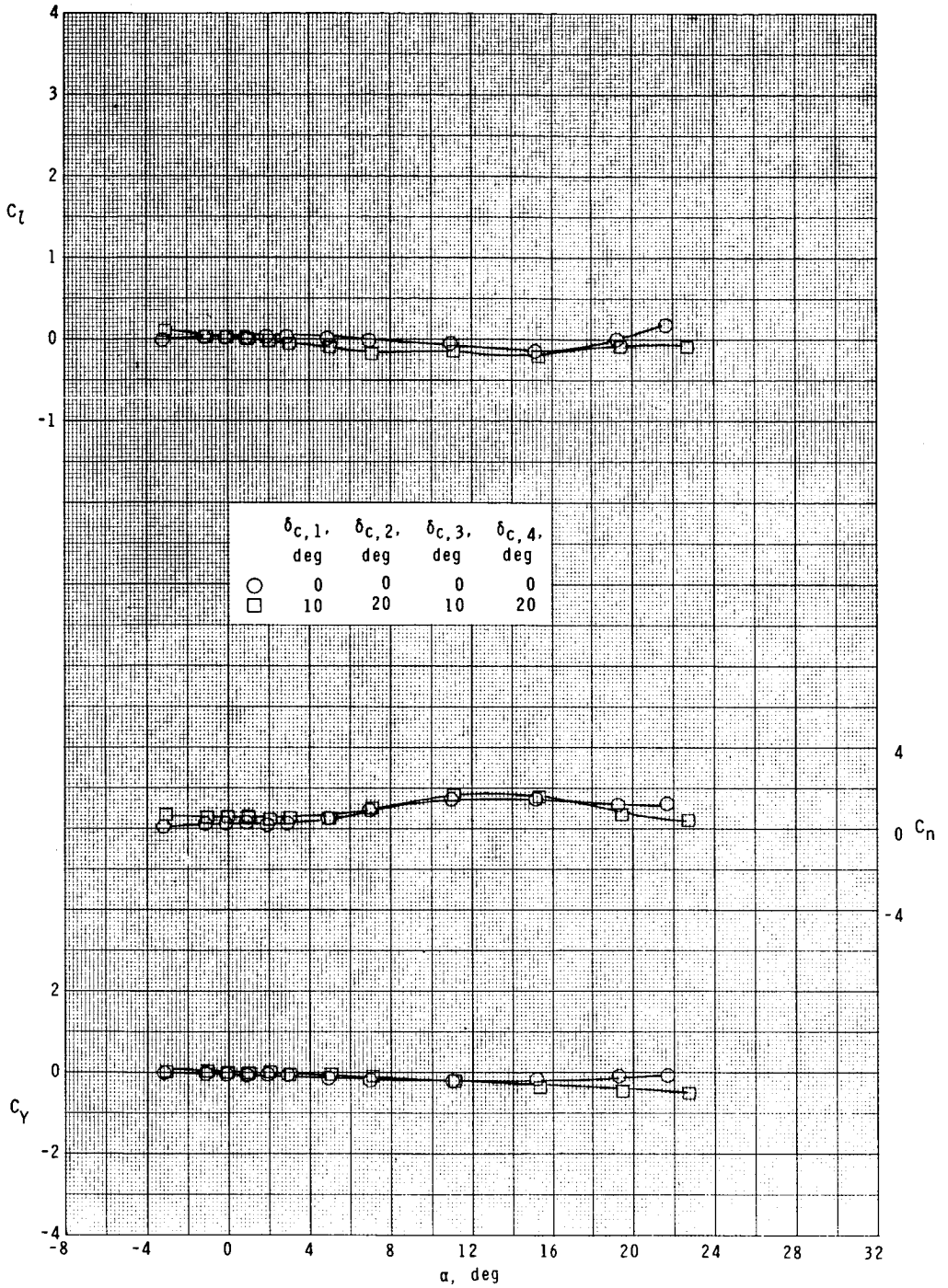

(f) M = 4.63.

Figure 15.- Concluded.

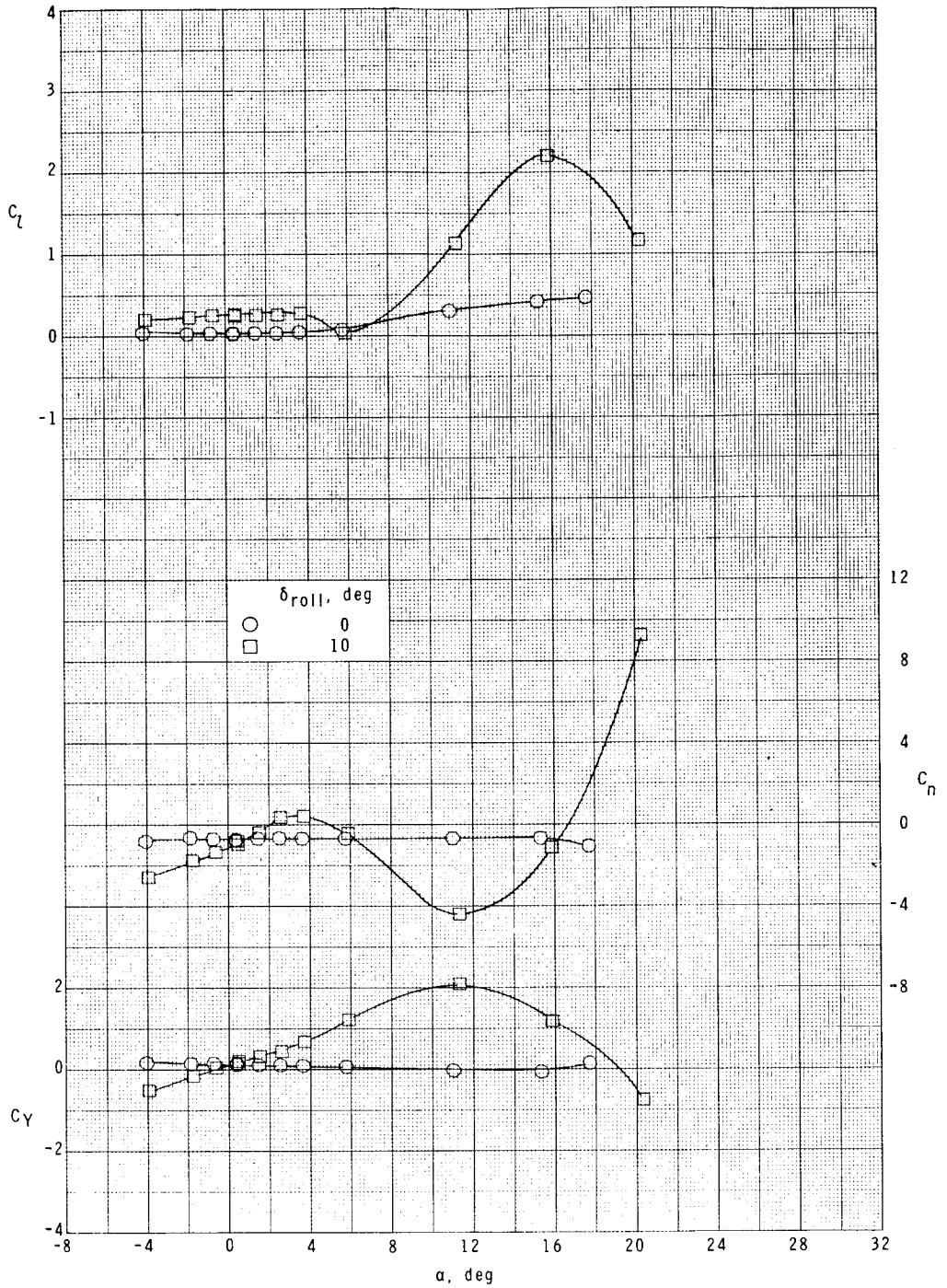

(a) M = 1.75.

Figure 16.- Roll control effectiveness. $\phi = 0^o$.

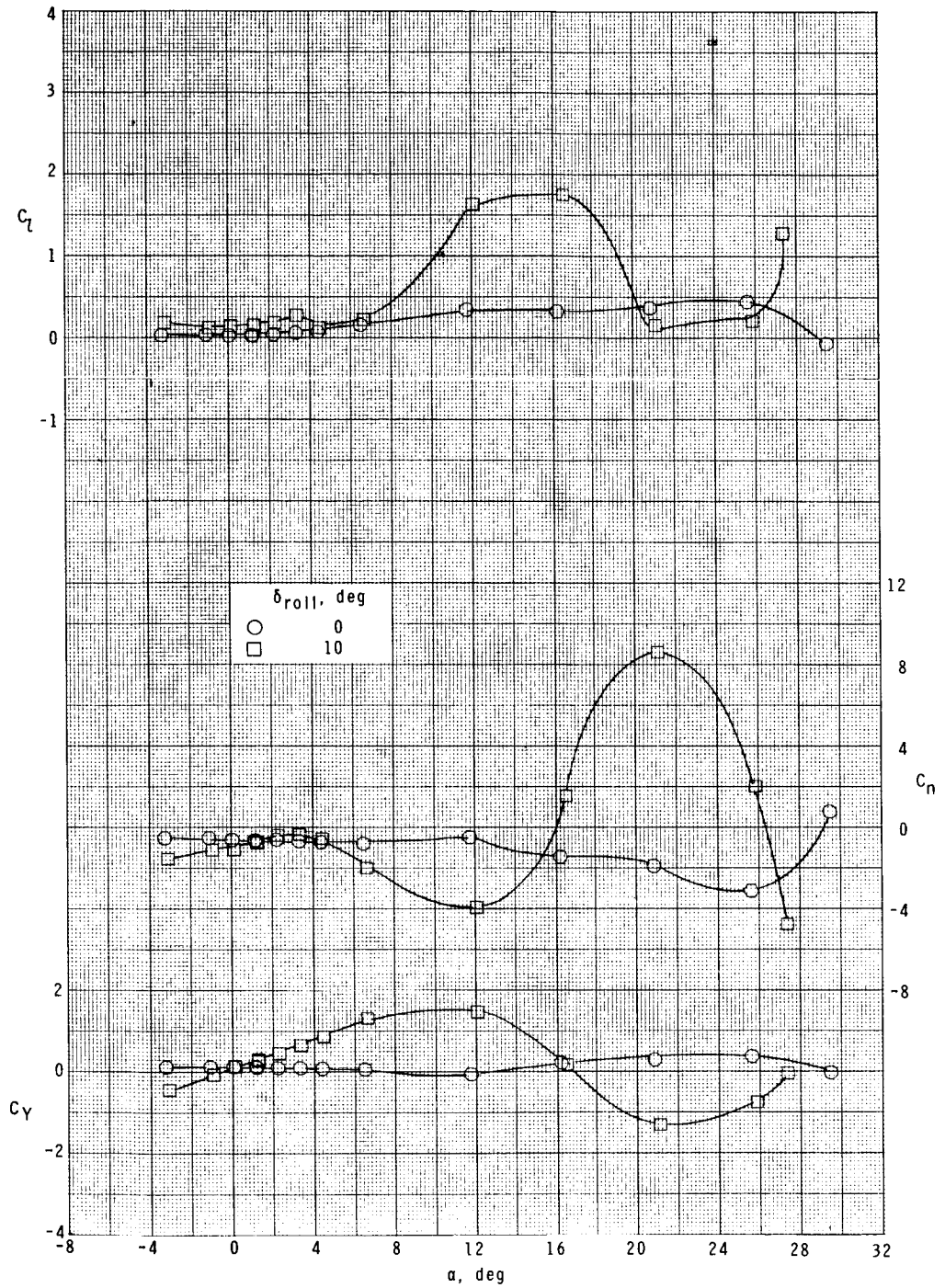

(b) M = 2.10.

Figure 16.- Continued.

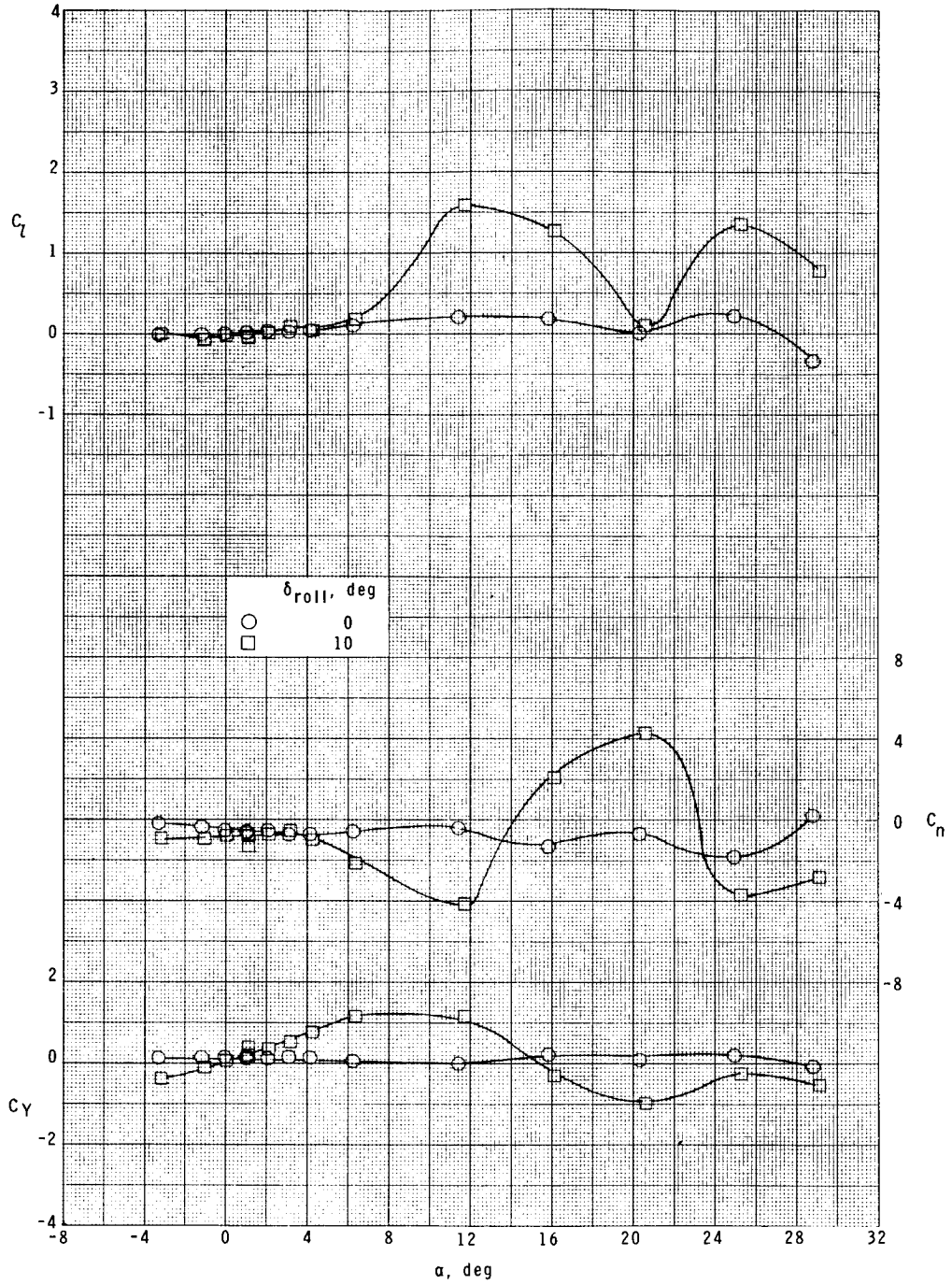

(c) M = 2.50.

Figure 16.- Continued.

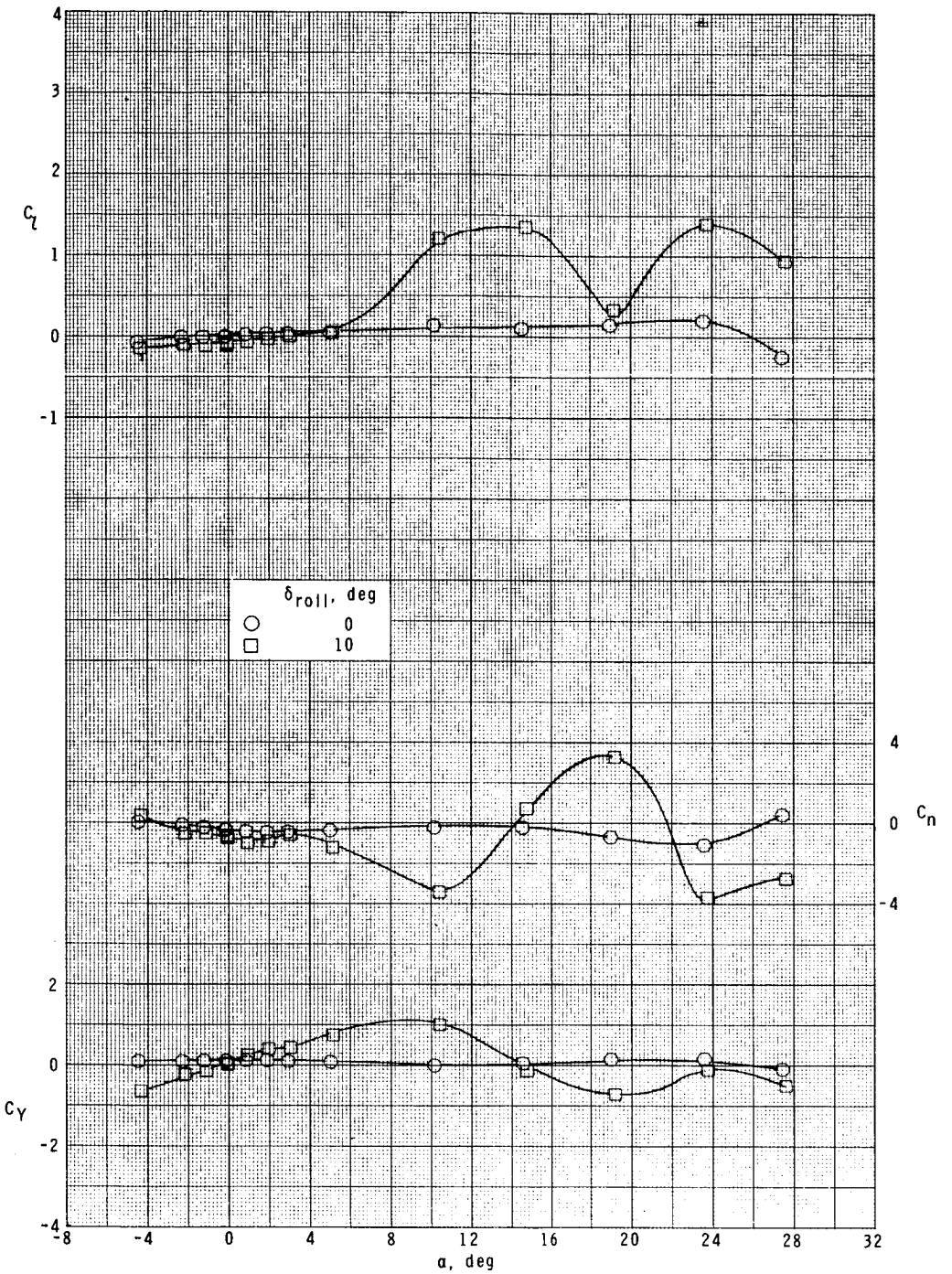

(d) M = 2.86.

Figure 16.- Continued.

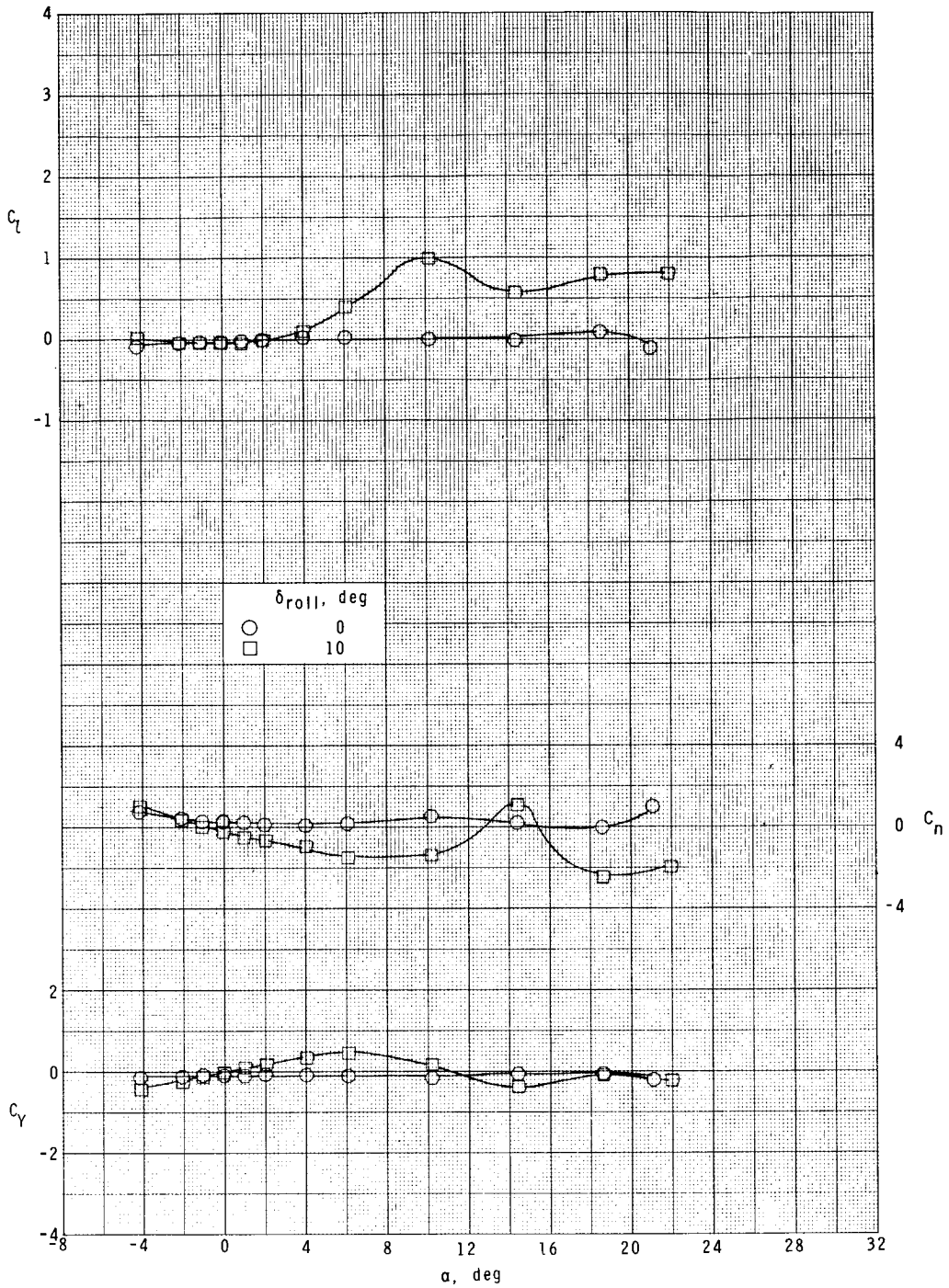

(e) M = 3.95.

Figure 16.- Continued.

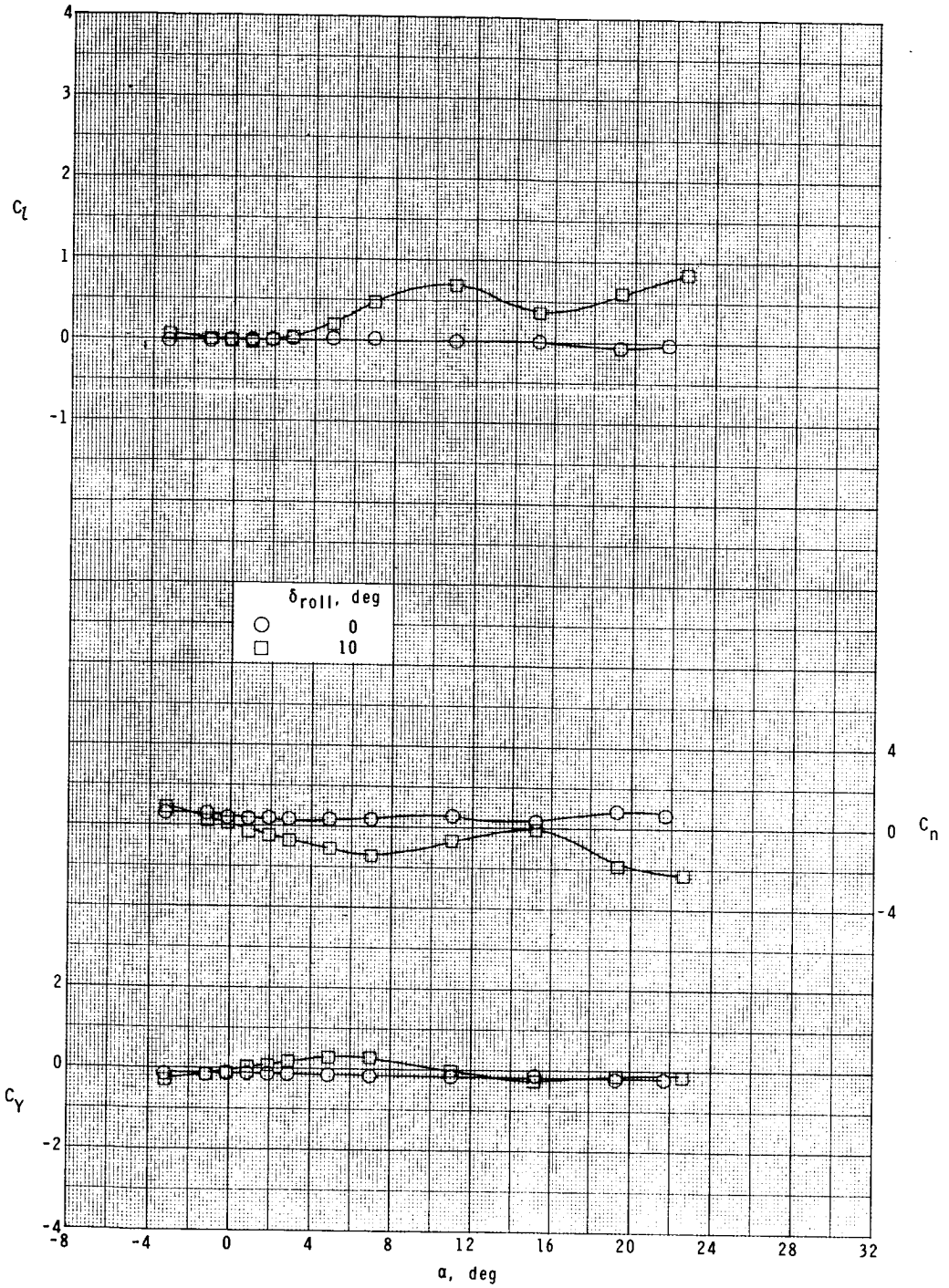

(f) M = 4.63.

Figure 16.- Concluded.

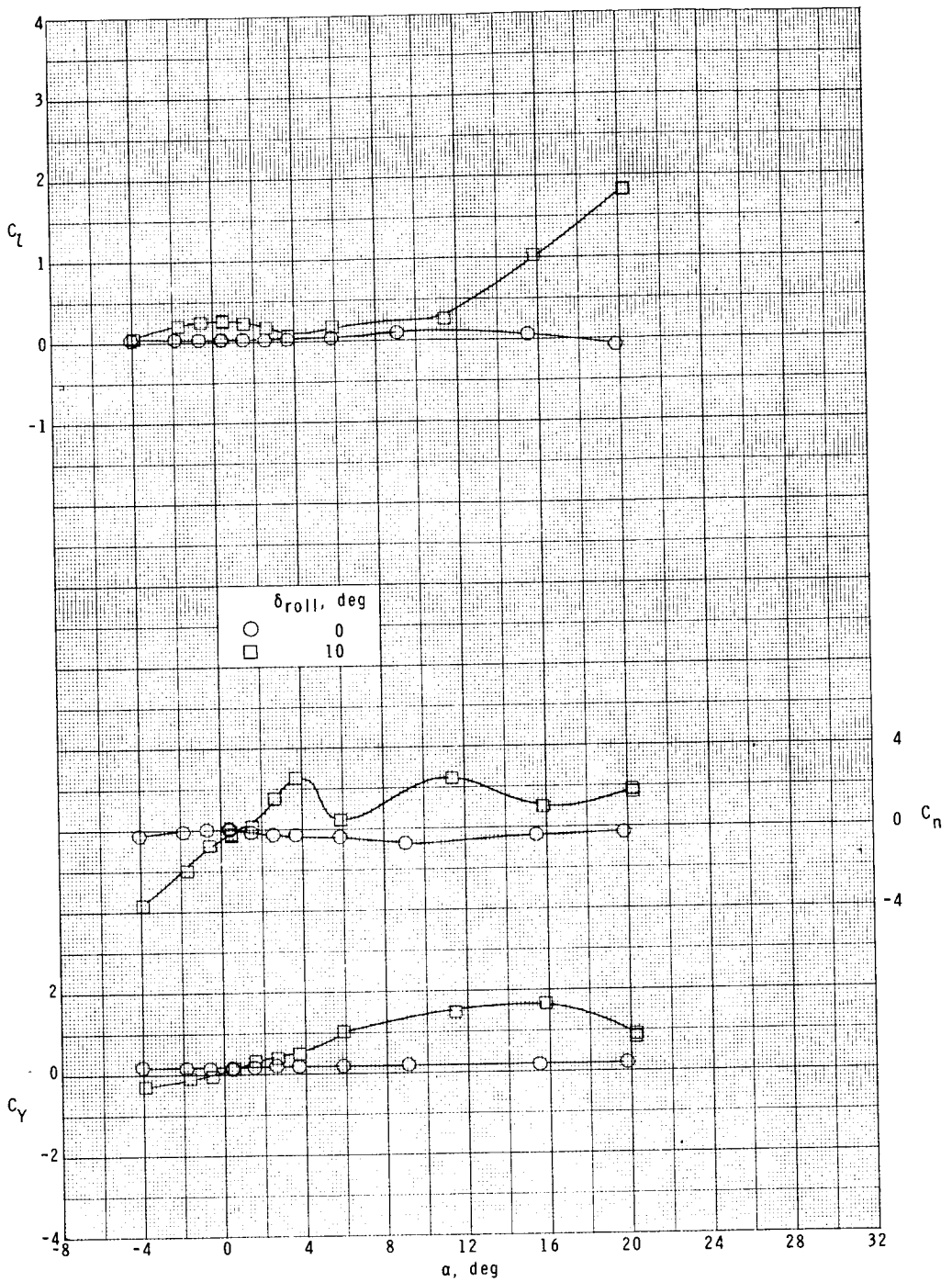

(a) M = 1.75.

Figure 17.- Roll control effectiveness. $\phi = -45^o$.

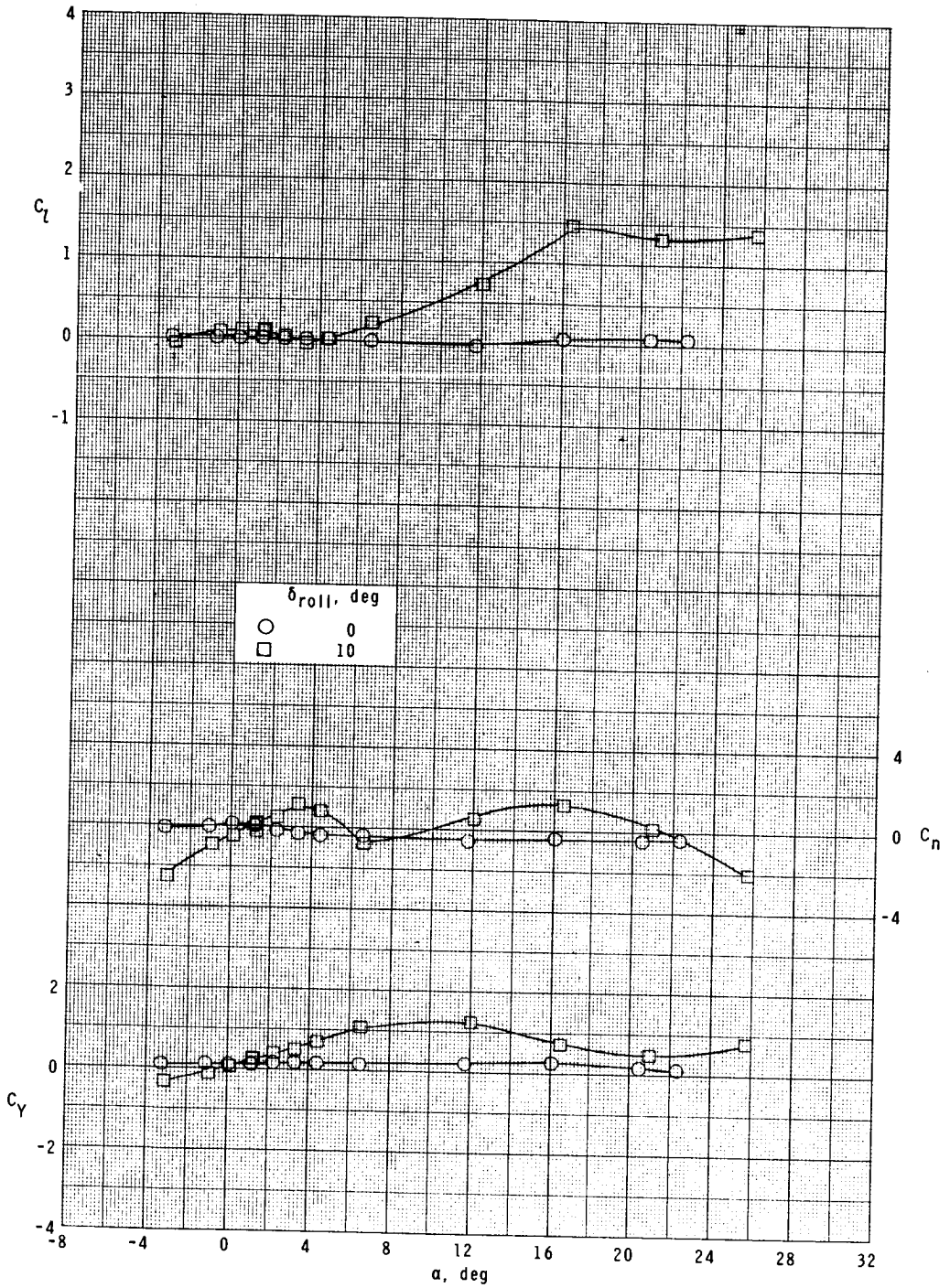

(b) M = 2.10.

Figure 17.- Continued.

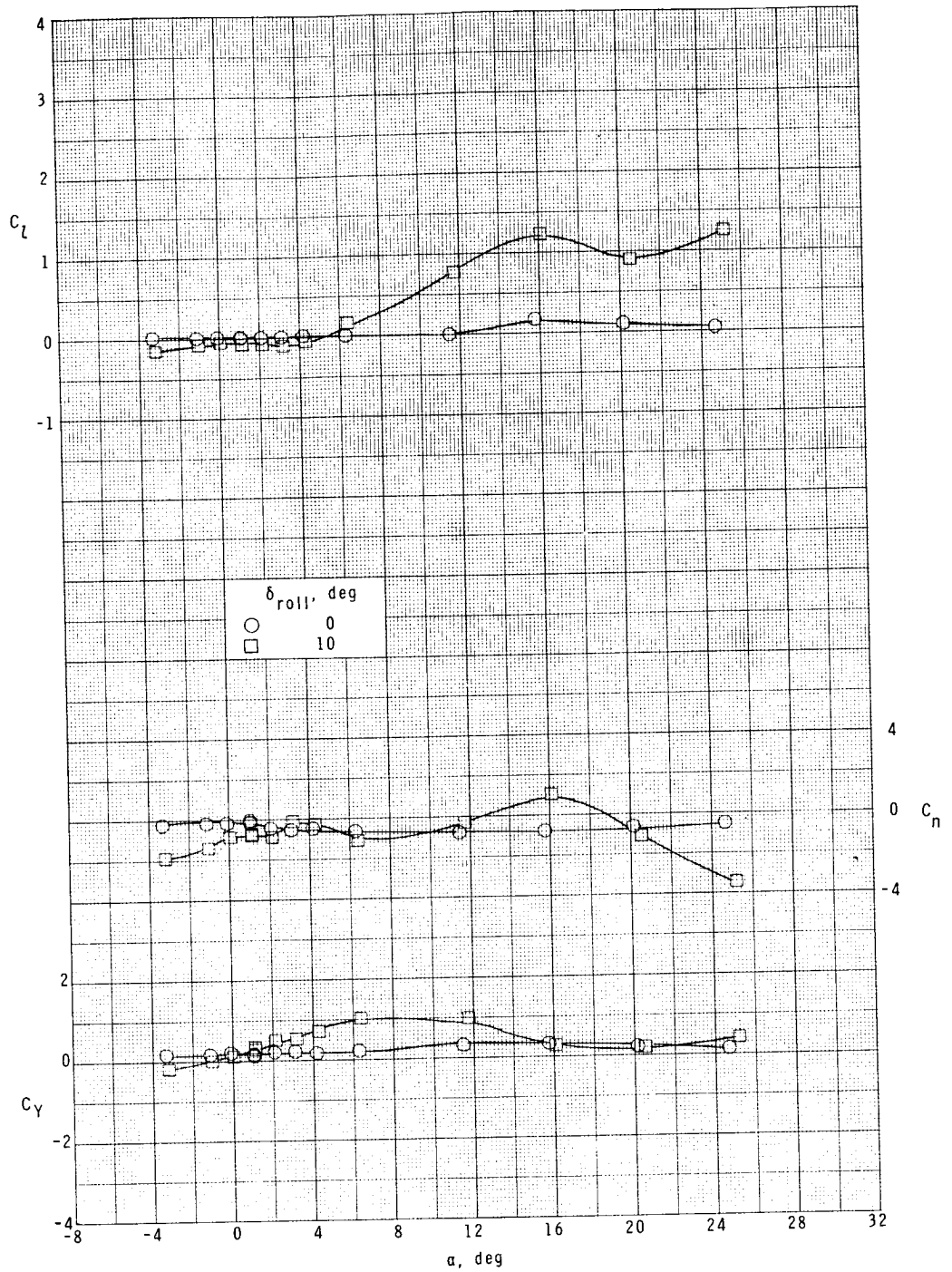

(c) M = 2.50.

Figure 17.- Continued.

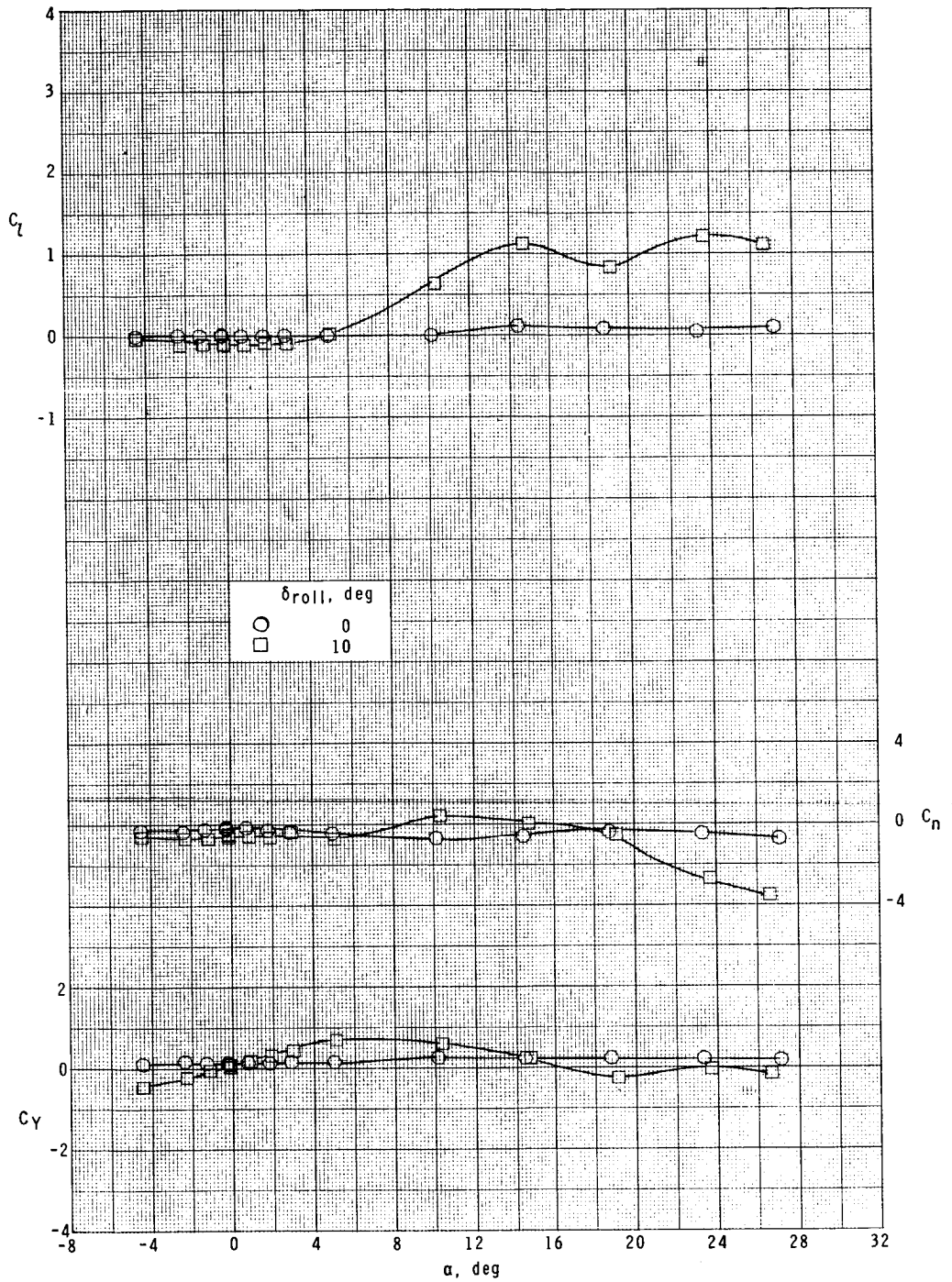

(d) M = 2.86.

Figure 17.- Continued.

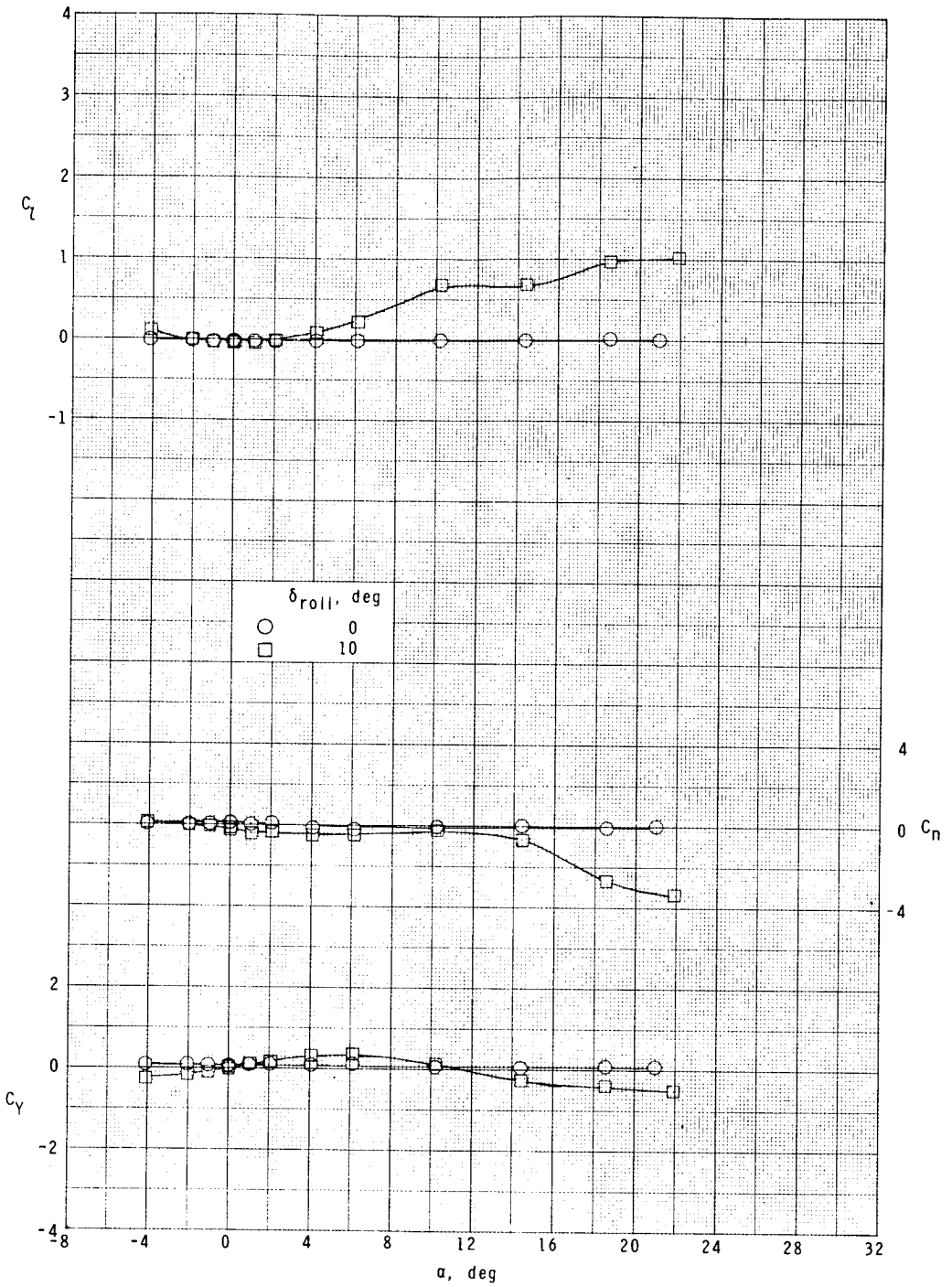

(e) M = 3.95.

Figure 17.- Continued.

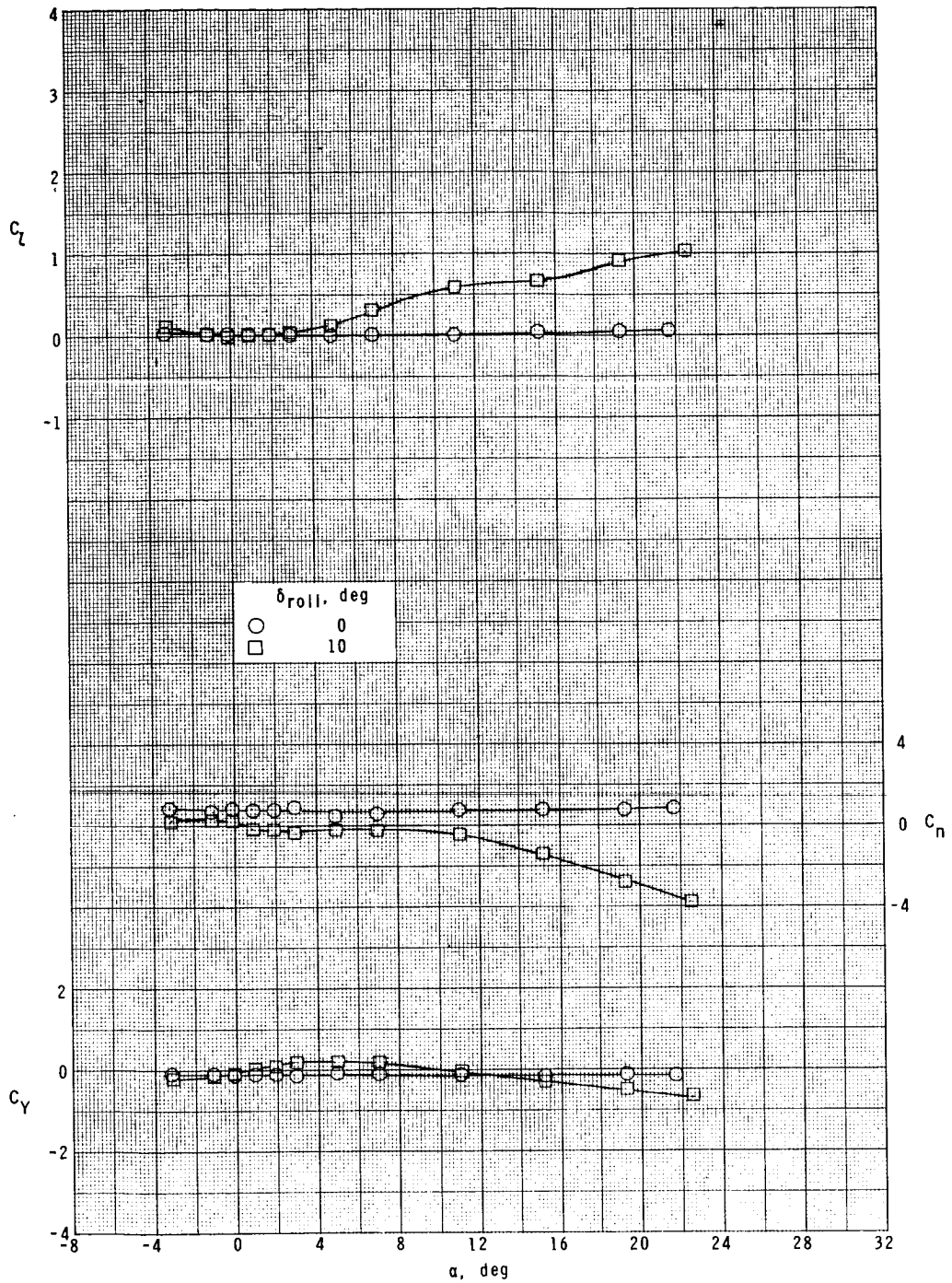

(f) M = 4.63.

Figure 17.- Concluded.

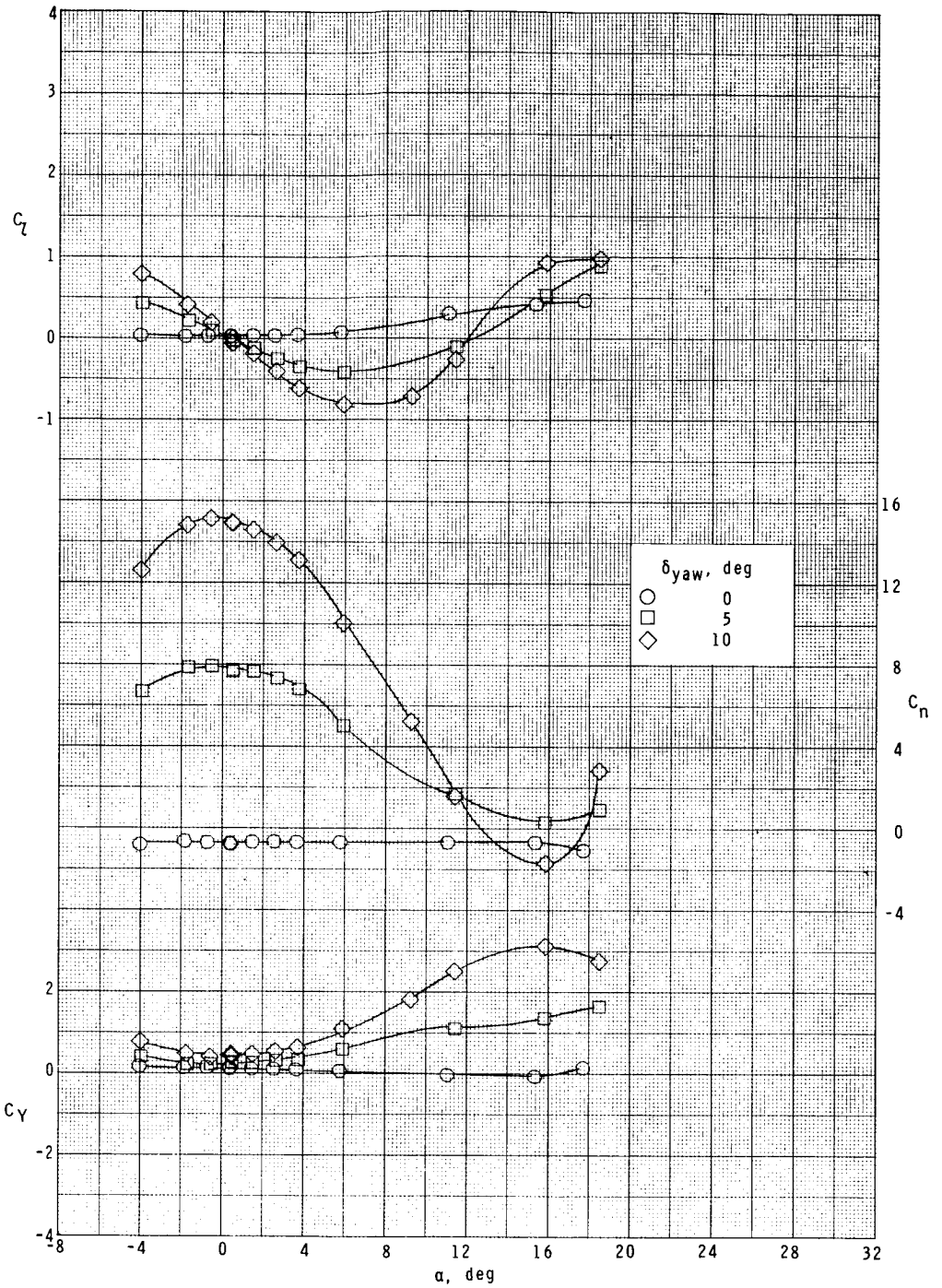

(a) M = 1.75.

Figure 18.- Yaw control effectiveness. $\phi = 0^o$.

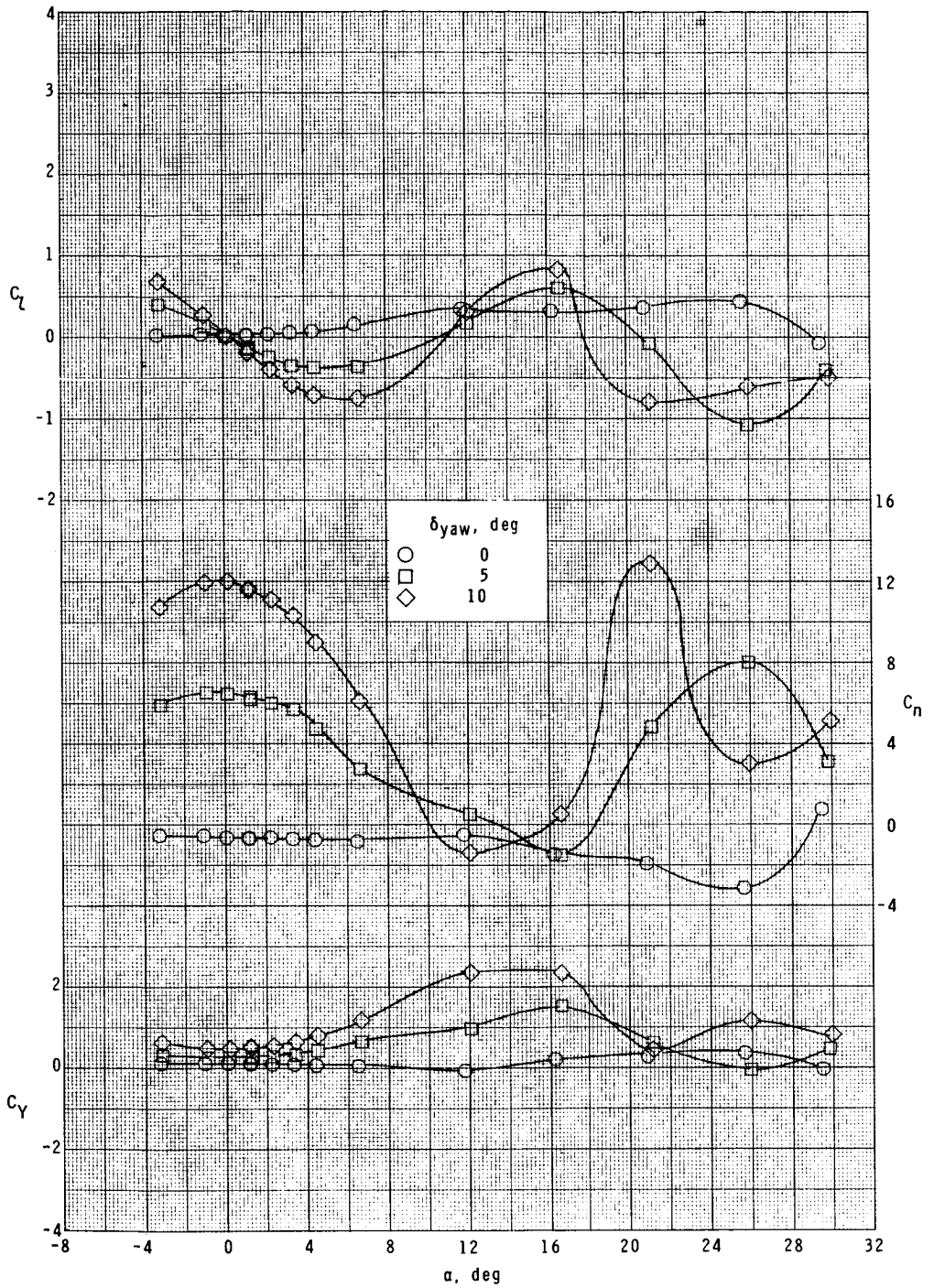

(b) M = 2.10.

Figure 18.- Continued.

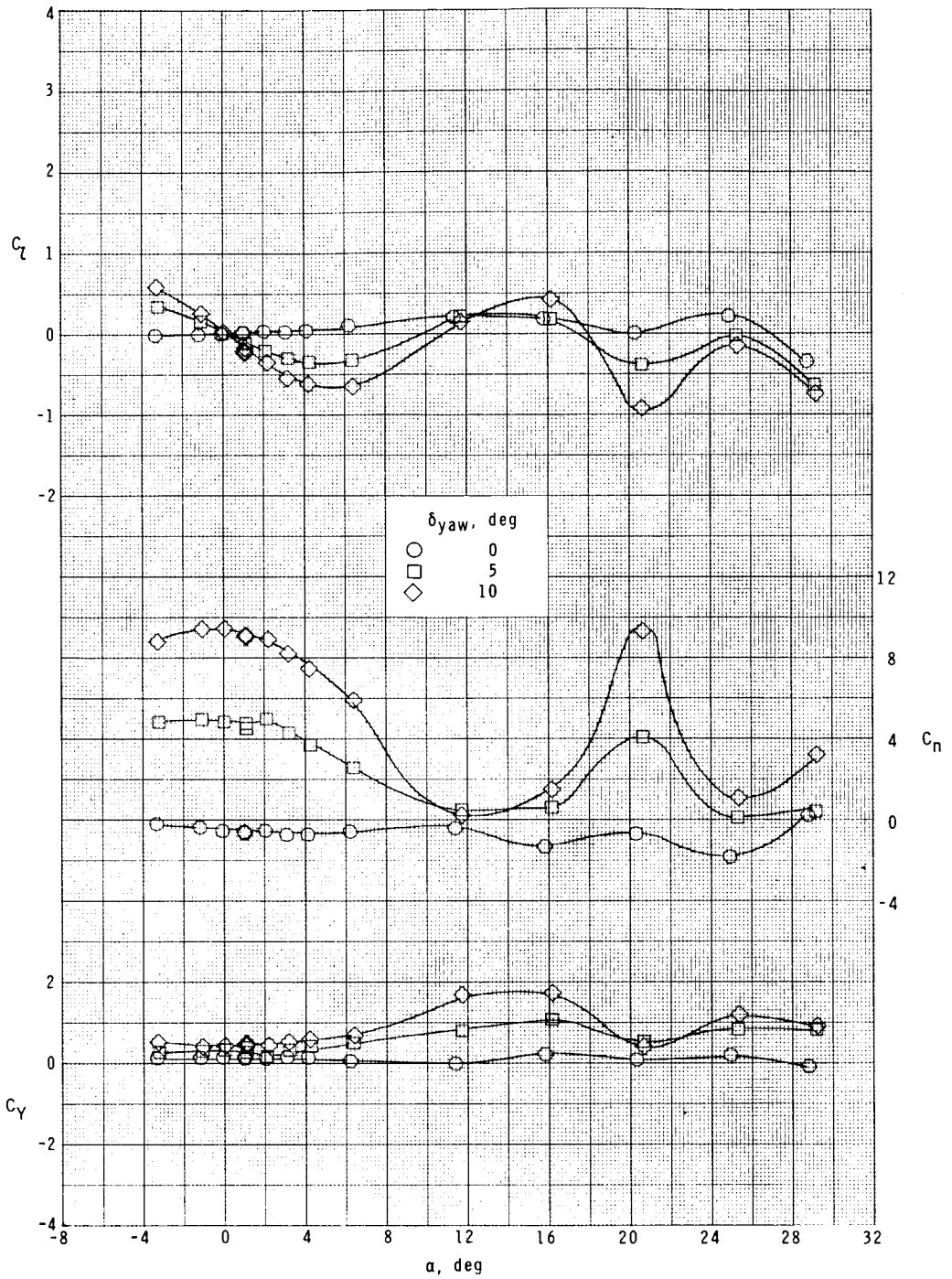

(c) M = 2.50.

Figure 18.- Continued.

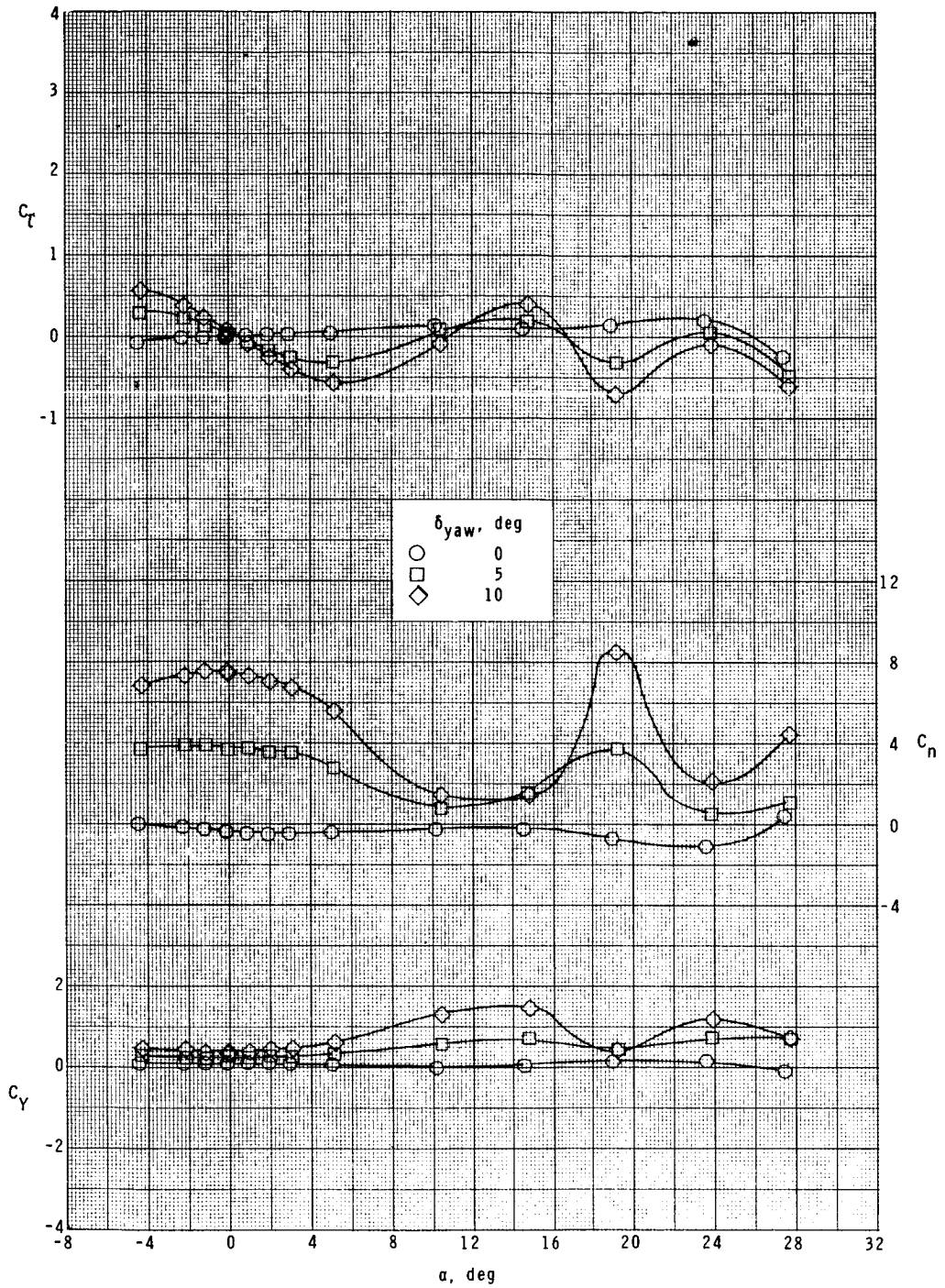

(d) M = 2.86.

Figure 18.- Continued.

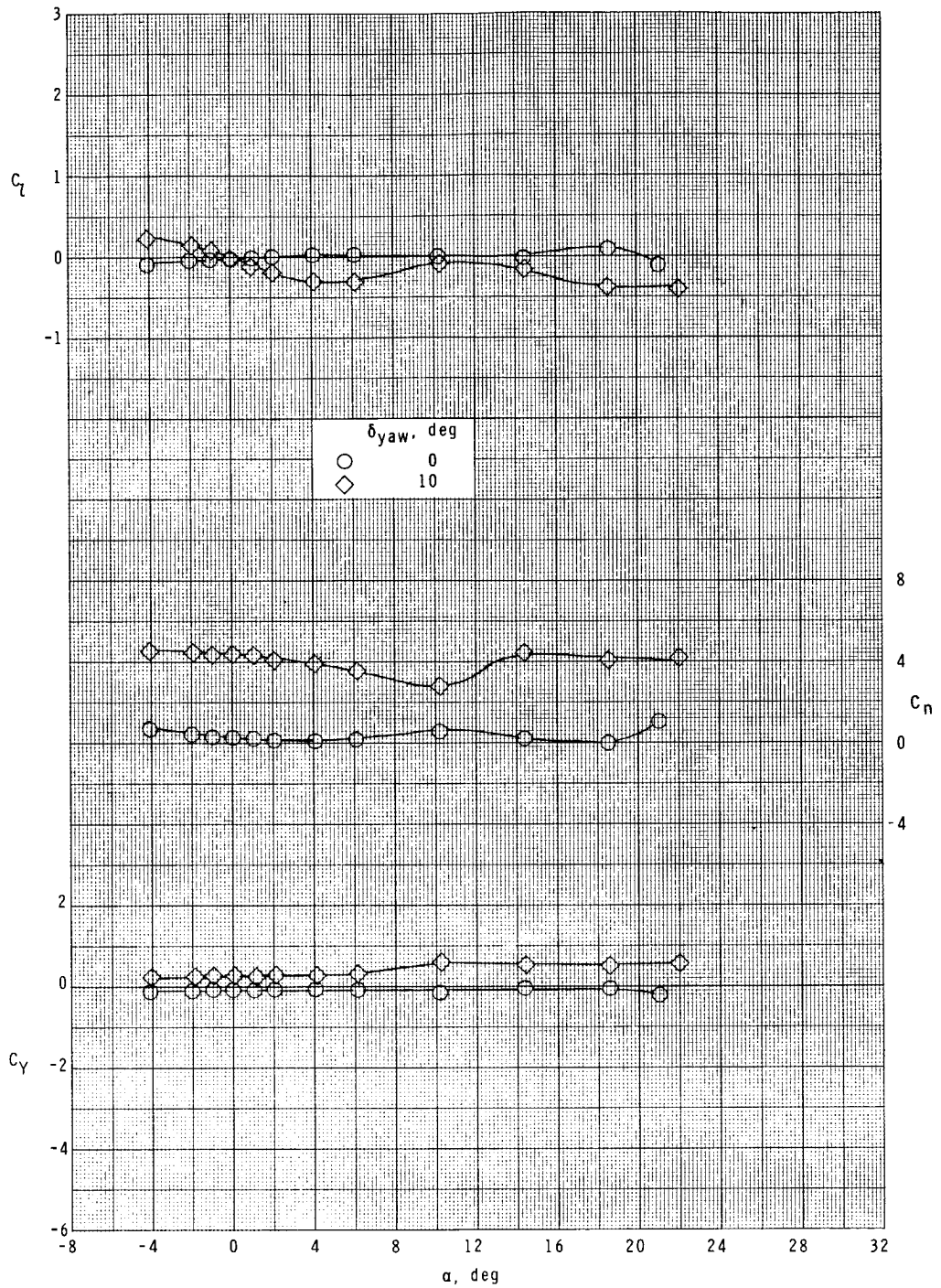

(e) M = 3.95.

Figure 18 .- Continued.

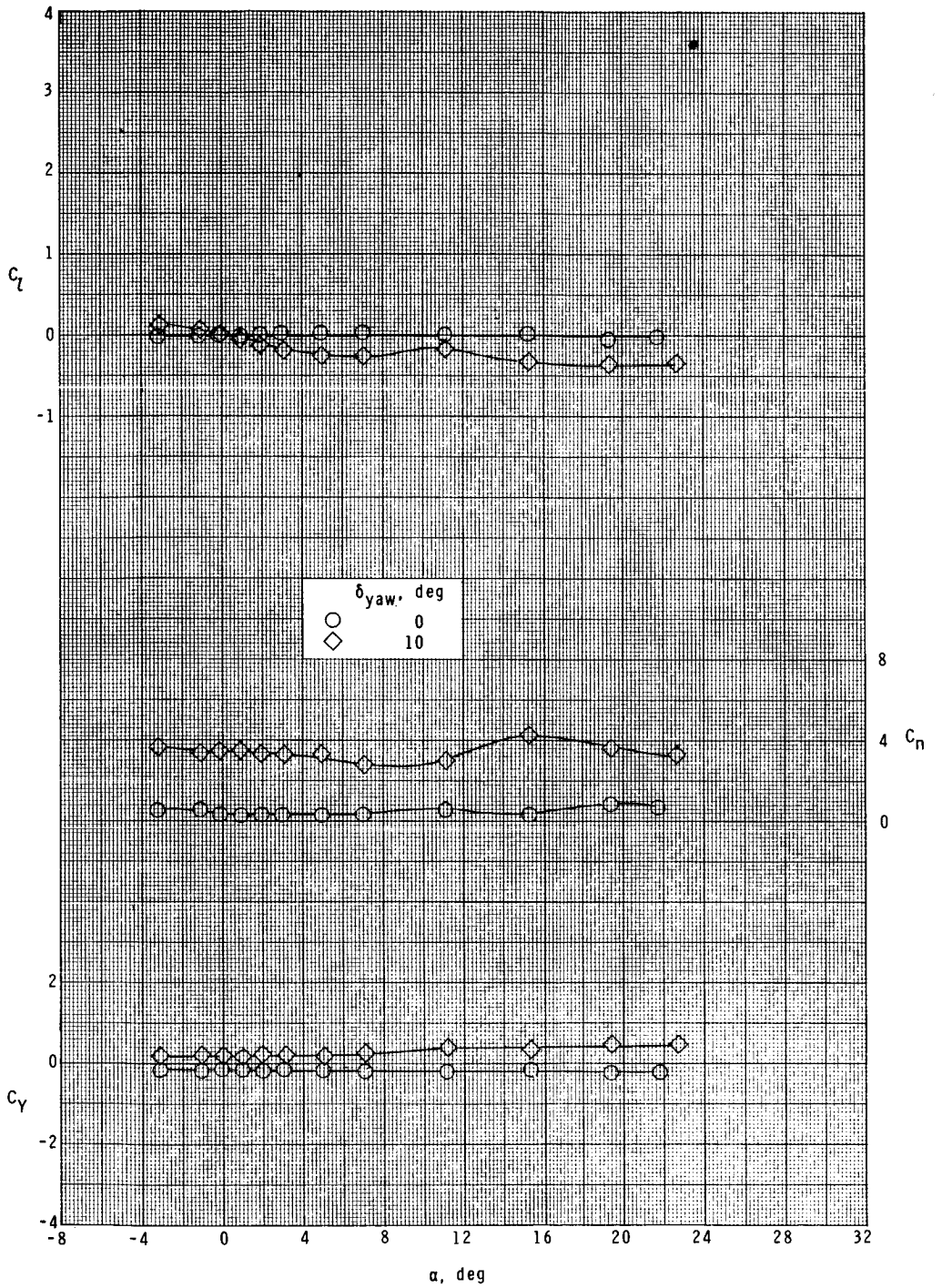

(f) M = 4.63.

Figure 18.- Concluded.

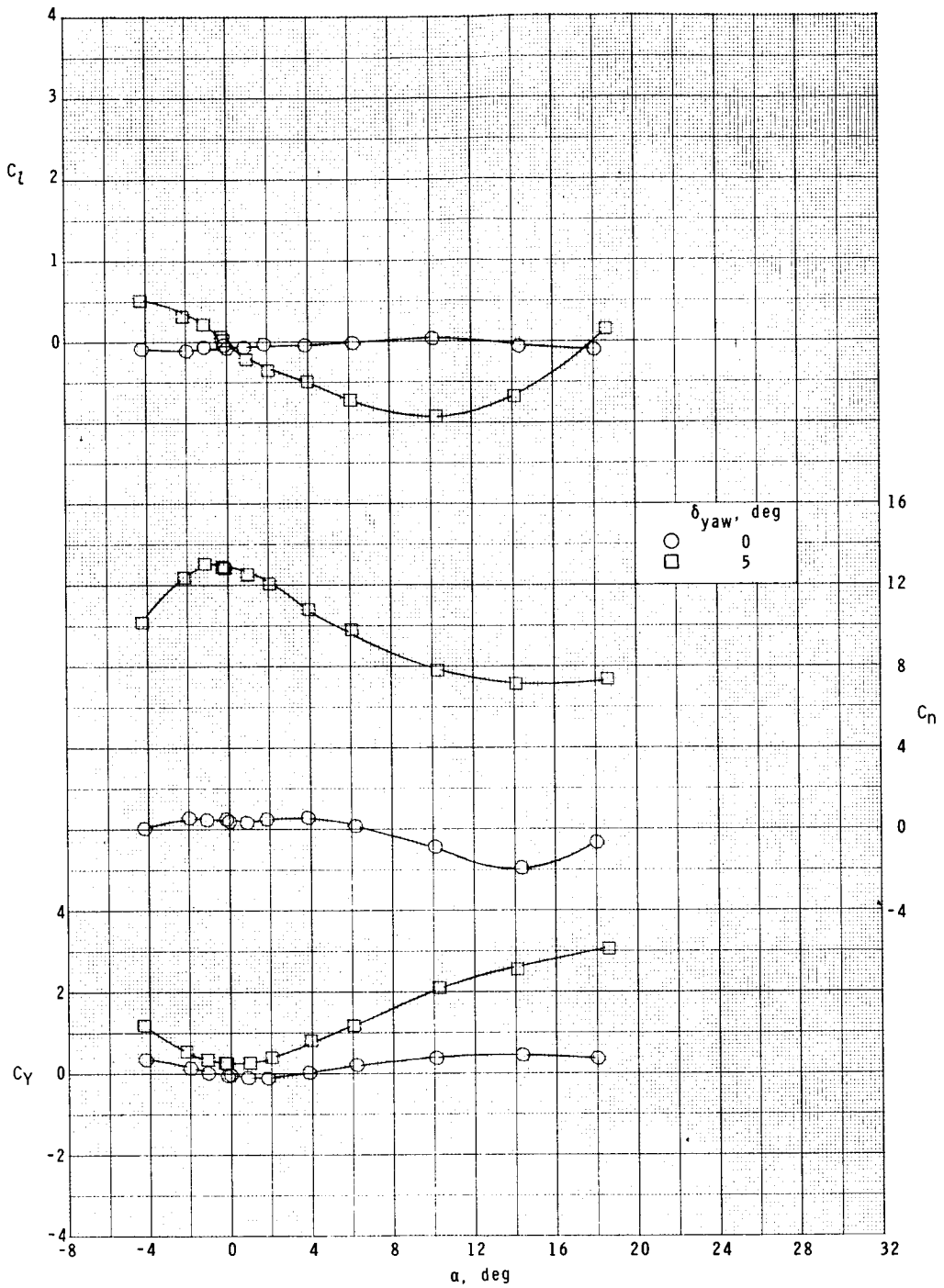

(a) M = 0.20.

Figure 19.- Yaw control effectiveness. $\phi = -45^{o}$.

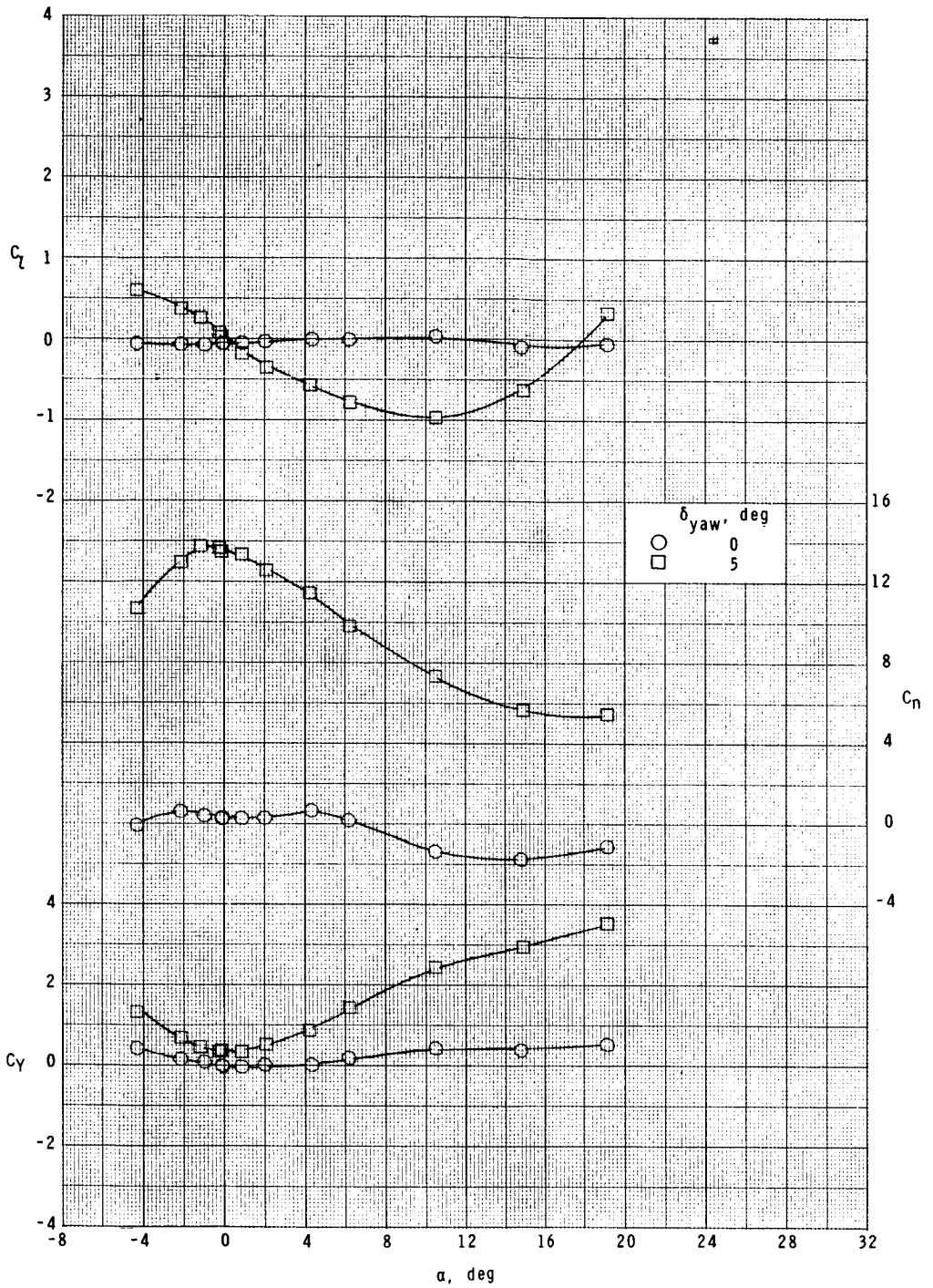

(b) M = 0.60.

Figure 19.- Continued.

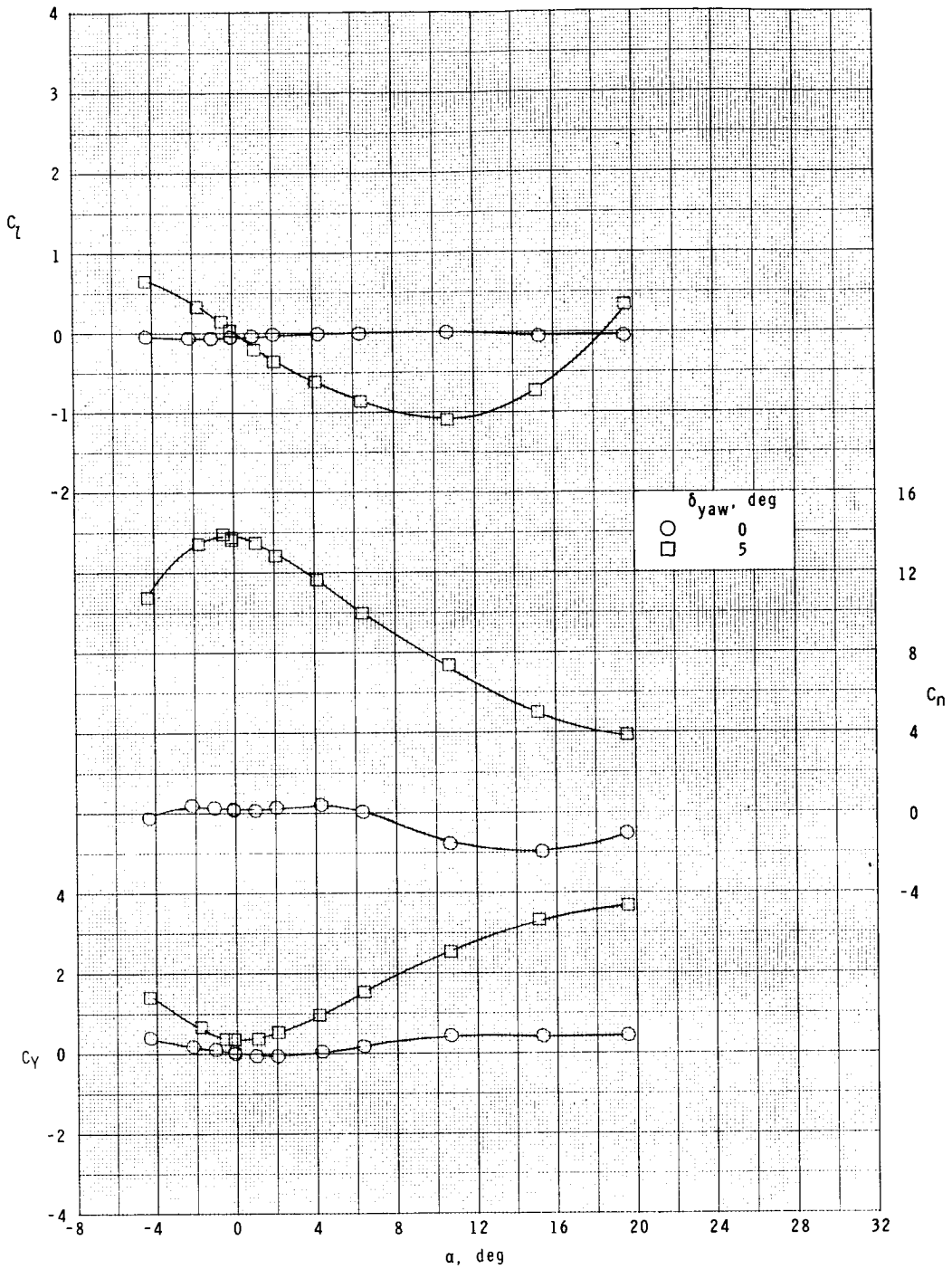

(c) M = 0.80.

Figure 19.- Continued.

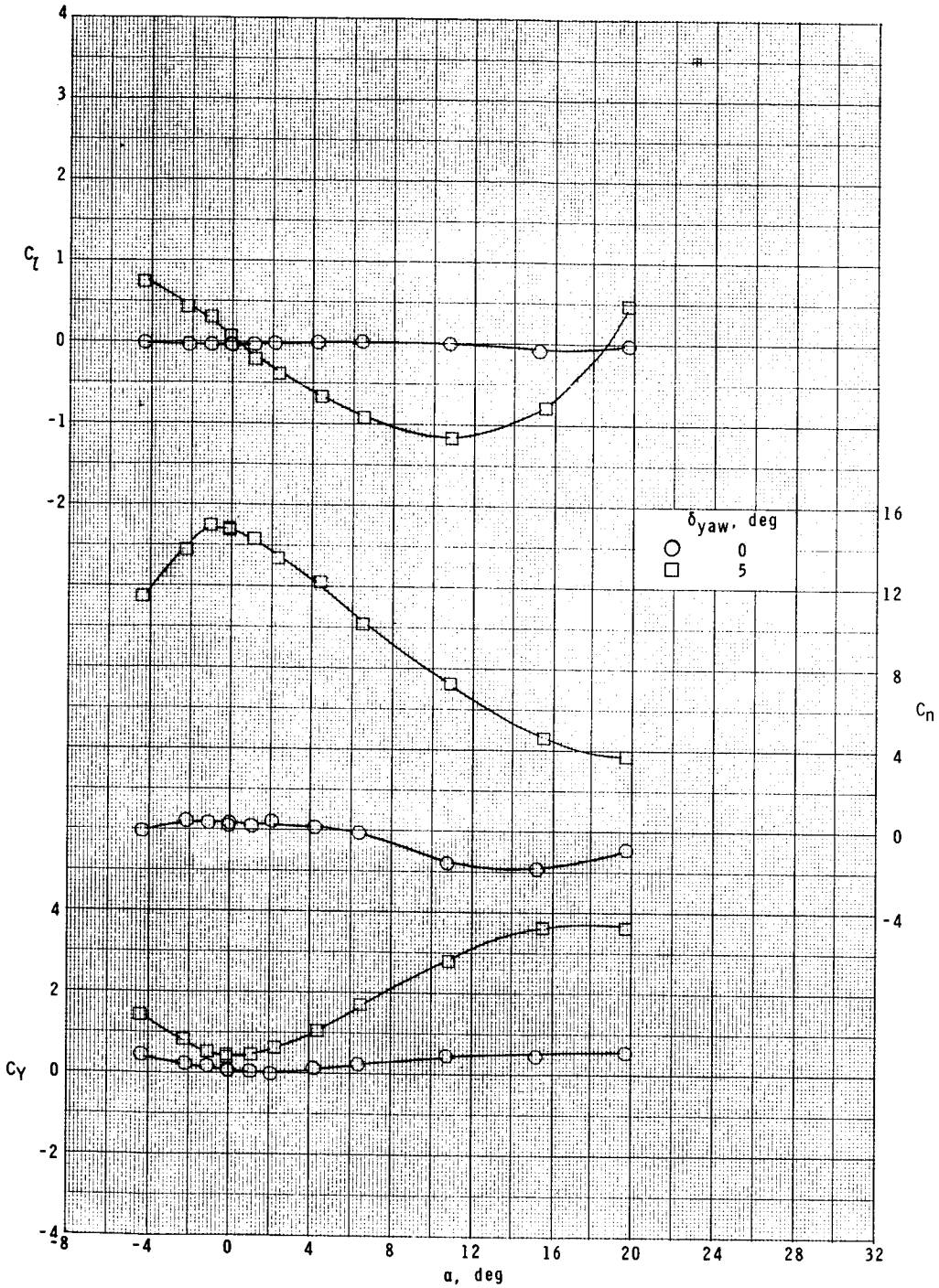

(d) M = 0.90.

Figure 19.- Continued.

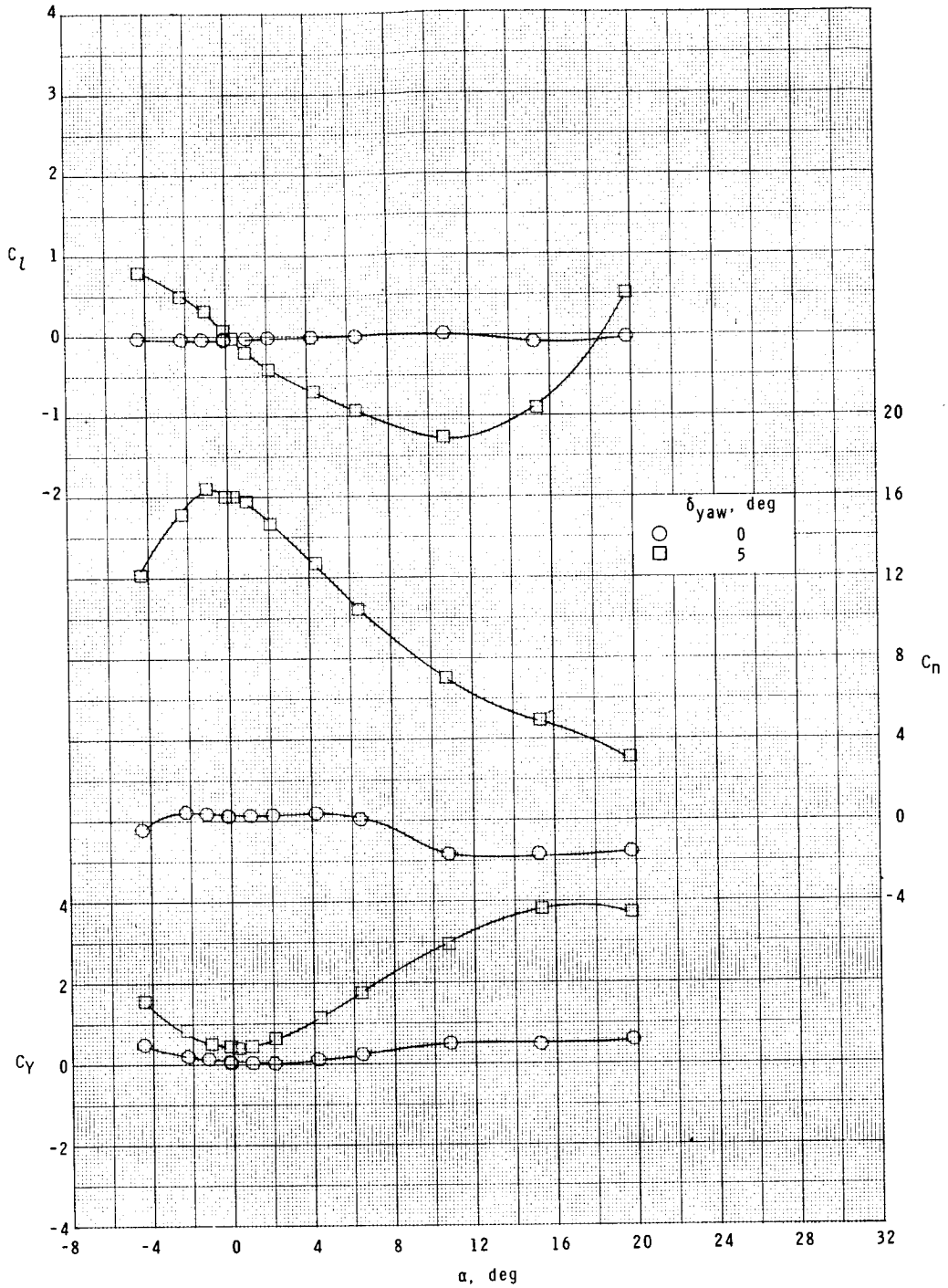

(e) M = 0.95.

Figure 19.- Continued.

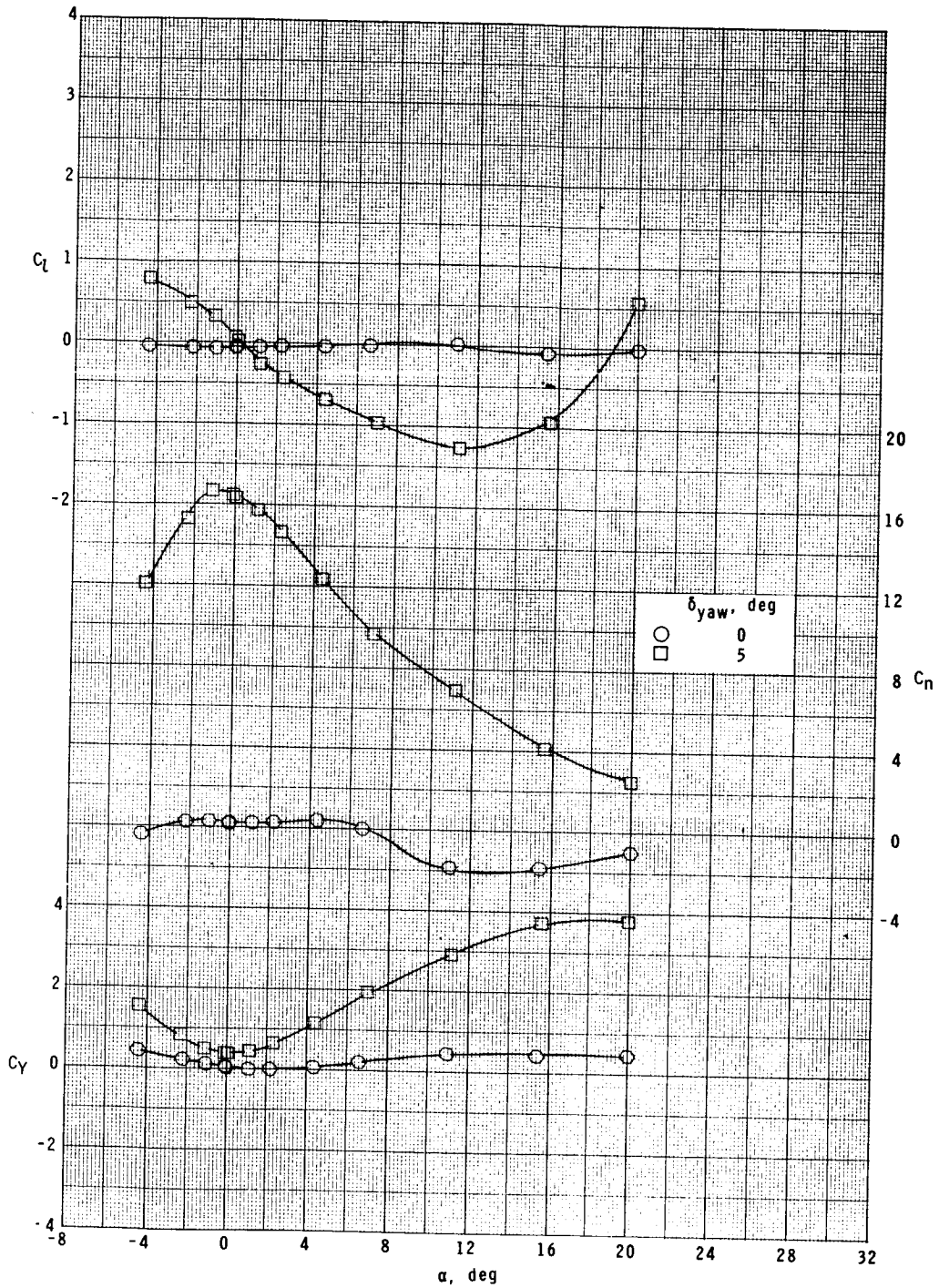

(f) M = 1.00.

Figure 19.- Continued.

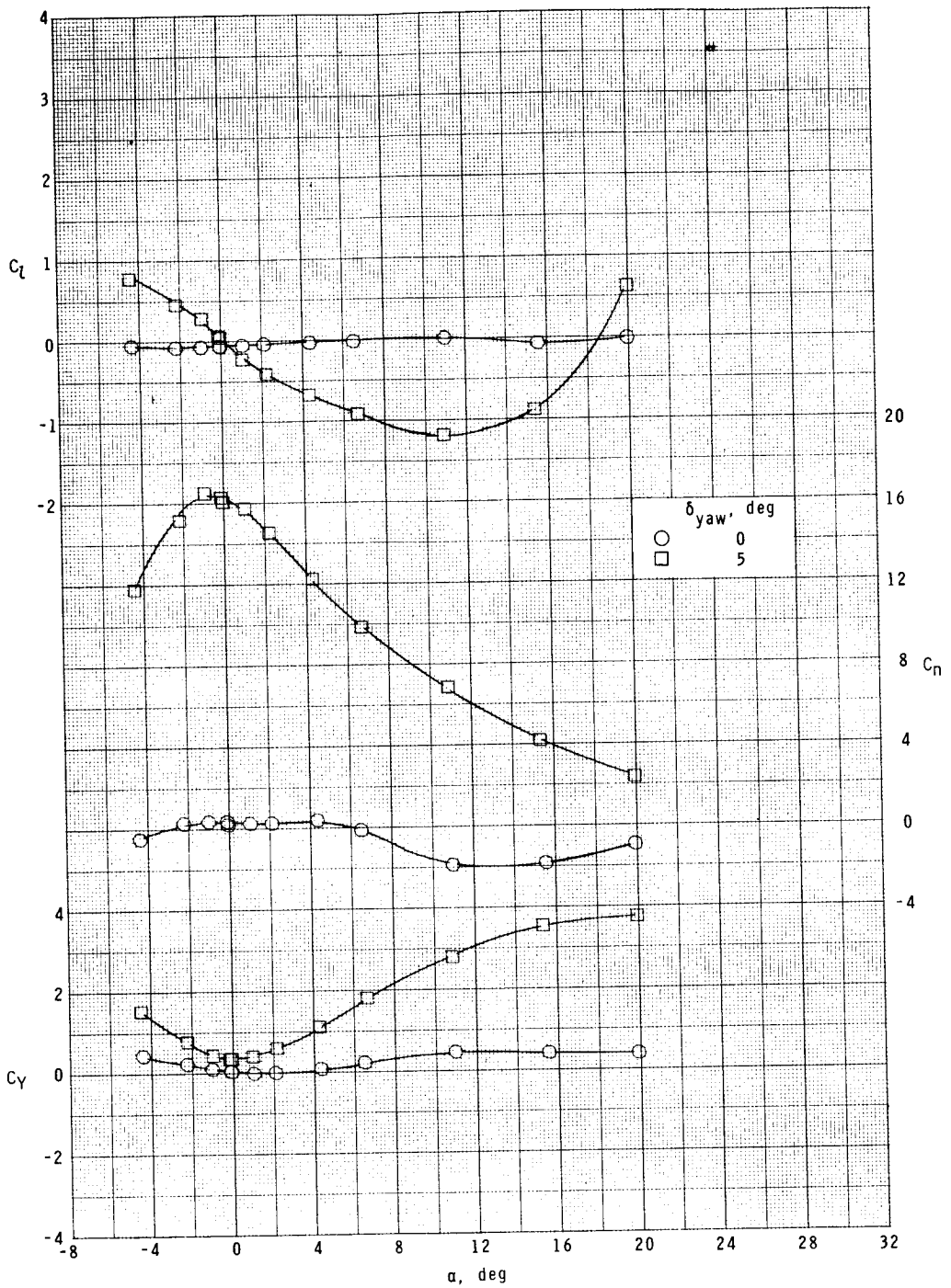

(g) M = 1.03.

Figure 19.- Continued.

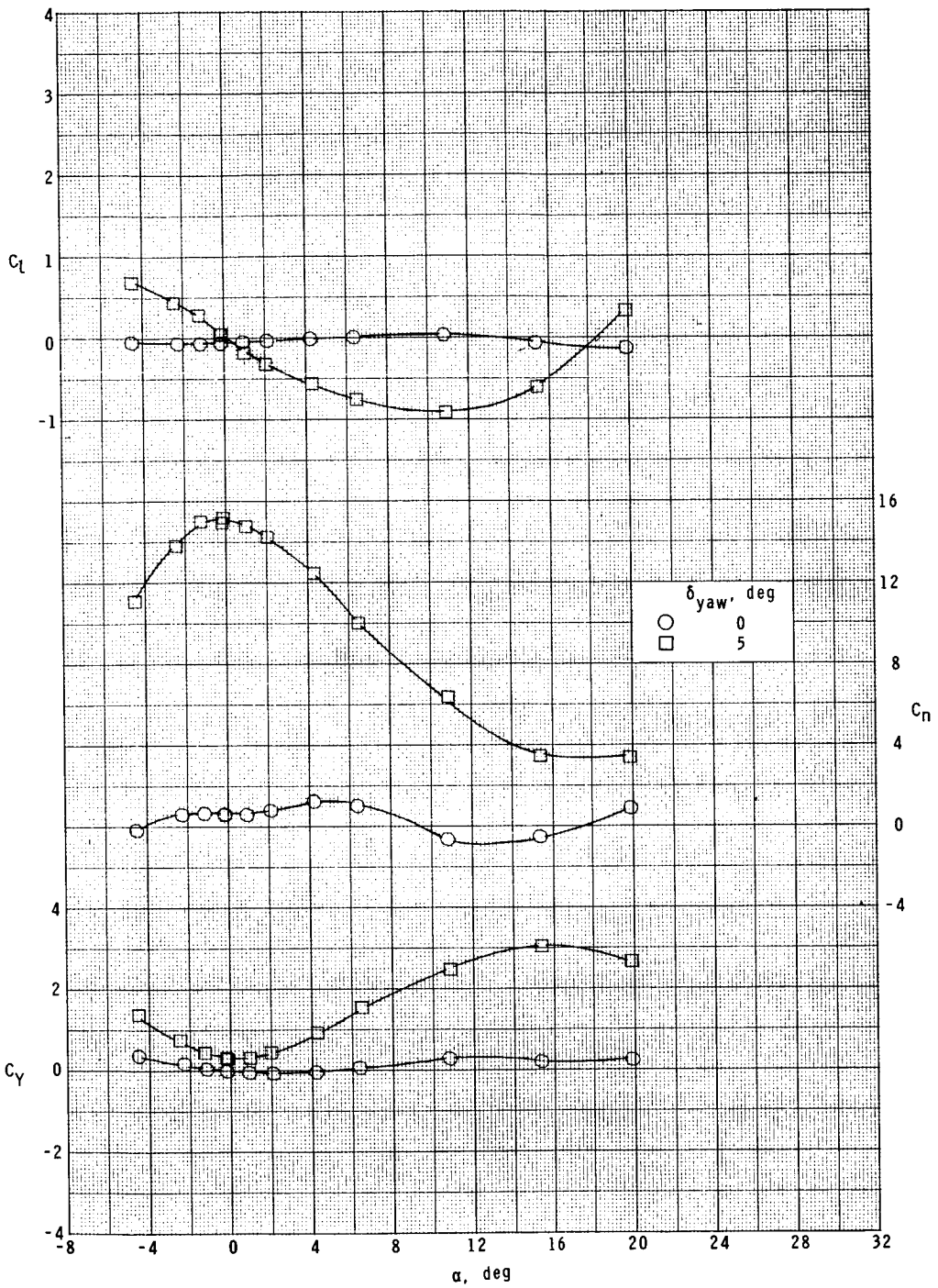

(h) M = 1.20.

Figure 19.- Continued.

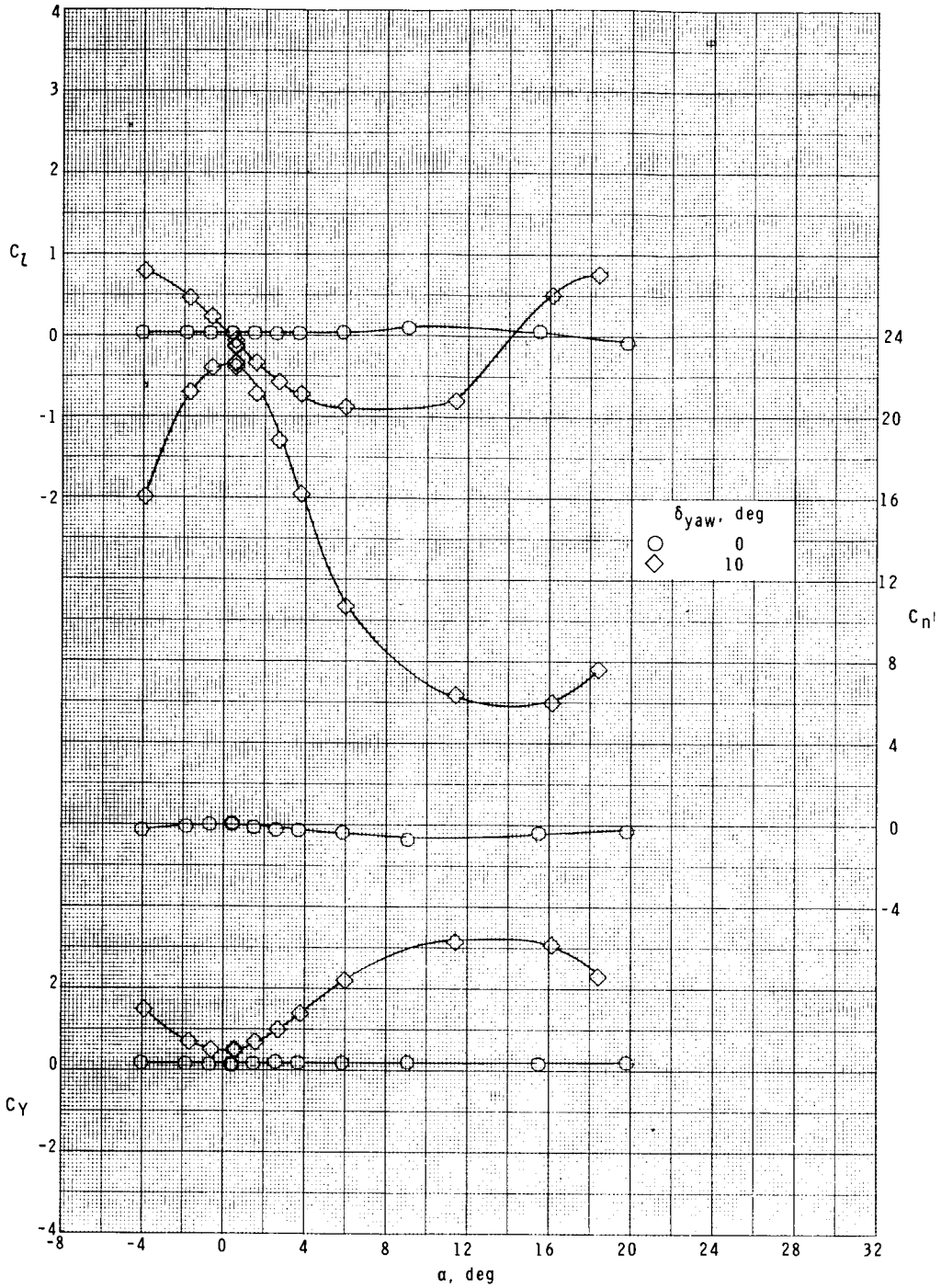

(i) M = 1.75.

Figure 19.- Continued.

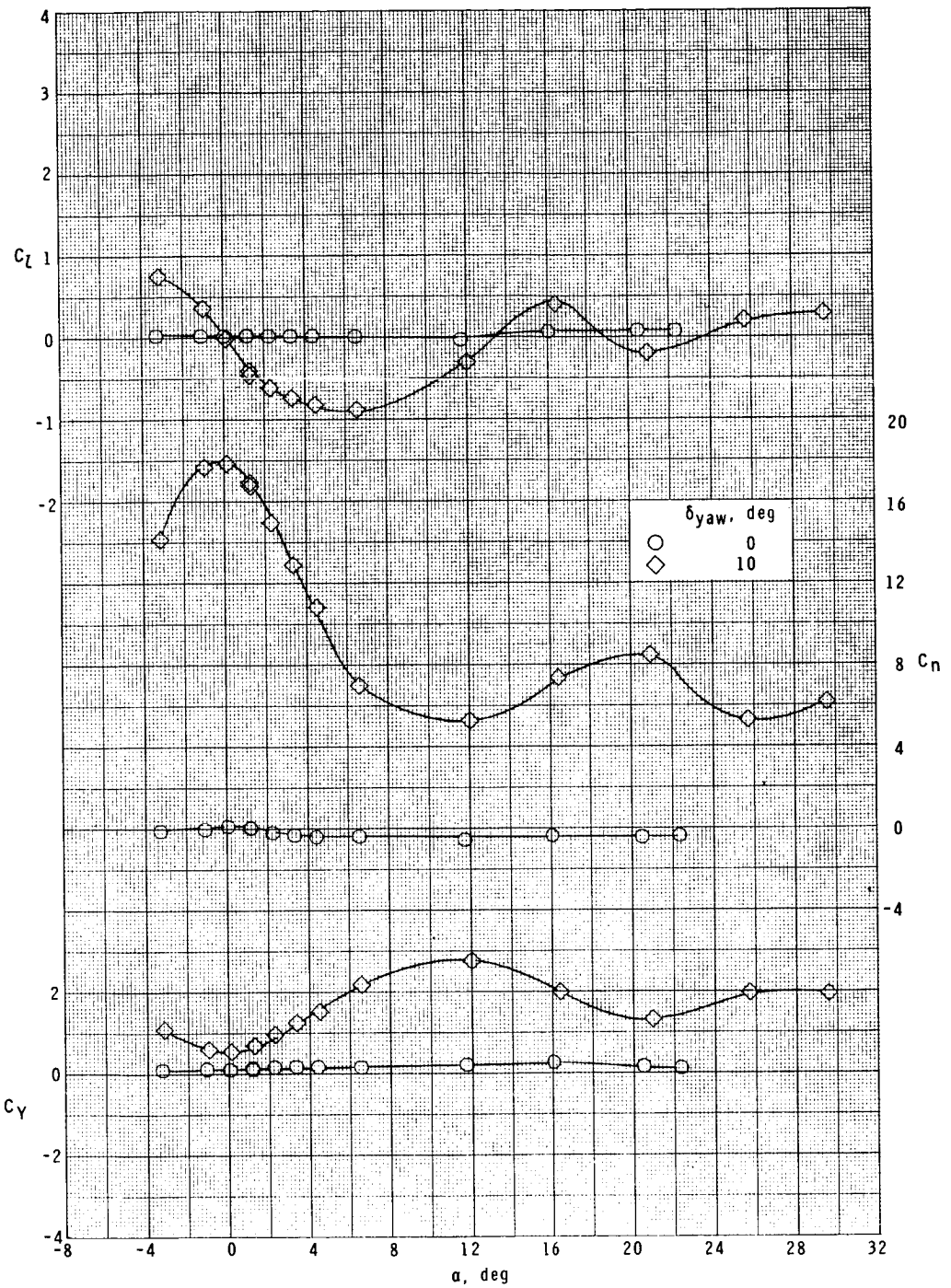

(j) M = 2.10.

Figure 19.- Continued.

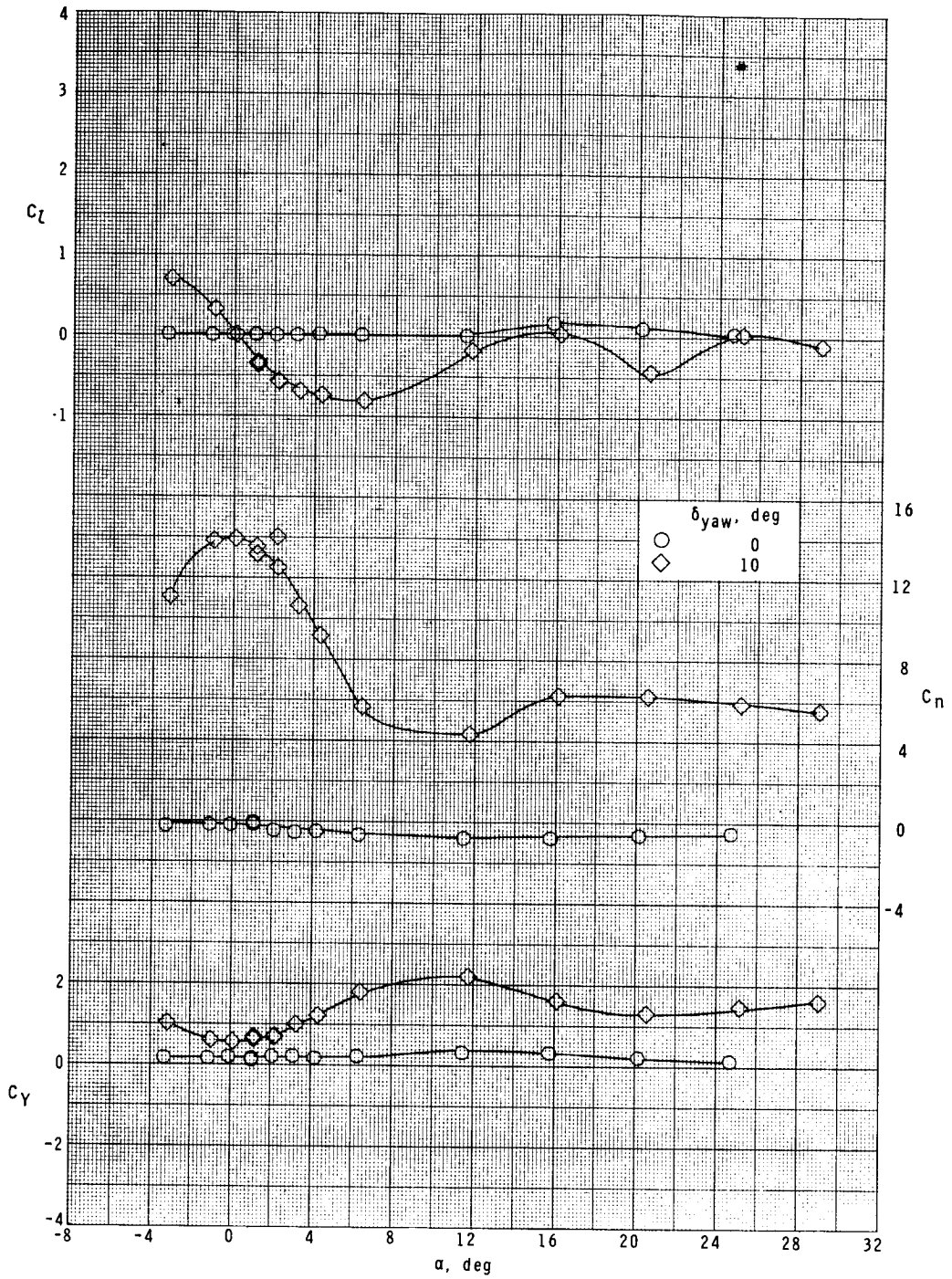

(k) M = 2.50.

Figure 19.- Continued.

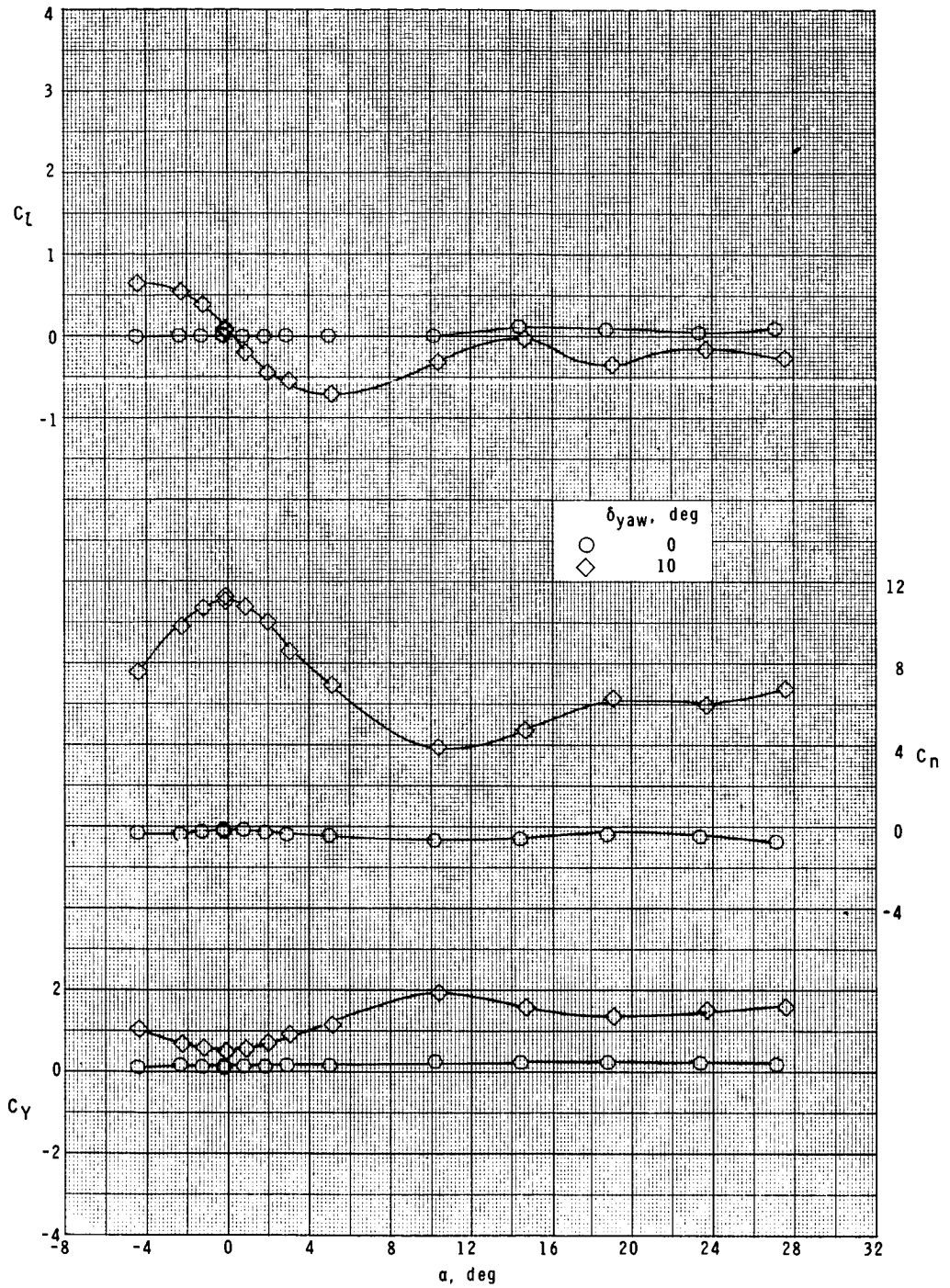

(l) M = 2.86.

Figure 19.- Continued.

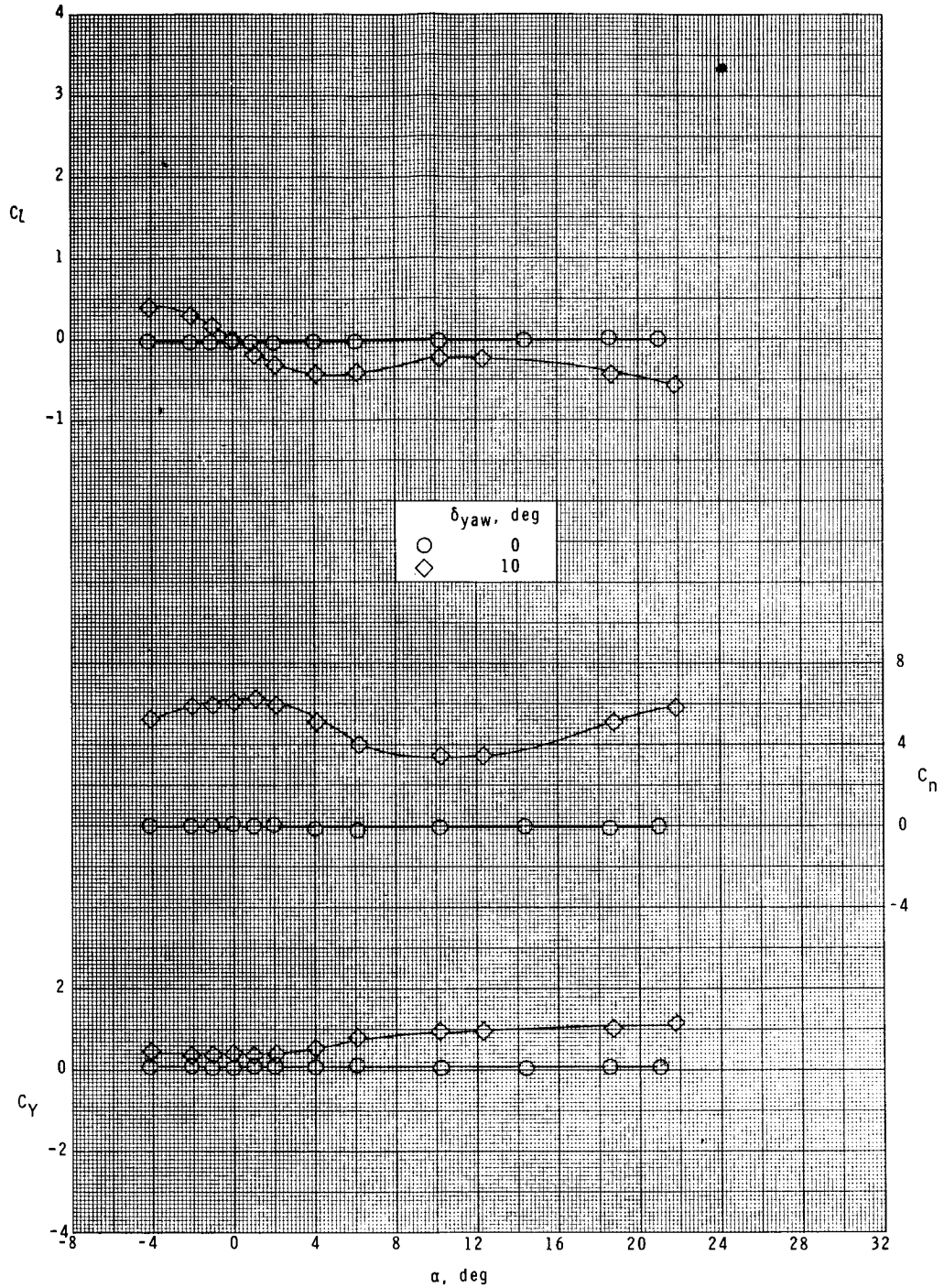

(m) M = 3.95.

Figure 19.- Continued.

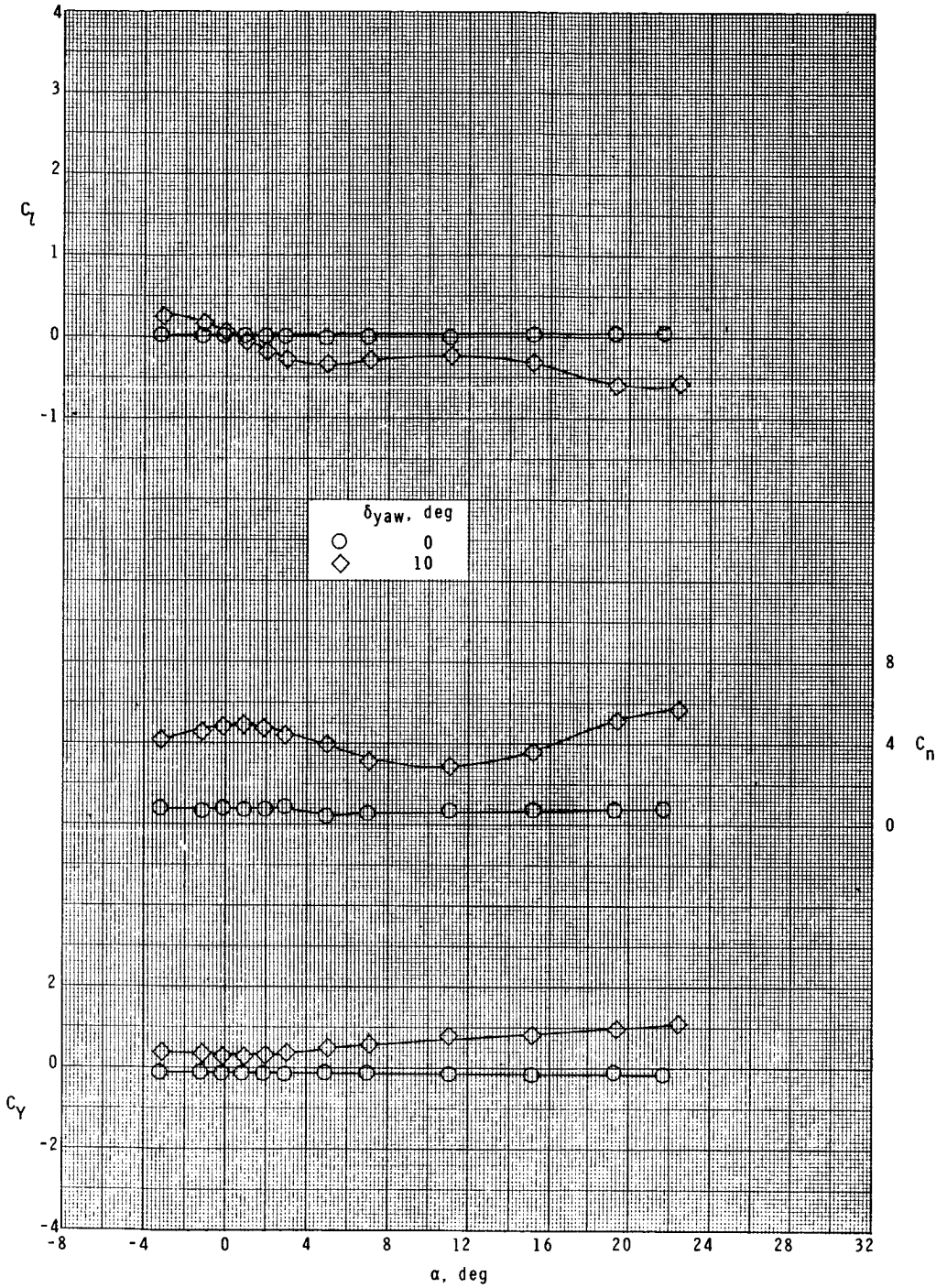

(n) M = 4.63.

Figure 19.- Concluded.

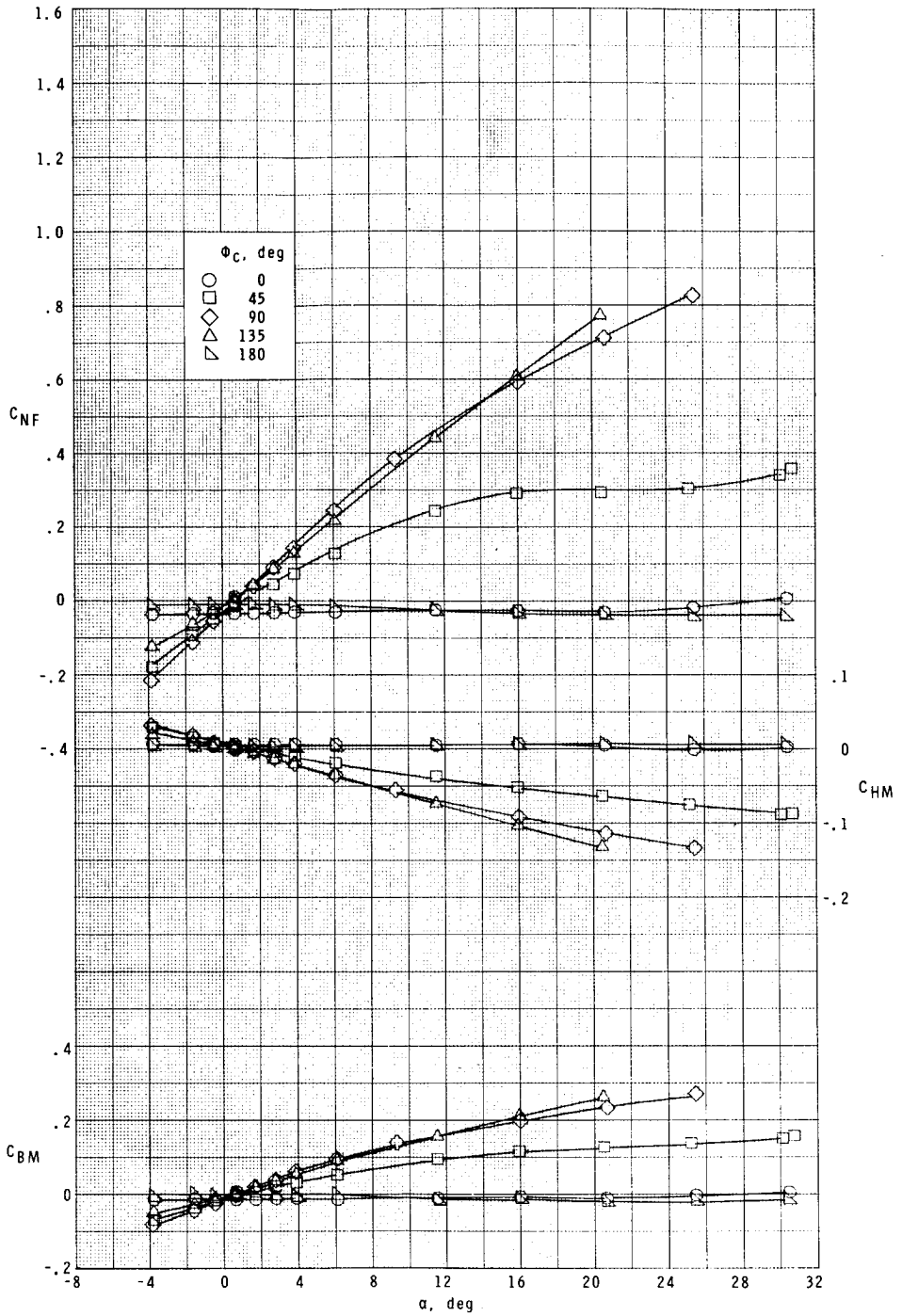

(a) M = 1.75.

Figure 20.- Variation of canard load coefficients with angle of attack. $\delta_c = 0^o$.

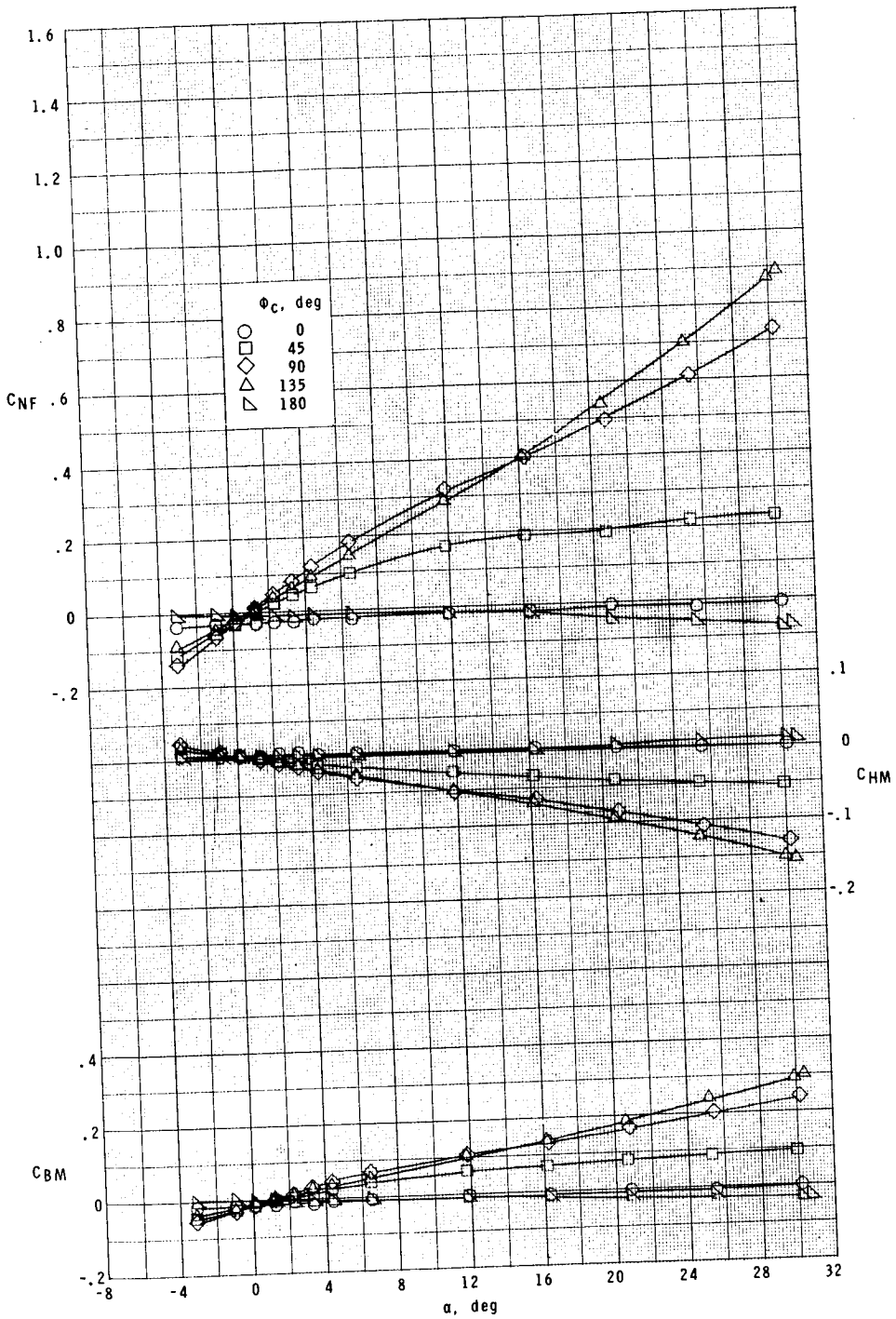

(b) M = 2.50.

Figure 20.- Concluded.

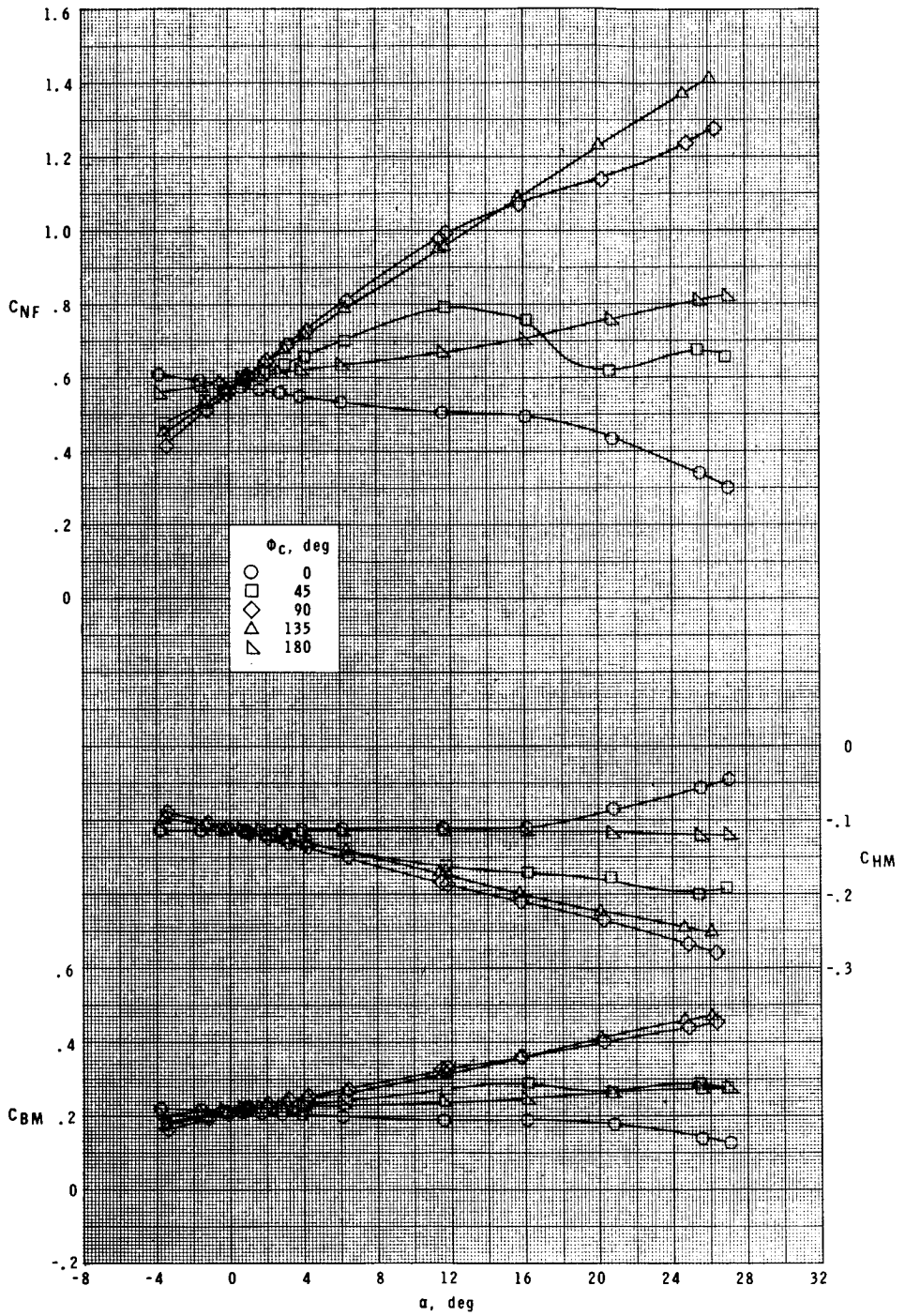

(a) M = 1.75.

Figure 21.- Variation of canard load coefficients with angle of attack. $\delta_c = -20^o$.

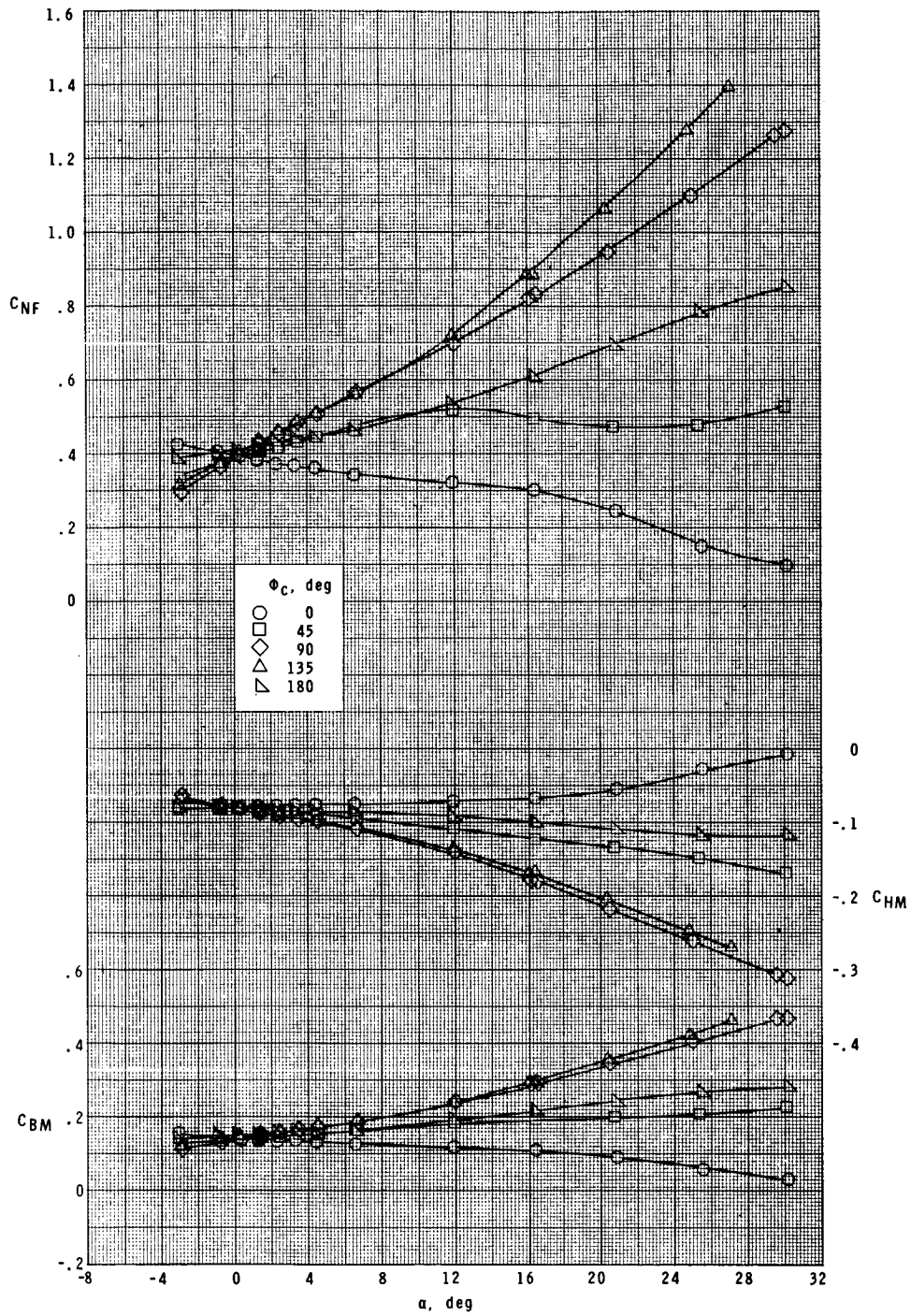

(b) M = 2.50.

Figure 21.- Concluded.